# Proceedings of the I·R·E

## A Journal of Communications and Electronic Engineering

(Including the WAVES AND ELECTRONS Section)

October, 1949

Volume 37 Number 10


Illinois U Library

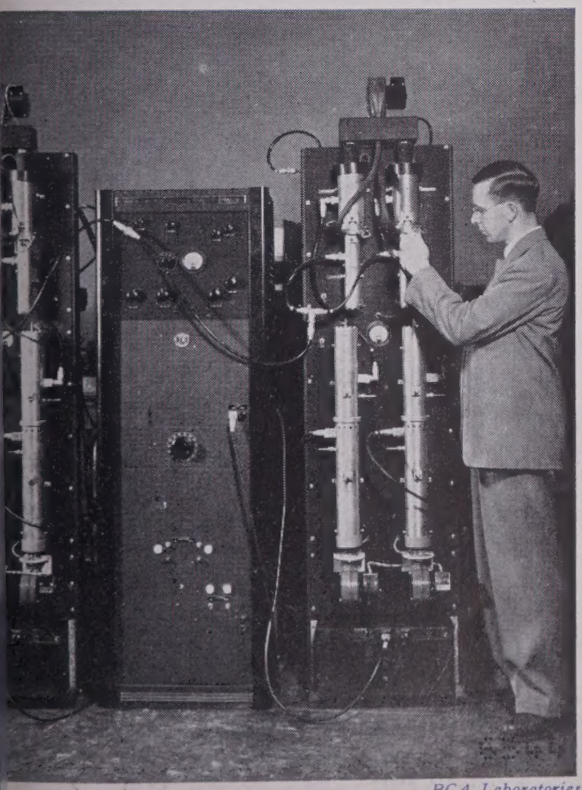

*RCA Laboratories*

**EXPERIMENTAL UHF TRANSMITTER**

negacycles, an output power of 400 watts is obtained by multiple n of tube groups.

PROCEEDINGS OF THE I.R.E.


Audio-Frequency Measurements
Error-Actuated Power Filters
Signal-to-Noise Ratios of Linear Detectors
A Video-Frequency Noise-Spectrum Analyzer
Terminal Impedance and Two-Wire-Line Theory
Energy Spectrum of Pulses
Field-Strength Measurements of HF Fields
RF Detection by Superconductivity
Band-Pass Low-Pass Theory


Waves and Electrons Section


What Kind of Engineers
Electronics Applied to the Betatron
The Influence of UHF Allocations on Receiver Design
Vacuum-Tube Electrodes by Photogravure
Short Antenna Characteristics
Diffraction of HF Radio Waves Around the Earth
Calculator and Chart for Feedback Problems
Voltage Variation in Pulsed *RC* Circuits
Impedance Measurements by Directional Couplers and Voltage Probe
Bilinear Transformations Applied to Transmitter Tuning
Abstracts and References


Table of Contents Follows Page 32A

1950 Convention Authors. See page 1160.

The Institute of Radio Engineers

# FOR COMPACT HIGH FIDELITY EQUIPMENT

Ultra compact, lightweight, these UTC audio units are ideal for remote control amplifier and similar small equipment. New design methods provide high fidelity in all individual units, the frequency response being ±2DB from 30 to 20,000 cycles. There is no need to resonate one unit in an amplifier to compensate for the drop of another unit. All units, except those carrying DC in Primary, employ a true hum balancing coil structure which, combined with a high conductivity outer case, effects good inductive shielding. Maximum operating level + 10 DB. Weight—8 ounces. Dimensions—1½" wide x 1½" deep x 2" high.

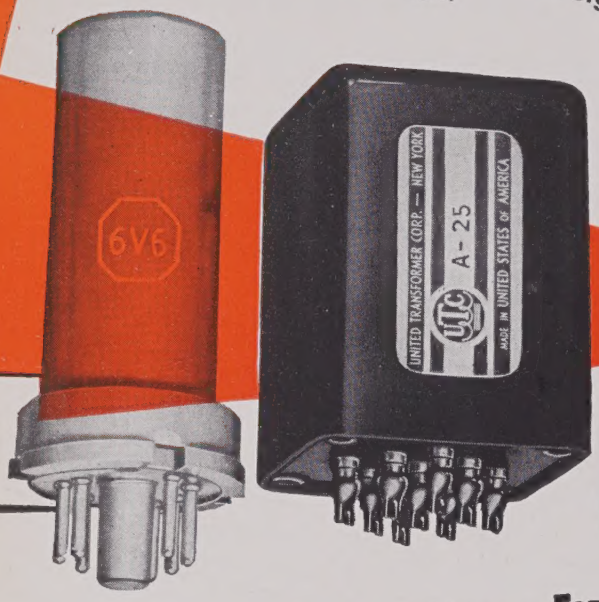


nit shown is ctual size. 6V6 ube shown r comparison nly.

## HERMETICALLY SEALED

On special order, we can supply any of the Ultra Compacts hermetically sealed per Jan T-27 Grade 1 Class A in our RC 50 case as illustrated. Dimensions: Height 2¼", Base 1 9/16" x 1 9/16".

## ULTRA COMPACT HIGH FIDELITY AUDIO UNITS

| Type No. | Application | Primary Impedance | Secondary Impedance | ±2 DB from | List Price |
|---|---|---|---|---|---|
| A-10 | Low impedance mike, pickup, or multiple line to grid | 50, 125/150, 200/250, 333, 500/600 ohms | 50,000 ohms | 30-20,000 | $15.00 |
| A-11 | Low impedance mike, pickup, or line to 1 or 2 grids. Multiple alloy shielded for extremely low hum pickup | 50, 200, 500 ohms | 50,000 ohms | 50-10,000 | 16.00 |
| A-12 | Low impedance mike, pickup, or multiple line to push pull grids | 50, 125/150, 200/250, 333, 500/600 ohms | 80,000 ohms overall in two sections | 30-20,000 | 15.00 |
| A-18 | Single plate to two grids, split primary | 8,000 to 15,000 ohms | 80,000 ohms overall, 2.3:1 turn ratio overall | 30-20,000 | 14.00 |
| A-19 | Single plate to two grids 8 MA unbalanced D.C. | 15,000 ohms | 80,000 ohms overall, 2.3:1 turn ratio overall | 50-20,000 | 18.00 |
| A-24 | Single plate to multiple line | 8,000 to 15,000 ohms | 50, 125/150, 200/250, 333, 500/600 ohms | 30-20,000 | 15.00 |
| A-25 | Single plate to multiple line 8 MA unbalanced D.C. | 8,000 to 15,000 ohms | 50, 125/150, 200/250, 333, 500/600 ohms | 50-12,000 | 14.00 |
| A-26 | Push pull low level plates to multiple line | 8,000 to 15,000 ohms each side | 50, 125/150, 200/250, 333, 500/600 ohms | 50-20,000 | 15.00 |
| A-30 | Audio choke, 300 henrys @ 2 MA 6000 ohms D.C., 75 henrys @ 4 MA 1500 ohms D.C., inductance with no D.C. 450 henrys | | | | 10.00 |

The above listing includes only a few of the many Ultra Compact Audio Units available . . . Write for our new catalog.

United Transformer Co.

150 VARICK STREET • NEW YORK 13, N. Y.

EXPORT DIVISION: 13 EAST 40th STREET, NEW YORK 16, N.Y., CABLES: "ARLAB"

BOARD OF DIRECTORS, 1949

Stuart L. Bailey
*President*

A. S. McDonald
*Vice-President*

D. B. Sinclair
*Treasurer*

Haraden Pratt
*Secretary*

Alfred N. Goldsmith
*Editor*

W. R. G. Baker
*enior Past President*

B. E. Shackelford
*unior Past President*

1949–1950

Ben Akerman
J. V. L. Hogan
F. H. R. Pounsett
J. E. Shepherd
J. A. Stratton
G. R. Town

1949–1951

W. L. Everitt
D. G. Fink

1949

J. B. Coleman
M. G. Crosby
E. W. Engstrom
R. A. Heising
T. A. Hunter
J. W. McRae
H. J. Reich
F. E. Terman
H. A. Zahl

●

Harold R. Zeamans
*General Counsel*

●

George W. Bailey
*Executive Secretary*

aurence G. Cumming
*Technical Secretary*

●

Changes of address th advance notice of een days) and com- nications regarding scriptions and pay- nts should be mailed the Secretary of the titute, at 450 Ahnaip Menasha, Wiscon- or 1 East 79 Street, w York 21, N. Y.

ll rights of republica- , including transla- into foreign lan- ges, are reserved by Institute. Abstracts apers, with mention heir source, may be ted. Requests for ublication privileges uld be addressed to Institute of Radio ineers.

# PROCEEDINGS OF THE I.R.E.

(Including the WAVES AND ELECTRONS Section)

*Published Monthly by*

The Institute of Radio Engineers, Inc.

VOLUME 37 — *October, 1949* — NUMBER 10

## PROCEEDINGS OF THE I.R.E.

Donald G. Fink, Director at Large, 1949–1951 ..... 1106
The Radio Engineer and the Armed Services ..... W. C. Tinus 1107
3450. Audio-Frequency Measurements ..... W. L. Black and H. H. Scott 1108
3451. Error-Actuated Power Filters ..... Gordon Newstead and D. L. H. Gibbings 1115
3452. Signal-to-Noise Ratios of Linear Detectors ..... R. H. DeLano 1120
3453. A Video-Frequency Noise-Spectrum Analyzer ..... Philip S. Jastram and Gordon P. McCouch 1127
3454. Terminal Impedance and Generalized Two-Wire-Line Theory ..... Ronold King and K. Tomiyasu 1134
3455. On the Energy-Spectrum of an Almost Periodic Succession of Pulses ..... G. G. Macfarlane 1139
3456. Problems Related to Measuring the Field Strength of High-Frequency Electromagnetic Fields ..... Rohn Truell 1144
3457. Detection at Radio Frequencies by Superconductivity ..... J. V. Lebacqz, C. W. Clark, M. C. Williams, and D. H. Andrews 1147
3458. Generalized Theory of the Band-Pass Low-Pass Analogy ..... P. R. Aigrain, B. R. Teare, Jr., and E. M. Williams 1152
Contributors to the PROCEEDINGS OF THE I.R.E. ..... 1156
Correspondence:
3096. "Positive-Grid Characteristics of a Triode" ..... Hsiung Hsu 1158

## INSTITUTE NEWS AND RADIO NOTES SECTION

Industrial Engineering Notes ..... 1161
IRE People ..... 1162
Books:
3459. "Principles of Radar" by Denis Taylor and C. H. Wescott ..... Reviewed by R. M. Page 1163
3460. "Transformations on Lattices and Structures of Logic" by S. A. Kiss ..... Reviewed by Claude E. Shannon 1163
Institute Committees—1949 ..... 1164
Technical Committees, May 1, 1949–May 1, 1950 ..... 1165
Special Committees—1949 ..... 1166
Institute Representatives in Colleges—1949 ..... 1166
Institute Representatives on Other Bodies—1949 ..... 1167

## WAVES AND ELECTRONS SECTION

3461. What Kind of Engineers? ..... J. D. Ryder 1168
3462. Electronics Applied to the Betatron ..... Theodore W. Dietze and Theodore M. Dickinson 1171
3319. Correction to "A Modulator Producing Pulses of $10^{-7}$ Second Duration at a 1-Mc Recurrence Frequency" by M. G. Morgan ... 1178
3463. The Influence of UHF Allocations on Receiver Design ..... John D. Reid 1179
3321. Correction to "The Effect of Pole Zero Locations on the Transient Response of Linear Dynamic Systems" by J. H. Mulligan, Jr. 1181
3464. Electrodes for Vacuum Tubes by Photogravure ..... Marshall P. Wilder 1182
3465. Short Antenna Characteristics—Theoretical ... Lynne C. Smeby 1185
3466. Diffraction of High-Frequency Radio Waves Around the Earth ..... M. D. Rocco and J. B. Smyth 1195
3467. Calculator and Chart for Feedback Problems ... Jean H. Felker 1204
3468. Abstract of "The High-Frequency Response of Cylindrical Diodes" ..... Edward H. Gamble 1206
3469. Response of *RC* Circuits to Multiple Pulses ..... Daniel Levine 1207
3470. Impedance Measurements with Directional Couplers and Supplementary Voltage Probe ..... B. Parzen 1208
3471. Bilinear Transformations Applied to the Tuning of the Output Network of a Transmitter ..... K. S. Kunz 1211
Contributors to Waves and Electrons Section ..... 1218
3472. Abstracts and References ..... 1220
Section Meetings ..... 34A
Student Branch Meetings ..... 34A
Membership ..... 36A
Positions Open ..... 50A
Positions Wanted ..... 52A
News—New Products ..... 18A
Advertising Index ..... 70A

*Copyright, 1949, by The Institute of Radio Engineers, Inc.*

EDITORIAL DEPARTMENT

Alfred N. Goldsmith
*Editor*

Clinton B. DeSoto†
*Technical Editor, 1946–1949*

E. K. Gannett
*Technical Editor*

Mary L. Potter
*Assistant Editor*

●

ADVERTISING DEPARTMENT

William C. Copp
*Advertising Manager*

Lillian Petranek
*Assistant Advertising Manager*

●

BOARD OF EDITORS

Alfred N. Goldsmith
*Chairman*

PAPERS REVIEW COMMITTEE

George F. Metcalf
*Chairman*

PAPERS PROCUREMENT COMMITTEE

John D. Reid
*General Chairman*

Responsibility for the contents of papers published in the PROCEEDINGS OF THE I.R.E. rests upon the authors. Statements made in papers are not binding on the Institute or its members.

† Deceased

MEMBER AUDIT BUREAU OF CIRCULATIONS

# Donald G. Fink

DIRECTOR-AT-LARGE, 1949–1951

Donald Glen Fink was born on November 8, 1911, in Englewood, New Jersey. He was graduated in 1933 from Massachusetts Institute of Technology with the B.Sc. degree in electrical communications. After a year as a research assistant on the staff of the departments of geology and electrical engineering at MIT, Mr. Fink joined the staff of the journal *Electronics*, as editorial assistant. In 1937 he became managing editor; in 1945, executive editor; and in 1946, editor-in-chief. In 1943 he was awarded the degree of M.Sc. in electrical engineering by Columbia University.

Obtaining a leave of absence from his editorial duties in 1941, Mr. Fink became a member of the staff of the radiation laboratory at MIT where, in 1943, he headed the loran division. He then transferred to the Office of the Secretary of War as an expert consultant on radio navigation and radar. During his war service Mr. Fink travelled over 80,000 miles from Cairo, Egypt, to Darwin, Australia, siting loran stations and arranging fo the use of the loran system by the allied forces. In 194 he participated in the atom bomb tests at Bikini, a a civilian consultant on the staff of Admiral Blandy

Mr. Fink is the author of numerous books, includin "Engineering Electronics," "Principles of Televisio Engineering," "Television Standards and Practice, "Microwave Radar," and "Radar Engineering." A editor of Proceedings of the National Television Syste Committee, member of the Television Panel of th Radio Technical Planning Board, and currently a chairman of the Joint Technical Advisory Committe he is active in standardization work, particularly in th field of television. In 1948 he was chairman of the IR Television System Committee. He is a member of th Committee on Navigation of the Research and Develop ment Board. Mr. Fink is a Fellow of the Institute and member of Tau Beta Pi, Sigma Xi and Eta Kappa Nu

The technical and industrial potentials of a modern country are vital factors in its military strength. Accordingly, increasingly extensive and close co-ordination between engineers and the Armed Forces is a timely matter, and one of major importance. It is ably discussed in the following guest editorial by a radio development engineer of the Bell Telephone Laboratories, who is a Senior Member of The Institute of Radio Engineers.—*The Editor.*

# The Radio Engineer and the Armed Services

W. C. TINUS

A great deal has been written during the past few years about the rapid growth of the radio and electronic engineering profession from adolescence to mature professional standing. This growth is particularly evident in the changed relation between radio engineers and the armed services. Radio engineers in industrial firms merit, and receive, a great deal more confidence than they did before the war from those in the services who are responsible for the development of new military electronic devices.

Not many years ago the first contact a typical industrial radio engineer had with a military electronic problem was a detailed equipment specification telling what was wanted and what the equipment was expected to do in its individual tests. The last contact the engineer had with the problem was when the equipment was designed, built, and made to pass its tests. What the military problem was and whether the specified equipment best solved it was the concern of others.

The situation today is very different. The military problems for which electronics may provide a solution are more complex. The engineer is on the job at a much earlier stage. His vision is broader and his opinion more respected. He frequently has the opportunity not only to become thoroughly acquainted with the basic military problem but also to help the military people define it. Many equipment design contracts are now preceded by study contracts in which the problem is defined and a solution is proposed. The solution may employ any of the multitude of things in electronics' bags of tricks.

These changes are all to the good. They are good for the military in getting more technical people studying their problems, and eventually in getting better solutions to them. They are good for radio engineers in enlarging their horizons of thought and their opportunities to apply their specialized knowledge. They are good for all of us in getting more value received for our money spent on national defense.

# Audio-Frequency Measurements*

W. L. BLACK†, SENIOR MEMBER, IRE, AND H. H. SCOTT‡, SENIOR MEMBER, IRE

*Summary*—**This paper indicates the theory involved in making measurements of gain, frequency response, distortion, and noise at audio frequencies, with particular emphasis on such measurements made on high-gain systems. There are also discussed techniques of measurement and factors affecting the accuracy of results. This subject is not new art but has not previously been published in correlated form, to the knowledge of the authors.**

## Introduction

DURING the last several years the Radio Manufacturers Association has given considerable attention to codifying minimum standards of performance for the major components of radio broadcasting systems. The engineering aspects of this subject have been considered by committees in the Transmitter Section of the Engineering Department of the Association.

Definitions and minimum standards for the audio facilities of a radio broadcasting system considered primarily as a complete electrical system have been issued as an RMA standard.[1] (Subscripts refer to numbered Bibliography on pages 1114–1115.) As defined in this standard, audio facilities comprise "all audio facilities from the input terminals of the microphone preamplifier to the input terminals of the main transmitter, excluding the studio-transmitter link which may be either wire line or radio. No pre-emphasis is included in the audio facilities."

Subsequently the RMA undertook to outline methods of measurement of audio facilities to insure comparable results from measurements, made at different times and on different apparatus, consistent with practical instrumentation. It is the purpose of this paper to summarize the technical background which is the basis for the RMA standardization activity and to outline possible pitfalls in making measurements on complex, high-gain audio systems. Emphasis is placed on system measurements, as ordinarily a complex, high-gain system presents more of a measurement problem than do system components.

As a practical matter, the important characteristics of audio systems for radio broadcasting which have been agreed upon for RMA standardization are: gain, frequency response (relative gain over a frequency range), single frequency harmonic distortion, and noise (in the sense of noise being extraneous sound or corresponding electrical energy tending to interfere with the proper and easy perception of desired sounds or their equivalent electrical waves).

* Decimal classification: R020×R200. Original manuscript received by the Institute, April 11, 1949; revised manuscript received, July 28, 1949. Presented, RMA-IRE Spring Meeting, Syracuse, N. Y., April 26, 1948.

† Bell Telephone Laboratories, Murray Hill, N. J.
‡ Hermon Hosmer Scott, Inc., Cambridge, Mass.

## Gain

Gain for the determination of performance characteristics is measured between resistances equal to the rated source and load impedances. For the purpose of measuring such gain (or loss) the concept of the ideal transformer[4,5,9,13] for impedance translation for optimum power transfer in the reference condition is useful. This is shown in Fig. 1. Then the gain is the ratio of the power in the load with the equipment under test in the circuit to the power delivered to the same load without the equipment under test, but including an ideal transformer. It is obvious that any further discussion of gain will refer with equal validity to frequency response, as the latter is relative gain over the specified frequency range.

Measurements using resistance terminations for the measurement of the component parts of a system may not agree in total with the results of over-all measurement of the system between resistances. Ordinarily the disagreement is, however, of relatively small magnitude

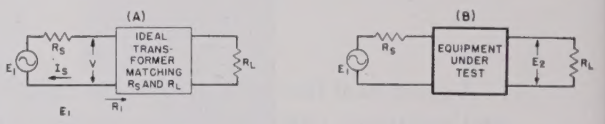


Fig. 1—Gain.

$$I_S = \frac{E_1}{R_S + R_1}$$

$R_S$ is the resistance equal to the rated source impedance of the equipment under test.
$R_L$ is the resistance equal to the rated load impedance of the equipment under test.
But $R_s = R_1$ (by definition), so

$$V = \frac{E_1}{2}$$

and

$$P_1 = \frac{V^2}{R_1} = \frac{E_1^2}{4R_S}.$$

By definition

$$P_{L1} = P_1,$$

where $P_{L1}$ is the power available in the load when the ideal transformer is in the circuit,
so

$$P_{L1} = \frac{E_1^2}{4R_S}.$$

Where $P_{L2}$ is the power in the load with the equipment under test inserted

$$P_{L2} = \frac{E_2^2}{R_L}.$$

$$\text{Gain (db)} = 10 \log_{10} \frac{P_{L2}}{P_{L1}} = 10 \log_{10} \frac{4E_2^2 R_S}{E_1^2 R_L} \text{ db}$$

$$= 20 \log_{10} \frac{2E_2}{E_1} \sqrt{\frac{R_S}{R_L}} \text{ db} = 6 + 20 \log_{10} \frac{E_2}{E_1} \sqrt{\frac{R_S}{R_L}} \text{ db}.$$

If the gain is negative then the equipment under test introduces a loss.

when the interrelations of the impedances of the components have been considered in conjunction with the system design. For large variations from rated impedances, distortion of gain-versus-frequency characteristics may be sufficient to require consideration of the coupling factors[2] involved and may indicate corrective equalization.

## Practical Test Circuit

For practical tests, Fig. 2 presents an essentially complete diagram showing all circuit elements which would

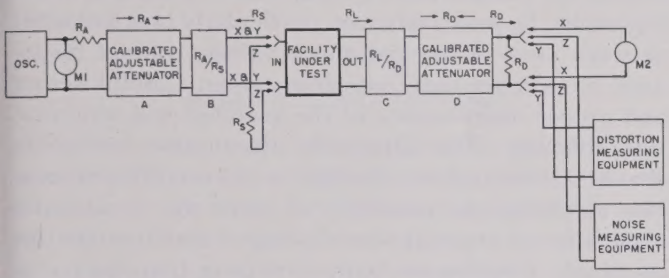


Fig. 2—Typical measuring system for audio facilities;
(B) and (C) are impedance matching networks at the input and the output, respectively.
$R_S$ and $R_L$ are resistances equal to the rated source and load impedances respectively, or facility under test.
Connections { $X$—for gain and response measurements. $Y$—for distortion measurements (single frequency). $Z$—for noise measurements.

Gain for facility under test

$$= A(\text{db}) + B(\text{db}) + C(\text{db}) + D(\text{db}) + 10 \log_{10} \frac{4(E_{M2})^2 R_A}{(E_{M1})^2 R_D}.$$

ordinarily be required for audio-frequency measurements. In many cases, several of the units may be combined in one physical instrument. Separate consideration of each of the various elements follows.

## Oscillator

The source of power for gain testing is ordinarily an audio-frequency oscillator. This oscillator should cover the range of frequencies involved in the tests. Ordinarily absolute frequency accuracy and stability with time are not practical limitations, except in the measurement of frequency selective devices such as filters, and in the use of some types of distortion measuring instruments containing sharply tuned rejection circuits. However, freedom from drift of output voltage with time and with variation in oscillator power supply voltage are of practical convenience. Except when distortion measurements are made, distortion and noise components ordinarily contributed by present-day oscillators are not limiting unless the equipment under test includes filters having sharp cutoff characteristics.

Some oscillators may be critical as to load impedance. Load impedance correction is ordinarily accomplished by a shunt or a series resistance, depending upon whether the optimum load for the oscillator is lower or higher respectively than that offered by the measuring circuit. It will also often be necessary to include a transformer having an electrostatic shield between windings between the oscillator output and the input of the testing circuit to control ground connections and parasitic coupling between the oscillator and the remainder of the testing system.

In any event, once the circuit at the output of the oscillator has been determined, the oscillator output circuit does not affect the measurements of gain or of response as a constant output voltage is maintained and the oscillator is then the equivalent of a zero internal impedance generator.

## Terminations

The desired objective of comparable results indicates the use of pure resistances for terminations. Such terminations include that for the output of the equipment under test, as well as any used for input termination including that used for equivalent generator internal impedance. The impedance of the resistors used for such terminations may therefore warrant consideration. Other factors in this connection include the absolute value of output terminating resistors and the stability of such resistors with temperature, particularly when the output distortion of a power amplifier is being measured.

## Meters

The input voltmeter may be of the vacuum tube, rectifier, or thermocouple type, or may be a standard volume indicator. This meter may be rms, average, or peak reading, except as noted in specific instances later. The stability of this meter must be such that its readings are not influenced by extraneous factors, such as power supply to a vacuum tube.

If a rectifier meter is used, its possible introduction of extraneous modulation products, particularly when making distortion measurements, as well as its possible variation in impedance with change in input are limiting factors. The loss introduced in the transmission circuit by the ordinary meters of this type (of which the "standard volume indicator"[3] is a special form) must be taken into account, particularly if the meter is alternately connected and disconnected during a test.

A thermocouple meter may be used, provided it is appropriately connected to the circuit so that its internal resistance is taken into account. Suitably calibrated thermocouple meters have good scale spread, practical freedom from frequency discrimination at audio frequencies, freedom from modulation, and adequate accuracy. The disadvantages are relatively slow speed of operation and danger of damage due to excessive current.

In this general connection, the indication of a rectifier type meter, typified by one using a copper oxide rectifier, approximates the average value of a sine wave while a thermocouple meter indicates the effective or

rms value. However, if the former is calibrated in terms of rms values no practical difficulty will be experienced on this score in making gain (and frequency response) measurements, even though one type is used at the input and the other type at the output, provided that the testing frequency has a sine wave form within the limits already mentioned. In the determination of harmonic distortion, wave-form errors due to the type of meter used may limit the accuracy of measurement.[12]

The output meter may be similar to the input meter or may actually be the same meter alternately connected at the input and at the output. If the other components of the measuring system are so arranged that the input and output voltages are the same, the measurements are expedited and errors due to absolute calibration of the meter and to its variation in indication with frequency are eliminated in making response measurements. However, convenient switching on this basis involves bringing wires from the input and the output of the system in close proximity and may cause undesirable coupling, particularly when a high-gain system is being measured. This may cause an error in absolute gain indication or an error changing with frequency during response measurements, or both. This procedure is, of course, impractical if the input and output of the equipment under test are not in approximately the same vicinity. For example, the input of the system being tested might be in a studio control booth and its output in a master control room.

Other factors to consider are the frequency response of the meter, accuracy of reading possible due to instrument scale spread and pointer structure and the sensitivity of the output meter in the case of loss measurements. Finally, the factors such as pivot friction and uniformity of magnetic field ordinarily affecting the accuracy of electrical instruments should be considered in conjunction with the absolute accuracy desired.

## Adjustable Attenuators

As a practical matter, greatest convenience of measurement is achieved if the meters used are held at constant readings, and the variations in gain are determined by calibrated adjustable attenuators at the input and at the output of the equipment under test as shown in Fig. 2. This method has several advantages. The meter scale range, absolute sensitivity, and possible variation in accuracy with indication are not factors in the choice of meters used. Possible observational errors due to the use of meter range switches are eliminated. The amount of calculation to obtain the desired result from observed readings is minimized. Further this arrangement has the merit that known input and output levels over a wide range of values can readily be provided. This is of particular practical importance if the same testing equipment is to be used to measure a wide range of gains and losses and various power levels.

The increments of attenuation available and the accuracy of their calibration, together with the scale sensitivity and accuracy of the meters used, govern the accuracy with which absolute gain can be determined. Response (relative gain) measurements require absolute accuracy such that relative gains are indicated within the desired limits of precision. A total measuring error of $\pm 0.2$ db from all causes is the order of precision required for frequency response (relative gain) measurements on equipment for broadcasting transmission. This limit includes frequency response errors in the attenuators. These may ordinarily be avoided by careful attenuator design. Failing this, recourse to calibration is possible. In some instances, particularly in attenuator-network arms of low resistance values, contact resistance in switches may introduce errors. Careful design and proper maintenance of the switches will minimize this difficulty. The adjustable attenuators preferably should be mounted in a shielded enclosure. This precaution minimizes the possiblity of errors due to parasitic capacities to external surroundings which become increasingly troublesome with increasing frequency.

## Impedance Matching Networks

The calibrated adjustable attenuators will have fixed input and output impedances determined during design. If the impedances from and into which it is desired to measure the equipment under test are other than those of the attenuators, it is necessary to add impedance matching networks. These ordinarily can be fixed pads. The addition of such pads to the testing circuit is shown in Fig. 3. The determination of the values of such pads is well covered in extant literature.[10,11]

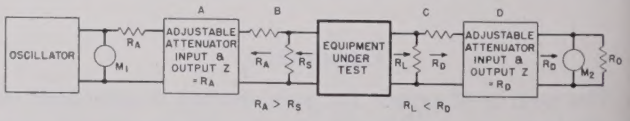


Fig. 3—Matching pads;
(B) and (C) are minimum loss "$L$" pads matching $R_A$ to $R_S$ and $R_L$ to $R_D$, respectively.
If $Z$ is the larger and $z$ is the smaller of the two impedances being matched by each matching pad, then

$$\text{loss (db)} = 20 \log_{10} \left( \sqrt{\frac{Z}{z}} + \sqrt{\frac{Z-z}{z}} \right).$$

The power handling capacity of the resistors used in pads may also require consideration on occasion. For example, when measurements are made on an amplifier for a high-powered sound system, an output pad might well be used to reduce the power to normal measuring level, but the difference between the power out of the amplifier and that in the meter circuit would be dissipated in the pad.

Ordinarily, one per cent accuracy will be adequate for the values of the resistors used for pads. However, the required accuracy (or alternative calibration of actual loss) will be governed by the accuracy desired in absolute gain indication. In addition, freedom from change of attenuation with frequency or calibration for such change of loss is also a necessary consideration.

In connection with the use of both adjustable attenuators and fixed pads, whether for impedance matching or to supplement limited range adjustable attenuators, it should be noted that Thevenin's theorem may be applied to reduce the input and the output networks to the equivalent of a generator in series with a resistance.

## Balance and Grounding

For measured results comparable to actual performance conditions, the equipment under test should be grounded in the same way for measurement as it is in actual use. In particular, the grounding or freedom from grounding of the input or output or both should be maintained. Among the practical problems which this introduces are: first, the balance of attenuators (both fixed and adjustable), and second, the control of oscillator grounding.

The attenuators, including those for impedance matching, should be of the "unbalanced" type for connection to a grounded circuit, and of the balanced type for connection to circuits intended for operation ungrounded or with a "center tap" ground. When using an unbalanced measuring circuit one side should always be grounded. The term "ground" is here used as meaning that zero potential plane used for reference. The impedance to ground for all points on the grounded side should be as low as possible, the interconnecting leads should be as short as possible, and no series resistors included in the ground circuits. For example, matching pads should have their series resistors in the ungrounded side of the circuit. A properly balanced attenuator requires both resistance balance between the two sides of the attenuator and capacity balance to ground on the two sides. The latter is ordinarily provided by the proper design of the calibrated adjustable attenuator switches. A ground at the center point of the shunt resistance element of the attenuator is usually necessary to insure balance in actual use. Tests to determine the adequacy of the balance (assuming freedom from parasitic coupling) may be made by reversing the connections either to the input or to the output of the attenuator in question and observing whether the output is affected due to such reversal, particularly at the higher audio frequencies. An alternative arrangement to the use of balanced attenuators is the use of an electrostatically shielded and balanced transformer between the attenuators and the equipment under test as shown in Fig. 4. This necessitates taking into account the loss and the possible frequency discrimination introduced by such a coil.

One practical check of the stability of the measuring circuit is to make a known change in the output level from the oscillator with a corresponding compensating change in the input attenuator setting. For example, a 10-db increase in test signal level and a 10-db increase in the input attenuator should result in the same input level to the equipment under test, and consequently no change in observed output level. This check should preferably be made at a frequency in the higher range of the frequencies to be used for testing.

The oscillator output circuit may be grounded, or even though not grounded, may have sufficient capacitance to ground to introduce errors (the usual practical case). Therefore, this circuit must also be considered in conjunction with the input ground. This condition can often be provided for by the use of an electrostatically shielded transformer at the oscillator output as shown in Fig. 4. As the reference input voltage is measured beyond this coil, its frequency response characteristic does not affect frequency response measurements. However, when making harmonic measurements, it should be borne in mind that such a coil may contribute undue harmonic distortion unless it is chosen to handle the desired oscillator output power adequately. The efficacy of an electrostatically shielded transformer is a function of the reduction of effective interwinding capacitance brought about by the shield which is a function of the transformer design.

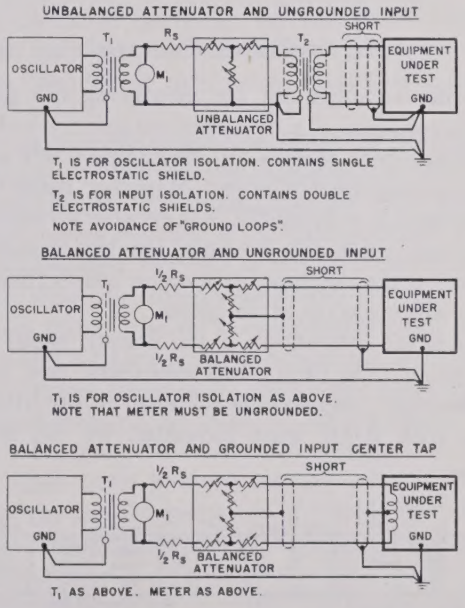


Fig. 4—Balance and grounding—input circuits.

In addition to the transmission circuit grounds, the shields ordinarily required on the interconnecting wiring must be grounded as shown in Fig. 4.

### Bridging Gain

A special condition of gain measurement occurs when it is desired to determine bridging gain which has been defined as "the ratio, expressed in db, of the power delivered to the bridging amplifier load to the power in the load across which the input of the amplifier is bridged."[1] For this measurement the output of the input attenuator is terminated by a resistance equal to the reference load, and the input of the equipment under test is connected in parallel with this load. Equipment intended for bridging operation will ordinarily have an input impedance high relative to that of the circuit on which it is bridged. However, it will still be necessary to take into account the reduction in power in the reference load due to the bridged input for accurate results. Otherwise, the measurement technique does not differ from that previously discussed.

### Illustrative Example

A specific arrangement for measuring the gain and frequency response of a hypothetical system is shown in Fig. 5. When both meters are indicating 0.001 watt, no meter correction need be added. However, using thermocouple meters, it is probable that greater accuracy of indication can ordinarily be obtained by reading small variations on the thermocouple meter scales than by the use of 0.1-db steps on attenuators.

In this same connection if the desired input level is equivalent to −50 dbm (2.45 millivolts, rms, in series with 150 ohms), this level is achieved in the illustrative example with 0.001 watt indicated by $M_1$ and 39.5 db in the adjustable attenuator. This 39.5 db plus the 10.5 db of the matching network provides the desired equivalent of −50 db referred to 0.001 watt.

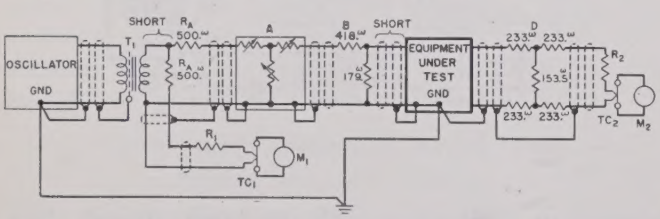


Fig. 5—Illustrative example:

(A) is adjustable attenuator for 500 ohms input and output impedances.
$R_1+TC_1$ = 500 ohms total ±1 per cent.
$R_2+TC_2$ = 600 ohms total ±1 per cent.
$R_A$ = each 500 ohms ±1 per cent.
All other resistors, ±1 per cent.

Loss in decibels due to matching network (B)

$$\text{db} = 20 \log_{10}\left(\sqrt{\frac{Z}{z}} + \sqrt{\frac{Z-z}{z}}\right)$$

$$= 10.5 \text{ db.}$$

Loss in db of (D) = 18 db (for +18 dbm from equipment under test and 0.001 watt in $R_2+TC_2$).
Source impedance of equipment under test = 150 ohms ($R_S$).
Load impedance of equipment under test = 600 ohms ($R_L$).
Meters $M_1$ and $M_2$ calibrated with reference to 0.001 watt in 500 ohms and 600 ohms, respectively.
Then, if 0.001 watt level is maintained in $R_1+TC_1$,
for equipment under test:
Gain (db) = $A$(db) + 10.5 db + 18 db = $A$(db) + 28.5 db.

The illustrative example of Fig. 5 is essentially similar to the general basic circuit of Fig. 2. However, it will be noted that the arrangement of the input meter circuit of Fig. 5 is such that the same input voltage appears across the input terminals of the input adjustable attenuator as that indicated by $M_1$, thus avoiding a 6-db correction required in the case in Fig. 2. With the arrangement of Fig. 5 the relative values of the series input resistances are, of course, factors in the accuracy of measurement.

### Distortion Measurement

*Distortion Measurements Using a Wave Analyzer*

Wave analyzer determination of harmonic distortion at the output of the equipment under test involves separate measurement of the individual harmonics and the calculation of the square root of the sum of their squares. The wave analyzer is connected as shown in Fig. 2. The wave analyzer can be used to check the signal source for harmonic content by connecting it directly to the output of the oscillator circuit. Such a check should be made to insure that measurements are being made of harmonics generated in the equipment under test.

For such tests on balanced equipment the same precautions must be observed as outlined in the section on response and gain measurements. In the case of wave analyzer measurements, it probably will not be possible to connect directly to the output terminals of the equipment under test without producing unbalance as the usual wave analyzer has one terminal at ground potential, unless an isolating transformer is inserted in the input leads to the wave analyzer.

The measurement of distortion with a wave analyzer tends to be more precise than measurements with a noise and distortion meter under some conditions, as discussed later. However, it has the disadvantages that the actual observations are more time consuming, and that calculations are necessary to determine the total distortion percentages.

In making distortion measurements, the same absolute gain as well as the same relative distribution of gains and losses in the equipment under test as were used for the gain and frequency response measurements must be used to insure correlation of results.

It is also advisable to make a check at the output of the equipment under test with the signal removed to see if actual components of the signal are causing the indication, or if it is due to noise or hum generated in the equipment. If noise causes a reading approaching the same order of magnitude of the expected distortion readings, the selective method of measuring the harmonics with a wave analyzer will ordinarily result in more accurate determination of distortion than a nonselective method.

*Distortion Measurements Using a Distortion Factor Meter*

A distortion factor meter,[15] when used for distortion measurements, attenuates the fundamental of the test signal output of the equipment under test and passes the remaining signal, which is composed of harmonics and noise. The rejection of the fundamental is achieved either by the use of a high-pass filter or by the use of a sharply selective circuit. Comparative measurements may thus be difficult to correlate, particularly if the amplitude of the remaining noise approximates that of the harmonics being measured. Such meters are sometimes so arranged that the frequency-selective circuits may be disconnected for use in measuring noise as discussed later. Such a device is ordinarily termed a distortion and noise meter.

A distortion factor meter may be substituted for the output meter as shown in Fig. 2. It will be necessary to preserve the desired grounding condition of the circuit under test and to terminate the output attenuator properly. This termination can be in part or in whole the input of the distortion and noise meter.

In addition to the errors caused by noise as already mentioned, this method of distortion measurement may be subject to other errors. The readings may be accentuated or reduced by phase relationships between different harmonics or between the same harmonics introduced by each of several elements in the equipment under test. Furthermore, when the magnitude of the harmonics exceeds a few per cent there is a metering error as the distortion factor meter indicates the ratio of the harmonics to the fundamental plus the harmonics rather than to the fundamental only.

*Intermodulation Distortion*

By substituting two signal sources at the input, two signals can be simultaneously applied to the equipment under test and, by means of an analyzer connected at the output, the intermodulation between the two signals can be measured. Different methods of making such measurements have been discussed in the literature.[16,17,18] However, the Committee on Audio Facilities of the Transmitter Section of RMA has taken the position that "there is not sufficient data available at this time based on subjective observation to establish recommended conditions for test for intermodulation measurement."[1]

## Noise

*General*

The measurement of electrical noise in a complex audio system such as the complete audio facilities for an eleborate broadcasting studio is very simple in theory. The reference output power at the reference frequency is first determined. The signal is then removed, the input is terminated with a resistance equal to the rated source impedance, and the residual output level is measured. The ratio of the two levels expressed in decibels is then the signal-to-noise ratio. In actuality there are two major complications in measuring the noise. These complications are the nature of the noise and the characteristics of the noise meter.

The nature of the noise is important basically because even though it is measured as electrical energy, in the actual application of the equipment under test it is ultimately converted to acoustical energy, and as such is a disturbance on a subjective basis to the listener. The noise energy present in audio facilities for radio broadcasting is ordinarily composed mainly of two types. The first is random energy distributed substantially uniformly over the frequency spectrum and of relatively uniform amplitude such as that caused by thermal noise in resistors. The second is energy concentrated at one or more frequencies. A typical cause of such noise is operation of equipment from an alternating-current power source. In addition to these two types ordinarily present, peaks of relatively high amplitude but of short duration may be experienced. Such peaks may occur at random intervals or may recur at repetitive time intervals.

The characteristics of the noise meter become a problem because of the possible variations in the nature of the noise energy. If all noises had the same wave shape, then any meter capable of indicating steady-state electrical energy and having the requisite sensitivity could be used. However, when noises have different frequency makeups, either due to various mixtures of single frequency and random noise or due to various mixtures of different single frequencies, then if the noise meter is to give equal readings on noises which are equally disturbing to a listener, the frequency response characteristic of the noise meter is important and should not be flat. Finally, the possible presence of random pulses emphasizes the time of integration of the meter and the ballistic properties of the indicating instrument.

As a temporary arrangement for measuring the noise on audio facilities for radio broadcasting (not including studio-transmitter links), the Committee on Audio Facilities has agreed upon making noise measurements with a device having a frequency response flat within plus or minus two decibels from 50 to 15,000 cps and having the ballistic characteristics of the "standard VU meter" but reading (responsive to) the rms value of a complex wave approximating a steady-state condition.[1] The Committee also notes that measurement of pulse noise conditions has not been included because of lack of definition and equipment.

The results of the measurement of noise with a meter having a substantially flat frequency response are ordinarily reasonably adequate for comparative use in the field outlined herein, particularly on like equipment. For example, in audio facilities for radio broadcasting, the noise problem frequently simplifies to that of the control of hum from power supply when power is supplied as alternating current to the heaters of indirectly heated cathodes and as rectified and filtered alternating

current for the other elements. Where a diversity of conditions exists, it may be necessary to qualify the results of noise measurements to insure proper interpretation; this results largely from employing flat response measurement of electrical noise, as generally the ultimate criterion is disturbance on an acoustical basis. For this reason, frequency weighting in the meter has been generally resorted to in noise tests on telephone systems and in acoustical measurements, to simulate human ears at representative listening levels. Examples of this are the Bell System program noise measuring equipment and the American Standard Sound Level Meter.[20,21,22] There are incorporated in the latter device two frequency weightings, corresponding to ear characteristics for 40 db and 70 db acoustical levels. Results of acoustical measurements with such a meter would of necessity require supplementary data for coordination with previous results of flat response measurements of the electrical noise in amplifiers intended as components of an electro-acoustical system. However, generally available data correlated with weighted electrical measurements made on amplifying systems do not appear to exist in sufficient volume to warrant abandonment at the present time of the existing use of flat weighting for electrical noise measurements on the audio systems under discussion. This decision is an expedient and is subject to review in the light of more adequate information which may become available later.

As noted above, the Committee on Audio Facilities has specified that the noise measuring device have the ballistic characteristics of a standard VU meter but that it read the rms value of a steady complex wave. The standard VU meter does not read this rms value as the exponent applying to the instantaneous value of voltage for it[3] is $1.2 \pm 0.2$, while the corresponding exponent is 2.0 for an rms device. However, it seems likely that on ordinary steady noises found in audio systems the difference between a VU meter reading and an rms reading would not exceed about 1 db. For noises of markedly peaked wave shapes, the difference would be greater[12]; but these are not ordinarily originated in audio facilities.

The Committee on Audio Facilities has not specified the frequency response of the noise measuring equipment above 15,000 cycles. It would seem desirable that this response cut off frequencies above 15,000 cycles, since the broadcast receiver and listener would ordinarily be insensitive to them. If measuring instruments of differing frequency response above 15,000 cycles are used to measure a noise having components above 15,000 cycles, different readings will be obtained, particularly if the equipment under test has a substantial frequency response above 15,000 cps. However, the difference between the readings of a standard volume indicator and an ordinary noise and distortion meter, contributed by the differences between their frequency response characteristics, will usually amount to only a few tenths of a decibel, though in particular cases (e.g., where the apparatus under test picks up the field from a long-wave radio-telegraph station) larger differences may be found.

### *Noise Measurement Using a Distortion and Noise Meter*

To make noise measurements with the distortion and noise meter of the general type already described, its calibration is first adjusted so that it indicates zero with a test signal at a medium frequency such as 1,000 cps after the input level is established at the normal or operating level. The gain and control settings of the equipment under test should again be the same as for previous measurements. The output of the equipment under test should be terminated by resistance equal to the rated load impedance. Noise measurement is then made by removing the test circuit from the input to the equipment under test and substituting a resistor equal to the rated input source impedance. The resistor should be noninductive and of a type, such as a wire-wound resistor, which will not in itself generate appreciable noise. In high-impedance, low-level circuits it may be necessary to shield it carefully to avoid hum pickup trouble.

## Acknowledgements

The authors wish to acknowledge the assistance of W. F. Byers of the General Radio Company for his help in the preparation of a preliminary draft. In addition, thanks are due to those who offered constructive comments to this presentation in manuscript form and to the many persons who, over the years, have published results of their work and thus made this compilation possible. The appended Bibliography is not intended to be all-inclusive, but it does indicate some of the sources of information available which bear on the subject matter.

## Bibliography

1. Radio Manufacturers Association, Standard TR-105A, "RMA Standard—Audio Facilities for Radio Broadcasting Systems," May, 1948.
2. F. F. Romanow and M. S. Hawley, "Proposed method of rating microphones and loudspeakers for systems use," Proc. I.R.E., vol. 35, pp. 953–960; September, 1947.
3. "American Recommended Practice for Volume Measurements of Electrical Speech and Program Waves," American Standards Association C16.5, 1942.
4. K. S. Johnson, "Transmission Circuits for Telephone Communication," D. Van Nostrand Co., New York, N. Y., 1925.
5. T. E. Shea, "Transmission Networks and Wave Filters," D. Van Nostrand Co., New York, N. Y., 1929.
6. W. L. Everitt, "Communication Engineering," McGraw-Hill Book Co., New York, N. Y., 1932.
7. "Electrical Engineers' Handbook—Electric Communications and Electronics," Ed. by H. Pender and K. McIlwain, John Wiley & Sons, New York, N. Y., 1936; 3rd edition.
8. F. E. Terman, "Radio Engineers' Handbook," McGraw-Hill Book Co., New York, N. Y., 1943.
9. "Motion Picture Sound Engineering," Research Council of the Academy of Motion Picture Arts and Sciences, D. Van Nostrand Co., New York, N. Y., 1938.
10. A. E. Thiessen, "Impedance matching networks," *Electronics*, vol. 2, pp. 552–553; March, 1931.
11. P. K. McElroy, "Designing resistive attenuating networks," Proc. I.R.E., vol. 23, pp. 213–234; March, 1935.

12. I. Wolff, "Alternating-current measuring instruments as discriminators against harmonics," Proc. I.R.E., vol. 19, pp. 647–655; April, 1931.
13. S. J. Haefner, "Amplifier—gain formulas and measurements," Proc. I.R.E., vol. 34, pp. 500–506; July, 1946.
14. N. B. Fowler, "Measurements in communications," *Elec. Eng.*, vol. 66, pp. 135–140; February, 1947.
15. W. N. Tuttle, "A method of measuring directly the distortion in audio-frequency amplifier systems," *Jour. Soc. Mot. Pic. Eng.*, vol. 18, pp. 199–206; February, 1932.
16. H. H. Scott, "Audible audio distortion," *Electronics*, vol. 18, pp. 126–132; January, 1945.
17. J. K. Hillard, "Distortion tests by the intermodulation method," Proc. I.R.E., vol. 29, pp. 614–620; December, 1941.
18. J. G. Frayne and R. R. Scoville, "Analysis and measurement of distortion in variable-density recording," *Jour. Soc. Mot. Pic. Eng.*, vol. 32, pp. 648–674; June, 1939.
19. H. H. Scott, "The measurement of audio distortion," *Communications*, April, 1946; and Engineering Handbook of National Association of Broadcasters.
20. "American Standard Sound Level Meters for Measurement of Noise and Other Sounds," American Standards Association, 224.3; 1944.
21. R. S. Tucker, "Measurements of noise on program circuits," *Bell Lab. Rec.*, vol. 14, pp. 233–236; March, 1936.
22. J. M. Barstow, "A new noise meter," *Bell Lab. Rec.*, vol. 15, pp. 252–256; April, 1937.

# Error-Actuated Power Filters*

GORDON NEWSTEAD† AND D. L. H. GIBBINGS†

***Summary*—A filter is described which is capable of handling large amounts of power using components rated at a small fraction of that power. The filter employs negative feedback to cancel out unwanted frequencies. Design equations are given and the operation of a typical filter circuit is examined.**

## I. Introduction

A PASSIVE filter achieves its results by presenting a frequency variable impedance to the supply which is to be filtered. An alternative method of filtering is to generate voltages to oppose and cancel those which it is desired to remove. In this paper we describe filters operating on this principle which may be likened to error-actuated servomechanisms, the error being the residual voltage at the unwanted frequencies. We have named such filters "error-actuated filters."

Error-actuated filters have distinct advantages over classical types of filter in respect to power-handling capacity, and their filtering action is not significantly affected by large variations in load impedance. In one stage of such a filter, the error can be reduced to a value fixed only by stability requirements, and, if necessary, a number of stages can be used in cascade. The lower limit to which harmonics can be reduced in this way is fixed by the production of harmonics in the filter itself.

In this paper we are mainly concerned with the purification of a fundamental frequency, by the removal of unwanted harmonic frequencies. However, there appears to be no fundamental limitations on the method which would prevent its being extended to apply to a given set or band of frequencies, and we intend, subsequently, to investigate error-actuated filters with wider pass bands.

Although the power to be filtered does not pass through the amplifiers used in the filter, it is necessary, as discussed below, for it to have a power rating. However, in the case where the unwanted frequencies are a small fraction of the wanted frequencies, this rating is only a fraction of the power handled by the filter. For example, with receiving tubes and small transmitting tubes, we have found it possible to remove the harmonics from about $\frac{1}{4}$ kw of alternating current containing 5 per cent harmonics. Larger powers could be handled using larger transmitting tubes.

* Decimal classification: R143.2×R386.2. Original manuscript received by the Institute, December 27, 1948.
† The University of Tasmania, Hobart, Tasmania, Australia.

## II. Notation and Symbols

The subscripts $i$ and $o$ are used to denote input and output quantities, and the subscripts $w$ and $u$ are used to denote wanted and unwanted quantities, respectively. The symbols $I$ and $V$ are used for current and voltage, respectively; for example, $V_{iw}$ means the wanted component of the voltage present in the input. The subscript $H$ is used to denote the difference between input and output quantities, thus

$$V_H = V_i - V_o.$$

In general, the $V$ and $I$ are complex numbers to take account of phase shifts, the modulus symbol being used for the rms value of their magnitudes. In the case where there is more than one wanted or unwanted component, symbols such as $V_{iu}$ are to be interpreted as applying to typical components, but $|V_{iu}|$ is to be interpreted as the rms value of all the $u$ components. We also use:

$D$ = the maximum allowable dissipation in the anode of the final amplifier tube. With the suffix $u$, $D$ means the actual power supplied by or to the tube at the unwanted frequencies.
$T$ = the turns ratio of the output transformer of the amplifier (see Fig. 2).
$G$ = the gain of the amplifier.
$\beta$ = a factor to take account of the attenuation of the network.
$I_o$ = the steady dc current in the anode of the final amplifier tube.
$E_o$ = the steady dc voltage on the anode of the final amplifier tube.
$E_c$ = the grid bias voltage on the final amplifier tube.
$r_a$ = the plate resistance of the final amplifier tube.
$n = |V_{iu}|/|V_{iw}|$ = ratio of unwanted to wanted voltages present in the input.

## III. Theory of the Error-Actuated Filter

The general arrangement of this type of filter is shown in Fig. 1. The unwanted frequencies are taken

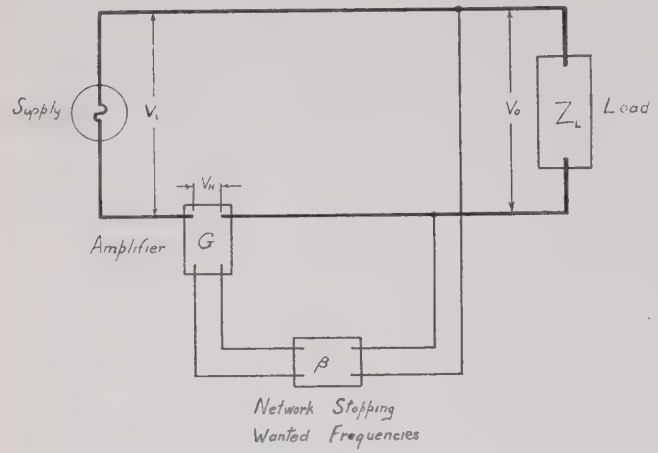


Fig. 1—General arrangement of error-actuated filter.

through a feedback path of gain $G\beta$ and reinserted further back in the circuit, the connection being such that the feedback is negative. The voltage gain $G\beta$ is defined as the ratio $V_H/V_o$ and is a function of frequency. It is convenient to take the gain as the product of two factors, $G$ depending on the amplification of the amplifier, and $\beta$ depending on the passive network. This method and notation will be familiar to those accustomed to servomechanisms and inverse feedback amplifiers, although so far as the authors are aware this method of filtering has not been described before. Terman[1] and others have described amplifiers whose gain versus frequency characteristics are controlled in a manner similar to that of Fig. 1. However, if such devices were to be used as filters, the whole of the power would have to pass through, and be delivered by, the amplifier.

In an arrangement such as in Fig. 1, it is easy to show that

$$V_o = V_i/(1 + G\beta). \tag{1}$$

By using a null network in the feedback path, $\beta$ can be made zero at the wanted frequencies, and we have

$$V_{ow} = V_{iw}. \tag{2}$$

The wanted frequencies are thus transmitted without attenuation. At the unwanted frequencies, however, $\beta$ is different from zero and we have

$$V_{ou} = V_{iu}/(1 + G\beta), \tag{3}$$

where the factor $1+G\beta$ can be made as large as stability considerations will allow. This aspect will be discussed later.

[1] E. E. Terman, R. R. Buss, W. R. Hewlett, and F. C. Cahill, "Some applications of negative feedback with particular reference to laboratory equipment," Proc. I.R.E., vol. 27, pp. 649–655; October, 1939.

An important matter is the power-handling capacitance required of the amplifier. The volt-amperes to be supplied by the amplifier at the unwanted frequencies are equal to

$$|V_{Hu}| \cdot |V_{ou}| / |Z_L|,$$

which, on substituting for $|V_{Hu}|$ and $|V_{ou}|$ and taking $|1+G\beta| \simeq |G\beta|$, reduce to

$$|V_{iu}|^2/|Z_L| \cdot |G\beta|.$$

The volt-amperes being supplied to the load at the wanted frequency are

$$|V_{iw}|^2/|Z_L|.$$

Thus the volt-amperes rating of the filter is

$$D_w \cdot |G\beta| /n^2. \tag{4}$$

Taking $|G\beta| = 50$ (a value typical of those we have achieved) and $n = 1/20$, e.g., 5 per cent unwanted voltages in the supply, we see that the amplifier is required to deliver only 1/20,000 of the volt-amperes supplied to the load. In practice the power-handling capacity of the amplifier at the unwanted frequencies is not a limiting factor on the power-handling capacity of the filter where the percentage of unwanted frequencies is not too large.

The load current $I_w$ flows through the output terminals of the amplifier and because of the impedance presented by these terminals, a voltage drop at the wanted frequencies occurs. Besides impairing the regulation of the supply, this voltage drop is impressed on the amplifier which must be capable of handling the requisite volt-amperes. The magnitude of the voltage drop is $|I_w| \cdot |Z_w|$, where $Z_w$ is the impedance looking into the amplifier terminals from the line side at the wanted frequency, and $|I_w|^2 \cdot |Z_w|$ volt-amperes are handled by the amplifier. If voltages at the wanted frequency are present or introduced further back in the amplifier, then $Z_w$ is not entirely a passive impedance and it can be controlled by controlling the magnitude and phase of these voltages. It has been found, for example, that by unbalancing the null network, the voltage drop at the wanted frequency can be reduced to zero. However, the amplifier is now supplying volt-amperes at the wanted frequency, and each case can only be examined in detail when its arrangement is completely known.

A typical arrangement is shown in Fig. 2. The final tube of the amplifier is shown there as a single-ended stage, whereas, in order to reduce the effect of the direct current through the transformer, push-pull arrangements are preferred in practice. However, the change in the analysis required is trivial, and Fig. 2 is discussed as having no irrelevant aspects which may tend to obscure the fundamental facts. In passing, it is important to note that any harmonics introduced by the amplifier or other components in the circuit are themselves divided by $|1+G\beta|$.

In order to select a tube which will be capable of filtering a given power and to fix its operating conditions at their optimum values, we require an analysis that will give the power-handling capacity of the filter in

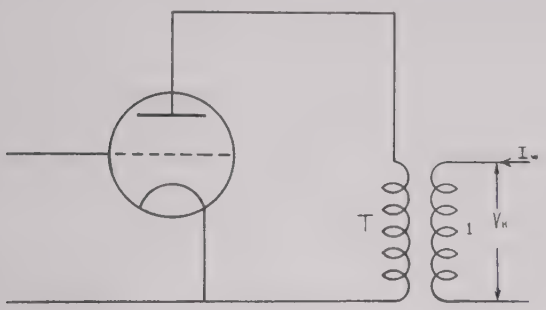


Fig. 2—Arrangement of power amplifier tube.

terms of the power-handling capacity of the tube. We will consider a tube restricted to operate class A on the linear portion of its characteristic and without voltages at the wanted frequencies applied to its grid. This last restriction can be removed, if desired, but as we have found that the voltage which can be applied to the grid is a limiting factor, it is not generally desirable to increase it by applying voltages at the wanted frequencies. There are four conditions to be fulfilled:

(i) The grid drive must be limited so that grid current does not flow during the positive half of the cycle, and plate current is not cut off during the negative half of the cycle. So far as the harmonics are concerned, the tube is working into a very large impedance, so that the load line is nearly horizontal and there is little possibility of driving the grid-to-plate current to cutoff. If $E_c$ is the grid bias voltage, the grid drive must not exceed $E_c/\sqrt{2}$, and, since the gain of the stage from tube grid to transformer secondary is $\mu/T$, we have

$$T \cdot |V_{iu}| \cdot /\mu \leqq E_c/\sqrt{2}$$

or

$$T \leqq \mu E_c/\sqrt{2} \cdot |V_{iu}|. \tag{5}$$

(ii) The plate voltage must not exceed the rated value on the positive half of the cycle or become negative on the negative half cycle. If the dc voltage $E_o$ is adjusted halfway between these limits, we have

$$|V_{iu}| \cdot T + r_a \cdot |I_w| /T \leqq E_o/\sqrt{2}. \tag{6}$$

(iii) Similar considerations as under (ii) above apply to the plate current $I_o$, and we have

$$|I_w| \cdot /T \leqq I_o \cdot /\sqrt{2}$$

or

$$|I_w| \leqq T \cdot I_0 \cdot /\sqrt{2}. \tag{7}$$

(iv) The dissipation in the tube at the wanted frequency must not be exceeded, and we have

$$|I_w|^2 \cdot r_a \leqq T^2(D - D_o). \tag{8}$$

With most tubes it is generally found that the restrictions due to (i) and (iii) are first reached and so the transformer ratio is chosen by making (5) an equation and limiting the load current in accordance with inequality (7). A check is then carried out to see that (6) and (8) are satisfied. In order to prevent distortion and to limit the dissipation it is necessary that these last inequalities are rather strongly fulfilled.

The following considerations show how to fix the operating conditions. Using (5) and (7) as equations, we obtain

$$\begin{aligned} |I_w| &= T \cdot I_o/\sqrt{2} \\ &= \mu E_c I_o/2 \cdot |V_{iu}|. \end{aligned}$$

Multiplying through by $|V_w|$ we have for the volt-amperes rating of the filter

$$|I_w| \cdot |V_w| = \mu E_c I_o/2n.$$

We therefore desire to maximize $\mu E_c I_o$. Assuming linear characteristics, we have

$$E_c = \frac{1}{\mu} \cdot (E_o - I_o r_a)$$

$$\therefore \quad |I_w| \cdot |V_w| = \frac{1}{2n} I_o(E_0 - I_o r_a)$$

$$= \frac{1}{2n}(D_o - I_o^2 r_a). \tag{9}$$

Thus the greatest power can be handled when $I_o$ is made as small as possible. In the limit, the volt-amperes that can be handled are given by

$$|I_w| \cdot |V_w| = D_o/2n. \tag{10}$$

A suitable design procedure is, then, as follows:

(i) Select a tube or decide on the number of tubes in parallel required, using (10). It has been our experience that a factor of safety of about 2 should be allowed at this stage.

(ii) Select $I_o$ as small as possible on the reasonably linear portion of the characteristics.

(iii) Work out $E_o$ from $E_o I_o = D_o$.

(iv) Find $E_c$ from $E_o$ and $I_o$.

(v) Find $T$ from equation (5).

(vi) Work out $I_w$ from equation (7).

(vii) Check inequality (6). If it does not hold it can generally be fulfilled by reducing $T$ and repeating (vi) and (vii).

It should be stressed that no great accuracy is claimed for the above analysis, but i does provide order of magnitude calculations useful for design purposes.

Investigations using the above methods show that in the receiving tube class the most suitable output tubes

are high-powered triodes such as the 2A3. The 807, as a triode with a small resistor in its screen to limit screen dissipation, has also proved very suitable. With two of these tubes in push-pull circuits, it is possible to filter about $\frac{1}{4}$ kw of alternating current containing 5 per cent harmonics, actual circuits and performances being given in section V. Greater power-handling capacity may be obtained by going to transmitting tubes or by using tubes in parallel; $m$ tubes in parallel increasing the capacity $m$ times. In the transmitting tube class it is found that two 833A's in push-pull would be able to filter a power of about $3\frac{1}{2}$ kw.

The alternating-current supply voltage at which filtering is carried out does not affect the power-handling capacitance of the filter, but as $|V_{iu}|$ increases with an increase of $|V_i|$, a smaller value of $T$ will be necessary (see (5)). Provided that the filter remains stable, the filtering action will be improved by the increase in gain brought about by the reduced value of $T$. If the value of $T$ found is such that it is not possible to obtain sufficient gain from a conventional voltage amplifier (because of the loss in the output tube), and as it is not desirable to increase the number of stages of voltage amplification for stability reasons (see section IV), a circuit of the type described by Jeffrey[2] can be employed. This circuit uses the high input resistance of the cathode follower as the load resistance of the voltage amplifier. A dc coupling is used between the output of the cathode follower and the grid of the power tubes, to avoid the introduction of further phase shifts.

## IV. Stability

In the theory given above there is no reason why $G$ should not be indefinitely increased, but in practice $G\beta$ is function of frequency and at some frequency the phase shift may be sufficient to cause the feedback to be positive. The requirements on $G\beta$ as a function of frequency for the system to be stable were discovered by Nyquist[3] and have been discussed in some detail by Bode.[4] In devices of this type it is not desirable to use conditionally stable arrangements, so the requirements reduce to ensuring that whenever the phase shifts become equal to odd multiples of $\pi$, $|G\beta| < 1$. We have confined ourselves to the cases in which phase shift is always less than $\pm\pi$ in the working range and arranged that the gain of the amplifier has dropped below the critical value before appreciable phase shift occurs. This limits us to the case of not more than two stages of resistance-coupled amplification, and, as discussed above, the last tube is essentially a power amplifier with no voltage gain: it often has a gain of about one-half. Under these conditions values of the order of 50 can easily be obtained. This means that unwanted voltages can be reduced in the ratio 1:50 (34 db) in a single stage.

Stability requirements also limit the types of passive network which can be inserted in the feedback path. Ladder type networks, because of their large phase shifts, are not suitable, in spite of their desirable attenuation characteristics. Parallel-$T$ null networks are very suitable as their phase shift does not exceed $\pm\pi/2$, and the greater part of it occurs within a relatively limited region near the null frequency. It is thus possible to design the amplifier to have relatively little phase shift where the parallel-$T$ has its greatest shift and vice versa, and so ensure that the phase shift of the network and amplifier do not greatly reinforce each other.

Bridged-$T$ networks are capable of greater selectivity than the parallel-$T$, and in applications where frequencies very close to the desired one are to be removed, their use is indicated. However, they were abandoned at 50~ because nonlinearity in the iron-cored inductances caused the balance point to vary with load.

## V. Some Experimental Results

Fig. 3 shows a circuit using 807 tubes which has been used for filtering a 250-volt, 50 ~ supply with 5 per cent harmonics.

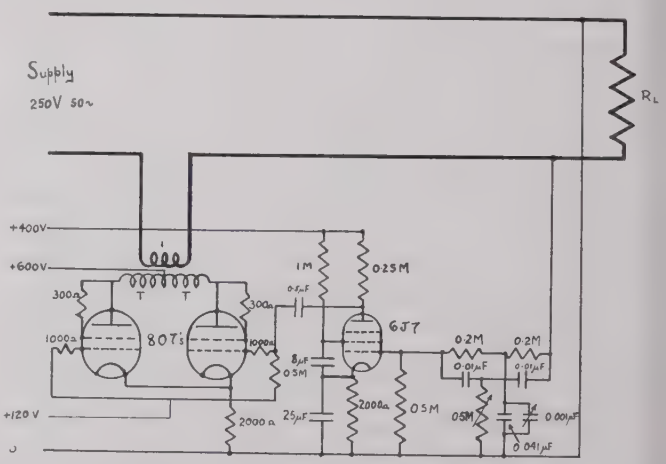


Fig. 3—Circuit of experimental filter.

The tube conditions are as follows:

| | |
|---|---|
| $\mu = 8$ | $r_a = 1600\ \Omega$ |
| $E_o = 450$ volts | $E_c = 40$ volts |
| $I_o = 40$ ma | $D_o = 18$ watts. |

Equations (5) and (7) give $T = 18$ and $I_w$ (for 2 tubes) as 1.02 amperes, and a check shows that inequality (6) is fulfilled.

The measured performance of this circuit with $T = 15$ is given in Table I (b). It will be seen that $I_w$ is 1.1 amperes so that the tubes must be operating with their anode current cut off over a small part of the cycle. This would explain the appearance of even harmonics in the output, but fortunately, as noted earlier, the harmonics produced by the device are also divided by the factor $1 + G\beta$.

[2] E. Jeffrey, "Push-pull phase-splitter," *Wireless World*, vol. LIII, p. 274; August, 1947.

[3] H. Nyquist, "Regeneration theory," *Bell Sys. Tech. Jour.*, vol. 11, pp. 126–148; January, 1932.

[4] H. W. Bode, "Network Analysis and Feedback Amplifier Design," 2nd Printing, D. Van Nostrand Company, Inc., New York, N. Y., 1946.

Table I (a) gives the measured performance with $T=8$, and as would be expected shows better filtering, since the gain of the amplifier is greater.

As the rated maximum dissipation of an 807 is 25 watts, equation (10) would lead us to expect a volt-ampere capacity for the filter of 500. The actual value achieved was 240. The discrepancy may be accounted for by 3 factors:

(1) The tubes were run at 18 watts dissipation.

(2) $I_o^2 r_a = 2.5$ and is not negligible.

(3) It was assumed that two tubes in push-pull would give twice the current-handling capacity, which is not true with the phase splitting device used.

If we take account of the first two factors, (9) gives us a theoretical volt-ampere capacity of 310, which is thus not greatly in excess of the achieved value.

The relative amounts of the individual harmonics can be adjusted by slightly unbalancing the parallel-$T$ network. We have found that the best procedure is to balance the parallel-$T$, as indicated by the vanishing of the fundamental frequency on an oscillograph connected across the grid of the 807, and then slightly unbalance it to increase the fundamental component or reduce any of the harmonics to a minimum. Failure of the filter shows itself in the presence of discontinuities of the wave form on the grid. The results given above represent the sort of typical compromise that can be obtained in practice.

TABLE I

(a)

$T=8$ $R_L=350\Omega$

| Frequency cps | Input | | Output | |
|---|---|---|---|---|
| | Volts | % Fundamental | Volts | % Fundamental |
| 50 | 250 | | 230 | |
| 100 | 0.18 | 0.07 | 0.08 | 0.03 |
| 150 | 1.85 | 0.74 | 0.15 | 0.07 |
| 200 | 0.11 | 0.04 | 0.02 | 0.01 |
| 250 | 7.65 | 3.06 | 0.20 | 0.09 |
| 300 | 0.40 | 0.16 | 0.04 | 0.02 |
| 350 | 1.48 | 0.59 | 0.08 | 0.03 |

(b)

$T=15$ $R_L=200\Omega$

| Frequency cps | Input | | Output | |
|---|---|---|---|---|
| | Volts | % Fundamental | Volts | % Fundamental |
| 50 | 250 | | 220 | |
| 100 | 0.12 | 0.05 | 0.08 | 0.04 |
| 150 | 2.15 | 0.86 | 0.14 | 0.06 |
| 200 | 0.08 | 0.03 | 0.16 | 0.07 |
| 250 | 8.20 | 3.28 | 0.42 | 0.19 |
| 300 | 0.07 | 0.03 | 0.16 | 0.07 |
| 350 | 1.70 | 0.68 | 0.06 | 0.03 |

## VI. Compensating Filters

It is possible to rearrange the circuit of Fig. 1 into the form of Fig. 4, where, with negative feedback connections, we have

$$V_o = V_i(1 - G\beta).$$

By making $\beta=0$ at the wanted frequencies we have

$$V_{ow} = V_{iw}$$

as before. If, at the unwanted frequencies, we make $G\beta=1$, we have

$$V_{ou} = 0.$$

It appears that this device would have advantages over the regulating type of filter previously described, and in special applications this might conceivably be so. However, in general, it is not possible to maintain the adjustment $G\beta=1$ over a frequency band or a period of time, and the regulating type of filter is to be preferred.

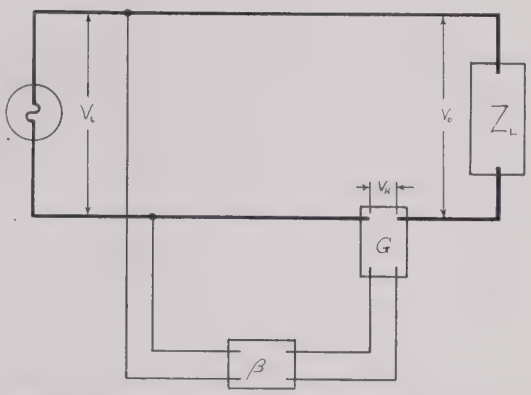


Fig. 4—General arrangement of compensating filter.

## VII. Conclusion

The method described above enables filters to be constructed which are capable of handling powers up to several kilowatts without requiring a large number of power-rated components. It appears that these devices are the most satisfactory means yet described for the production of a very pure wave form from an ac source and should have a number of applications, particularly in the field of electrical measurements. A further application that appears promising is the inclusion of a filter of this type between an ac voltage regulator that makes use of saturable reactors and a stabilized dc power supply. This should result in an improvement in the stability of the system, because if a filter is not used, changes in harmonic content, as the ac regulator operates, result in changes in average value of the ac voltage, even though its rms value remains constant. The over-all stability of the system, without the filter, is thus not as great as might be expected at first.

The actual filters described in this paper are of a rather specialized type, but it is felt that the principle of error-actuated filtering is capable of very wide extensions.

# Signal-to-Noise Ratios of Linear Detectors*

R. H. DeLANO†, ASSOCIATE, IRE

*Summary*—**A method is presented for obtaining the output signal and noise from a linear detector, including the output signal wave form and both the signal and the noise spectra. The method is applicable to any type of amplitude-modulated input signal at any signal-to-noise ratio, provided only that the bandwidth is small compared with the center-band frequency, and requires that certain steps be performed graphically rather than analytically. A comparison is made with square-law detection for a few useful cases. It is demonstrated that the linear detector gives a higher output signal-to-noise ratio than the square-law detector for some types of signal.**

## I. Introduction

THE METHOD presented here is a restatement and extension of principles discussed in the literature to the problem of the signal and noise output of a linear detector when the input signal is a general amplitude-modulated wave. As a rule, only amplitude-modulated waves, including any type of pulse-modulated signals, are detected by a single diode. The noise and signal output of a discriminator using linear detectors can also be derived by this same general method.

The general problem is to obtain the signal and noise spectrum of the output of a linear detector, given the input signal and the input noise power spectrum. From a mathematical standpoint this general problem is not solved until an analytic solution is obtained for the output signal and noise for any input signal (and noise) whatever. The method presented here is not such a solution. First of all, some graphical Fourier analyses have to be performed since the corresponding analytic expressions are much too cumbersome to handle. Secondly, the ratio of input bandwidth to the center frequency of the band is assumed to be small, and finally the input signal is subjected to more restrictive conditions than merely the one of having its components in the appropriate frequency band. If it is an amplitude-modulated wave, this fact is recognized, and use is made of the necessary relation between the phases of sidebands symmetrical around the carrier frequency. The type of input noise considered is normally distributed random noise. Several analytic solutions, both approximate and exact, have been given in the literature for certain less general problems connected with linear detection of signal and noise.[1–5]

The basic philosophy involved in the method is simple, and is commonly referred to as the adiabatic assumption. For the AM signal, for example, it is merely recognized that the signal may be factored into two parts, a slowly varying envelope and a carrier-frequency sine wave. The output signal for an unmodulated carrier is merely the dc output. Similarly, the output signal with modulation is this same dc, now varying slowly with time as a function of the amplitude of the input sine wave, and hence, of the envelope. Thus as a prerequisite, the solution for the dc output with noise and sine-wave signal input is required. Similarly, the output noise spectrum with AM signal can be modified from this simple case of a sine-wave signal at the input.

## II. The Output Signal with AM Signal Input

Consider first the dc output, which is the mean or average value of the output, when a sine-wave and noise are applied to the input of a nonlinear device. In general, this solution is given by

$$\bar{I} = F(V_s, \overline{V_n^2}) \tag{1}$$

where

$\bar{I}$ = mean or dc output current (output voltage for and envelope detector)

$V_s$ = peak amplitude of the input sine-wave (peak carrier amplitude)

$V_n(t)$ = input noise voltage

$\overline{V_n^2}$ = mean square input noise voltage.

For normally distributed random noise, whose probability distribution is not a function of its spectrum, it is easily demonstrated that the dc output is not a function of the spectral distribution of the input noise, but depends only on its mean square amplitude. Given the general detector characteristic

$$I = F_d(V_{\text{in}}) \tag{2}$$

$V_{in}$ = input voltage to the nonlinear device

$I$ = output current (or voltage) from the nonlinear device.

The probability density of the output, prior to filtering is

$$P_0(I)dI = P_i(V)dV \tag{3}$$

where

$P_0(I)$ = probability density of $I$, the output current,

$P_i(V)$ = probability density of the input voltage,

* Decimal classification: R362×R361.211. Original manuscript received by the Institute, November 22, 1948; revised manuscript received, March 21, 1949. Presented, 1948 West Coast Convention, Los Angeles, Calif., October 1, 1948.

† Hughes Aircraft Company, Culver City, Calif.

[1] W. R. Bennett, "Response of linear rectifier to signal and noise," *Bell Sys. Tech. Jour.*, vol. 23, pp. 97–113; January, 1944. See eq. (11).

[2] W. R. Bennett, "The biased ideal rectifier," *Bell Sys. Tech. Jour.*, vol. 26, pp. 139–169; January, 1947. See eqs. (1.23) and (1.24).

[3] S. O. Rice, "Mathematical analysis of random noise," *Bell Sys. Tech. Jour.*, vol. 23, pp. 282–332; July, 1944. Also, vol. 24, pp. 46–156; January, 1945.

[4] J. R. Ragazzini, "The effect of fluctuation voltages on the linear detector," Proc. I.R.E., vol. 30, pp. 277–288; June, 1942.

[5] D. Middleton, "Rectification of sinusoidally modulated carrier in noise," Proc. I.R.E., vol. 36, pp. 1467–1477; December, 1948.

and the mean value of the output is then

$$\bar{I} = \int_{-\infty}^{\infty} IP_0(I)dI = \int_{-\infty}^{\infty} P_i(V)F_d(V)dV. \qquad (4)$$

There is clearly no dependence on the input spectrum in this relation; in other words, the mean or dc output is a function only of the total input noise power. Furthermore, filtering of ac components of the output can have no effect on the dc value of the output, so this relation is always applicable.

For normally distributed random noise, the function $F(V_s, \overline{V_n^2})$ is uniquely determined by the detector characteristic $F_d(V)$. For the ideal linear detector whose transfer characteristic is

$$F_d(V) = \alpha V \quad \text{for} \quad V > 0$$
$$= 0 \quad \text{for} \quad V < 0.$$

The corresponding dc output has already been derived by Bennett[1]

$$\bar{I} = \alpha\sqrt{\frac{\overline{W_n}}{2\pi}}\,{}_1F_1\left(-\tfrac{1}{2};\,1;\,-\frac{W_s}{W_n}\right), \qquad (5)$$

Where

$W_n \equiv \overline{V_n^2}$

$W_s = \frac{1}{2}V_s^2$ = input power envelope

${}_1F_1(a;\,c;\,z)$ = confluent hypergeometric function[6]

$$= 1 + \frac{a}{c}\,\frac{z}{1!} + \frac{a(a+1)}{c(c+1)}\,\frac{z^2}{2!} + \cdots .$$

Furthermore, Bennett has shown that the output of an ideal envelope detector differs only by the constant factor $\pi$ from the low-frequency output of an ideal linear detector.[2] Since constant factors do not affect signal-to-noise ratios, this solution for the ideal linear detector is applicable to either case.

Since the frequency components of the envelope differ by at least one order of magnitude from the carrier frequency, the time variation of the actual envelope $V_s(t)$ may be introduced into this expression. The result is the output signal as a function of time, although, to be more exact, the contribution to the output due to noise must first be subtracted out, giving

$$I_s(t) = \alpha\sqrt{\frac{\overline{W_n}}{2\pi}}\left[{}_1F_1\left(-\tfrac{1}{2};\,1;\,-\frac{\frac{1}{2}V_s^2(t)}{W_n}\right) - {}_1F_1\left(-\tfrac{1}{2};\,1;\,0\right)\right]$$
$$= \alpha\sqrt{\frac{\overline{W_n}}{2\pi}}\left[{}_1F_1\left(-\tfrac{1}{2};\,1;\,\frac{-\frac{1}{2}V_s^2(t)}{W_n}\right) - 1\right]$$
$$= \alpha\sqrt{\frac{\overline{W_n}}{2\pi}}\left[{}_1F_1\left(-\tfrac{1}{2};\,1;\,-\tfrac{1}{2}y^2\right) - 1\right] \qquad (6)$$

where

$I_s(t)$ = output signal as a function of time

$$y \equiv \frac{V_s}{W_n^{1/2}} = \frac{\text{signal voltage envelope (peak)}}{\text{rms input noise voltage}}.$$

The frequency components of the signal must be obtained by a graphical Fourier analysis of $I_s(t)$. From a practical standpoint, such a procedure is much more effective than attempting to derive analytic expressions for the Fourier components of $I_s$ for any arbitrary $V_s(t)$. This process may be carried out with the help of Fig. 1 where $I_s$ is given as a function of $y$. To use a

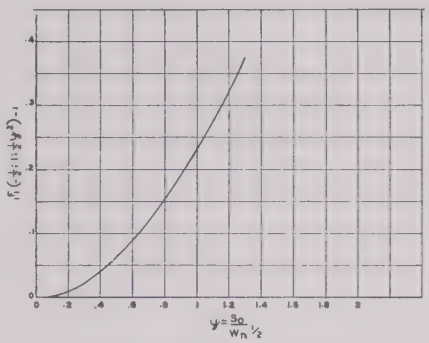

Fig. 1—Hypergeometric function used to obtain $I_s$.

simile, the signal output of an ideal linear detector with noise present is the same as the signal output of a hypergeometric function detector with no noise. Note that the output signal is not always proportional to the input envelope; therefore, the output signal contains distortion. This distortion is a function of three factors; (a) the average signal-noise ratio, (b) the per cent modulation, and (c) the relative phase of the modulation sidebands, in other words, the exact wave form of the envelope. Under these circumstances, a graphical approach is clearly the most practical one.

## III. Output Noise Spectra with AM Signal Intput

The modification of the output noise spectrum from the solution when the input is an unmodulated sinewave is entirely analogous, but a little more complicated. The mechanism whereby the output noise spectrum is obtained must first be reviewed to some extent. First, the normally distributed random noise input may be represented in the form of a Fourier series

$$V_n(t) = \sum_{n=1}^{\infty} C_n \cos\left(\omega_n t + \phi_n\right) \qquad (7)$$

$\omega_n = 2\pi(n/T) = 2\pi f_n$

$T$ = the time over which the expansion holds (since noise is not periodic, we allow $T$ to approach infinity)

$\phi_n$ = random phase angle (uniform probability density from 0 to $2\pi$).

The amplitude of the noise components $C_n$ is related to the noise power spectrum by the relation

[6] E. T. Whittaker and G. N. Watson, "Modern Analysis," Cambridge University Press, 1940; Chap. XVI.

$$\tfrac{1}{2}C_n^2 = w(f_n)\Delta f = w(f_n)\frac{1}{T}$$

$w(f)$ = noise power spectrum-mean square volts per cycle.

The input noise spectrum is determined by the band-pass characteristics of the narrow-band elements of the input circuits, since prior to narrow banding, the spectrum is uniform over all frequencies.

For a general nonlinear device, it has been demonstrated that the output noise can be represented as the sum of intermodulation products of all orders.[1] Since only the spectrum and statistical properties of the input noise are known, a direct Fourier integral of the output cannot be formulated, and this representation is the most convenient one. For a square-law detector the only nonzero intermodulation products are the second-order ones, signal-noise and noise-noise intermodulation. These products give difference frequency beats in the audio or video region. Since the phases of these difference frequency beats are also random for the case of noise, the mean square amplitudes or the "power" spectra of the two kinds of intermodulation add linearly in the output. It turns out conveniently that these second-order intermodulation products are the only significant contributors to the output of an ideal linear detector also.

For a sine-wave signal and noise, the difference frequency beat between signal and noise gives an output component whose amplitude is proportional to the product of the sine-wave amplitude and the noise-component amplitude. The proportionality constant is a function of the input signal-to-noise ratio (a constant for constant $W_s$). Thus, the shape of the signal-to-noise output spectrum is the same as that of the input noise, only shifted towards dc by the carrier or signal frequency. Of course, this shift leaves the lower half of the spectrum at negative frequencies. In the actual output it is necessary to reflect these portions back onto positive frequencies, and add the power spectra. Suppose, for the moment, that the spectrum is left as it is, with both positive and negative frequency components, and modified to take into account variations in signal amplitude with time.

As the input signal envelope varies, the amplitude of each of the beat-frequency output components varies in a related manner determined by the functional dependence of the proportionality constant on instantaneous signal-to-noise ratio. If the amplitude of a sine-wave, whatever its frequency or phase, varies periodically, the wave itself may be expanded into a carrier at the sine-wave frequency plus symmetrical modulation sidebands, even if some of the sidebands fall at negative frequencies and later have to be reflected back onto the positive half of the scale. Thus, the above spectrum becomes a function of time and the actual steady-state frequency spectrum is obtained by summing a series of power spectra corresponding to the carrier and sideband amplitudes in the above Fourier analysis of a single component. Mathematically this procedure is developed as follows:

The amplitude of the signal-to-noise beat at the difference frequency $f_n - f_s$ is given by Bennett[1]

$$A_{sn} = \frac{\alpha C_n}{2}\sqrt{\frac{\overline{W_s}}{\pi W_n}}\,{}_1F_1\left(\tfrac{1}{2};\,2;\,-\frac{W_s}{W_n}\right)$$

$$= \frac{\alpha C_n y}{\sqrt{8\pi}}\,{}_1F_1(\tfrac{1}{2};\,2;\,-\tfrac{1}{2}y^2). \qquad (8)$$

Plotting $A_{sn}$ over a cycle of the input modulation and performing a graphical Fourier analysis gives the expansion

$$A_{sn}(t) = \frac{\alpha C_n}{\sqrt{8\pi}}\left[a_0 + \sum_{n=1}^{\infty} a_n \cos\,(n\omega_m t + \theta_n)\right] \qquad (9)$$

$2\pi f_m = \omega_m = 2\pi$ times the fundamental envelope modulation frequency.

$A_{sn}$ is plotted versus $y$ in Fig. 2.

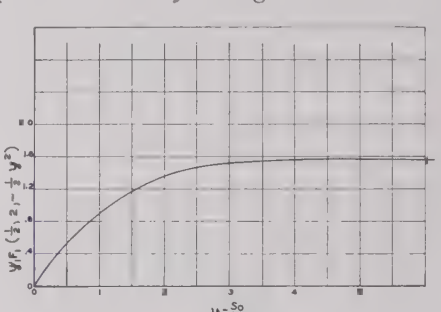


Fig. 2—Hypergeometric function used to obtain $A_{sn}$.

The $a_0$ coefficient gives the carrier amplitude of each beat component and the modulation sidebands are of amplitude $a_n/2$. The $a_0$ term gives an output spectrum equal to $\alpha^2 a_0^2/8\pi$ times the shifted input spectrum and the $a_n$ terms give similar spectra shifted in frequency by $nf_m$ relative to the $a_0$ spectrum. Thus, the output noise power spectrum due to signal-to-noise intermodulation is

$$w_{sn}(f) = \frac{\alpha^2}{8\pi}\left[a_0^2 w_s(f) + \sum_{n=1}^{\infty}\frac{a_n^2}{4}\left(w_s(f - nf_m) + w_s(f + nf_m)\right)\right] \qquad (10)$$

where

$w_s(f) = w(f_s + f)$ with $f$ both positive and negative

$f_s$ = input carrier frequency.

If the input noise power spectrum $w(f)$ is symmetrical around the signal carrier frequency, this expression simplifies to

$$w_{sn}(f) = \frac{\alpha^2}{8\pi}\left[a_0^2 w_s(f) + \sum_{n=1}^{\infty}\frac{a_n^2}{2} w_s(f - nf_m)\right]. \qquad (11)$$

At the conclusion of this summation process, all portions of the noise power spectrum at negative frequen-

cies may be reflected onto the positive side, and added to any portions already there.

The procedure for noise-to-noise intermodulation is identical, except that the output spectrum for an unvarying sine-wave signal is different. This spectrum is proportional to[1]

$$w_i(f) \equiv \frac{1}{W_n}\int_0^\infty w(\lambda)w(\lambda+f)d\lambda \tag{12}$$

with $f$ both positive and negative, and it is always symmetrical around zero frequency or dc. The expression for the amplitude of a single beat frequency component at the frequency $f_r - f_e$ is

$$A_{nn} = \frac{\alpha C_r C_e}{\sqrt{8\pi W_n}}\,{}_1F_1\left(\tfrac{1}{2};\,1;\,-\frac{W_s}{W_n}\right)$$
$$= \frac{\alpha C_r C_e}{\sqrt{8\pi W_n}}\,{}_1F_1(\tfrac{1}{2};\,1;\,-\tfrac{1}{2}y^2). \tag{13}$$

$A_{nn}$ is plotted versus $y$ in Fig. 3.

A graphical Fourier analysis of $A_{nn}$ plotted versus time over a period of the input modulation gives the expansion

$$A_{nn} = \frac{\alpha C_r C_e}{\sqrt{8\pi W_n}}\left[b_0 + \sum_{n=1}^{\infty} b_n \cos\,(n\omega_n t + \theta_n)\right]. \tag{14}$$

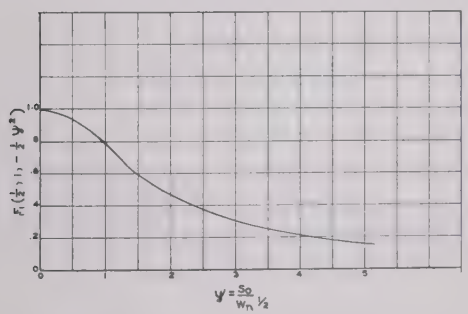


Fig. 3—Hypergeometric function used to obtain $A_{nn}$.

The corresponding noise spectrum, allowing both positive and negative frequencies, is[7]

$$w_{nn}(f) = \frac{\alpha^2}{8\pi}\left[b_0{}^2 w_i(f) + \sum_{n=1}^{\infty}\frac{b_n{}^2}{2}\,w_i(f+nf_m)\right]. \tag{15}$$

After summation, any portions of this spectrum at negative frequencies may be reflected onto the positive scale and added to any already at positive frequencies. Similarly, the total output noise spectrum is the sum of the spectra due to noise-to-noise and signal-to-noise intermodulation.

$$w_n(f) = w_{sn}(f) + w_{nn}(f). \tag{16}$$

## IV. The Total Output Signal and Noise

The preceding calculations, including the graphical Fourier analyses, are only necessary if the spectral distribution of the signal and noise in the output is desired. The total output signal and noise power for a sine-wave signal input are functions of the ratio of total input signal power to total input noise power only, provided none of the output components are removed by filtering. The total mean signal and noise power may be obtained by taking the average of these expressions over a period of the modulation for AM signal inputs. For signal, this mean power output is

$$\overline{I_s{}^2} = \frac{\alpha^2 W_n}{2\pi}\,\overline{\left[{}_1F_1(-\tfrac{1}{2};\,1;\,-\tfrac{1}{2}y^2) - 1\right]^2}. \tag{17}$$

The total output noise power due to signal-to-noise intermodulation is

$$W_{sn} = \frac{\alpha^2 W_n}{8\pi}\,\overline{y^2\,{}_1F_1{}^2(\tfrac{1}{2};\,1;\,-\tfrac{1}{2}y^2)}, \tag{18}$$

and due to noise-to-noise intermodulation is

$$W_{nn} = \frac{\alpha^2 W_n}{8\pi}\,\overline{{}_1F_1{}^2(\tfrac{1}{2};\,1;\,-\tfrac{1}{2}y^2)}$$
$$= \frac{\alpha^2 W_n}{8\pi}\,\overline{e^{-W_s/W_n}I_0{}^2\left(\frac{W_s}{2W_n}\right)}. \tag{19}$$

In general, the mean power for the signal is not too meaningful, since information is derived from the ac components of the signal. For the noise, however, the shape of the spectrum can be roughly estimated, and the total noise power is a useful quantity.

## V. Square-Law Detection

The same techniques are, of course, applicable to square-law detection except that the analytic solution is already known.[8] Given the square-law characteristic,

$$I = \alpha_d V_{\text{in}}{}^2 \tag{20}$$

$\alpha_d$ = detector coefficient.

The output signal and noise can be expressed directly in terms of the input signal and noise. Suppose the input signal is given by

$$E_i = V_c\left[c_0 + \sum_{n=1}^{\infty} c_n \cos\,(n\omega_m t + \theta_n)\right]\cos\,\omega_s t, \tag{21}$$

[7] In evaluating

$$w_i(f) = \frac{1}{W_n}\int_0^\infty w(\lambda)w(\lambda+f)df$$

it must be noted that this expression gives only the low-frequency output components. In treating square-law detection where double frequency output terms occur, S. O. Rice has used the convention $w(-f)=w(f)$ and evaluated the noise-to-noise output spectrum as

$$\alpha^2\int_{-\infty}^{\infty} w(x)w(f-x)dx.$$

This convention is not used here.

[8] See Section 4.5 of footnote reference 3.

and the input noise power spectrum by $w(f)$ again, then the low-frequency output signal is simply,

$$V_0(t) = \alpha V_c^2\left[c_0 + \sum_{n=1}^{\infty} c_n \cos(n\omega_m t + \theta_n)\right]^2 \overline{\cos^2 \omega_s t}$$

$$= \tfrac{1}{2}\alpha V_c^2\left[c_0 + \sum_{n=1}^{\infty} c_n \cos(n\omega_m t + \theta_n)\right]^2. \quad (22)$$

The signal-to-noise intermodulation output spectrum is

$$w_{sn}(f) = \alpha^2 V_c^2\left[c_0^2 w(f_s + f) + \sum_{n=1}^{\infty} \frac{c_n^2}{4}(w(f_s + f + nf_m) + w(f_s + f - nf_m))\right]$$

$$= \alpha^2 V_c^2\left[c_0^2 w_s(f) + \sum_{n=1}^{\infty} \frac{c_n^2}{4}(w_s(f + nf_m) + w_s(f - nf_m))\right] \quad (23)$$

where $f$ is both positive and negative.

If $w(f)$ is symmetrical around the signal carrier frequency, this expression is simply

$$w_{sn}(f) = \alpha^2 V_c^2\left[c_0^2 w_s(f) + \sum_{n=1}^{\infty} \frac{c_n^2}{2} w_s(f + nf_m)\right]. \quad (24)$$

Reflection onto the positive frequency scale is again applicable after this summation. The noise-to-noise power spectrum is also

$$w_{nn}(f) = \alpha^2 \int_{-\infty}^{\infty} w(\lambda) w(\lambda + f) d\lambda, \quad (25)$$

where $f$ is both positive and negative, or $w_{nn}(f)$ is twice as big as the above if $f$ is positive only. The total output noise power of both kinds is clearly

$$W_{sn} = \int_{-\infty}^{\infty} w_{sn}(f) df = 2\alpha^2 \overline{W}_s W_n \quad (26)$$

$$W_{nn} = \int_{-\infty}^{\infty} w_{nn}(f) df = \alpha^2 \int_{-\infty}^{\infty}\int_{0}^{\infty} w(\lambda) w(\lambda + f) d\lambda df$$

$$= \alpha^2\left[\int_0^{\infty} w(\lambda) d\lambda\right]^2 = \alpha^2 W_n^2 \quad (27)$$

where $\overline{W}_s$ = average input signal power.

These expressions will be used to obtain a simplified comparison of signal-to-noise ratios of gated, pulse-modulated signals for square-law and linear detectors in the next section. Let us, however, state the basic conclusions of the preceding theoretical development at this point.

Conclusions:

1. A general method has been presented for determining the output signal and noise of any nonlinear device, and in particular of an ideal linear detector, given the solution when the input signal is a constant sine wave.

2. Either the output spectra or the total output noise power, or both, may be derived.

3. The restrictions on the input signal and noise are as follows:

(a) The signal is an AM wave.

(b) The ratio of input bandwidth to center frequency is small.

(c) The noise is random.

## VI. A Simplied Comparison of Square-Law and Linear Detectors for Signal-to-Noise Ratio

The preceding method for obtaining the total output noise power for a linear or envelope detector and for a square-law detector offers a simple basis for comparison of these two types of detectors. The shape of the output noise spectra for the two cases is different, but usually not sufficiently different to produce any very large error if the shapes are assumed to be the same. In this case the total noise power output is the only possible variable. For small amounts of sinusoidal modulation either of a continuous carrier or of rectangular pulse signals, the ratio of total signal power to total noise power in the output for linear and square-law detectors can be calculated. The ratio of the output signal-to-noise ratios so obtained is a good basis for comparing the relative merits of the two detectors for a variety of applications. This calculation is made as follows:

### *A. Square-Law Detector*

Let us consider either an uninterrupted carrier or rectangular pulses of the carrier frequency. The input signal is then

$$E_i = V_s \sin \omega_s t \text{ during the pulses}$$

$$= 0 \text{ otherwise.} \quad (28)$$

Let the pulses have a duty cycle $k = f_r T$ where

$f_r$ = pulse repetition frequency

$T$ = pulselength

$k = 1$ for the uninterrupted carrier,

and the pulses be surrounded by a gate $t_g$ in length

$k_g = f_r t_g \geqq k$

$k_g = 1$ for the uninterrupted carrier.

The output signal is given by

$$V_0 = \alpha \overline{E_i^2} = \tfrac{1}{2}\alpha V_s^2 \text{ during the pulses}$$

$$= 0 \text{ otherwise.} \quad (29)$$

Referring to (26) and (27), the total output noise power is seen to be the sum of the following two quantities

$$W_{sn} = \alpha^2 V_s^2 W_n k \tag{30}$$

$$W_{nn} = \alpha^2 W_n^2 k_g. \tag{31}$$

The ratio of total output signal-to-noise power may be defined as

$$\lambda_s = \frac{(\frac{1}{2}\alpha V_s^2)^2 k}{\alpha^2[W_n^2 k_g + W_n V_s^2 k]} = \frac{\lambda_0^2}{\frac{k_g}{k} + 2\lambda_0} \tag{32}$$

where $\lambda_0$ is defined as $\lambda_0 = \frac{1}{2} V_s^2 / W_n$

$$= \frac{\text{peak input signal power}}{\text{average input noise power before gating}}.$$

If the pulses or the carrier is modulated sinusoidally at a small percentage modulation the output signal is

$$V_0 = \tfrac{1}{2}\alpha V_s^2(1 + a\cos\omega_m t)^2 \simeq \tfrac{1}{2}\alpha V_s^2(1 + 2a\cos\omega_s t); \tag{33}$$

the modulation frequency component of which is

$$V_{0m} = \alpha V_s^2 a \cos\omega_s t \tag{34}$$

$$\overline{V_{0m}^2} = \tfrac{1}{2}\alpha^2 V_s^4 a^2. \tag{35}$$

Hence, as far as the modulation frequency output is concerned, the output signal-to-noise ratio (in power) is

$$2\lambda_s a^2 = \frac{2\lambda_0^2 a^2}{\frac{k_g}{k} + 2\lambda_0}. \tag{36}$$

No attempt is made here to evaluate the psychological phases of such problems as visual detection of pulsed signals in the presence of noise. Signal-to-noise intermodulation is lumped in as noise, which it most assuredly is if any narrow-band filtering is used on the output signal and noise.

*B. Linear or Envelope Detector*

The analogous expressions for the linear detector are simply

$$V_0 = \alpha\sqrt{\frac{\overline{W_n}}{2\pi}}\left[{}_1F_1\left(-\tfrac{1}{2}; 1; -\frac{V_s^2}{2W_n}\right) - 1\right] \text{ during the pulses}$$

$$= 0 \text{ otherwise.} \tag{37}$$

$$W_{sn} = \frac{\alpha^2}{8\pi} k V_s^2 \, {}_1F_1\left(\tfrac{1}{2}; 2; -\frac{V_s^2}{2W_n}\right) \tag{38}$$

$$W_{nn} = \frac{\alpha^2}{8\pi}\left[k W_n \, {}_1F_1^2\left(\tfrac{1}{2}; 1; -\frac{V_s^2}{2W_n}\right) + (k_g - k) W_n\right] \tag{39}$$

$$\lambda_L = \frac{4[{}_1F_1(-\frac{1}{2}; 1; -\lambda_0) - 1]^2}{\left(\frac{k_g}{k} - 1\right) + {}_1F_1^2(\frac{1}{2}; 1; -\lambda_0) + 2\lambda_0 \, {}_1F_1^2(\frac{1}{2}; 2; -\lambda_0)}. \tag{40}$$

However, when a small sinusoidal modulation is applied, the signal-to-noise ratio for the output modulation component is not $2\lambda_L a^2$. In general, the output signal is

$$ay\left(\frac{dI_s}{dy}\right)\cos\omega_s t,$$

and the appropriate factor by which to multiply the ratio $\lambda_L/\lambda_s$ is

$$\tfrac{1}{2}a^2\left[y\frac{dI_s}{dy}\right]^2 \frac{1}{V_0^2}$$

$$= \tfrac{1}{2}a^2\left[\frac{y}{{}_1F_1(-\frac{1}{2}; 1; -\frac{1}{2}y^2) - 1}\frac{d}{dy}\left[{}_1F_1(-\tfrac{1}{2}; 1; -\tfrac{1}{2}y^2)\right]\right]^2$$

$$= \tfrac{1}{2}a^2\left(y\frac{d}{dy}\log\left[{}_1F_1(-\tfrac{1}{2}; 1; -\tfrac{1}{2}y^2) - 1\right]\right)^2$$

$$= a^2 2\lambda_0^2\left[\frac{d}{d\lambda_0}\log\left[{}_1F_1(-\tfrac{1}{2}; 1; -\lambda_0) - 1\right]\right]^2$$

$$\equiv 2a^2 P^2. \tag{41}$$

By definition

$$P^2 = \lambda_0^2\left[\frac{d}{d\lambda_0}\log_e\left({}_1F_1(-\tfrac{1}{2}; 1; -\lambda_0) - 1\right)\right]^2. \tag{42}$$

For some applications where the total energy in the pulse is of most importance, the ratio $\lambda_L/\lambda_s$ itself is the most accurate basis of comparison for the two detectors. However, when the modulation frequency component is the desired or useful output, the ratio $\lambda_L/\lambda_s P^2$ gives a better measure of the relative merits of square-law and linear detection. In Fig. 4 $\lambda_L/\lambda_s$ is plotted versus $\lambda_0$, and in

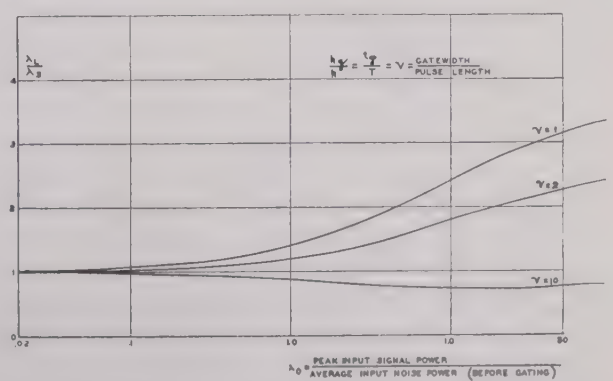


Fig. 4—Ratio of $S/N$ ratio obtained from a linear and from a square-law detector with ideal rectangular pulses at the input versus input $S/N$ ratio.

Fig. 5 the ratio $\lambda_L/\lambda_s P^2$ is plotted versus $\lambda_0$. In both cases $\nu = 1$ corresponds to the uninterrupted but modulated carrier. Several somewhat startling and very important conclusions are to be derived from these results. Note that in both cases the linear detector always gives

a higher output signal-to-noise ratio than the square-law detector for equal pulse and gate widths, or for the uninterrupted carrier. This result is in direct contrast to many well-known proofs that the square-law detector is optimum, regarding signal-to-noise ratio. The reason for this discrepancy is easily explained, however. First of all the series expansions for the hypergeometric functions show clearly that at very low signal-to-noise ratios

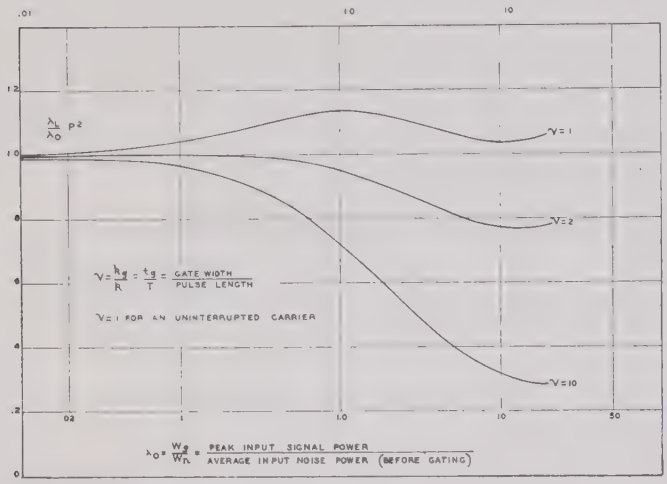


Fig. 5—Ratio of output $S/N$ ratios from a linear and from a square-law detector for modulated pulses or carrier when the useful signal is the output at the modulation frequency only.

the output of the linear detector is the same as the output of a square-law detector in signal-to-noise ratio, for at very low signal-to-noise ratios

$$I_s \to \alpha \sqrt{\frac{\overline{W_n}}{2\pi}} \left[ 1 + \frac{1}{2} \frac{W_s}{W_n} + \cdots - 1 \right]$$

$$= \alpha \frac{W_s}{\sqrt{8\pi W_n}} \tag{43}$$

$$W_{nn} \to \frac{\alpha^2 W_n}{8\pi} \tag{44}$$

$$\frac{I_s}{W_{nn}^{1/2}} \to \frac{W_s}{W_n}. \tag{45}$$

This result is identical to that obtained for a square-law detector. Naturally, signal-to-noise intermodulation is ignored at very low signal-to-noise ratios since noise-to-noise intermodulation is much larger. It is precisely because signal-to-noise intermodulation is ignored in these general proofs alluded to above that the results shown here are in contrast to them.

The reason for better signal-to-noise ratios from the linear detector is that the signal-to-noise intermodulation is of greater magnitude in the square-law detector than in the linear detector near unity signal-to-noise ratio, where it is beginning to be of importance. At very high signal-to-noise ratios also the two detectors give the same output modulation frequency signal-to-noise ratio, for at very high signal-to-noise ratios the linear detector gives,

$$I_s \to \frac{\alpha\sqrt{2W_s}}{\pi} = \frac{\alpha V_s}{\pi} \tag{46}$$

$$W_{sn} \to \frac{\alpha^2 W_n}{\pi^2} \tag{47}$$

$$\frac{I_s}{W_{sn}^{1/2}} \to \sqrt{\frac{W_s}{2W_n}} \tag{48}$$

whereas the square-law detector gives $\sqrt{W_s/2W_n}$ as (22) and (26) show. However, when small percentage modulations about the mean value of input are considered, the square-law detector doubles the percentage modulation in the output, whereas the linear detector is linear at high signal-to-noise ratios in this respect. Thus, the factor of two above is cancelled out, and the two detectors give identical output signal-to-noise ratios for the output modulation.

Finally, let us note the serious decrease in performance of the linear detector in the case of modulated pulses with very large gates regarding the output modulation frequency signal-to-noise ratio. The explanation of this result is likewise simple. As Fig. 3 shows, the signal suppresses the noise when it is large relative to the noise in the linear detector. During a wide gate, the signal is on only a small fraction of the time and most of the noise is not suppressed—the noise-to-noise intermodulation noise, that is. For these cases the linear detector is definitely inferior to the square-law detector. Experimental work in the Electronics Department of the Hughes Aircraft Company has shown excellent agreement with the theory presented here, and has clearly demonstrated the inaccuracies resulting from applying square-law theory to many calculations on circuits using linear detectors.

## APPENDIX I

### Relations between the Confluent Hypergeometric Functions and Bessel Functions

The expansions of the three confluent hypergeometric functions used in this paper in terms of imaginary Bessel functions are given below:

$${}_1F_1(-\tfrac{1}{2}; 1; -x)$$

$$= e^{-x/2}\left[ I_0\left(\frac{x}{2}\right) + xI_0\left(\frac{x}{2}\right) + xI_1\left(\frac{x}{2}\right)\right] \tag{49}$$

$${}_1F_1(\tfrac{1}{2}; 2; -x) = e^{-x/2}\left[ I_0\left(\frac{x}{2}\right) + I_1\left(\frac{x}{2}\right)\right] \tag{50}$$

$${}_1F_1(\tfrac{1}{2}; 1; -x) = e^{-x/2} I_0\left(\frac{x}{2}\right). \tag{51}$$

# A Video-Frequency Noise-Spectrum Analyzer*

PHILIP S. JASTRAM†, MEMBER, IRE, AND GORDON P. McCOUCH‡, ASSOCIATE, IRE

*Summary*—**A wave analyzer capable of measuring noise spectra n the video-frequency range is described. Part I of the paper dis-usses requirements in noise-analyzer design. Part II is a de-ailed description of a practical instrument.**

**A frequency range of 50 kc to 10 Mc is covered, without band-witching, at virtually constant sensitivity. The width of the ana-yzing pass band, 33 kc, remains constant over the measuring range. The lowest spectral level that can be measured is 7 microvolts per oot kilocycle.**

## Introduction

CERTAIN PROPERTIES of noise which have a direct bearing on the design of a noise-spectrum analyzer are found to differ considerably from hose of periodic signals.[1–7] The first section of the resent paper is devoted to a discussion of some of hese properties and the requirements which the nalyzer must fulfill. The relative advantages, in noise pplications, of the tuned-circuit and the heterodyne ıethods of frequency analysis are compared; the eterodyne proves to be preferable. In Part II, a prac-ical instrument is described.

## PART I

## Measurement of Noise Spectra

### . *Basic Considerations*

A wave analyzer should meet the following general onditions:

1. Adequate frequency coverage with maximum implicity of tuning and stability.
2. Adequate sensitivity, approximately the same at ll frequencies to be measured, with good gain stability.
3. Definition and identification of the measured fre-uency band.
4. Wide dynamic operating range.
5. Suppression, or at least accurate evaluation, of errors.

The frequency distribution of a given signal is experimentally determined by passing the signal through a circuit whose response is confined to a narrow band of frequencies, and then examining the result. The band must be movable over the frequency range to be measured. A periodic signal yields a set of sinusoidal components, harmonically related in frequency, each having definite amplitude and phase.

For a nonperiodic function, such as random noise, no single sinusoidal component can be isolated. The output of the filter retains the erratic behavior of noise, no matter how narrow the pass band is made. While, for the periodic case, the mean-square amplitude of an isolated component is independent of the bandwidth of the filter, for noise the mean-square value of the filter output approaches, as the bandwidth is decreased, direct proportionality to the bandwidth.

### II. *Analytical Representation of Noise Spectra*

These experimental facts imply that it is possible to express the time-average frequency distribution of a noise signal by a continuous function $y(f)$, which can be so chosen that the mean-square value associated with that part of the spectrum lying between any two frequencies $a$ and $b$ is given by

$$[E^2(a, b)]_{av} = \int_a^b y^2(f)df. \tag{1}$$

The time over which the average is taken is required to be large compared to $a^{-1}$ and $(b-a)^{-1}$. The definition of $y^2(f)$ is

$$y^2(f) = \lim_{\Delta f \to 0} \frac{[E^2(f, \Delta f)]_{av}}{\Delta f} \tag{2}$$

where $[E^2(f, \Delta f)]_{av}$ is the mean-square value of those components lying in a band of width $\Delta f$ and of center frequency $f$. Again the time over which the average is taken must be large compared with $f^{-1}$ and $(\Delta f)^{-1}$. The function $y^2(f)$ is the mean-square spectrum (or power spectrum) of the noise signal $e$; it is a continuous function of frequency. If the noise signal consists of a voltage-time function, then $y^2(f)$ has the units volts-squared-per-unit-frequency. In studying the frequency distribution of various noise sources, the rms spectrum $y(f)$ (referred to as the spectral level at frequency $f$) is of interest. Its measurement at a single, sharply defined frequency is an unattainable idealization, since the measuring bandwidth is necessarily finite.

The spectrum defined contains no quantity comparable to phase in the periodic case; our representation

* Decimal classification: R273.1. Original manuscript received by he Institute October 5, 1948; revised manuscript received, March 15, 949. This paper is based on work done for the Office of Scientific esearch and Development under Contract OEMsr-411 with the resident and Fellows of Harvard College.

† Formerly, Radio Research Laboratory, Harvard University, ambridge, Mass.; now, Washington University, St. Louis, Mo.

‡ Formerly, Radio Research Laboratory, Harvard University, ambridge, Mass.; now, Aircraft Radio Corp., Boonton, N. J.

[1] J. B. Johnson, "The Schottky effect in low-frequency circuits," *hys. Rev.*, vol. 26, July, 1925.

[2] J. B. Johnson, "Thermal agitation of electricity in conductors," *hys. Rev.*, vol. 32, pp. 97–109; July, 1928.

[3] F. B. Llewellyn, "A study of noise in vacuum tubes and at-ched circuits," PROC. I.R.E., vol. 18, pp. 243–265; February, 930.

[4] G. L. Pearson, "Fluctuation noise in vacuum tubes," *Bell Sys. ech. Jour.*, vol. 13, pp. 634–653; October, 1934.

[5] V. D. Landon, "A study of the characteristics of noise," PROC. R.E., vol. 24, pp. 1514–1521; November, 1936.

[6] C. J. Jansky, "An experimental investigation of the characteris-cs of certain types of noise," PROC. I.R.E., vol. 27, pp. 763–768; ecember, 1939.

[7] V. D. Landon, "Distribution of amplitude with time in fluctua-on noise," PROC. I.R.E., vol. 29, pp. 50–55; February, 1941.

is analogous to the power spectrum, consisting of the squares of the amplitudes.

### III. *Integrated Response of Circuits to Noise*[2]

We shall consider below a parameter called the "integrated response" of a circuit to noise. We proceed as follows: The mean-square value of the output of a circuit of amplitude response $m(f)$ to which noise having spectral level $y(f)$ is applied is, from (1),

$$[E^2]_{av} = \int_0^\infty m^2(f)y^2(f)df. \tag{3}$$

Suppose that $m$ has an appreciable value only within a certain range of frequencies. If the input spectrum is of constant level $y_c$ over this range,

$$[E^2]_{av} = y_c^2 \int_0^\infty m^2(f)df. \tag{4}$$

The integrated response $M$ of the circuit is defined as

$$M = \sqrt{\int_0^\infty m^2(f)df}. \tag{5}$$

This quantity relates the rms value of the output noise to the input spectral level, provided the latter is constant over the pass band of the circuit:

$$E = My_c. \tag{6}$$

$M$ may be calculated from (5). The integral may be computed when the analytic form of $m(f)$ is known, or it may be evaluated graphically from sine-wave determinations of $m(f)$. The value of $M$, together with a measurement of $E$, permits calculation of $y_c$. This is the basis for design of a noise-spectrum analyzer.

### IV. *Errors Due to Finite Bandwidth of Filter*

If noise is applied to a narrow-band-pass filter, then the rms output of the filter, together with the integrated response of the filter, gives approximately the spectral level at the center frequency of the filter

$$y_0 = \frac{E}{M} + \epsilon(y, m). \tag{7}$$

The error $\epsilon$ is a function of the filter characteristic and that part of the spectral distribution which lies within the pass band of the filter. Two theorems concerning this error, which have some practical importance, are as follows:

1. For a filter amplitude response that is symmetric about a frequency $f_0$, only the even derivatives of $y^2(f)$ computed at $f_0$ contribute to the error.
2. The error may be attributed to an error in the frequency at which the spectral level is measured; this error in frequency is always smaller than the filter pass band, and, for a symmetric characteristic, is smaller than half the pass band:

$$y(f_1) = \frac{E}{M}, \qquad |f_1 - f_0| < \text{pass band}. \tag{8}$$

These theorems depend on the continuity of the noise spectrum; they fail, for example, if a periodic component lies within the pass band.

The narrower the pass band, the more accurate the measurement of the spectrum. The width of the pass band has a lower limit, set by one or the other of two considerations: sensitivity, and meter fluctuations. The effective noise sensitivity of a filter is proportional to the square root of its bandwidth. More restrictive are fluctuations in the filter output. We may represent the noise output of a narrow filter as a sine wave, the amplitude of which varies in a random manner with time:

$$e = R(t) \sin 2\pi f_0 t. \tag{9}$$

The frequency $f_0$ is the center frequency of the filter, and the envelope $R(t)$ consists of noise having frequency components between zero and one-half the bandwidth of the filter. These low-frequency components cause objectionable fluctuations in the final measuring circuit. The narrower the filter, the more prominent are the lower frequencies in the spectrum of $R(t)$, and the greater the corresponding time required to obtain a measurement of prescribed accuracy.

The problem of measuring noise spectra is seen to reduce essentially to the design of a band-pass filter of variable center frequency, with band pass narrow enough to yield accurate measurements, but wide enough to satisfy practical requirements of sensitivity and reasonable time constants.

### V. *Basic Circuits*

Three fundamental circuits are available to meet the problem: the resonant inductance-capacitance-resistance circuit,[8] the selective feedback-amplifier circuit employing a bridged-$T$ or twin $T$,[9,11] and the heterodyne circuit.[12–16]

A high-selectivity inductance-capacitance resonant circuit satisfies conditions 3, 4, and 5. The measured frequency band is uniquely determined, the dynamic range of the input is restricted only to amplitudes for which the circuit components remain linear, and the response of the circuit to noise can be accurately calcu

[8] C. R. Moore and R. L. Wegel, "An electrical frequency analyzer," *Bell Sys. Tech. Jour.*, vol. 3, pp. 299–323; October, 1924.
[9] H. H. Scott, "A new type of selective circuit and some applications," PROC. I.R.E., vol. 26, pp. 226–235; February, 1938.
[10] H. H. Scott, "An analyzer for noise measurement," *Gen. Rad. Exper.*, vol. 13, pp. 6–12; February, 1939.
[11] H. H. Scott, "The noise primer: Part VI—Analysis of noise," *Gen. Rad. Exper.*, vol. 17, pp. 1–4; April, 1943.
[12] C. R. Moore and A. S. Curtis, "An analyzer for the voice-frequency range," *Bell Sys. Tech. Jour.*, vol. 6, pp. 217–229; April 1927.
[13] A. G. Landeen, "Analyzer for complex electric waves," *Bell Sys. Tech. Jour.*, vol. 6, pp. 230–247; April, 1927.
[14] L. B. Arguimbeau, "Wave analysis," *Gen. Rad. Exper.*, vol. 8, pp. 12–14; June and July, 1933.
[15] L. B. Arguimbeau, "The new wave analyzer—some of its features," *Gen. Rad. Exper.*, vol. 13, pp. 1–5; December, 1938.
[16] A. Peterson, "The communications receiver as a wave analyzer," *Gen. Rad. Exper.*, vol. 18, pp. 1–4; January, 1944.

ated from sine-wave calibration. For either series or arallel circuits, however, conditions 1 and 2 are extremely difficult to satisfy simultaneously.

The bridged-$T$ circuit, being a null-transmission arangement, must be employed as a feedback element in high-gain amplifier. For the frequency range under onsideration, this method is difficult to apply.

The heterodyne circuit shown in Fig. 1 can easily be nade to satisfy conditions 1 and 2 over very wide fre-

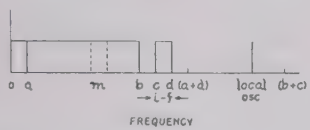


ig. 1—Arrangement of frequencies in heterodyne circuit. The range to be investigated is $ab$. The measured band $m$ consists of the input frequencies which, combining with the local oscillator, form difference frequency-modulation products lying in the intermediate-frequency band.

uency ranges. By suitable care in design, adequate perormance with regard to conditions 3, 4, and 5 may be ecured. The heterodyne system has the advantage that he width and character of the measured band are not unctions of the center frequency. The ultimate measring bandwidth is determined at audio frequency, vhere characteristics are readily controlled. Variations f the integrated noise gain with frequency depend nly on the frequency response of the first modulator nd the input filter.

### VI. *Considerations Pertinent to the Heterodyne Circuit*

(a) *Frequency Identification.* The identification of the neasured band is evident from consideration of Fig. 1. The intermediate-frequency band is placed between the ange to be measured and the local oscillator fundanental, and certain of the input signal components, as hown, lie within the intermediate-frequency band. To nsure that only frequencies below the intermediate requency are measured, a low-pass filter designed to ut off slightly below the intermediate frequency is inerted ahead of the first modulator. The measured omponents are then uniquely determined, and all other ossible primary modulation components are suppressed. Under certain conditions, secondary products lue to frequency components outside the band under crutiny may cause errors in measurement. This nethod, using simple difference-frequency components, ermits measurement of the entire range from near zero requency up to the intermediate-frequency band by uning the local oscillator over a frequency ratio of only to 1.

(b) *Effect of Internal Interference on Sensitivity.* The naximum sensitivity that may be obtained is intimately onnected with the interference that originates within he instrument. This interference may be periodic, or andom, or both.

The effectiveness of the interference in obscuring the ignal depends considerably on the output-circuit deign. The choice of the final meter circuit lies essentially between the linear rectifier and the quadratic rectifier.[17–19] When the signal is smaller than the interference, it is more completely obscured in the response of the linear rectifier than in the quadratic rectifier; also, the relation between the signal and the indication is more complicated. In the square-law circuit, the average output is just the sum of the mean-square values of the signal and interference. By use of a suitable bridge circuit, it is possible to cancel out the average effect of the interference, and leave a response due entirely to the signal. This cannot be done conveniently with a linear rectifier when the signal is smaller than the interference. Partially, in consequence of these considerations, the quadratic bridge circuit was adopted in the practical design.

There is a limit to the canceling-out process because of the fact that all amplifier stages must handle the entire interference-plus-signal amplitude, prior to cancellation, with linearity. As the signal becomes smaller this amplitude becomes larger, to produce sufficient output from the signal to actuate the meter circuit. Eventually, some stage will be overdriven because of the amplitude of the interference alone. If the signal and interference are both noise, then the least measurable signal level is independent of the analyzer bandwidth. When the minimum measurable output voltage $b$ is small compared with the overdrive voltage $a$, then the least measurable level is proportional to $b/a$.

A second limitation is associated with fluctuations of the output indicator due to interference of the random variety and to the random nature of the noise signal under observation. Such fluctuation may be reduced by use of a large time constant in the meter circuit. A compromise is necessary, however, as the time constant is limited by the practical consideration of the time required to obtain a reading, and ultimately by the rate at which the over-all sensitivity of the analyzer drifts. In the instrument as constructed, signals 6 db below the interference level could be accurately measured.

(c) *Errors Due to Nonlinearity.* The entire spectrum of the input signal which falls within the frequency range to be investigated is applied to the input of the first modulator. Thus the total signal at the first modulator may be many times larger than that portion of it which is effective in giving a measurement of the spectral level at any specific center frequency. In some cases, the resulting signal may be large enough to produce appreciable secondary modulation products in addition to the desired primary ones. In extreme cases, the signal may be large enough to cause overload of the modulator, with consequent reduction of the over-all gain of the analyzer. Simple broad filters of low attenuation

[17] J. R. Ragazzini, "The effect of fluctuation voltages on the linear detector," Proc. I.R.E., vol. 30, pp. 277–288; June, 1942.

[18] W. R. Bennett, "Response of a linear rectifier to signal and noise," *Bell Sys. Tech. Jour.*, vol. 23, pp. 97–113; January, 1944.

[19] D. Middleton, "The response of biased saturated linear and quadratic rectifiers to random noise," *Jour. Appl. Phys.*, vol. 17, pp. 778–801; October, 1946.

placed ahead of the first modulator[13] will minimize this by restricting the signal to the frequency band of interest at the moment. An important measure to reduce the significance of these effects is the introduction of attenuation ahead of the first modulator.[12] It is preferable to insert all attenuation at this point and operate subsequent amplifiers at full gain.

The error in measurement introduced by the presence of secondary modulation products is significant when dealing with portions of a spectrum which are considerably lower than the rest, such as narrow, deep holes, and the cutoff region of a sharp-cutoff filter. It is frequently found that the hole, as measured, appears narrower and less deep for noise than for sine waves. This effect is explained by the fact that, along with the primary modulation products, there is always a set of secondary products, consisting of noise components beating with each other and sometimes also subsequently with the local oscillator. These secondary products arise from frequencies outside the band nominally under measurement; they lie within the intermediate-frequency pass band and are indistinguishable from the primary ones. When the frequency region being measured has about the same amplitude as the rest of the spectrum, the secondary products are always drowned out by the primary ones; however, at a hole in the spectrum, the primary products may be so reduced as to be small compared with the secondary products. The reading then will be too large, and the hole will appear to be filled in; the deeper and narrower the hole, the smaller the primary components, and the larger the region which contributes secondary components. This same effect at the edge of a band-pass filter makes the noise appear to spill over outside the filter sine-wave characteristic. This type of error, caused by signal components outside the nominal measurement band, can be completely eliminated only by suppressing the extraneous frequencies with a band-pass filter preceding the first modulator. It can be minimized by careful choice of circuit and operating conditions. Furthermore, it can readily be detected by introducing additional attenuation ahead of the first modulator. If second- and higher-order products are of significant magnitude, the output of the analyzer will fall off *more* rapidly than the added attenuation would justify.

A somewhat different type of error is introduced when overload conditions occur. The over-all analyzer gain having been reduced by the overloading, peaks in the spectrum will be flattened out, and will appear to be of smaller amplitude than they really are. Actually, all parts of the spectrum would appear to be of lower than true amplitude, but, except at the peaks, there is an excellent chance that the extraneous secondary products discussed above will contribute so much energy to the band under measurement that the effect of gain reduction due to overload will not be very marked. Overload occurs only for larger amplitudes than those which produce objectionable secondary products. Hence, the net result of overload is to flatten out a spectrum containing peaks and holes. Overload can easily be detected, since it results in a nonlinear relationship between the input attenuator setting and the output reading. In this case, the output will decrease *less* rapidly than added attenuation at the input would justify.

If the signal mean-square voltage $E_s^2$ is greater than the maximum allowable mean-square voltage $E_m^2$ which may be applied to the modulator, then only the fraction $E_m/E_s$ of the signal amplitude $E_s$ can be applied to the first modulator. The expression for the minimum measurable signal amplitude is higher than before by the factor $E_s/E_m$. It should be noted that $E_m$ is dependent on the noise spectrum of the signal.

(d) *Dynamic Range.* The dynamic range of an instrument refers to the range of input amplitudes over which it may be used. The dynamic range may be extended indefinitely in the direction of large amplitudes by increasing the available attenuation ahead of the first modulator; in the other direction, little increase of sensitivity is gained by the use of untuned preamplifiers. The noise in the first modulator, which is the principal source of interference originating within the instrument, is only slightly above that of an amplifier stage, provided the modulator has been carefully designed. As we have seen, the range of spectral levels which can be measured in any particular case depends greatly on the nature of the signal. If large variations in level over the spectrum are present, removal of sufficient attenuation to permit measurement of the low-level portions may result in overdrive of the first modulator. A high peak-to to-rms ratio leads to overdrive at lower spectral levels than a low ratio. Whenever the level of the secondary products that lie in the intermediate-frequency pass band becomes comparable to that due to the primary components, serious errors will occur in the measurement. The significant quantity remains the minimum accurately measurable level, which can be computed from the effective peak-to-rms ratio of the signal, the maximum allowable input to the first modulator, and the maximum analyzer gain.

## VII. *Summary*

The foregoing comparison between the heterodyne and tuned-circuit methods of noise-spectrum analysis may be summarized as follows: the heterodyne method is greatly superior for obtaining wide frequency coverage at constant sensitivity and with simplicity of tuning. It is inferior in dynamic operating range and in the suppression of errors, but design procedures giving satisfactory performance with respect to these qualities can be worked out. The tuned circuit has the disadvantage that the entire amplifying and measuring system must be designed to operate at all frequencies in the range to be measured. In the heterodyne system, all circuits after the first modulator operate over fixed, narrow frequency bands. For the present purpose, the heterodyne circuit is decidedly preferable.

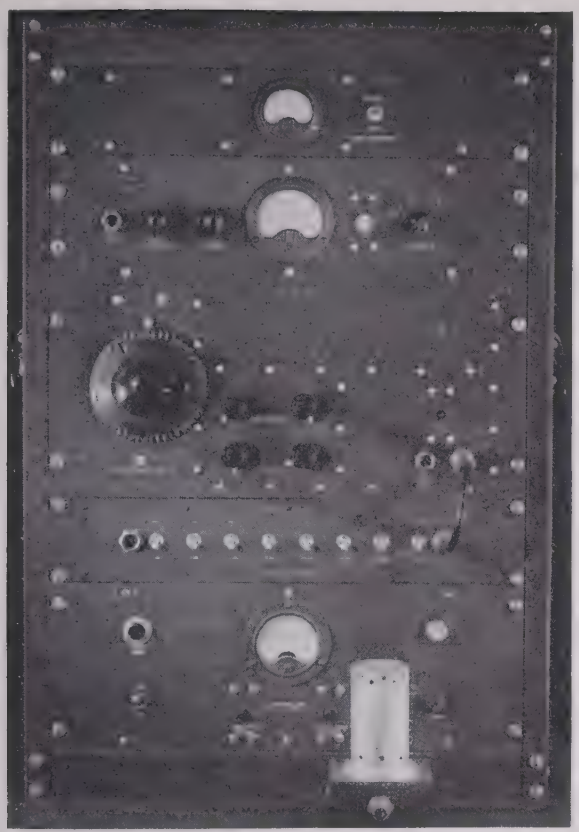

Fig. 2—Front-panel view of the video-frequency noise-spectrum analyzer.

## PART II

### Circuit Design

In this section the circuits of the practical instrument nown in Fig. 2 are discussed in the order of their appearance on the block diagram, Fig. 3.

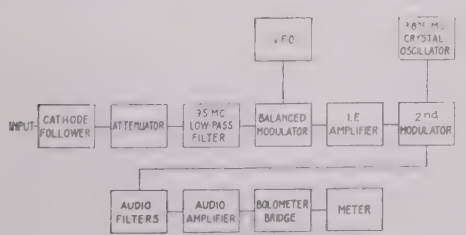


Fig. 3—Block diagram of the video-frequency noise-spectrum analyzer.

### . *Cathode-Follower Input Probe*

A cathode-follower input probe is used to provide a igh input impedance to the analyzer while giving the ide-band (100 kc to 10 Mc) impedance transformation ecessary to drive the input circuit. The input circuit ncludes a transmission line from the probe, an attenuaor, and a filter, all of which are necessarily of low characteristic impedance in view of the frequency range.

All circuits ahead of the first modulator must handle he voltage which corresponds to the entire spectrum of the source, at least up to 10 Mc. A noise signal 10 Mc wide of uniform level 0.1 volt per root kc has an rms value of 10 volts, and may have an effective peak value of 20 or 25 volts in the case of Gaussian noise.[7] In Part I it was shown that, given optimum design at subsequent circuits, the larger the nonoverdriving voltage which can be applied to the modulator, the lower the minimum measurable spectral level. The input probe should accordingly be designed not to overload at a lower voltage than the first modulator. In the instrument developed, the 6Y6G cathode follower handles 6 volts peak-to-peak at the input, driving a 100-ohm load with a voltage amplification of 0.3. The input capacitance is about 11 $\mu\mu$f, and the input resistance is greater than 0.1 megohm. The cathode follower is built into a probe unit which may be brought into close physical proximity of the source of signal being measured.

### II. *High-Frequency Attenuator*

The high-frequency attenuator is an integral part of the measuring system of the analyzer. Readings are taken by setting this attenuator so that the output meter indicates some standard value. The analyzer gain may be so adjusted that the loss introduced by the attenuator gives the input spectral level directly in decibels above a suitable arbitrary level. Location of the attenuator ahead of the first modulator provides the greatest possible dynamic operating range, but involves the difficulty of covering a wide band of frequencies. The attenuator is designed to provide a range of 70-db in 1-db steps at an impedance level of 100 ohms; there is negligible frequency discrimination up to 10 Mc.

The several sections consist of pi networks, individually shielded, each being controlled by a toggle switch. By connecting composition resistors directly to the lugs of the switches and soldering the returns securely to a heavy copper base plate, inductance and common-path effects were readily overcome.

### III. *Balanced Modulator*

A balanced modulator (Fig. 4) is used as a mixer in order to permit measurement at such low frequencies

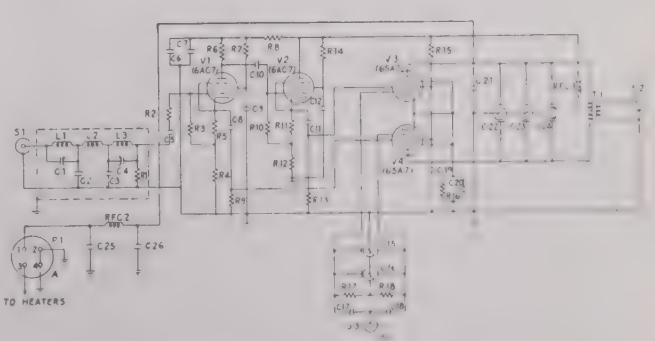


Fig. 4—Balanced-modulator schematic diagram.

that the local oscillator falls within the pass band of the intermediate-frequency amplifier. The balanced modu-

lator prevents the carrier of the local oscillator from appearing in the modulator output and overloading the intermediate-frequency amplifier.

Before being applied to the balanced modulator, the signal must be passed through a low-pass filter to prevent components at frequencies in the intermediate-frequency band or at image frequencies from contributing to the output of the modulator. The integrated response of the filter in the intermediate-frequency band of frequencies is about 100 db below the pass band. The filter response is flat within 1 db up to 9.3 Mc.

A signal balanced to ground for application to the balanced modulator is obtained by passing the output of the low-pass filter through a phase splitter ($V_1$ of Fig. 4). The difference in output impedance of the plate and cathode circuits (the latter, effectively a cathode follower, has a much lower impedance) results in difficult and critical balance of the modulator input circuits if the phase splitter is coupled directly to the modulator. The difficulties appear to be due to space-charge coupling[20] between the No. 1 and No. 3 grids of the 6SA7 converter tubes. The addition of an extra cathode follower ($V_2$ of Fig. 4), between the plate circuit of the phase splitter and the appropriate modulator grid, eliminates the need for neutralization of the space-charge coupling, and gives satisfactory operation.

In the design of the modulator circuit, 6SA7 pentagrid converter tubes ($V_3$ and $V_4$ in Fig. 4) are used to facilitate isolation of the signal circuits from the local oscillator. Means are provided for balancing both phase and amplitude. Amplitude balance is accomplished by means of a capacitance voltage divider which controls the relative proportion of the local-oscillator carrier fed to each converter tube. The phasing is done by means of a balancing capacitor across the output tank circuit. Both coarse and fine controls are provided for both amplitude and phase balancing.

Although exact settings of the balancing controls for optimum suppression of the carrier depend slightly on the frequency of the local oscillator, usually the balance obtained at some frequency in the neighborhood of 50 kc holds adequately over the entire range. Balancing is not required at all for readings at frequencies above 500 kc.

Provided the local-oscillator output remains reasonably constant over the tuning range, the modulator conversion gain is not dependent on frequency. The complete balanced modulator circuit is found to have a constant conversion gain from 10 cps to 10 Mc. Thus, with input circuits flat over the range to be measured, it is possible to realize essentially constant sensitivity.

## IV. *Variable-Frequency Local Oscillator*

The chief requirements in the design of the local oscillator (Fig. 5) are frequency stability and constancy of output over the tuning range. Stability is particularly important at the low-frequency end, since a small drift in oscillator frequency produces a large fractional change in the frequency of the band being measured.

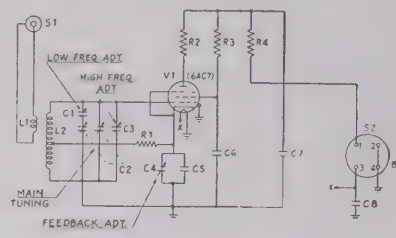


Fig. 5—Variable-frequency local oscillator schematic diagram.

Constancy of output over the tuning range is needed because, even with optimal choice of oscillator drive for the mixer tubes, the conversion transconductance of the latter varies with oscillator voltage. It was found that a typical grounded-plate Hartley oscillator operating between 10 and 20 Mc delivered approximately twice the voltage output at the high-frequency as at the low-frequency limit. A frequency-sensitive degenerative feedback network ($C_4$, $C_5$, and $R_1$ of Fig. 5) is added to make the output substantially constant over the band. By adjustment of $C_4$, the outputs can be made equal at any selected pair of high and low frequencies. By this means, a deviation of less than 1 db can be procured over the entire tuning range. The resistor $R_1$ acts both as part of the feedback circuit and also as the bias resistor for the oscillator.

It is necessary to shield the oscillator unit carefully and by-pass all power leads, including the heaters, thoroughly, in order to prevent undesired coupling with the rest of the instrument.

## V. *Intermediate-Frequency Circuits*

The intermediate-frequency amplifier employs two transformer-coupled stages giving a gain of 60 db at the center frequency of 9,875 kc.

The second modulator employs a 6SA7 pentagrid converter tube, with capacitance neutralization of the space-charge coupling between the oscillator and signal grids to prevent crystal oscillator voltage from appearing on the signal grid. A voltmeter may be switched to measure the bias on either grid. The bias on the oscillator grid is a measure of the drive secured from the crystal oscillator. The direct voltage developed by the signal grid is a useful preliminary indication of unbalance in the first modulator.

The crystal oscillator operates at 9,875 kc, the center of the intermediate-frequency-amplifier pass band. Thus frequencies both above and below this are converted to audio frequency in the mixer.

[20] F. L. Smith, "The Radiotron Designer's Handbook," The Wireless Press, Sydney, Australia, 3rd edition, 1941; chap. 15, pp. 103–104.

## VI. *Audio Circuit*

The audio circuit comprises a set of low-pass filters, an attenuator, an amplifier, and a square-law meter circuit.

The width of the sample of the input-signal spectrum which is measured is determined by the low-pass filter between the second modulator and the audio-frequency amplifier. The sample is just twice the bandwidth of the filter. Provision of a choice of several filters having different cutoff frequencies. specifically, 5 and 15 kc, permits the sample bandwidth to be varied.

A conventional amplifier employing two 6SJ7 pentodes in cascade to feed a 6J5 triode output stage provides the necessary audio-frequency amplification.

An attenuator providing up to 30 db loss in three 10-db steps is used as an auxiliary to the main video-frequency attenuator. A continuous gain control permits adjustment of the over-all sensitivity of the instrument to a predetermined standard calibration value.

The output indicator circuit consists of a thermistor bridge.[21] This has several advantages. It exhibits an accurately quadratic characteristic, high sensitivity, and tolerance of severe overload, and it maintains constant sensitivity over extended periods of use. Further, the bridge circuit can be rebalanced without affecting the sensitivity, so that the average effects of interference arising within the analyzer are suppressed. The thermistor arms of the bridge circuit are mounted within a temperature-controlled box in order to eliminate the effects of changes in the ambient temperature. The use of two thermistors permits cancellation of the effect of the small temperature changes which occur in the box due to lag in the thermostat response. Only one thermistor receives the signal to be measured.

A useful range of 10 db may be covered by the indicating scale. An input power of about 2 milliwatts will provide full-scale deflection of the meter. This power is readily supplied by the 6J5 final audio-amplifier tube with an excellent reserve capability for handling peaks. It is evident that any interference voltage present, whether originating internally or externally, may be combined with the direct current in the measuring thermistor to obtain the original bridge balauce. The addition of signal, even if considerably weaker than the interference, then produces a reading. The effect of interference evidently cannot be suppressed if, at an earlier point in the analyzer, it and the desired signal intermodulate.

[21] J. A. Becker, C. B. Green, and G. L. Pearson, "Properties and uses of thermistors," *Bell Sys. Tech. Jour.*, vol. 26, pp. 170–212; January, 1947.

## VII. *Conclusion*

The experience gained with two models of the video-frequency spectrum analyzer has shown that the instrument has a maximum sensitivity of 7 microvolts per root kilocycle with high impedance input. The sensitivity is constant to $\pm 0.5$ db over the range 50 kc to 9.3 Mc. The internal noise level, referred to the modulator input, is 5 microvolts per root kilocycle, or 15 microvolts per root kilocycle referred to the cathode-follower input.

The attenuators permit measurements over a wide range of signal-input levels, while the probe input permits these to be made with little disturbance of the signal source under investigation. The range of levels which the instrument will measure has a minimum set by the sensitivity, and a maximum determined by the voltage at which intermodulation begins. The maximum tolerable input is determined in terms of the effective peak voltage applied to the input circuit. Hence, the wave form and frequency distribution will affect the spectral level at which intermodulation occurs. It may occur that components in a remote part of the spectrum will overdrive the input before those under consideration can be measured, even though the latter be above the threshold level. If a noise signal is connected of which the effective peak value is four times its rms value and the spectrum is flat out to and negligible above 10 Mc, the greatest measurable spectral level is 7.5 millivolts per root kilocycle.

As long as the principal modulation products of the balanced modulator are the result of the signal noise components beating with the local oscillator, and not with each other, holes in the spectrum will be accurately measured; if a hole is narrow and deep, however, secondary-modulation products, consisting of difference frequencies between noise components beating with the local oscillator or of sum frequencies, may be sufficient to make the hole appear considerably filled in. No corresponding difficulty appears with peaks, for which second-order effects are always negligible. The presence of peaks may, however, interfere with measurements elsewhere in the spectrum.

The analyzer is not designed to measure signals with wave forms having large peak-to-rms ratios, such as radar pulses.

The exceptional tuning range without bandswitching and with constant sensitivity simplifies the use of the analyzer markedly. The method of determining bandwidth gives an almost ideal square-topped characteristic whose width is accurately known. If desired, selection between several such widths is possible. The output measuring circuit is simple, reliable, and rugged.

# Terminal Impedance and Generalized Two-Wire-Line Theory*

RONOLD KING†, SENIOR MEMBER, IRE, AND K. TOMIYASU†, MEMBER, IRE

*Summary*—**Conventional transmission-line theory takes no account of variations in the parameters of the line and of coupling near a terminating impedor, or near any other change in its uniform properties. A theory is derived which substitutes for these effects a simple terminal-zone network of lumped series and shunt elements which may be evaluated for each type of termination or discontinuity. The apparent terminal impedance $Z_{sa}$ (which is the impedance actually measured on a lossless line at a distance $\lambda/2$ from the termination) consists of this network in combination with the theoretical, isolated impedance, $Z_s$, of the load. $Z_{sa}$ for a *fixed* termination with a given $Z_s$ may vary greatly with the nature of the connection to the line, the relative orientation of line and load, and the type of line and its dimensions.**

## Introduction

THE DERIVATION of the transmission-line equations involves fundamental assumptions that are often overlooked. Among them is the requirement that all elements of length $\Delta z$ of a two-wire line be identical. Since this is not true near the ends of the line at $z=0$ and $z=s$ where it joins the generator and load, the conventional differential equations and the currents, voltages, and impedances derived from them are not accurate in terminal zones at each end. The length $d$ of each zone depends on the termination; it is of the order of magnitude $10b$, where $b$ is the spacing of the two-wire line, provided the terminations are completely outside the region bounded by the planes $z=0$ and $z=s$. In each terminal zone the parameters of the line vary, and the line may be coupled to adjacent parts of the termination. A physically significant impedance may be defined only outside the terminal zones; (i.e., at such distances from the load that the scalar potential difference between opposite points on the two conductors is equal to the line integral of the electric field from one point to the other).

The *apparent* terminal impedance of a particular impedor may be studied using Fig. 1 without specializing the formulation to this particular circuit. The load in this figure is to the right of the plane containing the line-load junction.

An essential postulate implied in the conventional equations is that the line must be balanced. Electrically, this means

$$q_{2L}(w') = -q_{1L}(w'); \quad I_{2zL}(w') = -I_{1zL}(w'), \qquad (1)$$

where $q_{1L}(w')$ $[q_{2L}(w')]$ is the charge per unit length on conductor 1 [2] of the line at a distance $w'$ from the load-line junction. $I_{1zL}(w')$ $[I_{2zL}(w')]$ is the total current in conductor 1 [2] at the same cross section. Distributions in the line that satisfy (1) involve restrictions on the charges and currents in the termination and, hence, on the electromagnetic field associated with *all* charges and currents in the entire circuit. Similar restrictions apply to the scalar and vector potentials as follows: All parts of the line, load, generator, and associated circuits must be so constructed that the scalar potential $\Phi$ and the axial component $A_z$ of the vector potential, at corresponding points on the surfaces of the conductors of the line, satisfy the following conditions:

$$\Phi_2(w) = -\Phi_1(w); \quad A_{2z}(w) = -A_{1z}(w). \qquad (2)$$

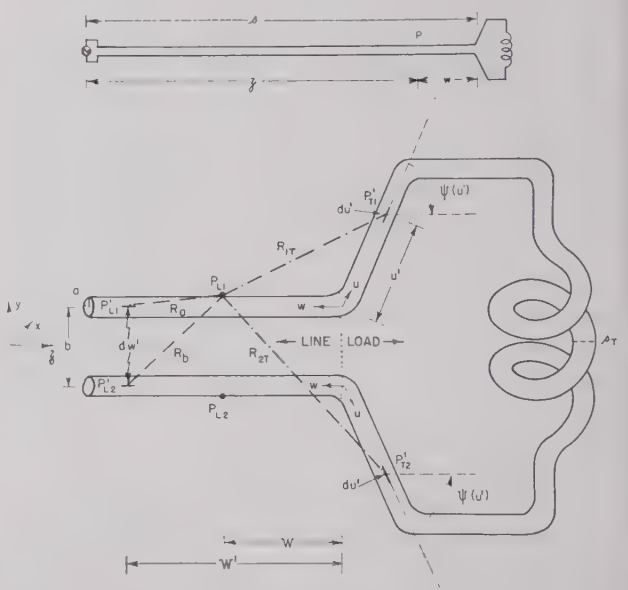


Fig. 1—Transmission line with load.

The potential differences are then given by:

$$V(w) = \Phi_1(w) - \Phi_2(w) = 2\Phi_1(w);$$
$$W_z(w) = A_{1z}(w) - A_{2z}(w) = 2A_{1z}(w). \qquad (3)$$

The total potentials and potential differences are the sums of components due to charges and currents on the line (subscript $L$) and on the terminations (subscript $T$). For example,

$$V(w) = V_L(w) + V_T(w);$$
$$W_z(w) = W_{zL}(w) + W_{zT}(w). \qquad (4)$$

Therefore, (2) and (3) are true if a subscript $L$ or $T$ is added to each potential.

The conditions (2) with added subscript $T$ imply that the load (or generator) consists of identical halves 1 and 2 of which #1 is attached or coupled to conductor 1 of the line, #2 to conductor 2 of the line. The following con-

* Decimal classification: R117.12. Original manuscript received by the Institute, January 17, 1949; revised manuscript received, April 25, 1949.

† Formerly, Cruft Laboratory, Harvard University, Cambridge 38, Mass.; now, Sperry Gyroscope Co., Great Neck, L. I., N. Y.

ditions must obtain at equal distances $u'$ from the junctions with the line along the *axes* of the *conductors* of each half of the termination:

$$q_{2T}(u') = -q_{1T}(u'); \qquad I_{2zT}(u') = -I_{1zT}(u');$$
$$I_{2xT}(u') = I_{1xT}(u'); \qquad I_{2yT}(u') = I_{1yT}(u'). \tag{5}$$

If the halves are geometrical images in the plane $y=0$, but with signs of charges and directions of currents opposite to those of mirror images, all conditions (1)–(5) are satisfied. However, there are configurations in which the halves are *not* geometrical images in the plane $y=0$, that also satisfy conditions (1)–(5).

## Generalized Potential Differences

Referring to Fig. 1, the potential differences between points $P_{L1}$ and $P_{L2}$ on the surfaces of the conductors of the line are given by (4) with[1]

$$W_{zL} = \frac{1}{2\pi\nu}\int_0^s I_{zL}(w')P_L(w, w')dw';$$
$$W_{zT}(w) = \frac{1}{2\pi\nu}\int_0^{s_T} I_{zT}(u')P_T(w, u')du' \tag{6}$$

$$V_L(w) = \frac{1}{2\pi\xi}\int_0^s q_L(w')P_L(w, w')dw';$$
$$V_T(w) = \frac{1}{2\pi\xi}\int_0^{s_T} q_T(u')P_T(w, u')du', \tag{7}$$

where

$$P_L(w, w') = \left[\frac{e^{-j\beta R_a}}{R_a} - \frac{e^{-j\beta R_b}}{R_b}\right];$$
$$P_T(w, u') = \left[\frac{e^{-j\beta R_{1T}}}{R_{1T}} - \frac{e^{-j\beta R_{2T}}}{R_{2T}}\right] \tag{8}$$

$$\beta = \omega\sqrt{\frac{\xi}{\nu}}; \qquad \xi = \epsilon_e - j\sigma_e/\omega \tag{9}$$

and where $\nu=\nu_0\nu_r$, $\nu_0=10^7/4\pi$ meters/henry; $\epsilon_e=\epsilon_{er}\,\epsilon_0$, $\epsilon_0=8.85\times10^{-12}$ farads/meters; $\nu_r=1/\mu_r$ is the relative reluctivity, $\epsilon_{er}$ is the real effective dielectric constant; and $\sigma_e$ is the real effective conductivity in mhos/meter of the medium in which the entire circuit is immersed. The distances $R_a=\sqrt{(w-w')^2+a^2}$, $R_b=\sqrt{(w-w')^2+b^2}$, $R_{1T}$ and $R_{2T}$ are in Fig. 1; $s$ in the length of the line, $s_T$ is half the distance around the contour of the termination.

In order to evaluate (6) and (7), the charges and currents at $w'$ in the line and at $u'$ in the termination are expanded in series. Currents and charges are continuous at the line-load junction so that

$$q_L(w'\to 0) = q_T(u'\to 0);$$
$$I_{zL}(w'\to 0) = I_{uT}(u'\to 0). \tag{10}$$

Using the equation of continuity, $dI_s/ds+j\omega q=0$, the following expansions may be written:

$$q_L(w') \doteq q_L(w) + (w'-w)\frac{1}{j\omega}\frac{\partial I^2_{zL}(w)}{\partial w^2} \tag{11a}$$

$$I_{zL}(w') \doteq I_{zL}(w) + (w'-w)j\omega q_L(w) \tag{11b}$$

$$q_T(u') \doteq q_L(w) - (u'+w)\cdot\frac{1}{j\omega}\cdot\frac{\partial^2 I_{zL}(w)}{\partial w^2} \tag{11c}$$

$$I_{uT}(u') \doteq I_{zL}(w) - (u'+w)\cdot j\omega q_L(w). \tag{11d}$$

Note that

$$I_{zT}(u') = I_{uT}(u')\cos\psi(u') \tag{12}$$

where $I_{uT}(u')$ is the total axial current at $u'$ in the termination, and $\psi(u')$ is the angle between the direction of the current at $u'$ and the $z$ axis.

Substitution of (11) and (12) in (6) and (7), and subsequent substitution of the resulting integrals in (4), gives:

$$W_z(w) = \frac{1}{2\pi\nu}\{I_{zL}(w)[k_0(w)+k_{0T}(w)] + j\omega q_L(w)[k_1(w)+k_{1T}(w)]/\beta\} \tag{13}$$

$$V(w) = \frac{1}{2\pi\xi}\left\{q_L(w)[k_0(w)+k_{0T}'(w)] + \frac{1}{j\omega}\frac{\partial^2 I_{zL}(w)}{\partial w^2}[k_1(w)+k_{1T}'(w)]/\beta\right\}, \tag{14}$$

where

$$k_0(w) \equiv \int_0^s P_L(w, w')dw' \doteq \int_0^s\left(\frac{1}{R_a}-\frac{1}{R_b}\right)dw'$$
$$= \sinh^{-1}\frac{w}{a} - \sinh^{-1}\frac{w}{b} + \sinh^{-1}\frac{z}{a} - \sinh^{-1}\frac{z}{b} \tag{15a}$$

$$k_{0T}(w) \equiv \int_0^{s_T} P_T(w, u')\cos\psi(u')du'$$
$$\doteq \int_0^{s_T}\left(\frac{1}{R_{1T}}-\frac{1}{R_{2T}}\right)\cos\psi(u')du' \tag{15b}$$

$$k_{0T}'(w) \equiv \int_0^{s_T} P_T(w, u')du'$$
$$\doteq \int_0^{s_T}\left(\frac{1}{R_{1T}}-\frac{1}{R_{2T}}\right)du' \tag{15c}$$

$$k_1(w) \equiv \beta\int_0^s (w'-w)P_L(w, w')dw'$$
$$\doteq \beta\int_0^s (w'-w)\left(\frac{1}{R_a}-\frac{1}{R_b}\right)dw'$$
$$= \beta[\sqrt{w^2+b^2} - \sqrt{w^2+a^2} - \sqrt{z^2+b^2} + \sqrt{z^2+a^2}] \tag{15d}$$

$$k_{1T}(w) \equiv -\beta\int_0^{s_T} (u'+w)P_T(w, u')\cos\psi(u')du'$$

[1] R. W. P. King, "Electromagnetic Engineering," vol. I., p. 472, McGraw-Hill Book Co., New York, N. Y., 1945.

$$\doteq -\beta \int_0^{u_T} (u' + w)\left(\frac{1}{R_{1T}} - \frac{1}{R_{2T}}\right) \cdot \cos \psi(u')du' \quad (15e)$$

$$k_{1T}'(w) \equiv -\beta \int_0^{u_T} (u + w)P_T(w, u)du'$$

$$\doteq -\int_0^{u_T} (u' + w)\left(\frac{1}{R_{1T}} - \frac{1}{R_{2T}}\right)du'. \quad (15f)$$

The approximate integrals in (15) differ negligibly from the exact integrals if $b$ satisfies the following inequality:

$$|\beta b| \ll 1. \quad (16)$$

The terms neglected on the right in (15) contribute to radiation from the line; (16) makes this negligible. Let

$$l^e(w) = l_0^e(w) + l_T^e(w) = [k_0(w) + k_{0T}(w)]/2\pi\nu \quad (17a)$$

$$\omega y^{-1}(w) \equiv j\omega[y_0^{-1}(w) + y_T^{-1}(w)] \equiv [k_0(w) + k_{0T}'(w)]/2\pi\xi \quad (17b)$$

$$y(w) = g(w) + j\omega c(w) \quad (17c)$$

$$p(w) = [k_1(w) + k_{1T}(w)]/[k_0(w) + k_{0T}(w)] \quad (17d)$$

$$p'(w) \equiv [k_1(w) + k_{1T}'(w)]/[k_0(w) + k_{0T}'(w)] \quad (17e)$$

$$p_0(w) \equiv k_1(w)/k_0(w). \quad (17f)$$

Note that

$$\beta^2 = \omega^2\xi/\nu = -j\omega l_0^e(w)y(w)[k_0(w) + k_{0T}'(w)]/k_0(w). \quad (18)$$

With (17) substituted in (13) and (14), the following expressions are valid at *all* points along the line:

$$W_z(w) = l^e(w)[I_{zL}(w) + j\omega q_L(w)p(w)/\beta] \quad (19)$$

$$V(w) = \frac{j\omega}{y(w)}\left[q_L(w) + \frac{1}{j\omega}\frac{\partial^2 I_{zL}(w)}{\partial w^2}\frac{p'(w)}{\beta}\right]. \quad (20)$$

For some purposes, the ratio functions $a_1(w)$ and $\phi_1(w)$ are useful.

$$a_1(w) \equiv l^e(w)/l_0^e(w) \doteq W_z(w)/W_{zL}(w);$$
$$\phi_1(w) \equiv c(w)/c_0(w) \doteq V_L(w)/V(w). \quad (21)$$

When $a_1(w) = 1$, there is no inductive coupling; when $\phi_1(w)$, there is no capacitive coupling between line and termination.

At points outside the terminal zones, where conventional line theory is adequate, these relations reduce to

$$W_z(w) = l_0^e I_{zL}(w); \quad V(w) = j\omega q_L(w)/y_0 \quad (22a)$$

$$l_0^e = k_0(w \to \infty)/2\pi = [\ln b/a]/2\pi\nu \quad (22b)$$

$$y_0 = g_0 + j\omega c_0 = j\omega 2\pi\xi/k_0(w \to \infty) = j\omega\pi\xi/[\ln b/a]. \quad (22c)$$

The functions $k_0(w)$, $k_1(w)/\beta_0 b$, and $p_0(w)/\beta_0 b$ which characterize the transmission-line-end effect for a line in air where $\beta = \beta_0$ (but do not include coupling to the termination) are shown in Fig. 2. The corresponding values of $l_0^e(w)$, $c_0(w)$, and $R_e(w) = [l_0^e(w)/c_0(w)]^{1/2}$ are in Fig. 3.

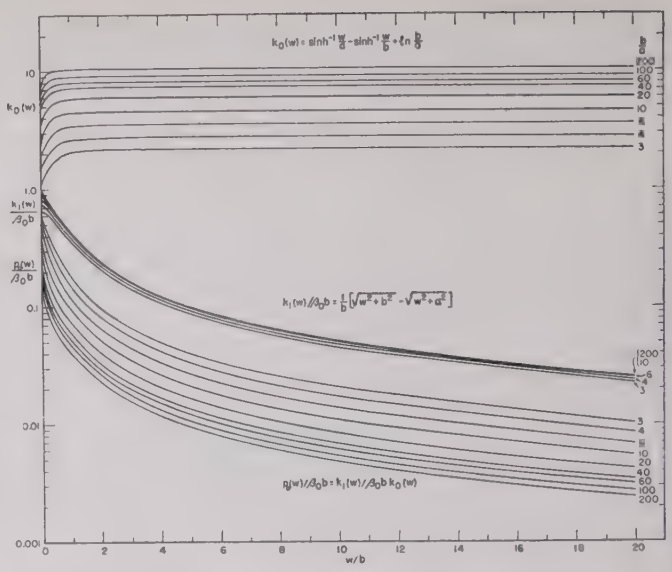


Fig. 2—The functions $k_0(w)$, $k_1(w)$, $p_0(w)/\beta_0 b$, at the load end of a long line in air which is not coupled to the load.

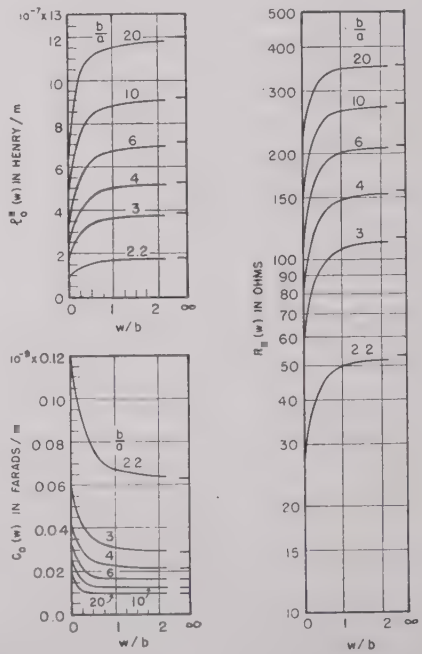


Fig. 3—The external inductance and capacitance per unit length and characteristic resistance at the load-end of a line in air with no coupling to the load, $l_0^e(w) = 2\times10^{-7}\ k_0(w)$ henry/$m$; $c_0(w) = 2\pi \times 8.85\times10^{-12}/k_0(w)$ farads/$m$; $R_e(w) = \sqrt{l_0^e(w)/c_0(w)}$.

## Generalized Differential Equations for Voltage and Current

The generalized differential equations for current and voltage may be derived from the equations defining the scalar and vector potentials, namely, $\vec{E} = -\text{grad}\ \Phi - j\omega A$; div $\vec{A} + j(\beta^2/\omega)\Phi = 0$; and the relation, $E_{z1} = z_1^i I_{z1}$, where $z_1^i$ is the internal impedance[2] per unit length of conductor 1 and $E_{z1}$ is the tangential electric field at its surface. Noting that $z_1^i = z_2^i = z^i/2$, where $z^i$

[2] See page 348 of footnote reference 1.

is the internal impedance per *loop unit* length of the line, and using (1), (3), and $w=s-z$, the following equations are obtained:

$$\frac{\partial V(w)}{\partial w} = z^i I_{zL}(w) + j\omega W_z(w) \tag{23}$$

$$\frac{\partial W_{zL}(w)}{\partial w} = \frac{j\beta^2}{\omega} V_L(w). \tag{24}$$

By eliminating $W_z(w)$ from (19), using (23), and $q_L(w)$ using (20),

$$z(w)I_{zL}(w) - \frac{j\omega l^e(w)p(w)p'(w)}{\beta^2}\frac{\partial^2 I_{zL}(w)}{\partial w^2} = \frac{\partial V(w)}{\partial w} - \frac{j\omega l^e(w)y'(w)p(w)}{\beta} V(w) \tag{25}$$

where

$$z(w) = z^i + j\omega l^e(w). \tag{26}$$

Since $p(w)$ and $p'(w)$ are small,

$$p(w)p'^d w) \ll 1; \tag{27}$$

and since, in order of magnitude,

$$\partial^2 I_{zL}(w)/\partial w^2 = -\beta^2 I_{zL}(w); \tag{28}$$

it follows subject to (27), that (25) with (18) reduces to,

$$I_{zL}(w) = \frac{1}{z(w)}\left[\frac{\partial V(w)}{\partial w} + \frac{k_0(w)+k_{0T}(w)}{k_0(w)+k_{0T}'(w)}\beta p(w)V(w)\right]. \tag{29}$$

When there is no inductive coupling between load and line, $k_{0T}(w)=0$ and the factor before $\beta$ reduces to $\phi_1(w)$. Outside the terminal zone (29) assumes the conventional form, namely,

$$I_{zL}(w) = \frac{1}{z_0}\frac{\partial V(w)}{\partial w}; \quad z_0 = z^i + j\omega l_0{}^e. \tag{30}$$

Differentiation of (23) with respect to $w$, using (4) gives

$$\frac{\partial^2 V(w)}{\partial w^2} + \beta^2 V_L(w) = \frac{\partial}{\partial w}[z^i I_{zL}(w) + j\omega W_{zT}(w)]. \tag{31}$$

This equation may be simplified by replacing the correction term $W_{zT}(w)$ by its principal part obtained from (13). Thus, with (26) and (17a),

$$z^i I_{zL}(w) + j\omega W_{zT}(w) \doteq I_{zL}(w)[z^i + j\omega l_T{}^e(w)] = I_{zL}(w)[z(w) - j\omega l_0{}^e(w)]. \tag{32}$$

With the leading term in (29), the derivative of (32) is given by

$$\frac{\partial}{\partial w}[z^i I_{zL}(w) + j\omega W_{zT}(w)] = \frac{\partial}{\partial w}\left[\frac{z(w) - j\omega l_0{}^e(w)}{z(w)}\frac{\partial V(w)}{\partial w}\right] \doteq \frac{z(w) - j\omega l_0{}^e(w)}{z(w)}\frac{\partial^2 V(w)}{\partial w^2}. \tag{33}$$

Since the leading part of $z(w)$ is $j\omega l_0{}^e(w)$ and this varies slowly with $w$ even in the terminal zone, the principal part in (33) is that given on the right. For terminations in which there is no $z$ component of current near the line load junction, $l_T{}^e(w)$ is zero, and (33) is exact. Substitution of (33) in (31), rearrangement of terms noting that $V_L(w)/V(w) = k_0(w)/[k_0(w)+k_{0T}'(w)]$, and use of (17a), gives the following final equation for $V(w)$:

$$\partial^2 V(w)/\partial w^2 - \gamma^2(w)V(w) = 0, \tag{34}$$

where

$$\gamma^2(w) \equiv z(w)y(w) = [z^i + j\omega l^e(w)][g(w) + j\omega c(w)]. \tag{35}$$

Since a small error in the small quantity $z^i$ in the terminal zone is of no consequence,

$$\gamma^2(w) \doteq \gamma^2 a_1(w)\phi_1(w), \tag{36a}$$

where

$$\gamma^2 \equiv \gamma^2(w \to \infty) = z_0 y_0 = (z^i + j\omega l_0{}^e)(g_0 + j\omega c_0). \tag{36b}$$

The parameter $\gamma$, which is independent of $w$, is the conventional complex propagation constant.

The scalar potential difference at any cross section of the line is obtained by solving (34); the current is then given by (29).

## Approximate Solutions of the Equations—Apparent Terminal Impedance

Transmission-line measurements usually depend on distribution curves or resonance curves obtained on parts of the line quite far from the terminations. The data so obtained are then interpreted using conventional formulas that are valid only outside the terminal zones. This procedure is correct only if sufficiently long sections of line are included as a part of the termination, so that $z=s$ is not the actual end of the smooth line. If conventional formulas are assumed to apply to the actual end of the line, the impedance *apparently* terminating it includes the effect of errors made in using incorrect line parameters and formulas in the terminal zone. This *apparent terminal impedance* $Z_{sa}$ at $z=s$ is not the ratio of the actual scalar potential difference to current. Since $Z_{sa}$ involves the properties of the transmission line, the *same* geometrical structure may have very *different* apparent terminal impedances when connected as load to different transmission lines. Merely varying the spacing of a line, for example, may change the apparent terminal impedance of a given load by a large amount.

For reasons similar to those which make it impossible to have the uniform properties of a long transmission line continue to its junction with an arbitrary impedor, it is also impossible to define for an arbitrary circuit element an impedance that is independent of the circuit to which it is connected. The degree of coupling of such an element to the adjacent parts of the circuit varies with the configuration of conductors; it may be large or small, but never zero. As explained in the literature,[3] it is for-

[3] See pages 419 and 461 of footnote reference 1.

mally possible to separate the coupling between two parts of a complete circuit into two self-impedances and a mutual impedance. Except when the distribution of current is greatly affected by the mutual term, the self-term of the load differs negligibly from the self-impedances when isolated with an equal potential difference maintained at its terminals by a fictitious "concentrated" source. This is true of the coupling between a transmission line and its load. Accordingly, the transmission-line may be analyzed as if it had a physically dimensionless load, and the load as if it were isolated and driven by a fictitious, dimensionless source that maintains the required potential difference $V(s)=\Phi_1(s)-\Phi_2(s)$ at its terminals (Fig. 4), provided account is taken of the

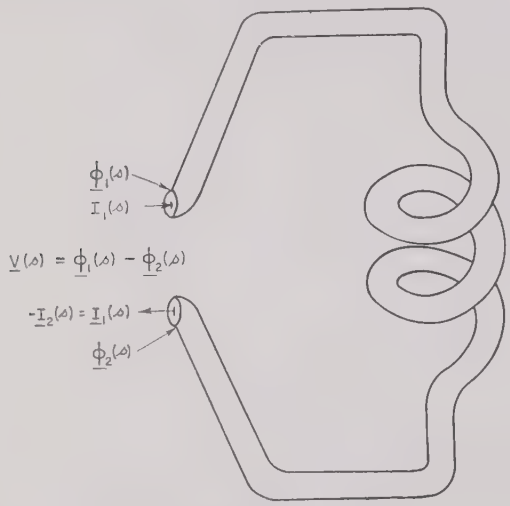


Fig. 4—"Isolated" load of Fig. 1

coupling between them. This may be done approximately by means of a suitable equivalent network that represents the coupling as if lumped at the junction instead of distributed over short distances near it. By concentrating end effects and coupling effects in the network of lumped elements, the terminal zone may be replaced by a fictitious section of conventional line that has as its termination the apparent terminal impedance $Z_{sa}$. This is composed of the fictitious impedance $Z_s$ of the load (treated as if isolated and given by $Z_s=V(s)/I(s)$ as shown in Fig. 4) in conjunction with the appropriate terminal-zone network that includes a series element $Z_T$ and a shunt element $Y_T$ defined as follows:

$$Z_T = \int_0^d [z(w) - z_0]dw \doteq j\omega \int_0^d [l^e(w) - l_0^e]dw$$

$$= j\omega \int_0^d [l_0^e(w)a_1(w) - l_0^e]dw \equiv j\omega L_T \qquad (38)$$

$$Y_T = \int_0^d [y(w) - y_0]dw \doteq j\omega \int_0^d [c(w) - c_0]dw$$

$$= j\omega \int_0^d [c_0(w)\phi_1(w) - c_0]dw \equiv j\omega C_T. \qquad (39)$$

The integrals (38) and (39) may be evaluated either in closed form or by numerical methods for a particul termination.

If $Z_T$ is assumed connected in series with the load an $Y_T$ in parallel with it, $\gamma^2$ may be substituted for $\gamma^2(v$ in (34), $z_0$ for $z(w)$, and zero for $p(w)$; also the fact before $\beta$ in (29) may be replaced by unity. It is no possible to obtain solutions in conventional form namely,

$$V(w) = V(s)[\cosh \gamma w + Y_{sa}Z_c \sinh \gamma w] \qquad (40a$$

$$I(w) = \frac{V(s)}{Z_c}[\sinh \gamma w + Y_{sa}Z_c \cosh \gamma w], \qquad (40b$$

where $Z_c$ is the conventional characteristic impedanc of the line and where $Y_{sa}$ consists of the impedance

$$Z_s = V(s)/I(s) \qquad (4$$

in series with $Z_T$ and in parallel with $Y_T$. $L_T$ and $C_T$ ar positive or negative depending on the terminatio Thus, an approximately equivalent circuit of an actu two-wire line of length $s$ *with* a terminal zone (extendin from $z=s-d$ to $z=s$ where the line joins the load) is

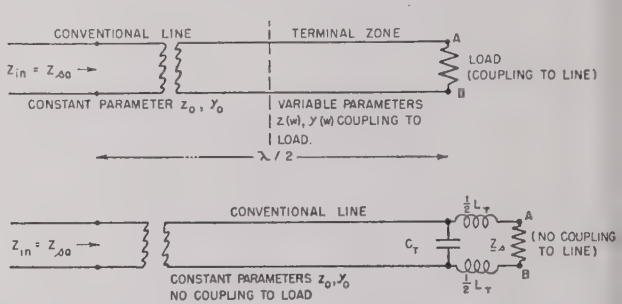


Fig. 5—Actual line and equivalent circuit with terminal zone ne work to take account of end-effects on the line and coupling line to load.

fictitious line of length $s$ *without* terminal zone, but wit the network of lumped elements shown in Fig. 5 servin as connection between the line and the "isolated" in pedance $Z_s$ of the load. Note that the impedances appa ently terminating both actual and fictitious lines a $Z_{sa}$. Neglecting line losses, this is the impedance lookin toward the load at a distance $\lambda/2$ from it. $Z_{sa}$ is a dire measurable quantity, $Z_s$ is not; $Z_{sa}$ varies with the typ of line and the nature of the connection, $Z_s$ is by defin tion independent of the line.

## Conclusion

A theory has been developed that is an essential su plement to conventional transmission-line analysis. has been applied to determine the apparent impedanc of an open end, of a bridged end, and of antennas co nected (1) as end loads[4-7] in the plane and perpendicul

[4] R. King, "Theory of antennas driven from a two-wire line Technical Report No. 41, Cruft Laboratory, 1948.
[5] R. King, "Antennas and open wire lines," Part I, *Jour. Ap Phys.*, September or October, 1949.
[6] K. Tomiyasu, "Problems of measurement on two-wire lines wi application to antenna impedances," Technical Report No. 48, Cru Laboratory, 1948.
[7] K. Tomiyasu, "Antennas and two-wire lines," Part II, *Jou Appl. Phys.*, October or November, 1949.

to the plane of the line, and (2) as center loads[8,9] on a line driven from both ends. For these three connections the values of $Z_{ta}$ for a given antenna with a single value of $Z_t$ differ greatly from one another, but corresponding theoretical and experimental values of $Z_{ta}$ are in good agreement. Differences in the apparent terminal impedance of the same antenna exceeding 50 per cent have been observed merely by changing the line spacing from $b/\lambda=0.01$ to $b/\lambda=0.1$. The theory is being applied to bends and other discontinuities on a two-wire line and, with some generalization, to coupled antennas driven or tuned by two-wire lines in a variety of arrangements.

In general principle, the analysis outlined in this paper resembles that of a corresponding problem in waveguides, but the mathematical method is different. The dominant mode on the line is that described by the conventional line equations. The effect on nonpropagating higher modes at junctions is represented by the terminal-zone network of lumped elements.

[8] P. Conley, "Impedance measurements with open-wire lines," Technical Report No. 35, Cruft Laboratory, 1948.
[9] P. Conley, "Antennas and two-wire lines," Part III, *Jour. Appl. Phys.*, November or December, 1949.

# On the Energy-Spectrum of An Almost Periodic Succession of Pulses*

G. G. MACFARLANE†, ASSOCIATE, IRE

*Summary*—**An analysis is presented of the effect of (i) irregularities in the amplitude of pulses, and (ii) jitter in the repetition rate on the energy-spectrum of a succession of pulses.**

**In both cases the spectrum has two components: (a) a line spectrum, and (b) a continuous spectrum. In case (i), the envelope of both spectra is proportional to the envelope of the energy-spectrum of a single pulse and the lines in the line spectrum are spaced by the repetition frequency (see Figs. 1 and 2). In case (ii), the envelopes of the spectra are not the same as the envelope of a single pulse, and the lines are spaced by the mean repetition frequency (see Figs. 3 and 4).**

## I. Introduction

IN THE FREQUENCY analysis of a succession of pulses it is generally assumed that the spacing and amplitude of pulses are perfectly constant. This allows the spectrum to be calculated by straightforward Fourier analysis. However, in practice owing to causes which may be systematic or random, all pulses are not equally spaced and/or do not have exactly the same amplitude. This paper is devoted to the description of a method for calculating the energy-frequency spectrum of such an almost periodic succession of pulses in which the irregularity occurs in a random way.

The method is illustrated in two cases of special interest. In the first, the pulses have all the same shape and are regularly spaced, but they vary in amplitude in a random manner about a mean value. The output from a superregenerative receiver operated in the linear mode is like this. In the second, the pulses are identically the same, but their spacing varies in a random manner about a mean spacing. Barkhausen noise in a magnetic amplifier is thought to be like this. The first case considered is PAM (pulse amplitude modulation) and the second is PPM (pulse position modulation), each using fluctuation noise as the modulation wave.

* Decimal classification: R148.6. Original manuscript received by the Institute, December 9, 1948.
† Ministry of Supply, Telecommunications Research Establishment, Great Malvern, England.

## II. The Energy Spectrum of a Regular Succession of Pulses All of the Same Shape, But of Different Amplitudes

We shall firstly derive an expression for the spectral energy-density of $2N+1$ pulses in terms of the amplitudes $a_n$ of the pulses.

Let the spectrum of a single pulse of unit amplitude occurring at zero time be $G(\omega)$. The spectrum of the same pulse occurring at time $t$ is

$$G(\omega)\exp(i\omega t). \tag{1}$$

The spectrum of $2N+1$ pulses spaced $T$ apart and

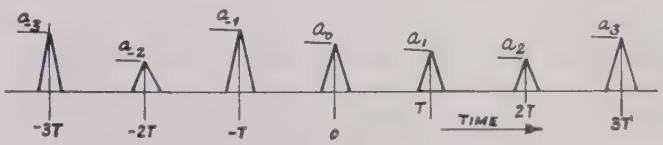


Fig. 1—A regular succession of similar pulses of different amplitudes.

with amplitudes $a_n$, as shown in Fig. 1, is the sum of the spectra of the individual pulses, and is therefore

$$S(\omega)=G(\omega)\sum_{-N}^{N}a_n\exp(in\omega T).. \tag{2}$$

The spectral energy density, which is the mean value of the square of the modulus of $S(\omega)$ per unit time, is

$$\begin{aligned}R_N(\omega)&=\frac{\overline{|S(\omega)|^2}}{(2N+1)T}\\&=\frac{\overline{|G(\omega)|^2}}{T}\left\{\frac{1}{2N+1}\left|\sum_{-N}^{N}a_n\exp(in\omega T)\right|^2\right\}_{\text{Av.}}\\&=\frac{\overline{|G(\omega)|^2}}{T}\left\{\frac{1}{2N+1}\left[\sum_{-N}^{N}a_n\cos(n\omega T)\right]^2\right.\end{aligned}$$

$$+\frac{1}{2N+1}\left[\sum_{-N}^{N} a_n \sin(n\omega T)\right]^2\Bigg\}_{\text{Av.}}. \qquad (3)$$

For an infinite succession of pulses the spectral energy-density is

$$R(\omega) = \lim_{N\to\infty} R_N(\omega). \qquad (4)$$

Let us now assume that the amplitudes $a_n$ are randomly distributed, and that the probability of the amplitude $a_n$ having a value between $x$ and $x+dx$ is $q_n(x)dx$. The function $q_n(x)$ is called the probability function. In order to evaluate the spectral energy-density, equation (4), we require to know the mean-square values of the sums

$$\sum_{N}^{N} a_n \cos(n\omega T), \qquad \sum_{-N}^{N} a_n \sin(n\omega T). \qquad (5)$$

They are readily obtained when we know the probability functions $P_N$ of these sums. We can find the functions $P_N$ in the following way.

Suppose the probability function of the random variable $x$ is $q(x)$, then the probability function $p_n(y)$ of an arbitrary function $y=f_n(x)$ is obtained from $q(x)$ by substituting

$$x = F_n(y), \qquad (6)$$

where $F_n(y)$ is the inverse of $f_n(x)$.

Thus

$$y = f_n(x). \qquad (7)$$

This gives

$$p_n(y) = q\{F_n(y)\}\frac{dF_n(y)}{dy}. \qquad (8)$$

Furthermore, there is a theorem in the theory of probability[1] which states that the mean and the mean-square deviation of the sum of any number of probability distributions is the sum of the means and the mean-square deviations respectively of the component distributions. By the sum of the probability distributions, $p_n(x)$, is meant the probability distribution of the sum of a number of functions $f_n(x)$ of the random variable $x$. Thus the sum of two probability distributions $p_1(x)$ and $p_2(x)$ is not $p_1(x)+p_2(x)$, but

$$\int_{-\infty}^{+\infty} p_1(x-y)p_2(y)dy. \qquad (9)$$

This theorem is directly applicable to our case, for we seek to find the mean-square value $\overline{x_N^2}$ of the sum $\sum_{-N}^{N} f_n(x)$ of $2N+1$ functions of the random variable $x$, and this is equal to the sum of the square of the mean, $(\bar{a}_N)^2$, and the mean-square deviation, $\rho_N^2$, of $\sum_{-N}^{N} f_n(x)$. Or

$$\overline{x_N^2} = \rho_N^2 + (\bar{a}_N)^2; \qquad (10)$$

[1] S. Chandrasekhar, "Stochastic problems in physics and astronomy," *Rev. Mod. Phys.*, vol. 15, pp. 2–89; January, 1943.

while the theorem above states that

$$\bar{a}_N = \sum_{-N}^{N} X_n \qquad (11)$$

and

$$\rho_N^2 = \sum_{-N}^{N} \sigma_n^2, \qquad (12)$$

where $X_n$ is the mean and $\sigma_n^2$ the mean-square deviation of the distribution $p_n(x)$ of the function $f_n(x)$. That is,

$$X_n = \int x p_n(x)dx = \int_{-\infty}^{+\infty} f_n(x)q(x)dx \qquad (13)$$

and

$$\sigma_n^2 = \int (x - X_n)^2 p_n(x)dx = \int_{-\infty}^{+\infty} [f_n(x) - X_n]^2 q(x)dx. \qquad (14)$$

Herein use is made of (8) to express $X_n$ and $\sigma_n^2$ in terms of the probability function $q(x)$ of the random variable $x$.

Having established these general formulas, let us return to the discussion of (3) for the spectral energy-density. Consider the series

$$\sum_{-N}^{N} f_n(a_n) = \sum_{-N}^{N} a_n \sin(n\omega T). \qquad (15)$$

Here

$$f_n(x) = x \sin(n\omega T).$$

Therefore, from (13) and (14),

$$X_n = \sin(n\omega T)\int_{-\infty}^{+\infty} xq(x)dx = \sin(n\omega T)\overline{A}, \text{ say,} \qquad (16)$$

and

$$\sigma_n^2 = \sin^2(n\omega T)\int_{-\infty}^{\infty} (x - \overline{A})^2 q(x)dx = \sin^2(n\omega T)\overline{(A - \overline{A})^2}, \text{ say.} \qquad (17)$$

Substitute $X_n$ and $\sigma_n^2$ from (16) and (17) into (10) to (12). This gives the mean-square value of the sum (15).

$$\left\{\left[\sum_{-N}^{N} a_n \sin(n\omega T)\right]^2\right\}_{\text{Av.}} = \overline{(A - \overline{A})^2}\sum_{-N}^{N} \sin^2(n\omega T) + (\overline{A})^2\left[\sum_{-N}^{N} \sin(n\omega T)\right]^2. \qquad (18)$$

Similarly,

$$\left\{\left[\sum_{-N}^{N} a_n \cos(n\omega T)\right]^2\right\}_{\text{Av.}}$$

$$= (A - \bar{A})^2 \sum_{-N}^{N} \cos^2 (n\omega T) + (\bar{A})^2 \left[ \sum_{-N}^{N} \cos (n\omega T) \right]^2. \quad (19)$$

Therefore,

$$\left\{ \frac{1}{2N+1} \left| \sum_{-N}^{N} a_n \exp (in\omega T) \right|^2 \right\}_{Av} = \overline{(A - \bar{A})^2} + \frac{(\bar{A})^2}{2N+1} \left[ \sum_{-N}^{N} \sin (n\omega T) \right]^2 + \frac{(\bar{A})^2}{2N+1} \left[ \sum_{-N}^{N} \cos (n\omega T) \right]^2. \quad (20)$$

Now let the number of pulses increase indefinitely, so that we can let $N \to \infty$. But

$$\lim_{N\to\infty} \frac{1}{2N+1} \left[ \sum_{-N}^{N} \sin (n\omega T) \right]^2 = 0$$

for all values of $\omega T$ and

$$\lim_{N\to\infty} \frac{1}{2N+1} \left[ \sum_{-N}^{N} \cos (n\omega T) \right]^2 = \frac{2\pi}{T} \delta\left(\omega - \frac{2m\pi}{T}\right),$$

where $\delta(x)$ is the unit impulse function of Dirac which is infinite at $x=0$ but zero everywhere else, although the integral of $\delta(x)$ over any range including the point $x=0$ is unity. The spectral energy-density of an infinite succession of pulses of equal spacing, $T$, and similar shape but with amplitudes which are randomly distributed according to the probability function $q(x)$ is therefore

$$R(\omega) = \lim_{N\to\infty} R_N(\omega) \left[ \overline{(A-\bar{A})^2} + (\bar{A})^2 \frac{2\pi}{T} \delta\left(\omega - \frac{2m\pi}{T}\right) \right] \frac{|G(\omega)|^2}{T}, \quad (21)$$

where

$$\bar{A} = \int_{-\infty}^{+\infty} x q(x) dx \quad (22)$$

and

$$\overline{(A - \bar{A})^2} = \int_{-\infty}^{+\infty} (x - \bar{A})^2 q(x) dx. \quad (23)$$

The energy spectrum consists of two distinct component spectra (i) a continuous distribution of density $\overline{(A-\bar{A})^2}|G(\omega)|^2/T$ with intensity proportional to the spectral density of a single pulse (Fig. 2a), and (ii) a line spectrum with separation of lines in frequency by $1/T$, the recurrence frequency of the pulses. The power in the line of frequency $m/T$ is

$$\frac{2\pi}{T} \frac{(\bar{A})^2}{T} \left| G\left(\frac{2m\pi}{T}\right) \right|^2.$$

If the power in the lines is plotted against frequency, the power spectrum of Fig. 2(b) is obtained. The envelope of the lines is proportional to the spectral density of a single pulse.

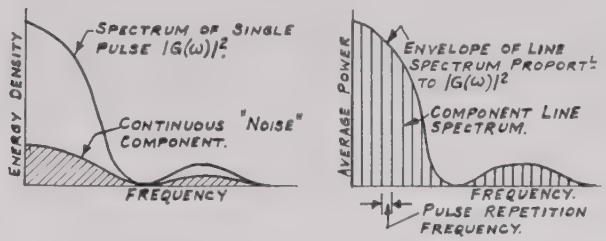


(a) (b)

Figs. 2—Spectrum of pulses of Fig. 1 has two parts: (i) Continuous energy-density spectrum shown in Fig. 2a. (ii) Line spectrum with power distributed as shown in Fig. 2b.

It is also of interest to know how the total power is divided between the continuous and the line spectra. The ratio is

$$\frac{\text{Power in continuous part}}{\text{Power in lines}} = \frac{\overline{(A-\bar{A})^2}}{(\bar{A})^2} \frac{\int_{-\infty}^{+\infty} |G(\omega)|^2 d\omega}{\sum_{-\infty}^{+\infty} \left| G\left(\frac{2m\pi}{T}\right) \right|^2 \frac{2\pi}{T}} \simeq \frac{\overline{(A-\bar{A})^2}}{(\bar{A})^2}. \quad (24)$$

The following example from the theory of the superregenerative receiver[2] under certain operating conditions will illustrate the use of these formulas. The output from the oscillator circuit of a superregenerative receiver is a regular succession of similar pulses with amplitudes which depend on the voltage of the incoming signal and on the noise present in the input circuit. It may be shown that these pulses have amplitudes $x$ which are distributed according to the probability function

$$q(x) = \frac{x}{\sigma^2} \exp\left[ -\frac{V^2 + x^2}{2\sigma^2} \right] I_0\left(\frac{Vx}{\sigma^2}\right), \quad (25)$$

where $V$ is the peak amplitude to which oscillations would build up from the incoming cw signal alone in the absence of any noise, and $\sigma$ is the root-mean-square noise voltage at the peak of the pulse, and $I_0$ is the modified Bessel function of order zero. $V^2/2\sigma^2$ is therefore the signal-to-noise power ratio before rectification of the pulses. $V/\sigma$ is the peak signal to root-mean-square noise voltage before rectification.

Substituting $q(x)$ from (25) into (21) we get, after some rearrangement,

$$\bar{A} = \sigma \sqrt{\frac{\pi}{2}} \exp\left(-\frac{r^2}{4}\right) \left[ \left(1 + \frac{r^2}{2}\right) I_0\left(\frac{r^2}{4}\right) + \frac{r^2}{2} I_1\left(\frac{r^2}{4}\right) \right] \quad (26)$$

and

$$\overline{(A-\overline{A})^2} = 2\sigma^2\left(1+\frac{r^2}{2}\right) - (\overline{A})^2, \tag{27}$$

where $r = V/\sigma$.

The energy spectrum is then obtained from (21). The ratio of power in the continuous part of the spectrum to power in the lines is thus determined. For a discussion of these results, reference should be made to the paper by Macfarlane and Whitehead.[2]

In the next section, we shall apply the method to another interesting example.

## III. The Energy Spectrum of a Succession of Identical Pulses of Uneven Spacing

Let the spectrum of a single pulse occurring at time $t=0$ be $G(\omega)$ and let the average periodicity be $T$. The spectrum of $2N+1$ pulses, as shown in Fig. 3, is therefore

$$S(\omega) = G(\omega)\sum_{-N}^{N}\exp\left[i\omega(nT+a_n)\right]. \tag{28}$$

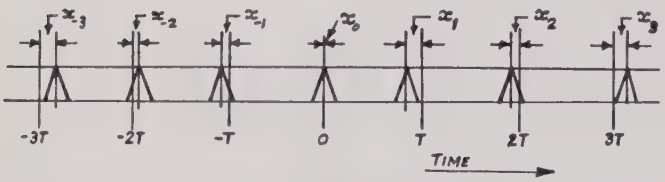


Fig. 3—Succession of identical pulses of uneven spacing.

Let the values $a_n$, which are the time intervals by which the pulses are delayed beyond their mean positions, be subject to a Gaussian probability distribution with mean of value zero and with root-mean-square deviation $\sigma$. Thus

$$q(a_n) = \frac{1}{\sigma\sqrt{2\pi}}\exp\left(-a_n^2/2\sigma^2\right). \tag{29}$$

We shall further assume that the deviation of $a_n$ from the mean value zero is small compared with $T$, the average time interval between pulses.

Following (3) we find that the energy spectrum of a succession of $2N+1$ pulses is

$$R_N(\omega) = \frac{|G(\omega)|^2}{T}\frac{1}{2N+1}\left\{\left[\sum_{-N}^{N}\cos\omega(nT+a_n)\right]^2 + \left[\sum_{-N}^{N}\sin\omega(nT+a_n)\right]^2\right\}_{\text{Av.}}. \tag{30}$$

In the limit when $N\to\infty$ $R_N(\omega)$ becomes the required spectral energy-density.

The terms $\begin{matrix}\sin\\ \cos\end{matrix}\left(\omega\cdot\overline{nT+x}\right)$ are now the functions $f_n(x)$ of the random variable $x$. For the first of these two, we have

$$f_n(x) = \sin\omega(nT+x).$$

From (13) and (14) the mean value and the square of the standard deviation of the probability distribution of $\sin\omega(nT+x)$ are, respectively,

$$X_n = \frac{1}{\sigma\sqrt{2\pi}}\int_{-\infty}^{+\infty}\sin\omega(nT+x)\exp\left(-\frac{x^2}{2\sigma^2}\right)dx = \exp\left(-\tfrac{1}{2}\sigma^2\omega^2\right)\sin(n\omega T) \tag{31}$$

and

$$\sigma_n^2 = \frac{1}{\sigma\sqrt{2\pi}}\int_{-\infty}^{+\infty}\sin^2\omega(nT+x)\exp\left(-\frac{x^2}{2\sigma^2}\right)dx - X_n^2 = \tfrac{1}{2}\left[1-\exp\left(-2\sigma^2\omega^2\right)\right] - \left[1-\exp\left(-\sigma^2\omega^2\right)\right]\exp\left(-\sigma^2\omega^2\right)\sin^2(n\omega T). \tag{32}$$

Therefore, from (10) and (11) the mean-square value of $\sum_{-N}^{N}f_n(x)$ is

$$\left\{\left[\sum_{-N}^{N}\sin\omega(nT+a_n)\right]^2\right\}_{\text{Av.}} = \frac{2N+1}{2}\left[1-\exp\left(-2\sigma^2\omega^2\right)\right] + \exp\left(-\sigma^2\omega^2\right)\left[\sum_{-N}^{N}\sin(n\omega T)\right]^2 - \exp\left(-\sigma^2\omega^2\right)\left[1-\exp\left(-\sigma^2\omega^2\right)\right]\sum_{-N}^{N}\sin^2(n\omega T).$$

Similarly

$$\left\{\left[\sum_{-N}^{N}\cos\omega(nT+a_n)\right]^2\right\}_{\text{Av.}} = \frac{2N+1}{2}\left[1-\exp\left(-2\sigma^2\omega^2\right)\right] + \exp\left(-\sigma^2\omega^2\right)\left[\sum_{-N}^{N}\cos(n\omega T)\right]^2 - \exp\left(-\sigma^2\omega^2\right)\left[1-\exp\left(-\sigma^2\omega^2\right)\right]\sum_{-N}^{N}\cos^2(n\omega T).$$

Therefore

$$\left\{\frac{1}{2N+1}\left|\sum_{-N}^{N}\exp\left\{i\omega(nT+a_n)\right\}\right|^2\right\}_{\text{Av.}} = 1-\exp\left(-\sigma^2\omega^2\right) + \frac{\exp\left(-\sigma^2\omega^2\right)}{2N+1}\left\{\left[\sum_{-N}^{N}\sin(n\omega T)\right]^2 + \left[\sum_{-N}^{N}\cos(n\omega T)\right]^2\right\}.$$

The energy spectrum is now obtained as before by letting $N\to\infty$. The result is

[2] G. G. Macfarlane and J. R. Whitehead, "The theory of the super-regenerative receiver operated in the linear mode," *Jour. IEE*, vol. 95, pp. 143–157; Part III, No. 35, May, 1948.

$$R(\omega) = \left\{1 - \exp(-\sigma^2\omega^2) + \exp - (\sigma^2\omega^2)\frac{2\pi}{T}\delta\left(\omega - \frac{2m\pi}{T}\right)\right\}\frac{|G(\omega)|^2}{T}. \quad (33)$$

Here again the energy spectrum consists of two distinct component spectra: a continuous spectrum and a line spectrum. If the pulses recurred with perfectly regular intervals $\sigma$ would be zero, and the spectrum would be solely a line spectrum. The average power in the lines would then be

$$\frac{2\pi}{T}\int_{-\infty}^{+\infty}\frac{|G(\omega)|^2}{T}\delta\left(\omega - \frac{2m\pi}{T}\right)d\omega = \frac{1}{T}\sum_{-\infty}^{+\infty}\left|G\left(\frac{2m\pi}{T}\right)\right|^2\frac{2\pi}{T} \simeq \frac{1}{T}\int_{-\infty}^{+\infty}|G(\omega)|^2 d\omega. \quad (34)$$

When, however, the repetition rate is not steady, the average power in the lines is reduced to

$$\frac{1}{T}\sum_{-\infty}^{+\infty}\left|G\left(\frac{2m\pi}{T}\right)\right|^2\exp\left(-\frac{4m^2\pi^2\sigma^2}{T^2}\right)\frac{2\pi}{T} \simeq \frac{1}{T}\int_{-\infty}^{+\infty}\exp(-\sigma^2\omega^2)|G(\omega)|^2 d\omega, \quad (35)$$

and energy is distributed continuously over the frequency band of a single pulse. The power in this continuous spectrum is noise power. The ratio of signal-to-noise powers is approximately

$$\frac{\int_{-\infty}^{+\infty}\exp(-\sigma^2\omega^2)|G(\omega)|^2 d\omega}{\int_{-\infty}^{+\infty}\{1 - \exp(-\sigma^2\omega^2)\}|G(\omega)|^2 d\omega}. \quad (36)$$

There is a difference in the forms of the energy spectra given by (21) and (33), which is interesting. In (21),

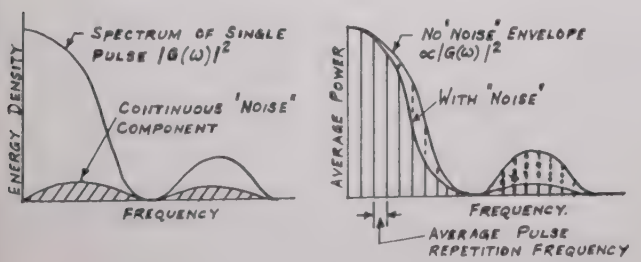


(a) (b)

Figs. 4—Spectrum of pulses of Fig. 3.
(a)—Illustrating continuous noise component.
(b)—Line spectrum.

where the pulse amplitudes are irregular, the form of the envelope of the energy-density spectrum of the noise component and the power spectrum of the lines is the same as the energy-density spectrum of a single pulse. In (33) however, this is not the case, for the factors multiplying $|G(\omega)|^2$ depend on $\omega$. Thus, the form of the envelope is altered for both signal line-spectrum and noise continuous-spectrum. The form of the energy-density spectrum of the noise is approximately $\omega^2$ times that of a single pulse. This is illustrated in Figs. 4(a) and 4(b).

## IV. The Spectrum of Regular Pulses of Unequal Length

The method of finding the energy-frequency spectrum of a temporal variation used in the two problems discussed in parts II and III, is applicable to many more cases. The above examples have been chosen for their practical importance. A further example would be the output from a superregenerative receiver operated in logarithmic mode. Successive pulses are then unequal in duration due to the noise in the input circuit.

If the spacing of pulses is $T$ and the spectrum of a pulse occurring at zero time is $G(\omega, x)$ where $x$ is the random variable that defines the pulse width, then the spectral energy-density is

$$R(\omega) = \frac{1}{T}\left\{\overline{(A - \overline{A})^2} + \frac{2\pi}{T}\delta\left(\omega - \frac{2m\pi}{T}\right)(\overline{A})^2\right\}.$$

In this equation

$$\overline{A} = \int_{-\infty}^{+\infty} G(\omega, x)q(x)dx,$$

$$\overline{(A - \overline{A})^2} = \int_{-\infty}^{+\infty} G^2(\omega, x)q(x)dx - (\overline{A})^2,$$

and $q(x)$ is the probability function.

If the pulses are all rectangular of amplitude $1/\tau$ and of mean width $\tau$, and if the distribution function is Gaussian about zero as mean with standard deviation $\sigma$

$$\overline{A} = \frac{1}{\omega}\int_{-\omega/2}^{\omega/2}\exp(iy\tau - 2\sigma^2y^2)dy$$

and

$$\overline{(A-\overline{A})^2} = \frac{1}{\omega^2}\int_{-\omega/2}^{\omega/2}dy\int_{y-\omega/2}^{y+\omega/2}\exp(i\tau x - 2\sigma^2x^2)dx - (\overline{A})^2.$$

## Acknowledgment

The author desires to thank the Chief Scientist, Ministry of Supply, England, for permission to publish this paper, which is reproduced with permission of the Controller of His Britannic Majesty's Stationery Office. British Crown Copyright reserved.

# Problems Related to Measuring the Field Strength of High-Frequency Electromagnetic Fields*

ROHN TRUELL†, SENIOR MEMBER, IRE

*Summary*—Discussion and comparison of the analysis of two cases of an electron of uniform velocity acted on by a uniform magnetic field parallel to the electron direction, and a high-frequency electromagnetic field with the electric component transverse to the beam, shows that, for both a plane parallel-plate field and a rectangular cavity field, the field amplitude may be expressed quite simply in terms of easily measurable parameters. The simple relationship in question requires that certain velocity conditions on the electron velocity be observed, and that the cyclotron frequency $|e|H/mc$ be equal to the frequency of the alternating electromagnetic field.

## Introduction

IN A PREVIOUS paper[1] the problem of an electron beam directed parallel to a uniform magnetic field and subjected to a transverse high-frequency electromagnetic field was discussed for a case where the alternating electromagnetic field was produced between two plane parallel plates, while the electron beam was directed along an axis midway between the plates.

The purpose of this paper is to present a more complete treatment of the parallel-plate case, and the extension to the case of a rectangular cavity. In the discussion presented here there appear certain velocity conditions on the electron beam which are necessary, if one wants to have the solutions in the simplest and most convenient form. The conditions mentioned did not appear in the earlier discussion because the analysis there was not carried out in sufficient detail.

## Plane Parallel-Plate Case

The plane parallel-plate situation is shown in Fig. 1. The electron beam of uniform velocity $v_z$ is introduced

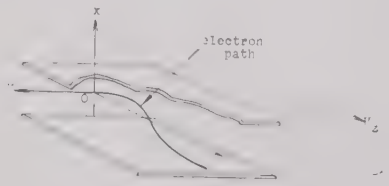


Fig. 1

at 0 in Fig. 1, with a uniform magnetic field $H_z$ as indicated. The electric component of the rapidly alternating electromagnetic field is $E_x$, and at any time $t$, $E_x$ is considered to be constant in magnitude over the region between the plates. The fringe field effect was discussed in the previous paper. The quantities $H_z$, $v_z$, and $E_x$ determine the motion of an electron.

The equations of motion and the differential equations to be solved are:

$$m\ddot{x} = -|e|E_x - \frac{|e|}{c}\dot{y}H_z \qquad \left.\begin{array}{ll} x=0 & \dot{x}=0 \\ y=0 & \dot{y}=0 \\ z=0 & \dot{z}=v_z \end{array}\right\} \text{ at } t=t_0,$$

$$m\ddot{y} = \frac{|e|}{c}\dot{x}H_z$$

$$m\ddot{z} = 0$$

where $t_0$ is the time of entrance of the electron into the field region. Using $E_x = E_{0x}\sin\omega t$, one has:

$$\ddot{x}+\omega_c^2 x = K_2\sin\omega t \qquad \ddot{y}+\omega_c^2 y = -\frac{\omega_c K_2}{\omega}(\cos\omega t - \cos\omega t_0$$

where

$$\omega_c = \frac{|e|H_z}{mc} \quad \text{and} \quad K_2 = -\frac{|e|}{m}E_{0x};$$

the complete solution for the $x$ equation is:

$$x = Ax_1(t) + Bx_2(t) + K_2\int_{s=t_0}^{s=t}\begin{vmatrix} x_1(s) & x_2(s) \\ x_1(t) & x_2(t) \\ \hline x_1(s) & x_2(s) \\ x_1'(s) & x_2'(s) \end{vmatrix}\sin\omega s\,ds$$

where

$$x_1(t) = e^{i\omega_c t}, \qquad x_2(t) = e^{-i\omega_c t}.$$

It turns out that only the particular solution, given by the integral, contributes to our solution. The particular solution in $x$ is:

$$x = -\frac{K_2}{\omega_c}\left[\frac{\sin(\omega_c-\omega)t - \sin(\omega_c-\omega)t_0}{2(\omega_c-\omega)} - \frac{\sin(\omega_c+\omega)t - \sin(\omega_c+\omega)t_0}{2(\omega_c+\omega)}\right]\cos\omega_c t$$
$$+\frac{K_2}{\omega_c}\left[\frac{\cos(\omega_c-\omega)t - \cos(\omega_c-\omega)t_0}{2(\omega_c-\omega)} - \frac{\cos(\omega_c+\omega)t - \cos(\omega_c+\omega)t_0}{2(\omega_c+\omega)}\right]\sin\omega_c t.$$

When $\omega=\omega_c$ the expression becomes:

$$x = -\frac{K_2}{2\omega_c}(t-t_0)\cos\omega_c t + \frac{K_2}{2\omega_c^2}[\sin\omega_c t - \sin\omega_c t_0\cos\omega_c(t-t_0)];$$

the corresponding solution in $y$ is:

$$y = -\frac{K_2}{2\omega_c}(t-t_0)\sin\omega_c t$$

* Decimal classification: R139×R270. Original manuscript received by the Institute, November 29, 1948; revised manuscript received, March 22, 1949.

† Brown University, Providence, R. I.

[1] Rohn Truell, "A method of measuring the field strength of high-frequency electromagnetic fields," PROC. I.R.E., vol. 36, pp. 1249–1252; October, 1948.

$$+\frac{K_2}{2\omega_c^2}\left[2\cos\omega_c t_0(1-\cos\omega_c(t-t_0))\right.$$
$$\left.+\sin\omega_c t_0\sin\omega_c(t-t_0)\right].$$

Let $(t-t_0)$ be the transit time $\tau$ for the electron in the region between the plates. The relations for $x$ and $y$ become:

$$x=-\frac{K_2}{2\omega_c}\tau\cos\omega_c(t_0+\tau)$$
$$+\frac{K_2}{2\omega_c^2}\left[\sin\omega_c(t_0+\tau)-\sin\omega_c t_0\cos\omega_c\tau\right]$$
$$y=-\frac{K_2}{2\omega_c}\tau\sin\omega_c(t_0+\tau)$$
$$+\frac{K_2}{2\omega_c^2}\left[2\cos\omega_c t_0(1-\cos\omega_c\tau)+\sin\omega_c t_0\sin\omega_c\tau\right].$$

If we regard $\omega_c$ and $\tau$ as fixed quantities, $x$ and $y$ are functions of the entrance time $t_0$. In other words, the distance $r$ of an electron from the $z$ axis in a plane $z$=constant at the exit end of the plates is a function only of $t_0$. It is apparent on looking at the component expressions for $x$ and $y$ that this expression for $r$ is in general complicated. If, however, we impose the condition:

$$\omega_c\tau=n\pi,\qquad n \text{ even}$$

the expressions for $x$ and $y$ become simply:

$$x=-\frac{K_2}{2\omega_c}\tau\cos\omega_c(t_0+\tau)$$
$$y=-\frac{K_2}{2\omega_c}\tau\sin\omega_c(t_0+\tau);$$

hence

$$r=\frac{K_2}{2\omega_c}\tau$$

since

$$\tau=\frac{z_0}{v_z}\quad\text{and}\quad K_2=-\frac{|e|}{m}E_{0z}$$
$$|E_{0z}|\doteq\left|\frac{2\omega_c r v_z}{\frac{|e|}{m}z_0}\right|=\left(\frac{2rv_zH_z}{z_0c}\right)\text{esu/cm.}$$

($z_0$ is the length of the plates).

It has been pointed out in (1) that neglecting the fringe field can introduce considerable error if the above expression is used to relate $E_{0z}$ to $r$, depending on the geometry and the frequency.

## Cavity Case

The use of a rectangular cavity (Fig. 2) in place of the parallel plates avoids the need of considering the fringe

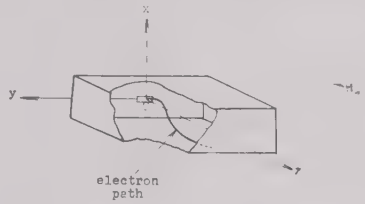


Fig. 2

field question. The equations of motion for an electron are as before except that the field $E_z$ now has a space dependence in the variables $y$ and $z$.

$$m\ddot{x}=-|e|\left(E_z+\frac{1}{c}\dot{y}H_z\right)\qquad x=0\ \dot{x}=0$$
$$m\ddot{y}=\frac{|e|}{c}\dot{x}H_z\qquad y=0\ \dot{y}=0$$
$$z=0^e\ \dot{z}=v_z\Big\}\ \text{at } t=t_0$$

$$E_z=E_{0z}\cos\frac{\pi}{y_0}y\sin\frac{\pi}{z_0}z\sin\omega t$$

(for the lowest mode in a rectangular cavity).

Now the quantity $\cos\pi/y_0\,y\cong1$ in the region of the electron path and is a slowly varying function as long as the beam deflection $r$ remains small in comparison with $y_0$. We write $z=v_z(t-t_0)$ where $t_0$ is the time of entrance of the electron into the cavity at $x=0$, $y=0$, $z=0$. Now with $E_z=E_{0z}\sin\pi/z_0\,v_z(t-t_0)\sin\omega t$ the differential equations in $x$ and $y$ are:

$$\ddot{x}+\omega_c^2x=K_2\sin b(t-t_0)\sin\omega t\qquad b\equiv\left(\frac{\pi}{z_0}v_z\right).$$
$$\ddot{y}+\omega_c^2\dot{y}=\omega_cK_2\sin b(t-t_0)\sin\omega t$$

The particular solutions are given by:

$$x=-\frac{K_2}{\omega_c}\int_{s=t_0}^{s=t}\sin\omega_c(s-t)\sin b(s-t_0)\sin\omega s\,ds$$
$$y=\frac{K_2}{\omega_c}\int_{s=t_0}^{s=t}(1-\cos\omega_c(s-t))\sin b(s-t_0)\sin\omega s\,ds,$$

and from the first of the two integrals one obtains:

$$x=\frac{K_2}{4\omega_c}\cos\omega_c t\cos bt_0\left\{\frac{\cos(-\omega_c+\omega+b)t-\cos(-\omega_c+\omega+b)t_0}{(-\omega_c+\omega+b)}-\frac{\cos(\omega_c+\omega+b)t-\cos(\omega_c+\omega+b)t_0}{(\omega_c+\omega+b)}\right.$$
$$\left.+\frac{\cos(\omega_c+\omega-b)t-\cos(\omega_c+\omega-b)t_0}{(\omega_c+\omega-b)}+\frac{\cos(\omega_c-\omega+b)t-\cos(\omega_c-\omega+b)t_0}{(\omega_c-\omega+b)}\right\}$$
$$+\frac{K_2}{4\omega_c}\sin\omega_c t\cos bt_0\left\{-\frac{\sin(-\omega_c+\omega+b)t-\sin(-\omega_c+\omega+b)t_0}{(-\omega_c+\omega+b)}-\frac{\sin(\omega_c+\omega+b)t-\sin(\omega_c+\omega+b)t_0}{(\omega_c+\omega+b)}\right.$$
$$\left.+\frac{\sin(\omega_c+\omega-b)t-\sin(\omega_c+\omega-b)t_0}{(\omega_c+\omega-b)}+\frac{\sin(\omega_c-\omega+b)t-\sin(\omega_c-\omega+b)t_0}{(\omega_c-\omega+b)}\right\}$$

$$+\frac{K_2}{4\omega_c}\cos\omega_c t\sin bt_0\left\{\frac{\sin(-\omega_c+\omega+b)t-\sin(-\omega_c+\omega+b)t_0}{(-\omega_c+\omega+b)}-\frac{\sin(\omega_c+\omega+b)t-\sin(\omega_c+\omega+b)t_0}{(\omega_c+\omega+b)}\right.$$
$$\left.-\frac{\sin(\omega_c+\omega-b)t-\sin(\omega_c+\omega-b)t_0}{(\omega_c+\omega-b)}+\frac{\sin(\omega_c-\omega+b)t-\sin(\omega_c-\omega+b)t_0}{(\omega_c-\omega+b)}\right\}$$
$$+\frac{K_2}{4\omega_c}\sin\omega_c t\sin bt_0\left\{\frac{\cos(-\omega_c+\omega+b)t-\cos(-\omega_c+\omega+b)t_0}{(-\omega_c+\omega+b)}+\frac{\cos(\omega_c+\omega+b)t-\cos(\omega_c+\omega+b)t_0}{(\omega_c+\omega+b)}\right.$$
$$\left.+\frac{\cos(\omega_c+\omega-b)t-\cos(\omega_c+\omega-b)t_0}{(\omega_c+\omega-b)}-\frac{\cos(\omega_c-\omega+b)t-\cos(\omega_c-\omega+b)t_0}{(\omega_c-\omega+b)}\right\}.$$

There are four values of $\omega$, ($\omega=\omega_c\pm b$ and $\omega=-\omega_c\pm b$) for which various terms in $x$ become indeterminate. In the parallel-plate case the corresponding situation arose only for $\omega=\pm\omega_c$. Consider now one of the four possible cases for which $\omega=\omega_c-b$; when the indeterminate terms are subjected to l'Hospital's rule one obtains:

$$x=\frac{K_2}{4\omega_c}\left\{-(t-t_0)\sin(\omega_c t-bt_0)\right.$$
$$+\frac{1}{(\omega_c-b)}[\sin(\omega_c-b)t\sin b(t-t_0)$$
$$-\sin(\omega_c-b)t_0\sin\omega_c(t-t_0)]$$
$$+\frac{1}{b}[\sin bt\sin[\omega_c t_0+(\omega_c-b)(t-t_0)]-\sin bt_0\sin\omega_c t]$$
$$\left.+\frac{1}{\omega_c}[\sin\omega_c t_0\sin[\omega_c(t-t_0)+bt_0]-\sin\omega_c t\sin bt_0]\right\}.$$

The corresponding expression for $y$ when $\omega=\omega_c-b$ is similar to that for $x$, but contains additional terms:

$$y=\frac{K_2}{4\omega_c}\left\{(t-t_0)\cos(\omega_c t-bt_0)\right.$$
$$-\frac{1}{(\omega_c-b)}[\sin(\omega_c-b)t\cos b(t-t_0)$$
$$-\cos\omega_c(t-t_0)\sin(\omega_c-b)t_0]$$
$$-\frac{1}{b}[\sin bt\cos[\omega_c t-b(t-t_0)]-\cos\omega_c t\sin bt_0]$$
$$+\frac{1}{\omega_c}[\sin\omega_c t\cos bt_0-\sin\omega_c t_0\cos[\omega_c(t-t_0)+bt_0]$$
$$-2\sin(\omega_c t-bt_0)+2\sin(\omega_c-b)t_0]$$
$$\left.+\frac{1}{(\omega_c-2b)}[2\sin[(\omega_c-b)t-b(t-t_0)]-2\sin(\omega_c-b)t_0]\right\}.$$

Let $(t-t_0)=\tau$, the transit time from entering cavity at $z=0$ to opposite end of cavity at $z=z_0$.

$$x=\frac{K_2}{4\omega_c}\left\{-\tau\sin[\omega_c(t_0+\tau)-bt_0]\right.$$
$$+\frac{1}{(\omega_c-b)}[\sin(\omega_c-b)(t_0+\tau)\sin b\tau-\sin(\omega_c-b)t_0\sin\omega_c\tau]$$
$$+\frac{1}{b}[\sin b(t_0+\tau)\sin[\omega_c t_0+(\omega_c-b)\tau]$$
$$-\sin bt_0\sin\omega_c(t_0+\tau)]$$
$$\left.+\frac{1}{\omega_c}[\sin(\omega_c\tau+bt_0)\sin\omega_c t_0-\sin\omega_c(t_0+\tau)\sin bt_0]\right\}.$$

$$y=\frac{K_2}{4\omega_c}\left\{\tau\cos[\omega_c(t_0+\tau)-bt_0]\right.$$
$$-\frac{1}{(\omega_c-b)}[\sin(\omega_c-b)(t_0+\tau)\cos b\tau-\cos\omega_c\tau\sin(\omega_c-b)t_0]$$
$$-\frac{1}{\omega_c}[\cos(\omega_c\tau+bt_0)\sin\omega_c t_0-\sin\omega_c(t_0+\tau)\cos bt_0$$
$$+2\sin(\omega_c(t_0+\tau)-bt_0)-2\sin(\omega_c-b)t_0]$$
$$-\frac{1}{b}[\sin b(t_0+\tau)\cos(\omega_c t_0+(\omega_c-b)\tau)$$
$$-\sin bt_0\cos\omega_c(t_0+\tau)]$$
$$\left.+\frac{2}{(\omega_c-2b)}[\sin(\omega_c-b)(t_0+\tau)-b\tau)-\sin(\omega_c-b)t_0]\right\}.$$

Now

$$b\equiv\frac{\pi}{z_0}v_z,$$

hence

$$b\tau=\frac{\pi}{z_0}v_z(t-t_0)=\frac{\pi}{z_0}z;$$

therefore, when $\tau$ is the transit time $(t\text{-}t_0)$ of the electron through the cavity in the $z$ direction, $z=z_0$ in the above expression, and

$$b\tau=\pi.$$

In addition, we may notice that use of the condition

$$(\omega_c-b)\tau=k\pi \qquad k \text{ odd}$$

will greatly simplify the expressions for $x$ and $y$.

Moreover, $b\tau=\pi$, making the above condition:

$$\omega_c\tau=(k+1)\pi \qquad k \text{ odd}$$

or

$$\omega_c\tau=n\pi \qquad n \text{ even},$$

so that this is the same condition on $\tau$ that was used in the parallel-plate case.

When one uses the condition just discussed, the expressions for $x$ and $y$ reduce to the following:

$$x = -\frac{K_2}{4\omega_c}\tau \sin (\omega_c - b)t_0$$

$$y = \frac{K_2}{4\omega_c}\tau \cos (\omega_c - b)t_0$$

then

$$r = \frac{K_2}{4\omega_c}\tau$$

and

$$|E_{0x}| = \frac{4v_z H_z r}{z_0 c}.$$

The quantity $E_{0x}$ has thus been obtained in magnitude in terms of the electron velocity $v_z$, the magnetic field $H_z$, the length of the cavity $z_0$, and the radius of the circle $r$; all measurable quantities in terms of which one can measure field strengths or compare field strengths. This expression differs by a factor of two from the expression for $|E_{0x}|$ in the plate case (neglecting fringe field).

The condition $\omega_c\tau = n\pi$ (with $n$ even) means that the electron velocity $v_z$ must take only selected-values given by:

$$v_z = \frac{\omega_c z_0}{n\pi} = \frac{2\nu_c z_0}{n} \qquad n \text{ even.}$$

If, for example, $\nu_c = 10^{10}$ cps and $z_0 = 3$ cm, $v_z = (6\times10^{10}/n)$, so that with $n = 100$, $v_z = 6\times10^8$ cm/sec (100 volt electrons). As $n$ becomes smaller and the corresponding value of $v_z$ increases, it becomes more important to adhere to the velocity condition, simply because the deviation of the $x$ and $y$ relations from the simple form derived will be larger when the velocity $v_z$ is such that $n$ is small and *not* even, than it will be when $n$ is large and *not* even. In other words, the larger the value of $v_z$, the more important it is that the velocity condition be adhered to, if one wants to use the simple relations obtained.

# Detection at Radio Frequencies by Superconductivity*

J. V. LEBACQZ†, MEMBER, IRE, C. W. CLARK‡, M. C. WILLIAMS†, AND D. H. ANDREWS†

*Summary*—**Detection of radio-frequency currents by superconducting columbium nitride has been studied as a function of rf current, bias current, and temperature. The existence of nonlinear resistance in the zone between super and normal conduction has been observed, with specially high values of $dR/dI$ for currents less than one ma; this is believed to be due to the effect of the magnetic field of the current superconductivity (Silsbee hypothesis). The observed values of $dR/dI$ account in a rough quantitative way for the observed rectified potentials and their variation with rf current, bias current, and temperature at 1 Mc. Increasing rectification at higher frequencies is observed, but not yet explainable.**

## INTRODUCTION

IN ONE OF the earliest series of experiments ever made at very low temperatures, the Dutch physicist, H. Kamerlingh Onnes, discovered[1] that many metals, when cooled to within a few degrees of absolute zero, suddenly lose all traces of electrical resistance and become perfect or "super" conductors. For any particular metal, the temperature interval in which this state of superconductivity is entered as the metal is cooled, is called the transition range. It is usually a zone a few hundredths of a degree wide, the midpoint of which is called the transition temperature.

This discovery was soon followed by another,[2] that although resistance had disappeared completely below the transition point, it could be restored by passing sufficient current through the metal, the amount of this restoring current increasing as the temperature was lowered further below the transition range. The resistance was also found to be restored by the presence of a sufficiently intense magnetic field around the metal.

In 1917, Silsbee[3] pointed out that the strength of the restoring current reported in a number of cases was just sufficient to produce at the surface of the metal a magnetic field equivalent to that which had been found just sufficient to restore resistance when externally applied. It was thus apparent that one had at these temperatures a resistance $R$ dependent on current $I$, providing a possible means of rectification of alternating currents and detection of radio signals. But the values of $dR/dI$ found were so small that this possibility was not investigated further for many years.

* Decimal classification: R282.11×R362.9. Original manuscript received by the Institute, November 1, 1948; revised manuscript received, April 11, 1949. The experiments described in this paper have been carried out as a part of a program of research under Contract N5-ori-166, Office of Naval Research, Physics Division, U. S. Navy.

† Johns Hopkins University, Baltimore, Md.
‡ U. S. Army Ballistic Research Laboratory, Aberdeen, Md.

[1] H. Kamerlingh Onnes, *Leiden Comm.*, No. 122b, 1911.

[2] H. Kamerlingh Onnes, *Leiden Comm.*, No. 133, 1913.

[3] F. B. Silsbee, Bureau of Standards Scientific Papers, No. 307; 1917.

Recently in studying the use of a superconducting alloy, columbium nitride (CbN) as a bolometer for detecting very weak infrared signals, it was found that, at certain values of the bias current, there was an abnormal amount of extraneous noise.[4] This turned out to be due to pick up from a local commercial broadcasting station. It appears that with very small bias currents in this alloy at special regions of temperature, $dR/dI$ attains values many times larger than in metallic elements and that considerable rectification therefore takes place, due to nonlinear resistance. Preliminary observations on this phenomenon have been reported recently[5] in addition to discussions of the use of CbN as an infrared bolometer,[6-8] so that we shall refer to the earlier papers to cover descriptions of the details of the preparation of the alloy and its mounting as a bolometer, and deal here with the results which point toward the Silsbee hypothesis[3] as the explanation of the detection observed.

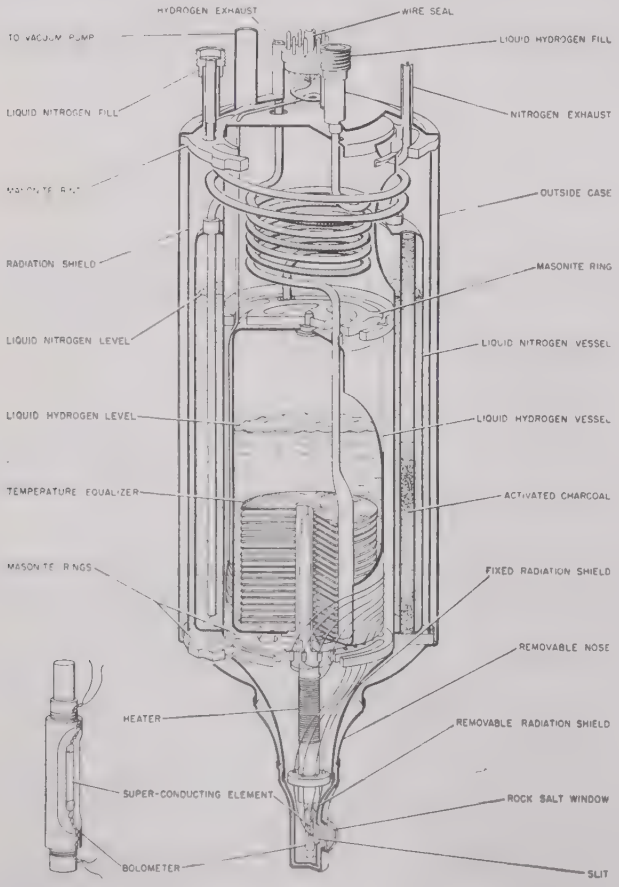


Fig. 1—Cryostat or refrigerating can to maintain bolometer at 15.5°K. Bolometer is shown enlarged ×2 in lower left corner.

[4] D. H. Andrews and C. W. Clark, "Demodulation by superconductivity," *Nature*, vol. 158, pp. 945–946; December 18, 1946.
[5] J. Lebacqz and D. H. Andrews, "Properties of CbN at radio frequencies," Nat. Electronics Conf. Proc., pp. 11–23, 1948.
[6] D. H. Andrews, R. M. Milton, and W. DeSorbo, "A fast superconductivity bolometer," *Jour. Opt. Soc. Amer.*, vol. 36, pp. 518–524, September, 1946.
[7] N. Fuson, "The infrared sensitivity of superconducting bolometers," *Jour. Opt. Soc. Amer.*, vol. 38, pp. 845–853; October, 1948.
[8] N. Fuson, "Effect of current magnitude upon the behavior of a superconducting bolometer in its transition region," *Jour. Appl. Phys.*, vol. 20, pp. 59–66; January, 1949.

## Apparatus

The bolometer is normally made from a 1-cm lengt of columbium nitride ribbon, 1 mm wide and 0.025 mm thick, cemented on the flattened face of a small coppe rod by a thin layer of bakelite lacquer which insulate the ribbon from the rod electrically, but leaves it in goo thermal contact. The normal resistance $R_N$ at 15.8°K i about 1 ohm. Fig. 1 shows such a bolometer in the lowe left-hand corner, and in the main drawing shows the re frigerating can or cryostat in which the bolometer i mounted. The cryostat holds about a liter each of liqui hydrogen and liquid nitrogen, and will maintain th bolometer in the sensitive region of temperature fo about twenty hours before refilling. A rock salt windo is provided for passing in infrared signals; radio signal are sent down the electrical leads from the upper end o the can or through two special short leads (not shown which can be placed next to the rock salt window.

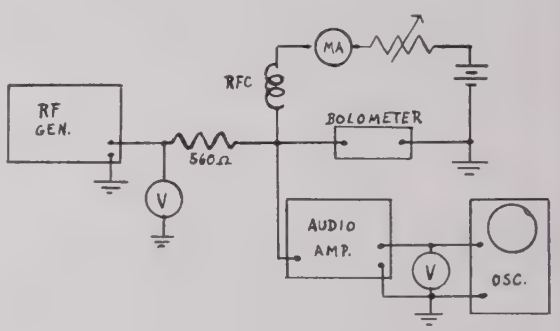


Fig. 2—Electrical circuit.

The electrical circuit is shown in Fig. 2. Provision also made for connecting a Brown recording potentiom eter (BRP-1) across the bolometer to measure the I drop due to the dc bias current ($I_d$). Another Brown re cording potentiometer (BRP-2) equipped with a rect fier, can be connected in parallel with the oscillograph t record audio signals received. A type K, Leeds an Northrup potentiometer is sometimes connected d

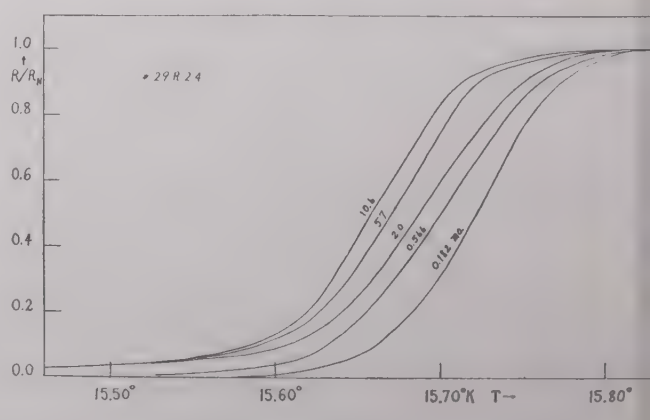


Fig. 3—Values of resistance ($R/R_N$) as a function of temperatur ($T$) and bias current ($I_d$) for bolometer #29 R 24.

rectly across the bolometer to measure rectified potential from unmodulated rf input signals. The audio amplifier gives a band pass of about 200–2,000 cps, the signal from the bolometer passing first into a low-impedance transformer and then through two stages of audio amplification. The rectified signal will be denoted by $\Delta E_R$, and given in microvolts (rms) denoted by $\mu$v.

## Results

Fig. 3 shows the variation of resistance with temperature for five different values of direct current passing through the sample. By cross plotting these and inter polating, there were obtained the values of $dR/dI$ given in the second column of Table I corresponding to the values of dc in the first column labelled $I_d$.

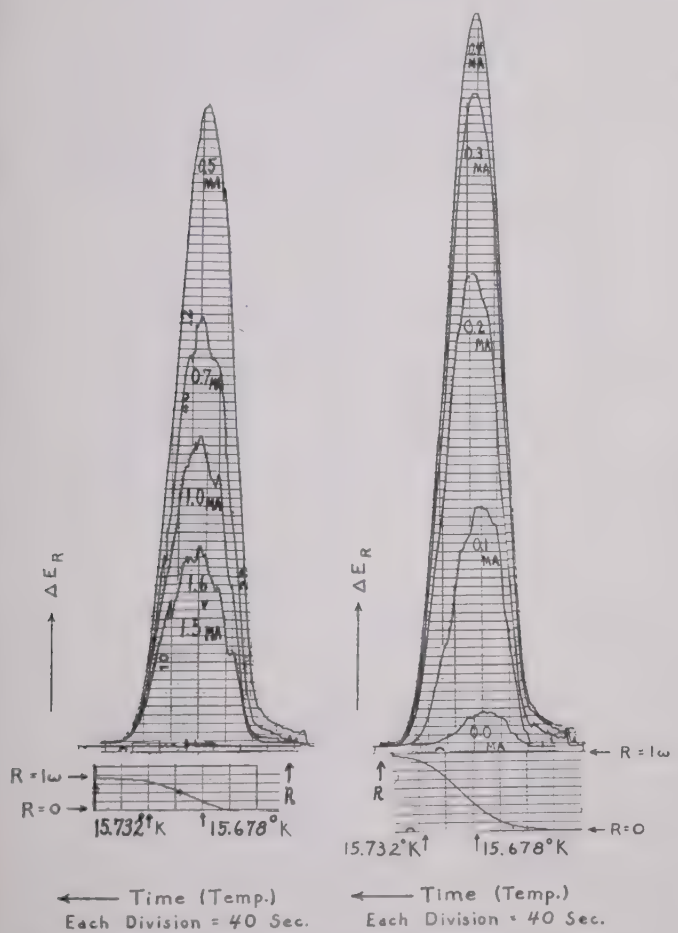


Fig. 4—Superimposed Brown recording potentiometer tracings showing rectified voltage ($\Delta E_R$) obtained as temperature is varied from region of normal resistance through transition to region of superconductivity with various values of bias current. Lower curves show change of dc voltage with temperature for same region.

Fig. 4 shows a typical variation of audio signal with temperature and with bias current. This figure was prepared by cutting out and superimposing the BRP-2 tracings. The BRP-1 tracings showing the corresponding change of dc potential (and thus of resistance) are shown below each set, for 0.1 ma dc on the left and for 0.2 ma on the right. The rf signal used had a frequency of 1 Mc, 80 per cent modulated at 400 cps, and a current of about 1 ma was flowing through the bolometer. It is seen that the audio signal reaches a peak value at a temperature in the middle of the transition zone where $dR/dT$ is a maximum. It reaches a maximum with bias current at about 0.4 ma.

TABLE I

Rectification voltages, $\Delta E_R$, calculated by (a) stepwise integration; (b) calculation from equation (5); (c) by calculation from equation (4). There is also included for comparison purposes a column of experimentally observed rectification voltages.

| | $I_d$ ma | $dR/dI$ ohm amp$^{-1}$ | $\Delta E_R$ (calc.) microvolts | $\Delta E_R$ (obs.) microvolts |
|---|---|---|---|---|
| | | Values for $I_{rfp}=0.535$ ma | | |
| (a) | 0.0 | 500 | 0 | 6.7 |
| | 0.1 | 485 | 17 | 18 |
| | 0.2 | 415 | 24 | 28 |
| (b) | 0.1 | 485 | 14 | 18 |
| | 0.2 | 415 | 24 | 28 |
| | 0.3 | 375 | 32 | 53 |
| | 0.4 | 335 | 38 | 48 |
| (c) | 0.5 | 295 | 42 | 48 |
| | 0.6 | 250 | 36 | 35 |
| | 0.7 | 220 | 32 | 30 |
| | 0.8 | 180 | 25.6 | 23.8 |
| | 0.9 | 160 | 22.8 | 18.8 |
| | 1.0 | 120 | 17.1 | 16.2 |
| | 1.5 | 80 | 11.4 | 9.7 |
| | 2.0 | 70 | 10.0 | 6.3 |
| | 3.0 | 60 | 8.6 | 4.0 |
| | 4.0 | 50 | 7.2 | 2.9 |
| | 5.0 | 40 | 5.7 | 2.3 |
| | | Values for $I_{rfp}=1.07$ ma | | |
| (b) | 0 | 500 | 0 | 16 |
| | 0.1 | 485 | 27.5 | 31 |
| | 0.2 | 415 | 47 | 48 |
| | 0.3 | 375 | 65 | 65 |
| | 0.4 | 335 | 79 | 80 |
| | 0.5 | 295 | 83 | 103 |
| | 0.6 | 250 | 90 | 118 |
| | 0.7 | 220 | 96 | 125 |
| | 0.8 | 150 | 106 | >125 |
| | 0.9 | 100 | 108 | >125 |
| (c) | 1.0 | 90 | 109 | >125 |
| | 1.5 | 80 | 69 | 92 |
| | 2.0 | 70 | 40 | 41 |
| | 3.0 | 60 | 34 | 35 |
| | 4.0 | 50 | 29 | 26 |
| | 5.0 | 40 | 23 | 22 |

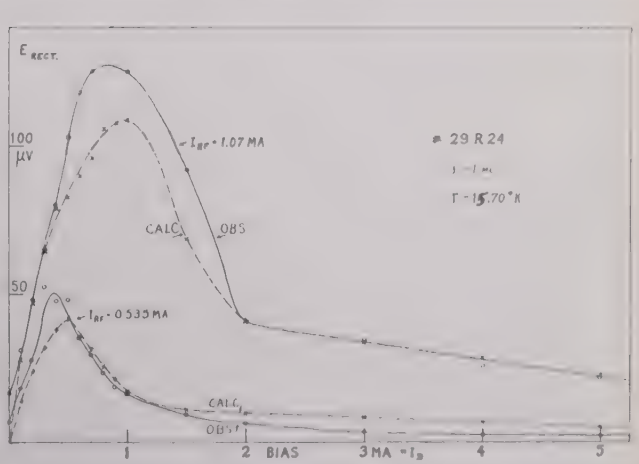


Fig. 5—Maximum rectified voltage for bolometer #29R24 as observed and calculated (see Table I), plotted against bias current $I_d$ for two values of $I_{rfp}$.

In the right-hand column of Table I there are shown the maximum (with temperature variation) audio voltages (rms) observed when passing in an rf signal at 1 Mc, 80 per cent modulated at 500 cps, using bolometer 29R24. The first part of the table gives the results obtained when an rf current of 0.535 ma was passing through the bolometer; and the second part of the table, when the rf current was 1.07 ma. Fig. 5 shows these results plotted as $\Delta E_R$ against $I_d$, the bias current. The calculated results in the third column will be discussed in the following section on Theory.

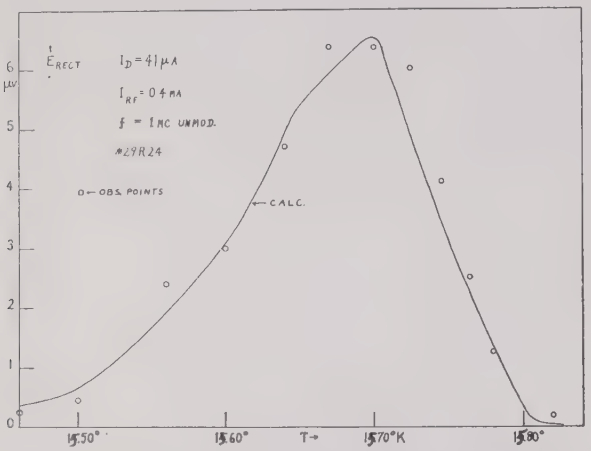


Fig. 6—Rectified voltage ($\Delta E_R$) as a function of temperature ($T$) for constant bias current of 41 $\mu$a and rf current of 0.4 ma. Calculated values are shown as solid line, observed values as circles. bolometer #29 R 24.

Fig. 6 shows the values of rectified voltage obtained when an rf signal at 1 Mc, unmodulated, was applied, the rf current being 0.4 ma and the bias current, 41 $\mu$a, being held constant as temperature was varied. The calculated curve is discussed below in the section on Theory.

In order to show variation with frequency, percentage modulation, and direction of bias current, three other sets of curves from a previous paper[5] are included as Figs. 7 and 8. These are the maximum audio signal voltages observed as temperature is varied in the superconducting transition. These maxima, in turn, are a function of the above variables.

## Theory

Since we are dealing with a strip of metal mounted as a bolometer for infra red detection, it is natural to ask whether rectification is not due in part to heating. Fuson[7,8] has made a careful study of the response of these bolometers to chopped infrared radiation and has determined their thermal time constants with considerable accuracy, finding values between 0.005 and 0.0005 second in general. The heat capacity of the CbN has been measured by Armstrong,[9] so that the thermal conductivity away from the sample can be calculated in the

[9] G. Armstrong, "The low temperature heat capacity of columbium nitride," *Jour. Amer. Chem. Soc.*, (in press).

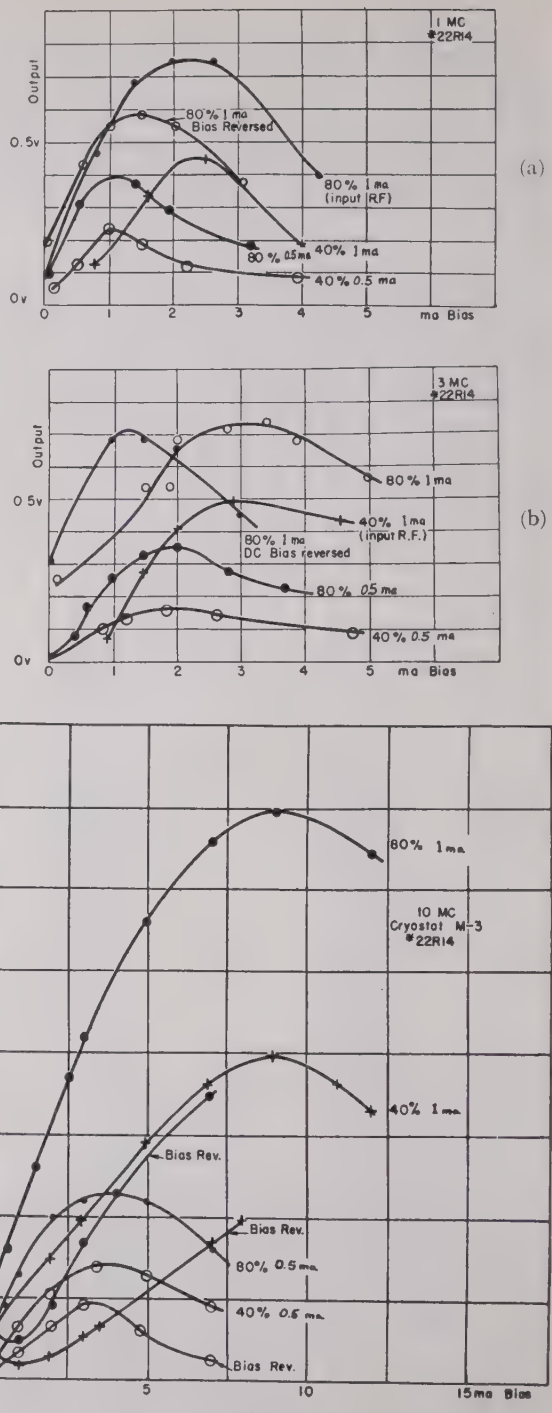


Fig. 7—Maximum rectified voltages obtained in transition for various values of bias current, rf current, percentage modulation, and direction of current flow at (a) 1 Mc, (b) 3 Mc and (c) 10 Mc

usual manner. As previously shown,[5] this is sufficiently large so that the heating from the relatively small currents used should produce less than 1 microvolt of rectified potential. Moreover, the bias current,[7,8] which gives maximum response with infrared signals, i.e., with modulated external heating, is about 20 ma, whereas the bias current which gives maximum response with modulated rf is less than 1 ma. In addition to this, there are the large rectified voltages observed with *unmodulated*

rf, which cannot be explained on the basis of a "heating bolometer effect." Therefore we conclude that rectification due to heating is negligible.

On the other hand, the observed values of $dR/dI$, apparently due to the displacement of electrons from the superconducting to the normal state by the magnetic field of the current, can explain the major part of the observed rectified voltages and their dependence on temperature, rf current, and bias current as variables.

Consider first the condition of zero bias current and the passage of unmodulated rf through the CbN. As the current rises from zero to its peak value $I_{rfp}$ in the first quarter of the rf cycle, the resistance will rise rapidly, giving a larger value of instantaneous potential across the sample at the peak value of the rf current than would be obtained for constant $R$. However in the third quarter of the cycle with the current passing in the opposite direction, the *same* excess of potential is created in the opposite direction, since the resistance rises as a function of the magnetic field, and does *not* depend on the direction of the current. Thus no rectified potential is to be expected for zero bias current.

If, now, a bias current $I_d$ is introduced, somewhat less than the peak rf current, the excess $E$ will be greater when the instantaneous rf current $I_{rf}$ flows with the bias current than when it flows against it, and rectification should result. Thus, if $dR/dI$ were constant, the rectified potential $\Delta E_R$ should rise to a maximum at the point where $I_{rfp}$ equals $I_d$; and as $I_d$ is increased beyond $I_{rfp}$, $\Delta E_R$ should remain constant at its maximum value.

This can be summarized in the following equations, which are similar to the usual expressions for nonlinear resistance:

$$E = R(I_d + I_{rf}) \tag{1}$$

$$R = R_0 + (dR/dI)(I_d + I_{rf}) \tag{2}$$

$$I_{rf} = I_{rfp} \sin 2\pi ft, \tag{3}$$

where, in addition to the symbols already defined, we have $R_0$, resistance for zero current; $E$, instantaneous potential; $f$, frequency; and $t$, time.

Substituting and integrating over a complete cycle, we get, for the rectified potential:

$$\Delta E_R = \tfrac{1}{2}(dR/dI)I_{rfp}^2. \tag{4}$$

Actually $dR/dI$ is not a constant but falls with increasing $I$, as may be seen from Table I. The result is that $\Delta E_R$ does not reach a constant maximum value with increasing $I_d$, but goes through a maximum and then falls rapidly, as may be seen from Fig. 5, this fall being due to the rapid decrease in $dR/dI$ at values where $I_d > I_{rfp}$.

The problem of calculating $\Delta E_R$ thus falls into two parts:

(i) The region where $I_d > I_{rfp}$ and the variation of $dR/dI$ is appreciable;

(ii) The region where $I_d < I_{rfp}$ and the rectification is incomplete, approaching zero as $I_d$ tends to zero.

For the second of these two parts, we can use the approximate expression:

$$\Delta E_R = \frac{I_d}{I_{rfp}} \cdot \frac{1}{2}\left(\frac{dR}{dI}\right) I_{rfp}^2, \tag{5}$$

or we can integrate graphically from a plot of $E$ against $I$, which is constructed from the observed values of $dR/dI$.

In Table I, the second and third values of $\Delta E_R$ calculated in the series marked (a), have been obtained by graphical integration, the first value for zero bias current being identically zero.

The series of values marked (b) have been calculated from (5), using the mean value of $dR/dI$ for the range covered.

The series of values marked (c) have been calculated from (4), in the range where $I_d > I_{rfp}$.

Because the rf was modulated, the rms values of the observed voltages have been used as an approximation to compensate for this additional complication in the variation of the current.

It is to be observed, first, that the difference between the values of series (a), calculated by graphical integration, differ only slightly from those of series (b), calculated on the basis of a mean value for $dR/dI$. It thus appears that the shape of the curve for $dR/dI$ is such that, for a rough comparison such as we are making, this approximation is permissible.

Considering the difficulties of the measurements, problems of temperature control, losses in the wires leading into and out of the low-temperature chambers, and the as yet unexplained frequency dependence, we cannot expect too close a correspondence between calculated and observed values actually found. The agreement may, under these circumstances, be regarded as tending to confirm the explanation of the rectified voltages as due to the Silsbee phenomenon.

The calculated curve in Fig. 6 is also obtained with the help of (5) and explains the variation of $\Delta E_R$ with temperature as due to the variation of $dR/dI$, which is a maximum in midtransition, and becomes zero at temperatures both above and below the transition.

The presence of rectified voltage in the absence of bias current is not explained by this theory, and must be attributed to some additional phenomenon which is dependent on the direction of the current, as may be seen from the curves in Fig. 7 (a), (b), (c).

Since the publication of the first report on superconducting rectification, several investigators have checked[10–12] on the rectification to be expected when relatively large currents are used, in general, sufficient to carry the resistance completely through the transi-

[10] B. G. Lazarev, A. A. Galkin, and V. I. Khotkevich, "Some experiments on superconductivity at radio frequencies," *Doklady Acad. Sci. Ukraine*, vol. 55, p. 817; 1947.

[11] A. A. Galkin and B. G. Lazarev, "Detecting properties of superconductors," *Doklady Acad. Sci. Ukraine*, vol. 59, pp. 669; 1948.

[12] Privately printed report under O. N. R. Contract, Physics Dept., Rutgers University, to be published shortly.

tion from the superconducting to the normal state; and they have confirmed the customary Silsbee theory as applying in such cases.

The rectification in the case of CbN using small currents appears to be due, however, to a kind of Silsbee effect several orders of magnitude larger than has been found with relatively larger currents in metals and alloys previously studied. The explanation of this "hyper Silsbee effect" must await a more detailed understanding of superconductivity itself.

Finally, it must be noted that although the simple equations (4) and (5) appear to be applicable at a frequency of 1 Mc, the curves in Figs. 7 (a), (b), (c) show that, at higher frequencies, the rectified voltages increase very considerably. This raises the question of how long it takes for electrons to go from the normal to the superconducting state, or vice versa. This has been recognized as a most interesting problem for some years. It was first studied extensively by Silsbee, Brickwedde and Scott[13,14] and has assumed special importance in connection with the behavior of microwaves in superconductors. It is possible that the frequency dependence of rectification in CbN may be a function of the response time of electron regional transition.

ACKNOWLEDGMENT

The authors wish to thank Roys H. Sause and William Asher for invaluable assistance and co-operation in the investigation.

[13] F. B. Silsbee, R. B. Scott, J. W. Cook, and F. G. Brickwedde, "Superconductivity with respect to alternating currents," *Phys. Rev.*, vol. 39, pp. 379–380; January 15, 1932.

[14] F. B. Silsbee, F. G. Brickwedde, and R. B. Scott, "Some experiments at radio frequencies on superconductors," *Jour. Res. Nat. Bur. Stand.*, vol. 20, pp. 109–123; February, 1938.

# Generalized Theory of the Band-Pass Low-Pass Analogy*

P. R. AIGRAIN†, STUDENT, IRE, B. R. TEARE, JR.‡, SENIOR MEMBER, IRE, AND E. M. WILLIAMS‡, SENIOR MEMBER, IRE

*Summary*—**A generalized theory of band-pass low-pass equivalents is developed using Laplace transform analysis, and it is shown that video equivalents exist not only for symmetrical systems, but also for dissymmetrical systems with low-level modulation. Several illustrations are given.**

THE BAND-PASS low-pass analogy[1] provides a means of simplifying the analysis of amplitude-modulated carrier systems which otherwise would be extremely tedious, especially when transient phenomena are involved.

This useful alternative analysis has not been extensively applied, however, possibly because its general theory, breadth of application, and limitations have not been widely understood. The purpose of this paper is to give a rigorous derivation of the band-pass low-pass analogy, and to discuss and illustrate its use in the classes of transient and steady-state problems in which it is applicable.

The concept of the equivalent video amplifier is illustrated by the two systems of Fig. 1. Fig. 1(a) shows a generalized amplitude-modulated carrier system comprising an oscillator as carrier source, a modulated stage in which the carrier envelope is made to vary linearly with the instantaneous amplitude of the signal $a(t)$, a band-pass network which includes all the high and intermediate frequency sections of the transmitter, receiver, and transmission link, and a linear detector, the output $b(t)$ of which is similar in form to the variable part of the carrier signal envelope at its input. In an ideal system $b(t)$ would be identical (except for a possible constant multiplying factor) with $a(t)$. However, in most realizable systems there are distinct differences between $b(t)$ and $a(t)$. The equivalent video system, shown in Fig. 1(b), is a hypothetical low-pass amplifier which, for the same input signal $a(t)$, has a signal output of the same form $b(t)$ as the band-pass system. The elements of the equivalent system are usually, though not necessarily, physically realizable.

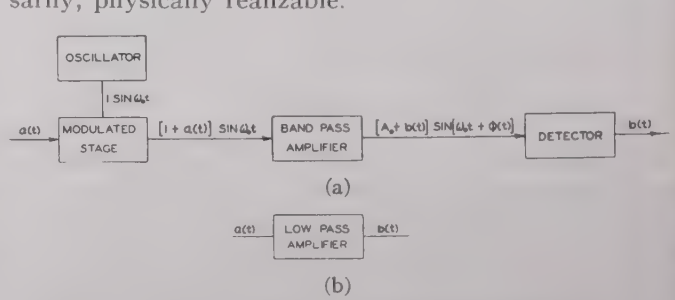


Fig. 1—(a) Above, generalized amplitude-modulated carrier system. (b) Below, the video equivalent.

It has been pointed out by Cherry[2] that the existence of an equivalent video system is a sufficient condition

* Decimal classification: R143.2. Original manuscript received, July 22 1948; revised manuscript received, April 7, 1949.

† Service d'Etudes et de Recherches de la Marine Francaise, Ecole Normale Superieure, Paris, France.

‡ Carnegie Institute of Technology, Pittsburgh, Pa.

[1] V. D. Landon, "The band-pass low-pass analogy," PROC. I.R.E., vol. 24, pp. 1582–1584; December, 1936.

[2] E. Colin Cherry, "The transmission characteristics of asymmetric-sideband communication networks," in two parts, Pt. I, *Jour. IEE* (London), vol. 89, pt. III, pp. 19–42; March, 1942. And Pt. II, *Jour. IEE* (London), vol. 90, pt. III, pp. 75–88; June, 1943.

for a linear relation between $b(t)$ and $a(t)$ and that the nonexistence of a video equivalent in any system is an indication of a nonlinear relationship between detector signal output and modulated stage signal input. For this reason the theory of the band-pass low-pass analogy takes on an interesting general significance quite apart from its utility in the solution of specific problems.

The theory of the video equivalent is derived by use of the Laplace transform.[3] An alternative approach using Fourier transforms could be adapted from Cherry.[2]

We begin by considering the carrier system of Fig. 1(a) in detail. An oscillator supplies a sinusoidal voltage of unit amplitude and frequency $\omega_0$ to a modulated stage in which the modulating input signal $a(t)$ is applied. The modulated stage is assumed to have such idealized properties that its output is a voltage $(1+a(t))\sin\omega_0 t$ which is the input to a band-pass amplifier. The output of the band-pass amplifier is a voltage of form $[A_0+b(t)]\sin(\omega_0 t+\phi(t))$, in which $A_0$ is a constant, and this voltage is supplied to a detector whose properties are assumed to be such that the output voltage is the variable part of the envelope of the input; that is, $b(t)$. The arbitrary part of the system, the band-pass amplifier, is described by its transfer function $G_B(j\omega)$, the ratio of output to input under steady-state ac operation. The transfer function may also be written as $A(\omega)\epsilon^{j\theta(\omega)}$ in which $A$ and $\theta$ are the amplitude and phase functions.

The problem is to determine under what conditions there is a low-pass amplifier which is equivalent to the carrier system, an amplifier which will give the same output $b(t)$ for the same input $a(t)$.

The form of the response $h(t)$ of the band-pass amplifier when the input is $f(t)\sin\omega_0 t$ may be expressed in terms of Laplace transforms as

$$h(t) = \frac{1}{2j}\{\epsilon^{j\omega_0 t}L^{-1}[F(s)G_B(s+j\omega_0)] - \mathfrak{I}^{-j\omega_0 t}L^{-1}[F(s)G_B(s-j\omega_0)]\} \quad (1)$$

in which $F(s)$ is the transform of $f(t)$, and $L^{-1}$ indicates the operation of taking the inverse transform. If $s$ is considered to be real, and this can be assumed without loss of generality,[4] the expression (1) may be simplified[5] to

$$h(t) = \mathfrak{I}\epsilon^{j\omega_0 t}L^{-1}[F(s)G_B(s+j\omega_0)]. \quad (2)$$

This may be expressed more usefully by introducing new quantities $p(t)$, $q(t)$, $m(t)$, and $\phi(t)$ as follows:

$$L^{-1}[F(s)G_B(s+j\omega_0)] = p(t)+jq(t) = m(t)\epsilon^{j\phi(t)}, \quad (3)$$

where $p(t)$ and $q(t)$ are the real and imaginary parts of the inverse transforms, and

$$m(t) = [\{p(t)\}^2+\{q(t)\}^2]^{1/2} = |L^{-1}[F(s)G_B(s+j\omega_0)]| \quad (4)$$

$$\phi = \tan^{-1}\frac{q(t)}{p(t)} = \text{angle of } L^{-1}[F(s)G_B(s+j\omega_0)]. \quad (5)$$

Then

$$h(t) = \mathfrak{I}m(t)\epsilon^{j[\omega_0 t+\phi(t)]} = m(t)\sin[\omega_0 t+\phi(t)]. \quad (7)$$

In the case under consideration

$$f(t) = 1+a(t); \quad (8)$$

hence its transform is

$$F(s) = \frac{1}{s}+A(s) \quad (9)$$

and we are concerned only with $m(t)$, the envelope of the modulated carrier wave $h(t)$, since the variable part of $m(t)$ is the output of the system. From (4) and (9)

$$m(t) = \left|L^{-1}\left\{\frac{1}{s}G_B(s+j\omega_0)+A(s)G_B(s+j\omega_0)\right\}\right|. \quad (10)$$

It is assumed that the carrier frequency has been applied for a very long time, and it will next be shown that the first term of (10) is the steady-state response to the carrier alone. The final value theorem[3] gives for the first term of (10)

$$\lim_{t\to\infty} L^{-1}\frac{1}{s}G_B(s+j\omega_0) = G_B(j\omega_0). \quad (12)$$

In terms of amplitude and phase functions this is $A(\omega_0)\,\epsilon^{j\theta(\omega_0)}$. For brevity $A(\omega_0)$ will be written $A_0$ and $\theta(\omega_0)$ as $\theta_0$. Then $m(t)$ may be written as the absolute value of the sum of the two complex numbers,

$$m(t) = |A_0\epsilon^{j\theta_0}+L^{-1}A(s)G_B(s+j\omega_0)| \quad (13)$$

in which $s$ is real ($s$ is integrating variable and integration is over a contour in complex $s$ plane). The first term gives the response to the carrier alone and is contant, and the second term is, in general, a function of time. Reference to (2) to (5) shows that the whole expression (13) is the amplitude of a rotating vector $\omega_0$ which represents the output of the band-pass amplifier. At any time $t$ this expression may be represented by the vector diagram in the complex plane shown in Fig. 2. The out-

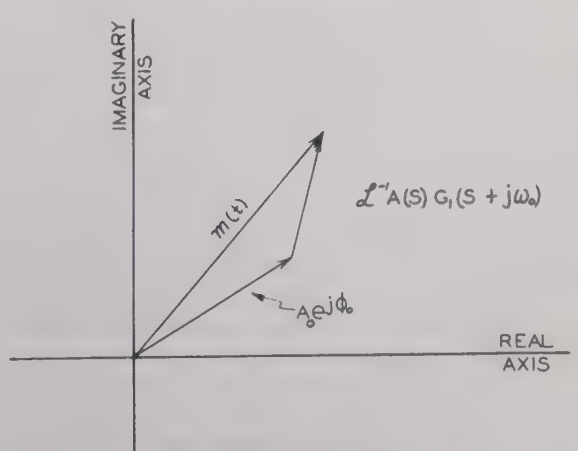


Fig. 2—Vector diagram for $m(t)$ giving the envelope of the output of the band-pass amplifier.

[3] M. F. Gardner and G. L. Barnes, "Transients in Linear Systems," vol. I, John Wiley and Sons, Inc., New York, N. Y., 1942.

[4] R. V. Churchill, "Modern Operational Mathematics in Engineering," McGraw-Hill Book Co., New York, N. Y., 1944; particularly Chapter VI, Section 53.

[5] The symbols $R$ and $\mathfrak{I}$ will be used to designate operations of taking the real and imaginary parts, respectively.

put of the detector consists of the varying or ac component $m(t)$, that is, the second term (13).

Consider now the equivalent video amplifier shown in Fig. 1(b) which has a transfer function $G_L(s)$. The equivalence means that for the same input $a(t)$, its output $b(t)$ is the same as the variable part of the output $m(t)$ of the amplitude-modulated carrier system. Now

$$b(t) = L^{-1}G_L(s)A(s), \tag{14}$$

and the problem of determining the video equivalent reduces to that of finding whether and when it is possible to find a function $G_L(s)$ which is the transfer function of some circuit, not necessarily a physically realizable one, such that

$$b(t) = m(t) - C, \tag{15}$$

$C$ being constant or the dc component of $m(t)$ attributable to the first term of (13). A necessary condition for the existence of a single video equivalent circuit is that when $a(t)$ is multiplied by a constant factor $K$, $b(t)$ is also multiplied by the same factor $K$, and $m(t)$ is changed to

$$\left| A_0\epsilon^{j\theta_0} + L^{-1}KA(s)G_B(s + j\omega_0) \right| = Kb(t) + C.$$

Thus there is equivalence only if the variable part of $m(t)$ is proportional to

$$\left| L^{-1}A(s)G_B(s + j\omega_0) \right|.$$

From Fig. 2 it may be seen that this is true in general for only two distinct conditions: *Case I*, in which $A_0\epsilon^{j\theta_0}$ and $L^{-1}A(s)G_B(s+j\omega_0)$ have the same phase angle ($s$ being real) $\theta_0$, and *Case II*, in which

$$A_0\epsilon^{j\theta_0} \gg L^{-1}A(s)G_B(s + j\omega_0)$$

and changes in the resultant vector are proportional to the magnitude of the second, very small component. These cases will be considered separately.

*Case I*: $A_0\epsilon^{j\theta_0}$ and $A_sG_B(s+j\omega_0)$ have the same phase angle $\theta_0$ hence $\epsilon^{-j\theta_0}A_sG_B(s+j\omega_0)$ is real. A comparison of (13) and (14) shows that the video equivalent exists and

$$G_2(s) = \epsilon^{-j\theta_0}G_B(s + j\omega_0). \tag{16}$$

The fact that both members of (16) are real means that $A(\omega)$, the amplitude function for $G_B(j\omega)$, is symmetrical[6] and the phase function $\theta(\omega) - \theta_0$ is antisymmetrical about $\omega = \omega_0$ and, conversely, any system which has this symmetry will make (16) real and falls into this case. The case in which there is symmetry of amplitude and phase characteristics about the carrier frequency is the case previously discussed in the literature.[1] It may be observed that no physically realizable system can be exactly symmetrical about a frequency $\omega_0$, since network theory requires that $A(\omega)$ shall always be symmetrical about $\omega = 0$, and any function having two axes of symmetry must extend to infinity. Symmetry can be obtained approximately, however, if the amplifier passband is only a small fraction of $\omega_0$. The effect of this approximation on the accuracy of results obtained from the video equivalent for any real network can be shown to be related to the "switching angle," or phase of the carrier voltage within its signal envelope. The actual transient response of an approximately symmetrical carrier system is independent of this switching angle at all instants of time except those immediately following the initiation of the transient, and it is during this initial period that the video-equivalent response is not very precisely indicative of the prototype carrier system response.

*Case II*:

$$\left| A_0\epsilon^{j\theta_0} \right| \gg \left| L^{-1}A(s)G_B(s + j\omega_0) \right|. \tag{17}$$

This is the case in which the depth of modulation in the input signal to the detector is small. The expression (13) for $m(t)$ can be simplified because of low modulation depth as follows:

$$m(t) = \left| A_0\epsilon^{-j\theta_0} + R\epsilon^{-j\theta_0}L^{-1}A(s)G_B(s + j\omega_0) + \Im\epsilon^{-j\theta_0}L^{-1}A(s)G_B(s + j\omega_0) \right|.$$

Because of inequality (17) the imaginary part contributes a negligible amount to the magnitude, and since $\epsilon^{j\theta_0}$ is a constant independent of $s$, it may be moved inside the operator $L^{-1}$ giving

$$m(t) \simeq A_0 + L^{-1}A(s)R[\epsilon^{-j\theta_0}G_B(s + j\omega_0)]. \tag{18}$$

By comparison of (18), (14), and (15) it is evident that a circuit with a transfer function[7]

$$G_L(s) = R\epsilon^{-j\theta_0}G_B(s + j\omega_0)$$

is the video equivalent.

The case has not previously been fully developed in the literature although it may be deduced from Poch and Epstein.[8] A small depth of modulation at the detector can be the result either of small modulation depth at the modulated stage or of reinserted or "exalted" carrier operation, such as with injection of a large locally

[6] That this symmetry is implied may be shown by considering the right-hand member of (16) to be a function of $s$ and expanding it in a power series in $s$:

$$\epsilon^{j\theta_0}G_B(s + j\omega_0) = c_0 + c_1s + c_2s^2 + \cdots.$$

Since this function is real when $s$ is real, the coefficients are real. By substituting first $s = +j\omega$ and then $s = -j\omega$ it may be shown that

$$\epsilon^{-j\theta_0}G_B(j\omega_0 + j\Delta\omega) \text{ is conjugate to } \epsilon^{-j\theta_0}G_B(j\omega_0 - j\Delta\omega).$$

Now the transfer function $G(j\omega)$ may be written in polar form $A(\omega)$. Thus

$$A(\omega_0 + \Delta\omega)\epsilon^{j[\theta(\omega_0+\Delta\omega)-\theta_0]} \text{ is conjugate to } A(\omega_0 - \Delta\omega)\epsilon^{j[\theta(\omega_0-\Delta\omega)-\theta_0]}.$$

Accordingly, if $\Delta\omega$ is any departure of frequency from $\omega_0$

$$A(\omega_0 + \Delta\omega) = A(\omega_0 - \Delta\omega) \quad \text{and}$$
$$\theta(\omega_0 + \Delta\omega) - \theta_0 = -[\theta(\omega_0 - \Delta\omega) - \theta_0],$$

which are statements of the symmetry conditions.

[7] In taking the real part of the right-hand expression $s$ is considered to be real. After having taken the real part $s+j\omega$ is substituted in the new expression to obtain the equivalent video transfer function.

[8] W. J. Poch and D. W. Epstein, "Partial suppression of one-sideband in television reception," PROC. I.R.E., vol. 25, pp. 15–31; January, 1937.

generated carrier, or by the use of a sharply tuned carrier emphasis filter.

It is important to note that the video equivalent of a circuit in this case is not the same as that of the same circuit or form of circuit under symmetrical conditions.

When the conditions of either cases I or II are not met, there is no video equivalent and, furthermore, the carrier system is nonlinear in the sense described in this paper. This case is treated in detail by Cherry,[2] who derives a more elaborate equivalent low-pass system, the output of which is the square root of the sum of the squares of the individual outputs of two parallel linear low-pass networks. In conclusion, several illustrations are given in video equivalents for some common carrier systems.

*Case I:* Consider a carrier amplifier with the characteristics of a series $R$, $L$, $C$ circuit, Fig. 3(a), to

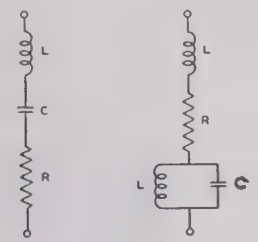


(a) (b)

Fig. 3—(a) Series $R$, $LC$ circuit used in Fig. 1. (b) Video equivalent for (a) in the case of low-level modulation.

which there is applied an amplitude modulated signal at the resonant frequency. We may take $G_B(\omega)$ as

$$G_B(\omega) = R + j\left(\omega L - \frac{1}{\omega C}\right)$$

or, in terms of $\omega_0 = 1/\sqrt{LC}$, with the approximation $\omega/\omega_0 + \omega_0/\omega \simeq 2$,

$$G_B(\omega) = R + \frac{2j[\omega - \omega_c]}{\omega_0^2 C} \quad G_B(s + j\omega_0) = R + 2sL$$

and $\theta_0$ is zero so that $G_L(s) = R + 2sL$. The video equivalent, as is generally known for the case,[1] consists of a resistance $R$ in series with an inductance equal to twice the inductance in the original band-pass system.

As a second illustration consider the two-stage amplifier of Fig. 4(a), which is made approximately symmetrical for a carrier frequency $\omega_0$ by setting

$$\begin{aligned} Q_1 &= Q_2 & \frac{1}{Q} &\ll 1 \\ \omega_1 &= \omega_0 + D & & \\ \omega_2 &= \omega_0 - D & D &\ll \omega. \end{aligned}$$

The steady-state gain is of the form

$$\frac{E_{\text{out}}}{E_{\text{in}}} = g_m^2 Z_1 Z_2.$$

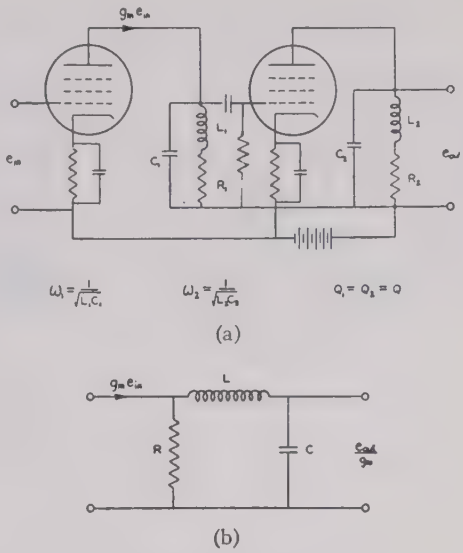


Fig. 4—(a) Two-stage symmetrical amplifier used as Fig. 2. (b) Video equivalent for (a).

The impedance transfer function is

$$G_R(\omega) = Z_1(\omega) Z_2(\omega),$$

or in symmetrical form

$$G_B(\omega) = \frac{1}{C_2 C_3 [\omega_0^2 Q^2 + 4D^2 - 4(\omega - \omega_0)^2 + j4Q\omega_0(\omega - \omega_0)]}$$

and

$$G_B(s + j\omega_0) = G_L(s) = \frac{1}{C_2 C_3 [\omega_0^2 Q^2 + 4D^2 + 4s^2 + 4Q\omega_0 s]}.$$

This video equivalent is realized in Fig. 4(b) if

$$\begin{aligned} R &= \frac{1}{C_2 C_3 [\omega_0^2 Q^2 + 4D^2]} \\ C &= 4Q\omega_0 C_2 C_3 \\ L &= \frac{1}{Q\omega_0 C_2 C_3 [\omega_0^2 Q^2 + 4D^2]}. \end{aligned}$$

*Case II:* Consider again the series $R$, $L$, $C$ circuit of Fig. 3(a) with $\omega_0 = 1/\sqrt{LC}$, but in the case in which $Q$ is too low to make the approximation $\omega/\omega_0 + \omega_0/\omega \simeq 2$. Then it can be shown that

$$G_L(s) = R + Ls + \frac{Ls}{1 + LCs^2},$$

and the circuit of Fig. 3(b) is a video equivalent for low modulation levels.

# Contributors to the Proceedings of the I.R.E

Donald H. Andrews was born in Southington, Conn., on June 11, 1898. He spent one year at Phillips Academy, Andover, and entered Yale in the Fall of 1916, receiving the B.A. degree in 1920. In 1923 he was awarded the Ph.D. degree, and remained at Yale for one year as research assistant to Dr. John Johnston. Following this he went to the University of California on a National Research Fellowship to continue research in low temperature calorimetry during 1924–1925. He was granted an International Research Fellowship and went to Leiden, Holland, in August, 1925, where he continued research at the Physics Laboratory of the University in absolute zero temperature studies. In August, 1926, he was appointed Research Fellow at the Bartol Research Foundation of the Franklin Institute in Philadelphia, Pa., where he remained until September, 1927. At that time he came to The Johns Hopkins University to teach thermodynamics and direct research in calorimetry.

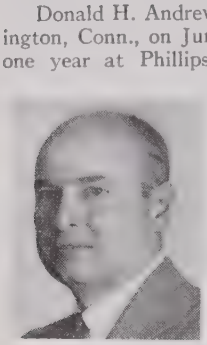

D. H. ANDREWS

Dr. Andrews was promoted to associate professor in 1929, and to professor of chemistry in 1930, the chair which he had held since that time. Since 1943 he has devoted full research time to the "Cryogeny Laboratory," a research unit which he organized for studies at very low temperatures. Dr. Andrews served as Director of the Chemistry laboratory from 1936 to 1942. He initiated the organization of an atomic research unit in 1936, which was carried on by members of the staff, later becoming associated with the atomic bomb project. He has served as chairman of the Baltimore branch of the Association of Scientists for Atomic Education, and as a member of the Board for Foreign Policy Association, of the United Nations Association, and of the United World Federalists in Maryland. In 1936 he was asked to serve as a member of the First Scientific Commission of L'Institut International de Froid, and in 1948 he served as a representative of the United States on the organizational commission which met in Amsterdam.

❖

For a photograph and biography of PIERRE R. AIGRAIN, see page 900 of the August, 1949, issue of the PROCEEDINGS OF THE I.R.E.

❖

For a photograph and biography of E. M. WILLIAMS, see page 902 of the August, 1949, issue of the PROCEEDINGS OF THE I.R.E.

W. Lindsay Black (M'36—SM'43) was born on February 8, 1900, at Asbury Park, N. J. In 1918 he joined the engineering department of the Western Electric Co. which became the Bell Telephone Laboratories in 1925, where he is now a member of the technical staff. He has been engaged in the development and installation of radio and carrier apparatus and systems and, more recently, of apparatus and systems particularly, including such equipment for radio broadcasting and sound reproduction.

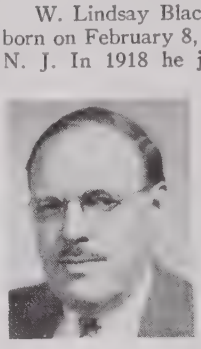

W. L. BLACK

Mr. Black is a member of the Acoustical Society of America, the American Institute of Electrical Engineers, and the Audio Engineering Society.

❖

Chester W. Clark was born in San Francisco, Calif., on July 18, 1906. He received the B.S. and M.S. degrees in chemistry from the University of California in 1927 and 1929, respectively. In 1935 he was awarded the Ph.D. degree in physics from the University of Leyden, Netherlands. During 1929–1933 he was associated with the Standard Oil Company of California, as a research chemist. He taught in the College of Chemistry at the University of California from 1935 to 1937, and at the San Francisco Junior College from 1937 to 1941. During the period 1941–1946 Dr. Clark was a member of the Ordnance Department of the U. S. Army, returning to teaching in 1946 at the Johns Hopkins University. In 1947 he became a low-temperature consultant and physicist at the Naval Research Laboratory, leaving there to accept the position of scientific assistant to the director, Ballistic Research Laboratories, at the Aberdeen Proving Grounds, Md., where he is now engaged. He holds the rank of lieutenant colonel in the U. S. Army.

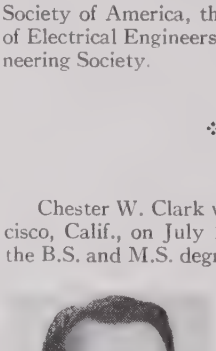

CHESTER W. CLARK

❖

For a photograph and biography of ROHN TRUELL, see page 1260 of the October, 1948, issue of the PROCEEDINGS OF THE I.R.E.

Richard H. DeLano (A'48) was born Los Angeles, Calif., on August 13, 1925. H received the B.S. and M.S. degrees electrical engineerin from the Californ Institute of Techno ogy in 1946. Sinc 1946 Mr. DeLan has been with ele tronics departme of the Hughes Ai craft Company, e gaged in investig tions on automat tracking radar an missile control sy tems.

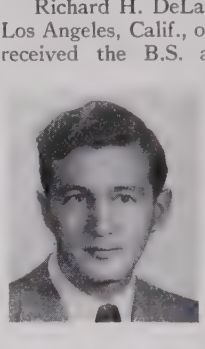

RICHARD H. DELANO

Mr. DeLano is a member of Tau Beta and the American Institute of Electric Engineers.

❖

Dennis L. H. Gibbings was born Hobart, Tasmania, on October 18, 1925. 1942 he entered the University of Tasman receiving the degr of Bachelor of Eng neering in 1946, a Bachelor of Scien in 1948. Since grad ating in engineerir Mr. Gibbings h been employed as research student the electrical en neering departme of the University, e gaged on resear work concern chiefly with transient phenomena in ele tric wave filters.

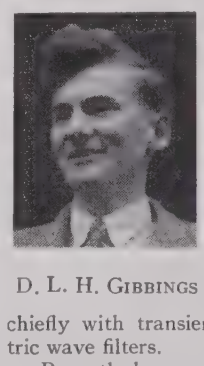

D. L. H. GIBBINGS

Recently he was awarded a Studentsh by the Australian Commonwealth Scie tific and Industrial Research Organizatio and is shortly to proceed to England to stu electronics at the University of Manchest

❖

Philip S. Jastram (M'45) was born Providence, R. I., on February 28, 1920. received the S.B. degree from Harvard U versity in 1943, a the Ph.D. deg from the Univers of Michigan in 19 From 1943 to 19 he was a member the staff at Ra Research Laborato in Cambridge.

P. S. JASTRAM

During the l two years, Dr. J tram has been car ing on research nuclear physics at University of Michigan, where he is an structor in physics. He is a member of American Physical Society, Sigma Xi, a Phi Beta Kappa.

# Contributors to the Proceedings of the I.R.E.

Ronold King (A'30–SM'43) was born on September 19, 1905, at Williamstown, Mass. He received the B.A. degree in 1927 and the M.S. degree in 1929 from the University of Rochester, and the Ph.D. degree from the University of Wisconsin in 1932. He was an American-German exchange student at Munich from 1928 to 1929; a White Fellow in physics at Cornell University from 1929 to 1930; and a Fellow in electrical engineering at the University of Wisconsin from 1930 to 1932. He continued at Wisconsin as a research assistant from 1932 to 1934. From 1934 to 1936 he was an instructor in physics at Lafayette College, serving as an assistant professor in 1937.

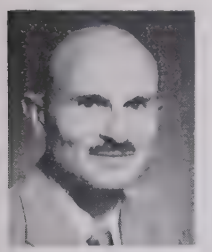

RONOLD KING

During 1937 and 1938, Dr. King was a Guggenheim Fellow at Berlin. In 1938 he became instructor in physics and communication engineering at Harvard University, advancing to assistant professor in 1939 and to associate professor in 1942. He was appointed Gordon McKay professor of applied physics at Harvard University in 1946.

Dr. King is a Fellow in the American Physical Society, the American Association for the Advancement of Science, and the American Academy of Arts and Sciences.

❖

Jean V. Lebacqz (M'46) was born in Tilff, Belgium, on July 30, 1911. He received the E.E. degree from the University of Brussels in 1933, and the Ph.D. degree from Stanford University, in 1935. He was employed by by the SOFINA, in Brussels, until 1939, when he joined the teaching staff of the electrical engineering department of the University of California, as an instructor.

JEAN V. LEBACQZ

In 1943, Dr. Lebacqz became a staff member of the Massachusetts Institute of Technology, leaving in 1946 to go to The Johns Hopkins University, as an assistant professor on the electrical engineering staff.

❖

G. G. Macfarlane (S'35–A'39) was born in 1916 at Airdrie, Scotland. He received the B.Sc. degree with first class honors in electrical engineering in 1937 from Glasgow University. From 1937 to 1939 he pursued postgraduate research at the Technische Hochschule, in Dresden, and was awarded the Dr. Ing. degree.

G. G. MACFARLANE

Since 1939 Dr. Macfarlane has been engaged in mathematical research at the Telecommunications Research Establishment, Ministry of Supply, in Malvern, England, where he is in charge of the theoretical physics division. He has published a number of papers on waveguides, tropospheric wave propagation, noise, and mathematics.

Dr. Macfarlane is an associate member of the Institute of Electrical Engineers, and a Fellow of the Physical Society, London.

❖

Gordon P. McCouch (S'41–A'45) was born on May 5, 1920 in London, England. He received the A.B. degree in 1941, and the M.A. degree in 1948, both from Harvard University. He has been a licensed radio amateur since 1936. From 1942 through 1945, he was a research associate at the Radio Research Laboratory; of this period, the latter two years were spent in England and continental Europe with the Telecommunications Research Establishment and the American British Laboratory. At this time he was engaged in field applications of radar countermeasures and vhf radiotelephone equipment; for this work he received the Army-Navy Certificate of Appreciation.

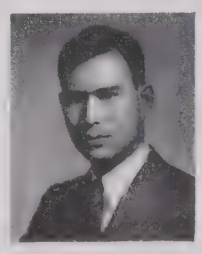

G. P. MCCOUCH

Since 1945 Mr. McCouch has been a member of the engineering staff of Aircraft Radio Corp., where he has been principally concerned with signal generator development. While on leave of absence from ARC during 1948, Mr. McCouch held a teaching fellowship at Harvard University.

❖

Gordon Newstead was born in Cairo, Egypt, on July 1, 1917. In 1939 he received the degree of Bachelor of Engineering with Honours from the University of Melbourne, and also obtained first class Honors in Applied Mathematics. After graduation Mr. Newstead was employed as a senior demonstrator in electrical engineering by the University of Melbourne, and then as a communications engineer with the department of Civil Aviation. In 1945 he was awarded the degree of Master of Electrical Engineering for a thesis on aviation radio covering the work on which he was engaged while with the department.

GORDON NEWSTEAD

Since 1944, Mr. Newstead has been lecturer in electrical engineering at the University of Tasmania, concerned with electronics and communications. His research work and publications have been on circuit theory and the ionosphere. Mr. Newstead is an associate member of the Institution of Engineers of Australia.

❖

Hermon H. Scott (M'35–SM'43) was born in Somerville, Mass., on March 28, 1909. He holds the degrees of B.Sc. and M.Sc. from the Massachusetts Institute of Technology, and was associated with the General Radio Co. for 15 years, first as sales and development engineer, and later as executive engineer in charge of audio frequency, acoustic, and broadcast developments. He is the inventor of *RC* tuned circuits and oscillators, the dynamic noise suppressor, and other circuits. Leading companies throughout the world are licensed to use these inventions, including Electric and Musical Industries, Ltd., the British manufacturers of His Master's Voice and Columbia records and phonographs.

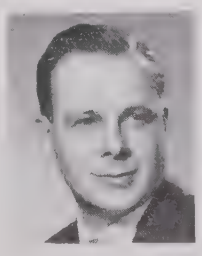

H. H. SCOTT

At the present time, Mr. Scott is president and director of engineering of Hermon Hosmer Scott, Inc., Cambridge, Mass., which company manufactures dynamic noise suppressors, amplifiers, broadcast station and laboratory equipment, and sound-measuring apparatus. The company is also active in the development of electronic musical instruments.

Mr. Scott is also a fellow of the Acoustical Society of America, a member of the American Institute of Electrical Engineers, the Audio Engineering Society, and the American Institute of Physics, and associate member of the Society of Motion Picture Engineers. He is also Chairman of the Boston Section of The Institute of Radio Engineers.

K. Tomiyasu (S'41–A'42–M'49) was born on September 25, 1919, at Las Vegas, Nev. He received the B.S. degree in electrical engineering from the California Institute of Technology in 1940, and the M.S. degree in communication engineering from Columbia University in 1941. After further graduate study at Stanford University, and at Harvard University, he was awarded the Ph.D. degree in engineering science and applied physics from Harvard in 1948.

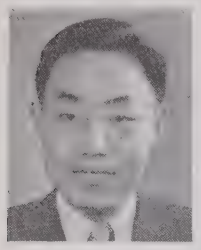

K. Tomiyasu

In 1947–1948, Dr. Tomiyasu was a research assistant at Harvard, under the ONR Contract N5-ori-76 T.O.1, supported jointly by the Navy Department, Office of Naval Research, and the Signal Corps of the U. S. Army. He was appointed a teaching fellow in 1946 and instructor in 1948 in the department of engineering sciences and applied physics, Harvard University, where he was engaged until September, 1949. At present he is employed as a project engineer in the microwave department of the Sperry Gyroscope Co.

❖

B. R. Teare, Jr., (A'41–SM'45) was born in 1907 in Menomonie, Wis. He received the B.S. degree in 1927, and the M.S. degree in 1928, both from the University of Wisconsin. After another year of graduate work he was employed by the General Electric Company, where he was associated with the advanced course in engineering. He was an instructor and assistant professor of electrical engineering at Yale University from 1933 to 1939, and completed the work for the degree of doctor of engineering in 1937.

B. R. Teare, Jr.

Dr. Teare now is Buhl Professor of electrical engineering at the Carnegie Institute of Technology, and head of the department of electrical engineering. He is a past Chairman of the IRE Pittsburgh section, a member of Sigma Xi, and a Fellow of the American Institute of Electrical Engineering. In 1937 he received the George Westinghouse Award in Engineering Education from the American Society of Electrical Engineering.

❖

Mary Camilla Williams was born in Albany, N. Y., in 1923. She attended the Calvert and Bryn Mawr Schools, in Baltimore, Md., receiving the A.B. degree from Bryn Mawr College in 1946. Miss Williams has been engaged in laboratory work since 1944, when she became a technician at the Cryogeny Laboratory of The Johns Hopkins University. She is now a research assistant, attached to the same institution.

M. C. Williams

# Correspondence

## Positive-Grid Characteristics of a Triode*

In a recent paper by Wood,[1] the grid in a positive-grid triode was considered as a virtual cathode, and the author sought to explain the deviation of his theoretical curves from the experimental ones by means of secondary emission, as stated in his observation (C). I cannot agree with him in his explanation.

At first, as Wood indicated in his paper, when the plate voltage is greater than the grid voltage, secondary-emission current, if any, can only flow from the grid towards the plate, and thus adds to the plate current. Consequently, any secondary emission present in this condition will simply alter his result in the opposite sense to his observation (C).

Regarding his deviations, I should like to state that they actually came from his assumption that the grid could be considered as a "virtual cathode." Thus, when he directly applied his equation (1), he actually fixed the field pattern of the potential distribution to one which corresponds to the maximum or space-charge-limited current, assuming the grid plane to be replaced by an emitter. This is a limit which usually cannot be realized in an actual triode. Should we insist on assuming the grid plane as an emitter, the emission would be mostly temperature-saturated, instead of space-charge-limited.

In order to clarify this point, it is well to refer back to Jaffé's paper,[2] where Jaffé indicated that the equation (1) used by Wood corresponds to the maximum current which can enter the fixed discharge space. In that case, we always observe a fixed potential distribution pattern with a minimum located somewhere beyond the emitter. As a result we certainly cannot apply that equation if the current is not space-charge-limited, especially when there is no potential minimum in the space. In the latter case, we have the Branch I condition in Jaffé's paper. The current is much smaller than the space-charge limit calculated by Wood, since there is a positive potential gradient on the emitter.

In a triode we certainly do not always have a potential minimum between grid and plate. The potential distribution itself depends largely on the space current which can enter the grid-plate space. Furthermore, the plate current of a triode obviously depends on the total emission from the cathode; it cannot be simply fixed by the grid and plate voltages. As an example, let us suppose that the grid is of the same potential as the neighboring potential of the grid plane. The presence of the grid will, therefore, have no effect on the potential distribution in this case. In other words, we get the same potential distribution as would occur in a diode degenerated from a triode with the grid omitted. There, the potential-distribution curve between the grid and plate electrodes is obviously monotonously increasing according to $V = V_a \cdot (x/a)^{3/4}$, in the case of plane electrodes, or to $V = V_a \cdot (\beta^2 r/\beta_a^2 r_a)^{2/3} \doteq V_a \cdot (r/r_a)^{2/3}$, in cylindrical electrodes, where, for simplicity, the cathode radius is assumed to be negligibly small, so that the Langmuir's function $\beta^2 \doteq \beta_a^2 \doteq 1$. The flow of current is here limited by space charge, and cannot be larger; or it would be better to say that the current is limited by the space charge in the entire space from cathode to plate, and is by no means limited by the space charge between the grid and plate planes only. This is a simple example where no potential minimum is present. The actual current is, naturally, much smaller than that predicted from Wood's equation (1). We cannot consider the grid as an emitter or virtual cathode. Instead, we have to use the complete solution from Jaffé's paper. It is easy to see that the deviation will be large when $E_0$ and $V_0$ are larger, as was observed by Wood. The same reasoning explains the deviation of the results of Table I also, where $J$ becomes too small as $E_0$ increases.

For these problems it would seem to be more convenient to choose the potential gradient or the slope of the potential-distribution curve at the grid plane as a parameter. A potential minimum will appear only when that gradient becomes negative.

So far as current distribution in triodes is concerned, it is rather unnecessary to work out the problem in the way proposed. A much simpler and more accurate method was developed by Chaffee.[3] Based on that method, we have obtained a complete solution of current distribution of primary current, and secondary current in power tubes.

Hsiung Hsu
Cruft Laboratory
Harvard University
Cambridge 38, Mass.

* Received by the Institute, March 14, 1949.

[1] George W. Wood, "Positive-grid characteristics of a triode," Proc. I.R.E., Vol. 36, 804–809; June, 1948.

[2] George Jaffé, "On the currents carried by electrons of uniform initial velocity," *Phys. Rev.*, vol. 65, pp. 91–98, February, 1944.

[3] E. L. Chaffee, "The characteristic curves of the triode," Proc. I.R.E., vol. 30, pp. 383–395; August, 1942.

# Institute News and Radio Notes

## Technical Committee Notes

The **Standards Committee** at a meeting held July 14 reviewed and approved a scope of activities for each of the technical committees, and will submit the plans to the Board of Directors for final approval. Preliminary arrangements were made for the formation of a technical committee on **Measurements.** It was announced that a proposed standard for reference designations (for the identification of electrical, electronic, and mechanical parts and their associated graphic symbols) has been prepared by the **Symbols Committee** and presented to the Standards Committee and to the RMA for approval and for possible co-sponsorship. The Master Index of IRE, and tentative definitions prepared by the **Definitions Co-ordinating Subcommittee** under the chairmanship of Axel G. Jensen, will be published in August. This Subcommittee has set up a task group to co-ordinate the definitions of pulse, another group to deal with definitions of transducer and another with electronics. The joint IRE/AIEE group on **Noise Definitions** has been given full committee status. It is hoped this group will be able to co-ordinate definitions of all types of noise as related to various fields. . . . A member from each of the technical committees has been appointed to represent his committee on the **Annual Review Committee** to prepare a Radio Progress Report for 1949 in the field covered by his committee. The Report will be published in the Proceedings of the I.R.E. early in 1950. Ralph Batcher, of Caldwell-Clements Inc., is serving as Chairman of the **Annual Review Committee.** . . . **The Audio Techniques Committee,** meeting August 2, approved a set of definitions prepared by the Subcommittee for **Definitions of Audio Systems and Components** under the chairmanship of O. L. Angevine, Jr. The definitions are being submitted to the **Standards Committee** for approval. Standardization work is underway on methods of measurement for audio systems and components by a subcommittee under the chairmanship of D. E. Maxwell. The Committee has established two subcommittees, one dealing with **Noise in Audio Systems,** and the other concerned with the **Psychology of Aural Perception.** . . . The **Committee on Electron Tubes and Solid States Devices** held a meeting July 15. Approved and submitted to the Standards Committee for standardization was the following material: *Grid Emission Currents, Methods of Testing,* and *Radio Frequency Operating Tests for Power-Output High Vacuum Tubes.* . . . The **Sound Recording and Reproducing Committee,** in session on July 28, formed a new Subcommittee on **Optical Recording** under the chairmanship of Everett Miller of RCA Victor. The **Mechanical Recording** Subcommittee, H. E. Roys, Chairman, has written several methods of testing for cutter calibration of disk recording. Because the art is so new, the Subcommittee has not been able to standardize on one method. It is felt that the material prepared by the group will be of value to engineers, however, and copies will be distributed through the IRE Professional Group on **Broadcast Engineers.** S. J. Begun's Subcommittee on **Magnetic Recording** has prepared a preliminary draft on *Noise Methods of Measurement and Definitions.* . . . A proposed standard, *Methods of Measurement of Television Signal Levels,* prepared by a subcommittee of the **Video Techniques Committee,** is being circulated widely in the IRE and in industry to obtain comments on the work prior to its acceptance by the Committee. L. W. Morrison is Chairman. . . . The **Joint Technical Advisory Committee,** convening at all-day sessions July 19 and August 1, was concerned primarily with the forthcoming FCC hearing and the results of the carrier offset tests conducted by JTAC at the RCA Laboratories at Princeton July 6 and 7. The report of these tests will be included in the JTAC's recommendations to the FCC for the September hearing. The JTAC's full report to the FCC will be published and issued as Vol. IV, Proceedings of the JTAC. . . . A petition for the formation of a **Professional Group On Broadcast and Television Receivers** was approved by the Executive Committee August 9. The sponsor is Virgil M. Graham, Sylvania Electric Products Inc., Flushing, L. I. . . . The **Administrative Committee of the Antennas and Propagation Group** met July 15 at Washington, D. C. Constitution and By-Laws were adopted and a membership committee appointed. Plans are being made to hold this group's first national meeting in conjunction with the URSI meeting at Washington October 31 and November 2, 1949. . . .

## IRE/AIEE Slate Second Annual Conference for Oct. 31, Nov. 1, 2

Electronic instrumentation in nucleonics and medicine will be the theme of the second annual IRE/AIEE joint conference scheduled for October 31, November 1 and 2 at the Hotel Commodore, New York, N. Y. "Evaluation of Radiation Hazards" will be the topic of a special round-table discussion planned for the evening session on November 1.

A four-man panel of scientific experts will lead the discussion and then will answer questions from the audience. Dr. Karl T. Compton, chairman of the Research and Development Board of the National Military Establishment, will address the gathering.

Following the program plan of last year's conference, the coming meeting will devote the first day's proceedings to electronics in medicine, the second day's to nucleonics in medicine, and the third day's to the physical aspects of nucleonics instrumentation.

Simultaneously with the conference, the Nucleonics Manufacturers' Exhibit will be held on November 1 and 2 at the Hotel Commodore. This exhibit of nucleonics instrumentation is expected to be one of the largest ever held. Featured will be scalars, Geiger tubes, survey meters, scintillation counters, and industrial instrumentation utilizing radiation.

## URSI—IRE Groups Will Confer at Fall Session in Washington

In lieu of the regular fall session of the URSI and the IRE, a joint meeting of the USA National Committee of the URSI and the IRE's newly organized Professional Group on Antennas and Propagation has been scheduled for October 31, November 1 and 2, at Washington, D. C. The session will convene at the National Academy of Sciences, 2101 Constitution Ave., N.W., and in the auditorium of the State Department Building, 21 St. and Virginia Ave., N.W.

Sponsoring the conference are the National URSI Commissions as follows: Commission 2—Tropospheric Radio Propagation, Chairman: Dr. Charles R. Burrows, Director of School of Electrical Engineering, Cornell University; Commission 3—Ionospheric Radio Propagation, Chairman: Dr. Newbern Smith, Chief of Central Radio Propagation Laboratory, National Bureau of Standards; Commission 5—Extraterrestrial Radio Noise, Chairman: Dr. D. H. Menzel, Harvard College Observatory; Commission 6—Radio Waves and Circuits, including General Theory and Antennas, Chairman: Dr. L. C. Van Atta, Naval Research Laboratory.

The IRE Professional Group on Antennas and Propagation will be co-sponsors of the sessions of Commissions 2, 3, and 6.

## Florida Broadcasting Company Starting Television Programs

Radio station WMBR-TV, owned by the Florida Broadcasting Company, commenced broadcasting test patterns last month, and planned to open officially early in October with local television program with a four and one-half hour daily and Sunday schedule. Station officials reported that it might be "at least a year" before network programs can be picked up for local television fans.

WMBR-TV purchased complete transmitter and studio equipment from General Electric, including a 3-bay antenna which is mounted on a 500-foot tower, and other equipment such as wave-form rack, film camera channel, rack of transmitter monitoring equipment, and two 16-mm movie projectors.

## Electronics Conference Aids Research, New Developments

Electronic research, development, and application were the concern of the National Electronics Conference held September 26, 27, and 28 at the Edgewater Beach Hotel, Chicago, Ill., with technical sessions devoted to the general topics of Electronic Instrumentation, Solid-State Studies, Computers, Television, Antennas, Measurements, Magnetic Amplifiers, Research Management, Theory of Communications, Vacuum Tubes, Electromagnetics, Supersonics, and Audio-Frequency.

## Radio Fall Meeting To Be Held at Syracuse

Authorities in their respective fields will address sessions of the Radio Fall Meeting conducted under auspices of the IRE and the RMA Engineering Department on October 31, November 1 and 2, at the Hotel Syracuse, Syracuse, N. Y.

R. H. Williamson is chairman of the technical session starting at ten o'clock in the morning of the conference's opening. The session will be devoted to discussion of the following topics: "Measurement of Transient Response of Television Receivers" by J. Van Duyne, of Allen B. DuMont Laboratories Inc.; "Television Transient Response Measurement" by Jerry Minter, of Measurements Corporation; and "Underwriters' Requirements for Television Receivers" by K. S. Geiges, of Underwriters' Laboratories, Inc.

The afternoon session with J. R. Steen, chairman, will hear the following addresses: "Quality Control from the Producer and Consumer Viewpoints" by A. B. Mundel, of Sonotone Corporation; "Quality Control Gets a Job in Television Manufacturing" by L. Lutzger, of Allen DuMont Laboratories, Inc.; and "The Navy's Interest in Quality Control" by William R. Pabst, Jr., Navy Department, Bureau of Ordnance.

Dr. Ralph E. Lapp of the Research and Development Board, Washington, D. C., will speak on the topic, "The Atomic Bomb and National Security," at the evening session, jointly sponsored by the Syracuse Section of the IRE and the Technology Club of Syracuse.

Chairman of the November 1 morning session is R. A. Hackbusch who has arranged the following program: "An Intercarrier Sound System for Television Receivers Using the 6BN6" by Walter Stroh, of Zenith Radio Corporation; "Simplification of Television Receivers" by W. B. Whalley, of Sylvania Electric Products Inc.; and "Came the Television Revolution" by Dorman B. Israel, of Emerson Radio and Phonograph Corporation; "Universal Application-Cathode Ray Sweep Transformer with Ceramic Iron Core" by C. E. Torsch, of General Electric Company. The afternoon session, with J. E. Brown, as chairman, will hear addresses as follows: "An Evaluation of Television Viewing Filters," by A. E. Martin and R. M. Bowie; and "Characteristics of High-Efficiency Deflection and High Voltage Supply Systems for Kinescopes" by O. H. Schade, of RCA. At the dinner meeting Kenneth W. Jarvis will discuss "The Engineering Aspects of Sin."

At the November 2 morning session topics will be "Pickup Tracking" by H. E. Roys, of RCA Victor Division; "New Audio Amplifier Circuit" by Frank H. MacIntosh, consulting engineer; "The Safety-Vox, A Novel Continuous Tape Magnetic Recorder-Reproducer for Industrial Purposes" by R. A. York, of General Electric Company; and "A New Type of Dual Cone Loudspeaker" by Harry F. Olson and John Preston of RCA Laboratories and D. H. Cunningham, RVA Victor Division.

H. C. Sheve, chairman, has arranged for the afternoon session the following program: "Design and Application of a New Miniature High-Frequency Transmitting Pentode" by Robert M. Cohen and George F. Elston of RCA; "A VHF Remotely Tunable Receiver" by Leonard A. Mayberry, of the Hallicrafters Company; and "The Advantages of Toroidal Transformers in Communication Systems" by H. W. Lamson of General Radio Company.

**Second Call!**

**Authors for National Convention**

**R. M. Bowie, Chairman of the Technical Program Committee for the 1950 IRE National Convention, requests that prospective authors of papers to be considered for presentation submit the following information to him as soon as possible:**

**(1) Name and address of author.**

**(2) Title of paper.**

**(3) Abstract of sufficient length to permit the Committee to assess the paper's suitability for inclusion in the Technical Program. Since the merit of the prospective paper must necessarily be judged by the abstract, it should be clear and informative.**

**Material should be mailed to R. M. Bowie, Sylvania Electric Products Inc., Box 6, Bayside, L. I., N. Y. The deadline for acceptance of abstracts is November 21, 1949. Your prompt submissions will be appreciated.**

## Rider Publishes Index for Electronics Information

John F. Rider, president of the Electronics Research Publishing Co., Inc., has announced that the Electronics Engineering Master Index for 1947 and 1948, and the index for January-June, 1949, will be published next month.

According to Mr. Rider the institution of a new idea in the contents of these publications will be of significance to the electronic engineering industry. Beginning with 1947–1948 index, the contents will cross reference published technical papers and related U. S. patents allowed during the period covered by the volume. The work will provide a single source listing all technical articles published in the United States and abroad, the titles, patentees, serial number and number of claims, of all electronic and related-subject patents issued in the United States during 1947 and 1948.

## Atomic Unit Grants Funds to Minnesota University

Construction of a 50 million-volt proton linear accelerator, which will be the world's most powerful "atom smasher" of its type, will be started at the University of Minnesota this year under a $728,000 grant from the Atomic Energy Commission, according to an announcement by President J. L. Merrill of the University.

## DuMont Laboratory Studies New Television Allocation

Dr. Thomas T. Goldsmith, Jr. (A'38–SM'46–F'49), research director of Allen B. DuMont Laboratories Inc., has announced the development of a program to utilize vhf and uhf as intergrated components of a national television system that will assure viewers a choice of television services provided by a multinetwork system and protect owners of television receivers from the need to buy additional equipment, including converters and extra antennas. The DuMont plan, which was presented to the FCC at a hearing in September, also provides 10 additional channels for service to smaller localities and seven uhf channels for the use of educators. It constitutes an alternative to the proposals put forward July 11 by the FCC.

According to Dr. Goldsmith, "DuMont enthusiastically approves the policy of providing more channels for additional television services, but there are certain features of the FCC proposal which should be modified to provide better service to the public and a more competitive national television operation."

For example, while the FCC program provides four vhf channels in only 20 of the first 50 cities of the United States, under the DuMont proposal, approximately 35 of the same 50 cities will be provided with four or more vhf channels.

Dr. Goldsmith also states that the DuMont studies, which have been carried on for nearly two years, indicate that FCC proposed allocations, mixing uhf and vhf frequencies in the same market, would impose an unnecessary financial burden on both station owner and receiving set owner.

**Calendar of COMING EVENTS**

National Radio Exhibition, Olympia, London, England, September 28 to October 8

SMPE 66th Semiannual Convention, Hollywood, Calif., October 10–14

AIEE Midwest General Meeting, Cincinnati, Ohio, October 17–21

**Technical Conference on Antennas, Kansas City Section, IRE, Kansas City, October 28–29**

**Radio Fall Meeting, Syracuse, N. Y., October 31, November 1–2**

**1949 Nucleonics Symposium, New York City, October 31, November 1–2**

**URSI/IRE Joint Meeting, October 31, November 1–2, Washington, D. C.**

**Southwestern IRE Conference Dallas, Tex., December 9–10**

**1950 IRE National Convention, New York, N. Y., March 6–9**

# Industrial Engineering Notes[1]

## National Bureau of Standards Develops Electron-Optic Tool

As the result of a series of electron-microscope experiments at the National Bureau of Standards, Dr. L. L. Marton of the Electron Physics Laboratory has developed an electron-optical shadow technique which provides a valuable tool for the quantitative study of electrostatic and magnetic fields of extremely small dimensions. An electron lens system is used to produce a shadow image of a fine wire mesh placed in the path of the electron beam. From the distortion in the shadow network caused by the deflection of the electrons as they pass through the field under study, accurate values of field strength are computed.

According to Dr. Marton, it is thus possible to investigate quantitatively fields that have not been susceptible to other methods of investigation; for example, the fringe fields from the small domains of spontaneous magnetization in ferromagnetic materials.

The new development, which is based on extensive theoretical analysis, should provide a powerful means for broadening present knowledge concerning space-charge fields, fields produced by contact potentials, patch fields in thermionic emission, charge distribution in a gaseous plasma, waveguide problems, and the basic magnetic properties of metals. Though similar in some respects to the electron-optical Schlieren method previously developed at the Bureau, the shadow method is better adapted to precise determinations of field intensity.

According to the Bureau, perhaps the greatest value of the electron-optical shadow method lies in its utility for exploring complex electric and magnetic fields of extremely small dimensions or in which a probe of size greater than the electron would disturb the field under study. It provides data for accurate calculation of the absolute value of the intensity in the neighborhood of a specimen of any size or shape without altering or disturbing the field.

## Television News

**The FCC has issued proposals for expanding television broadcasting** into the uhf band and has scheduled a broad television hearing, involving the proposed allocations and consideration of color video proposals as the first step toward lifting the current "freeze" on new television stations. The FCC simultaneously has reaffirmed previous vhf allocations with only three assignment changes in as many cities. The television allocations proposals provide for 42 uhf channels, plus retention of the present 12 vhf bands, both on present TV standards. They would permit construction of a nation-wide television system embodying a total of 2,245 television stations in 1,400 cities and communities. Uhf channels alone allow for 1,702 stations in 1,179 areas in addition to any rural coverage. Uhf channel allocations, in general, are in virgin territory with a minimum of over-lap of uhf and vhf stations, as recommended early this year by the FCC Conference Committee of RMA. For instance, no channels were assigned to New York City, Chicago, or Los Angeles, and only one uhf channel was allocated to Philadelphia and Washington. Baltimore got two uhf channels. Uhf channels will be numbered 14 through 55. Thirty-two were assigned for metropolitan television stations and ten for community stations. The uhf assignments will begin at 470 or 500 Mc, depending on the outcome of a Bell Laboratories petition for assignment of the 470-500 Mc band to multichannel mobile radio communications. Vhf channel assignments are identical with previous FCC allocations except in three cities, Cleveland, Syracuse, and Rochester, where channel changes within vhf were proposed. . . . With the view of encouraging the adoption by foreign countries of American television standards, the **U. S. Delegation** attending an international meeting on Television standards at Zurich, Switzerland **were authorized to invite representatives** of the study group to attend a **television demonstration** in this country. The position of the various delegations with respect to the number of picture frames and lines was as follows: U. S. 30 frames, all others 25; British and French, 405 and 819 lines, respectively; U. S. 525; Denmark, Hungary, Netherlands, Sweden, Switzerland, and Czechoslovakia, 625 lines. The Conference agreed that further study was required to determine maximum brightness usuable with 50 and 60 cycles per second. . . . A dispatch from the American Consulate General in the **Netherlands** to the U. S. Department of Commerce indicates that **experimental television broadcasting stations** are **operating** in that country but the government has no official plans for regular broadcasts. An experimental station at Eindhoven, uses 567-lines interlaced 2×25 (synchronized on 50-cycle line frequency). There is also an experimental television transmitter at Gronigen, built by amateurs, which broadcasts on the 144-Mc amateur band, using a 250-line system. The Eindhoven station uses 67.75 Mc for video and 63.75 for sound. . . . Following receipt of complaints from television receiver owners that **diathermy equipment** and some **other radiation devices** have been the **cause of considerable interference to television broadcasts,** the FCC has proposed to amend its rules to clarify the responsibilities of operators of these devices. It has announced the following statement: "an analysis of these complaints shows that in many instances the interfering signal is the fundamental signal emitted by the diathermy or other equipment in the channel centering on 27.120 Mc prescribed for such use in Part 18 of the Commission's rules. The interference involved results from the fact that most TV receiver manufacturers have selected intermediate frequency passbands in the 27 Mc region, making such receivers presently in use susceptible to interference from medical diathermy and other devices operating on 27.120 Mc."

## FCC Actions

Two stations, one in Baltimore and one in New York, have been authorized by the FCC to conduct **experimental television broadcasts in color** with the view of further studying compatibility of color standards and the present black-and-white standards and the problem of converting present receivers to color. CBS has granted authority to begin broadcasting in color during the hours when its regular television programs are not being broadcast in order to gather information for the FCC television hearings. The other action authorized station WMAR-TV in Baltimore to broadcast **color television programs originating at Johns Hopkins University Hospital** in connection with the American Medical Association convention in Washington, and also to gather information for the television hearings. WMAR utilized equipment furnished by a Philadelphia pharmaceutical concern which had previously demonstrated color television operations at Philadelphia and Atlantic City. The program was microwaved from Johns Hopkins to WMAR-TV and then broadcast to Washington. . . . Letters have been sent to all experimental television stations asking for reports on their research and experimentation in both the uhf and vhf bands. Full details on the operation and findings of these stations, including questions on color if that type of transmission has been undertaken, have been asked. With respect to color, the FCC requested information concerning color break-up, flicker, color fringing, image registration, color fidelity, picture brightness, camera light efficiency, definitions, field tests and details with respect to modification of transmitters and receivers to provide the degree of compatability contemplated by the recent television notice of the Commission. . . . **Bound volumes of decisions and orders of the FCC,** exclusive of annual reports, covering the period July 1, 1945, through June 30, 1947, are now on sale at the Superintendant of Documents, Government Printing Office, Washington, D. C., at $3.75 a copy, according to an announcement by the RMA.

## Signal Corps Crystal Discovery May "Revolutionize" Industry

Industry is expected to benefit from a new discovery in the processing of quartz crystals, according to an announcement by the U. S. Army Signal Corps. The development which may revolutionize the quartz crystal industry "promises proportionate savings in the future for all types of modern communications services, including television, radio broadcasting, point-to-point radio, and in hundreds of types of military equipments which depend on crystal control for their operation."

More channels may be available in the future due to the ability of these crystals to hold precisely to an assigned frequency. Chances of overlapping or drowning out of one station by another on an adjacent channel will be greatly reduced, the Signal Corps said. The discovery involves the super-heating to approximately 900 degrees Fahrenheit, followed by slow cooling for 24 hours.

[1] The data on which these NOTES are based were selected, by permission, from "Industry Reports," issues of July 12, July 15, and July 22, published by the Radio Manufacturers' Association, whose helpful attitude is gladly acknowledged.

# IRE People

**Ralph A. Hackbusch** (A'26–M'30–F'37), formerly vice-president and general manager of Stromberg-Carlson Co., Limited of Canada, has been named president and managing director of that company.

Born in Hamilton, Ontario, on September 18, 1900, he was educated at Hamilton and later specialized in electrical engineering. Prior to his employment with Stromberg-Carlson, he was associated with the Canadian Westinghouse Company and with the Canadian Brandes Co. (Kolster Radio).

In 1930 he became chief engineer and factory manager of the Stromberg-Carlson Telephone Manufacturing Company in Toronto, a position he held for a period of ten years. In 1940 he was named vice-president and general manager.

During the war Mr. Hackbusch was requisitioned by the Canadian government and placed in charge of the radio division of the government's Research Enterprises Ltd., later being elected its vice-president in charge of radio and director of the radio division. He returned to Stromberg-Carlson as managing director, a position he held until his recent election by the board of directors for office as president.

Mr. Hackbusch, who was elected vice-president of the IRE in 1944, served as Chairman of the Toronto Section of the Institute in 1933, a member of the Sections committee in 1936, and on the Board of Directors in 1938, 1944–1946. He was the director of engineering for the RMA of Canada for ten years, member of the Canadian electrical code committee, the main committee of the Canadian Engineering Standards Association, and the RMA's general standards committee. In addition he has been a guest member of the joint co-ordination committee of the Edison Electric Institute, the National Electric Manufacturers Association, and the RMA. He has for many years been a guest member of the general standards committee of the Radio Manufacturers Association of the United States.

Mr. Hackbusch, a professional engineer in the province of Ontario, has also served as the official observer on the main RTPB committee for the RMA of Canada, as vice-president of the Canadian Radio Technical Planning Board, and as chairman of the Canadian Building-Fund Committee.

❖

**Frederick E. Llewellyn** (A'23–F'38), consulting engineer of Bell Telephone Laboratories, has been elected a member of the executive committee of the United States National Committee of the International Electrotechnical Commission to serve for the coming year.

Dr. Llewellyn, who served as President of IRE in 1946, has been concerned with radio and circuit research and analysis of the electronic behavior of vacuum tubes at high frequencies. He was awarded the Morris Liebmann prize for his outstanding original work on constant-frequency oscillators and on vacuum-tube electronics at high frequencies in 1935.

**Ernst F. W. Alexanderson** (A'13–M'13–F'15), consultant to the General Electric Engineering and Consulting Laboratory, was recently named "Man of the Year" at Sweden Day ceremonies attended by 5,000 Swedes and Swedish-Americans.

Dr. Alexanderson was born in Upsala, Sweden, on January 25, 1878. He was graduated from the Royal Technical Institute in Stockholm and did post-graduate work at the Royal Technical Institute at Charlottenburg. Prior to his recent retirement, Dr. Alexanderson had completed forty-six years of service with General Electric.

During that time he was awarded 314 patents, or an average of one patent every seven weeks. The Alexanderson high-frequency alternator made possible reliable trans-oceanic radio transmission. His other patents cover such fields as radio telephony, radio telegraphy, television, vacuum tubes for radio and power rectifiers, and electronic circuits.

Dr. Alexanderson was the recipient of the IRE's Medal of Honor in 1919 and served as the Institute's President in 1921. He has published numerous papers in the PROCEEDINGS OF THE I.R.E. and in the *Journal of the AIEE*. He is also a Fellow of the AIEE.

❖

**Frederick Emmons Terman** (A'25–F'37), Dean of engineering at Stanford University, has been elected vice-president in charge of the Engineering College Administrative Council of the American Society of Engineering Education as the result of the Society's annual convention held this summer at Rensselaer Polytechnic Institute. More than 1,700 engineering educators administrators of engineering colleges and industrial leaders attended the session.

Born on June 7, 1900, in English, Ind., Dr. Terman received the B.S. degree in 1920 and the degree of engineer in 1922 from Stanford University, and the Sc.D. degree from Massachusetts Institute of Technology in 1924. From 1925 to 1937 he served as instructor, assistant professor, and associate professor of Stanford's electrical engineering department. In 1937 he was named professor and head of the department.

During the war Dr. Terman assumed the directorship of the Radio Research Laboratory at Harvard University which developed counter measures to nullify radar equipment. He was Vice-President of the IRE in 1940 and President in 1941.

❖

**Harold S. Osborne** (A'14–M'29–SM'43–F'45), chief engineer for the American Telephone and Telegraph Corporation, has been elected by the United States National Committee of the International Electrotechnical Commission to serve as its chairman for the coming year. The IEC is the electrical division of the International Organization for Standardization.

Dr. Osborne spent the summer in Europe serving as one of the United States delegates to IEC meetings held in June at Stresa, Italy.

A former vice-president and treasurer of the USNC, Dr. Osborne also is affiliated with the American Institute of Electrical Engineers, Acoustical Society of America, and American Physical Society. He is a member of the Joint Conference Committee on Standards, U. S. Department of Commerce, and the Industry Advisory Council, Federal Specifications Board. He is also vice-president and member of the Board of Directors of the American Standards Association.

❖

**Edwin A. Speakman** (A'43-M'44-SM'48), branch head of the National Radio Laboratory's Countermeasures Section, has been appointed executive director of the Committee on Electronics, Research, and Development, National Military Establishment.

Associated with the National Radio Laboratory since 1940, Mr. Speakman has held his present post since 1945. In 1947 he received the Navy's Meritorious Civilian Service award for his work in radar.

Mr. Speakman was born in Gratz, Pa., on August 14, 1909, and has been a radio amateur since 1925, with the call letters W3AUR and W8RSJ. While attending Haverford College in Haverford, Pa., from which he was graduated in 1931 with the bachelor of science degree in physics, he invented the first automatic photoelectric timing system for use in timing sports events. He served as instructor in radio at Haverford for three years following his graduation; then became a radio engineer with the Philco Corp. in Philadelphia and Detroit, remaining with that company until 1939.

Subsequently he was employed for a year as physicist by the Curtis Publishing Co. in Philadelphia, where his work consisted of research in electron-physics as applied to printing processes. His specific duties were to investigate special electronic devices for the improvement of high-speed four-color printing.

The inventor of the telescopic rod antenna system, Mr. Speakman is a member of the American Physical Society, the U. S. Naval Institute, and the Board of Civil Service Examiners for the Potomac River Naval Command.

❖

**Charles N. Kimball** (A'34-M'40-SM'43) was recently appointed technical director of the Bendix Aviation Corp's research laboratories in Detroit, Mich.

Born in Boston, Mass., on April 21, 1911, Dr. Kimball received the B.E.E. degree from Northeastern University in 1931 and the S.M. and Sc.D. degrees in communications from Harvard University in 1933 and 1934, respectively. After graduation he was employed by the National Union Radio Corp. as a tube development engineer until 1935, when he joined the research staff of

the Radio Corporation of America's license division laboratory in New York City. There he worked on television, frequency modulation, and special communication studies.

From 1940 through 1946 Dr. Kimball was vice-president in charge of engineering at the Aireon Manufacturing Corp. in Kansas City, as well as a member of the Board of Directors. His duties included supervision of work on a variety of projects, including radio countermeasure equipment and underwater sound techniques. He was one of the original workers in the field of high-frequency communications for railroads. In 1947 and 1948 he worked privately on instrumentation problems in the food processing industries.

The author of several papers on television and electronic instrumentation, Dr. Kimball holds patents in these fields. He is a member of Tau Beta Psi and the Harvard Engineering Society, and is a former officer of the Kansas City Section of the Institute.

❖

## Correction

In the announcement of the appointment of **Roger E. Robertson** (A'48) to the staff of the National Bureau of Standards in the August issue of PROCEEDINGS, inadvertently it was erroneously stated that Mr. Robertson had been affiliated with Bell Telephone Company. His prior business association as electronics engineer was with Bell Aircraft Corp.

❖

**James Rennie Whitehead** (SM'45) has been appointed to the post of Principal Scientific Officer in the Telecommunications Research Establishment, Ministry of Supply at Malvern, Worcester, England.

A native of England, where he was born April 8, 1917 in Lancastershire, he received his preparatory education at Clitheroe Royal Grammar School. He was graduated with honours from the University of Manchester, receiving the B.Sc. degree in 1939.

Mr. Whitehead recently obtained a Ph.D. degree from the University of Cambridge. He formerly was engaged in scientific research and development at the Ministry of Aircraft Product Research Establishment, Malvern.

❖

**Robert D. Teasdale** (S'44–A'46–M'49) has joined the teaching staff of the School of Electrical Engineering, Georgia Institute of Technology. Dr. Teasdale has been appointed associate professor of electrical engineering. Recently he earned the Ph.D. degree from Illinois Institute of Technology, where he has done some part-time teaching.

Dr. Teasdale, who is a native of Pennsylvania, received the bachelor's degree at Carnegie Institute of Technology under a George Westinghouse Scholarship. He held a Gerard Swope Fellowship for 1947–1948, and an RCA Fellowship in Electronics for 1948–1949. He is a member of the American Institute of Electrical Engineers, Sigma Xi, Tau Beta Pi, and Eta Kappa Nu.

❖

# Books

### Principles of Radar, by Denis Taylor and C. H. Wescott

Published (1949) by the Cambridge University Press, 51 Madison Ave., New York, N. Y. 136 pages+3-page index+x pages. 56 figures. 5½×8½. $3.50.

Radar, a specific application of the principles of radio, was responsible for a large-scale development of new radio techniques. Much of modern radio technique is consequently erroneously classified in current literature as radar. As one turns wearily from the resulting congested volumes under that title, the first reaction to Taylor and Wescott is that it can't be done in 136 easily readable pages.

The authors, however, have very nearly succeeded in doing exactly that! Each fundamental of the "Principles of Radar" is lucidly set before the reader in a volume that will delight any technical student. In fact, so condensed and so well classified is the material that the work could easily pass as an engineering handbook on radar. However, it is by no interpretation a mere tedium of facts. Based on systems engineering concepts, the quantitative facts mathematically expressed are backed up by qualitative logic clearly identifying the physical significance of every term, and further clarified by numerical examples based on historical equipments.

In only rare exceptions is clarity sacrificed to brevity. It is suggested that the lack of exact correspondence between text and figure 4.5 on "Electronic Range Marker" and ommission of a statement on axial orientation of the microwave variable elevation beam equipment on page 94, be corrected in future editions. In both cases, the intent is clear to the expert, but possibly confusing to the student.

The question of what to exclude ultimately taxes the judgment of any author who attempts to put so much information in so little space. The omission of any treatment of signal storage, radar camouflage, and corner reflectors might be debated.

To one familiar with the development and application of radar on both sides of the Atlantic, this text displays a disappointing national limitation. The historical introduction, the examples, the application problems, the techniques themselves, are all limited to British experience. Were a similar work based on American experience, some statements of fact would appear in disagreement with Taylor and Westcott, simply because American and British radar developments, while similar, were not identical. Historically, original conceptions and significant observations would be earlier in the American Version, with development more rapid and military application earlier in the British version. Technically, American experience in common antenna working, rapid scan, IFF, and shipborne radar would lead to rather different treatment of these subjects, and there might be disagreement on the relationship between bandwidth and range accuracy due to employment of different techniques. This restriction renders the book a bit thin, both historically and technically, in those areas where the contribution was significantly American.

In spite of the above-noted limitation, since no American equivalent is known to this reviewer, Taylor and Westcott's "Principles of Radar" is recommended as a text in radar engineering for those who prefer less detail than is found in Ridenour's 735-page microwave version of "Radar Systems Engineering." It is also recommended as a handbook for radar systems engineering for practicing engineers. It is excellent for the technically inclined reader who seriously wants to know about radar. The merely curious will find it intellectually too strenuous.

ROBERT M. PAGE
Naval Research Laboratory
Washington 25, D. C.

### Transformations on Lattices and Structures of Logic, by Stephen A. Kiss

Published (1948) by Stephen A. Kiss, 11 E. 92 St., New York 28, N. Y. 315 pages+4-page index+2-page bibliography+x pages. 6 figures. 7×10.

Mathematics develops by successive abstraction and generalization. Modern algebra is particularly subject to this tendency, with many of its concepts, such as those of group and lattice, now permeating the entire range of mathematical thought. In this book Dr. Kiss develops a generalization of Boolean algebra based upon its lattice theoretic properties. Naturally such a work will be of principal interest to the logician and the pure mathematician.

The book falls into three main parts of about the same length. The first consists of an orderly exposition of the pertinent results from modern algebra and lattic theory. In the second part the author defines his generalized Boolean algebras with 4, 8, 16 or generally $2^n$ elements, and develops their algebraic and lattice theoretic properties. These algebras have a natural and elegant mathematical structure. The third part of the book is an exposition of the calculus of classes and of propositions, and an application of the preceding algebraic theory to an extension of these fields.

Classical Boolean algebra and the calculus of propositions have been applied in such fields as switching theory and the study of nerve networks, and it is possible that the author's extensions of these disciplines may find similar applications. Dr. Kiss conjectures that an adequate description of physical and biological phenomena require 4 and 16 class logics, without, however, developing this thesis. At any rate, considered as a purely algebraic theory, the author has added a significant contribution to mathematical literature.

CLAUDE E. SHANNON
Bell Telephone Laboratories, Inc.
Murray Hill, N. J.

# Institute Committees—1949

## Executive

S. L. Bailey, *Chairman*
D. B. Sinclair, *Vice-Chairman*
Haradan Pratt, *Secretary*

W. R. G. Baker
M. G. Crosby
A. N. Goldsmith
B. E. Shackelford

## Board of Editors

A. N. Goldsmith, *Chairman*

F. W. Albertson
J. S. Allen
G. M. K. Baker
W. L. Barrow
R. R. Batcher
A. E. Bowen
R. M. Bowie
Ralph Bown
R. S. Burnap
O. H. Caldwell
C. W. Carnahan
C. C. Chambers
L. M. Clement
J. D. Cobine
M. G. Crosby
R. B. Dome
W. G. Dow
E. W. Engstrom
W. L. Everitt
W. G. H. Finch
D. G. Fink
H. C. Forbes
I. A. Getting
P. C. Goldmark
A. W. Graf
F. W. Grover
L. B. Headrick
E. W. Herold
J. A. Hutcheson
C. M. Jansky, Jr.
J. K. Johnson
L. F. Jones
H. S. Knowles
J. D. Kraus
J. B. H. Kuper
J. L. Lawson
D. G. Little
F. B. Llewellyn
S. S. Mackeown
Nathan Marchand
E. D. McArthur
Knox McIlwain
J. W. McRae
L. A. Meacham
G. F. Metcalf
E. L. Nelson
D. O. North
H. F. Olson
R. M. Page
H. O. Peterson
G. W. Pickard
Haraden Pratt
C. A. Priest
J. R. Ragazzini
Simon Ramo
H. J. Reich
J. D. Reid
F. X. Rettenmeyer
P. C. Sandretto
S. W. Seeley
V. W. Sherman
L. C. Smeby
C. E. Smith
J. A. Stratton
W. C. Tinus
K. S. Van Dyke
E. K. Van Tassel
E. C. Wente
H. A. Wheeler
J. R. Whinnery
W. C. White
L. E. Whittemore
Jerome Wiesner
G. W. Willard
Irving Wolff
V. K. Zworykin

## Awards

Keith Henney, *Chairman*

Austin Bailey
W. L. Barrow
D. E. Chambers
E. W. Engstrom
W. L. Everitt
V. M. Graham
R. A. Hackbusch
R. W. Hickman
A. V. Loughren
J. W. McRae
David Packard
E. R. Piore
S. W. Seeley
G. R. Town

## Education

H. J. Reich, *Chairman*

C. D. Albert
R. G. Anthes
R. E. Beam
L. J. Black
C. C. Chambers
R. M. Fano
G. H. Fett
R. A. Galbraith
A. W. Graf
A. E. Harrison
R. W. Hickman
G. B. Hoadley
L. N. Holland
G. L. Hollander
A. H. Howell
A. W. Melloh
P. H. Nelson
J. M. Pettit
W. H. Pickering
L. R. Quarles
J. R. Ragazzini
J. D. Ryder
B. E. Shackelford
R. P. Siskind
W. R. Smith
K. R. Spangenberg
F. R. Stansel
F. E. Terman
L. A. Ware
Ernst Weber
L. E. Williams
A. H. Wing, Jr.
Irving Wolff

## Constitution and Laws

J. E. Shepherd, *Chairman*

F. W. Albertson
I. S. Coggeshall
R. A. Heising
H. J. Reich
G. T. Royden
H. R. Zeamans

## Professional Groups

W. L. Everitt, *Chairman*

O. L. Angevine, Jr.
A. B. Chamberlain
W. H. Doherty
V. M. Graham
R. A. Heising
(Professional Group Chairmen Ex-Officio)

## Tellers

G. F. Metcalf, *Chairman*

J. F. Byrne
J. L. Callahan

## Admissions

T. H. Clark, *Chairman*

H. S. Bennett
P. S. Christaldi
H. P. Corwith
F. M. Deerhake
D. D. Donald
G. A. Downsbrough
T. M. Ferrill, Jr.
C. A. Hachemeister
G. B. Riley
R. H. Siemens
Rohn Truell

## Policy Development

B. E. Shackelford, *Chairman*

R. E. Beam
K. C. Black
M. G. Crosby
A. E. Cullum, Jr.
A. V. Eastman
R. A. Heising
T. A. Hunter
F. B. Llewellyn
J. A. Stratton
F. E. Terman
W. N. Tuttle

## Sections

A. W. Graf, *Chairman*

R. A. Heising
J. F. Jordan
C. A. Norris
B. E. Shackelford
J. E. Shepherd
E. T. Sherwood
W. O. Swinyard
R. N. White
(Section Chairmen Ex-Officio)

## Nominations

T. A. Hunter, *Chairman*

W. L. Barrow
Ralph Bown
A. E. Cullum, Jr.
Melville Eastham
W. L. Everitt
I. J. Kaar
F. H. R. Pounsett
B. E. Shackelford
F. E. Terman

## Membership

R. F. Guy, *Chairman*

F. W. Albertson
J. E. Brown
A. B. Chamberlain
J. B. Coleman
G. W. Fyler
V. M. Graham
George Grammer
G. L. Hollander
R. V. Howard
A. S. Kramer
F. B. Llewellyn
F. L. Marx
J. D. Reid
D. B. Smith
F. E. Terman
W. C. White
(Chairmen of Section Membership Committees Ex-Officio)

## Public Relations

R. F. Guy, *Chairman*

W. J. Barkley
O. H. Caldwell
W. C. Copp
O. E. Dunlap, Jr.
R. A. Hackbusch
Keith Henney
T. R. Kennedy
M. B. Sleeper
Lewis Winner

## Finance

W. R. G. Baker, *Chairman*

I. S. Coggeshall
F. B. Llewellyn
D. B. Sinclair, ex-officio

## Papers Review

G. F. Metcalf, *Chairman*

H. A. Affel
C. F. Baldwin
J. L. Barnes
B. de F. Bayly
P. H. Betts
F. J. Bingley
D. S. Bond
Kenneth Bullington
H. A. Chinn
J. K. Clapp
S. B. Cohn
J. M. Constable
M. G. Crosby
F. W. Cunningham
A. R. D'Heedene
R. L. Dietzold
M. J. Di Toro
H. D. Doolittle
O. S. Duffendack
R. D. Duncan, Jr.
E. H. Felix
V. H. Fraenckel
R. L. Freeman
Paul Fritschel
E. G. Fubini
Stanford Goldman
W. M. Goodall
G. L. Haller
O. B. Hanson
A. E. Harrison
T. J. Henry
C. N. Hoyler
P. K. Hudson
D. L. Jaffe
Hans Jaffe
D. C. Kalbfell
A. G. Kandoian
Martin Katzin
J. G. Kreer, Jr.
Emile Labin
J. J. Lamb
V. D. Landon
M. T. Lebenbaum
C. V. Litton
B. D. Loughlin
Louis Malter
W. P. Mason
R. E. Mathes
H. F. Mayer
H. R. Mimno
Jerry Minter
R. E. Moe
F. L. Moseley
G. G. Muller
A. F. Murray
J. R. Nelson
K. A. Norton
Ernest Pappenfus
H. W. Parker
L. J. Peters
A. P. G. Peterson
W. H. Pickering
A. F. Pomeroy
Albert Preisman
T. H. Rogers
H. E. Roys
J. D. Ryder
M. W. Scheldorf
Samuel Seely
Harner Selvidge
R. E. Shelby
C. M. Slack
J. E. Smith
R. L. Snyder
E. E. Spitzer
J. R. Steen
E. K. Stodola
G. C. Sziklai
H. P. Thomas
Bertram Trevor
W. N. Tuttle
Dayton Ulrey
A. P. Upton
G. L. Usselman
S. N. Van Voorhis
J. R. Weiner
M. S. Wheeler
R. M. Wilmotte
W. T. Wintringham
J. W. Wright
H. R. Zeamans

## Papers Procurement

J. D. Reid, *Chairman*

Andrew Alford
B. B. Bauer
R. M. Bowie
J. T. Brothers
G. H. Brown
J. W. Butterworth
I. F. Byrnes
T. J. Carroll
K. A. Chittick
B. J. Chromy
J. T. Cimorelli
L. M. Clement
G. V. Eltgroth
M. K. Goldstein
R. C. Guthrie
J. R. Harrison
John Hessel
T. A. Hunter
Harry Huskey
Hans Jaffe
J. J. Jakosky
Martin Katzin
C. E. Kilgour
N. L. Kiser
A. V. Loughren
I. G. Maloff
H. R. Marvin
W. P. Mason
Pierre Mertz
B. J. Miller
I. E. Mouromtseff
A. F. Murray
L. L. Nettleton
G. M. Nixon
D. E. Noble
K. A. Norton
T. M. Odarenko
W. C. Osterbrock
W. E. Reichle
F. X. Rettenmeyer
H. W. G. Salinger
K. M. Schafer
R. E. Shelby
W. P. Short
W. E. Shoupp
Daniel Silverman
P. L. Smith
J. Q. Stansfield
G. R. Town
L. G. Trolese
H. J. Tyzzer
W. L. Webb
J. R. Whinnery
W. C. White
G. S. Wickizer
R. H. Williamson
R. J. Wise

# Technical Committees, May 1, 1949–May 1, 1950

## Annual Review

Ralph Batcher, *Chairman*
Frank A. Cowan, *Vice-Chairman*

. L. Black
revor Clark
D. Crawford
V. Dimock
G. Fick
eorge Graham
T. Hamlett
R. Hodges
V. L. Hogan
C. Jordan
E. Keister
G. Kreer, Jr.
R. Meahl
H. R. Mimno
J. Minter
L. S. Nergaard
H. F. Olson
A. F. Pomeroy
George Rappaport
Nathaniel Rochester
Harner Selvidge
Harry Smith
W. N. Tuttle
K. S. Van Dyke
H. P. Westman
L. E. Whittemore

## Antennas and Wave Guides

L. C. Van Atta, *Chairman*
L. J. Chu, *Vice-Chairman*
A. G. Fox, *Vice-Chairman*

M. Bloomer
S. Carter
E. Eaton
dney Frankel
dward Hamilton
F. Holtz
C. Jordan
E. Kienow
E. Kock
W. Mieher
Theodore Moreno
J. D. Parker
D. C. Ports
M. W. Scheldorf
S. A. Schelkunoff
J. C. Schelleng
S. Sensiper
J. P. Shanklin
George Sinclair
P. H. Smith

## Audio Techniques

E. J. Content, *Chairman*
R. A. Miller, *Vice-Chairman*

L. Angevine, Jr.
W. Augustadt
L. Beranek
L. Black
H. Castle
I. G. Easton
J. A. Green
D. E. Maxwell
Ralph Schlegel
W. E. Stewart

## Circuits

W. N. Tuttle, *Chairman*
Cledo Brunetti, *Vice-Chairman*

A. Antman
R. Bennett
G. Brainerd
R. D'Heedene
L. Dietzold
L. Everitt
M. Foster
anford Goldman
A. Guillemin
H. Huggins
Herbert Krauss
John Linville
D. O. McCoy
E. E. Overmier
C. H. Page
E. H. Perkins
J. B. Russell, Jr.
Wolcott Smith
Ernst Weber
J. R. Weiner

## Electroacoustics

E. S. Seeley, *Chairman*
B. B. Bauer, *Vice-Chairman*

N. Arnold
ginhard Dietze
J. Di Toro
D. Goodale, Jr.
C. Gregg
Martin Greenspan
F. V. Hunt
W. F. Meeker
H. F. Olson
Vincent Salmon
P. S. Veneklasen

## Electron Tubes and Solid State Devices

L. S. Nergaard, *Chairman*

S. Burnap
W. Clark
G. Dow
E. Fay
M. Glover
E. Gorham
W. Greer
B. Headrick
A. Hendricks
C. Homer
B. Ingram
J. Koch
Herbert Krauss
Louis Malter
J. A. Morton
I. E. Mouromtseff
G. D. O'Neill
O. W. Pike
P. A. Redhead
H. J. Reich
A. C. Rockwood
R. M. Ryder
A. L. Samuel
R. W. Slinkman
C. M. Wheeler

## Electronic Computers

J. W. Forrester, *Chairman*
Nathaniel Rochester, *Vice-Chairman*

S. N. Alexander
J. H. Bigelow
D. R. Brown
Perry Crawford, Jr.
J. P. Eckert, Jr.
E. L. Harder
John Howard
J. H. Kusner
E. Lakatos
B. R. Lester
G. D. McCann
R. D. O'Neal
C. H. Page
G. W. Patterson
J. A. Rajchman
Robert Serrell
R. L. Snyder
D. L. Stevens
G. R. Stibitz
P. B. Taylor
J. R. Weiner
C. F. West
Way Dong Woo

## Facsimile

J. V. L. Hogan, *Chairman*
C. J. Young, *Vice-Chairman*

James Barnes
Henry Burkhard
J. J. Callahan
A. G. Cooley
W. G. H. Finch
F. A. Hester
Pierre Mertz
N. A. Nelson
R. J. Wise

## Industrial Electronics

D. E. Watts, *Chairman*
H. R. Meahl, *Vice-Chairman*

G. P. Bosomworth
J. M. Cage
E. W. Chapin
John Dalke
C. W. Frick
G. W. Klingaman
Eugene Mittelmann
P. E. Ohmart
H. W. Parker
H. O. Peterson
Walther Richter
W. C. Rudd
C. F. Spitzer
R. S. Tucker
Julius Weinberger

## Modulation Systems

H. S. Black, *Chairman*
Bertram Trevor, *Vice-Chairman*

B. V. Blom
F. L. Burroughs
C. C. Chambers
M. G. Crosby
W. J. Cunningham
L. A. W. East
C. W. Finnigan
A. C. Goodnow
D. D. Grieg
R. F. Guy
L. B. Hallman, Jr.
D. M. Hill
J. G. Kreer, Jr.
E. R. Kretzmer
V. D. Landon
C. T. McCoy
L. A. Meacham
Dale Pollack
S. W. Seeley
W. G. Tuller
J. B. Wiesner

## Navigation Aids

Henri Busignies, *Chairman*
H. R. Mimno, *Vice-Chairman*

W. B. Burgess
G. C. Comstock
J. N. Dyer
D. G. Fink
C. J. Hirsch
Wayne Mason
Marcus O'Day
A. C. Omberg
J. A. Pierce
J. A. Rankin
W. M. Richardson
P. C. Sandretto
W. J. Sen
Ben Thompson
R. R. Welsh

## Nuclear Studies

L. R. Hafstad, *Chairman*
R. E. Lapp, *Vice-Chairman*

R. M. Bowie
A. H. Dahl
John Dalke
W. F. Davidson
J. W. Heyd
M. M. Hubbard
J. L. Lawson
Harner Selvidge
W. E. Shoupp

## Piezoelectric Crystals

K. S. Van Dyke, *Chairman*
R. A. Sykes, *Vice-Chairman*

C. F. Baldwin
W. L. Bond
W. G. Cady
J. K. Clapp
Clifford Frondel
Hans Jaffe
W. P. Mason
P. L. Smith

## Radio Transmitters

J. F. McDonald, *Chairman*
A. E. Kerwien, *Vice-Chairman*

E. L. Adams
T. J. Boerner
M. R. Briggs
H. R. Butler
L. T. Findley
Harold Goldberg
J. B. Heffelfinger
J. B. Knox
L. A. Looney
John Ruston
Berthold Sheffield
Harry Smith
J. E. Smith
I. R. Weir

## Railroad and Vehicular Communications

G. M. Brown, *Chairman*
P. V. Dimock, *Vice-Chairman*

E. H. B. Bartelink
F. T. Budelman
D. B. Harris
C. M. Heiden
C. N. Kimball, Jr.
D. E. Noble
J. C. O'Brien
David Talley
George Teommey
R. W. Tuttle
Alexander Whitney

## Receivers

R. F. Shea, *Chairman*
S. C. Spielman, *Vice-Chairman*

J. Avins
G. L. Beers
J. E. Brown
W. F. Cotter
A. R. Hodges
K. W. Jarvis
J. K. Johnson
I. E. Lempert
B. D. Loughlin
C. R. Miner
Garrard Mountjoy
J. F. Myers
J. M. Pettit
F. H. R. Pounsett
J. D. Reid
William O. Swinyard

## Research

D. E. Chambers, *Chairman*
C. G. Fick, *Secretary*

W. L. Barrow
Ralph Bown
Gregory Breit
E. L. Chaffe
J. W. Coltman
W. G. Dow
E. W. Engstrom
W. R. Jones
A. L. Samuel
L. C. Van Atta
J. B. Wiesner

## Sound Recording and Reproducing

S. J. Begun, *Chairman*
H. E. Roys, *Vice-Chairman*

A. W. Friend
George Graham
F. L. Hopper
E. W. Kellogg
R. A. Lynn
J. Z. Menard
Everett Miller
A. R. Morgan
G. M. Nixon
R. A. Schlegel
Lincoln Thompson

## Standards

J. G. Brainerd, *Chairman*
L. G. Cumming, *Vice-Chairman*
A. G. Jensen, *Vice-Chairman*

R. R. Batcher
S. J. Begun
H. S. Black
G. M. Brown
C. R. Burrows
Henri Busignies
W. G. Cady
P. S. Carter
A. B. Chamberlain
Dudley Chambers
E. J. Content
Jay W. Forrester
R. A. Hackbusch
L. R. Hafstad
J. V. L. Hogan
E. J. Keister
E. A. Laport
J. F. McDonald
Wayne Mason
L. S. Nergaard
A. F. Pomeroy
George Rappaport
E. S. Seeley
R. F. Shea
J. R. Steen
W. N. Tuttle
L. C. Van Atta
K. S. Van Dyke
D. E. Watts
L. E. Whittemore

### Symbols

A. F. Pomeroy, *Chairman*
A. L. Samuel, *Vice-Chairman*

K. E. Anspach
C. R. Burrows
A. G. Clavier
H. F. Dart
E. T. Dickey
W. J. Everts
W. A. Ford
R. T. Haviland
V. R. Hudek
O. T. Laube
C. D. Mitchell
C. Neitzert
M. B. Reed
Duane Roller
E. W. Schafer
W. F. Snyder

### Television Systems

A. G. Jensen, *Chairman*
R. E. Shelby, *Vice-Chairman*

G. W. Andrew
W. F. Bailey
M. W. Baldwin
R. M. Bowie
J. E. Brown
K. A. Chittick
C. G. Fick
D. G. Fink
C. J. Franks
P. C. Goldmark
R. N. Harmon
J. L. Hollis
I. J. Karr
R. D. Kell
P. J. Larsen
H. T. Lyman
Leonard Mautner
J. Minter
J. H. Mulligan, Jr.
A. F. Murray
J. A. Ouimet
D. W. Pugsley
David Smith
M. E. Strieby
Norman Young, Jr.

### Video Techniques

J. E. Keister, *Chairman*
W. J. Poch, *Vice-Chairman*

M. W. Baldwin, Jr.
A. J. Baracket
P. F. Brown
R. H. Daugherty, Jr.
V. J. Duke
G. L. Fredendall
R. L. Garman
L. W. Morrison, Jr.
R. S. O'Brien
J. F. Wiggin

### Wave Propagation

C. R. Burrows, *Chairman*
H. G. Booker, *Vice Chairman*

E. W. Allen, Jr.
S. L. Bailey
A. B. Crawford
A. E. Cullum, Jr.
W. S. Duttera
A. G. Fox
E. G. Fubini
I. H. Gerks
M. C. Gray
D. E. Kerr
J. E. Keto
K. A. Norton
H. O. Peterson
J. A. Pierce
George Sinclair
Newbern Smith
A. W. Straiton
E. F. Vandivere
A. H. Waynick
H. W. Wells
J. W. Wright
R. L. Smith-Rose

## Special Committees

### Armed Forces Liaison Committee

G. W. Bailey, *Chairman*

### Convention Policy

J. E. Shepherd, *Chairman*

Austin Bailey
G. W. Bailey
E. J. Content
B. E. Schackelford

### Editorial Administrative

A. N. Goldsmith, Editor, *Chairman*

G. M. K. Baker
H. S. Black
R. S. Burnap
E. F. Carter
H. F. Dart
R. L. Dietzold (alternate for H. S. Black)
A. V. Haeff
E. W. Herold
F. B. Llewellyn
Knox McIlwain
Donald McNicol
K. A. Norton (alternate for Newbern Smith)
Haraden Pratt
J. R. Ragazzini
F. X. Rettenmeyer (alternate for Haraden Pratt)
Newbern Smith
G. C. Sziklai (Alternate for E. W. Herold)
Ernst Weber
H. A. Wheeler
L. E. Whittemore
Harold Zahl

### Professional Recognition

G. B. Hoadley, *Chairman*

C. C. Chambers
H. F. Dart
W. E. Donovan
C. M. Edwards

### Founders

R. F. Guy, *Chairman*

## INSTITUTE REPRESENTATIVES IN COLLEGES—1949

*Agricultural and Mechanical College of Texas: Tom Prickett, Jr.
Akron, University of: P. C. Smith
*Alabama Polytechnic Institute: G. H. Saunders
*Alberta, University of: J. W. Porteous
*Arizona, University of: H. E. Stewart
*Arkansas, University of: G. H. Scott
British Columbia, University of: H. J. MacLeod
*Brooklyn, Polytechnic Institute of: A. B. Giordano
*California Institute of Technology: S. S. MacKeown
*California State Polytechnic College: Clarence Radius
*California, University of: L. J. Black
Carleton College: G. R. Love
*Carnegie Institute of Technology: E. M. Williams
*Case Institute of Technology: J. D. Johannesen
Cincinnati, University of: A. B. Bereskin
*Clarkson College of Technology: F. A. Record
*Colorado, University of: H. W. Boehmer
*Columbia University: J. R. Ragazzini
Connecticut, University of: L. E. Williams
Cooper Union: J. B. Sherman
*Cornell University: True McLean
Dartmouth College: M. G. Morgan
*Dayton, University of: Appointment later
*Detroit, University of: Appointment later
Drexel Institute of Technology: R. T. Zern
Duke, University of: W. J. Seeley
Evansville College: J. F. Sears
*Fenn College: K. S. Sherman
*Florida, University of: P. H. Nelson
*George Washington University: W. S. Carley
*Georgia School of Technology: M. A. Honnell
Harvard University: E. L. Chaffee
*Illinois Institute of Technology: G. F. Levy
*Illinois, University of: E. C. Jordan
*Iowa, State University of: L. A. Ware
*Iowa State College: W. L. Cassell
*John Carroll University: J. L. Hunter
Johns Hopkins University: Ferdinand Hamburger, Jr.
*Kansas State College: J. E. Wolfe
Kansas, University of: D. G. Wilson
*Kentucky, University of: Appointment later
*Lafayette College: F. W. Smith
Lawrence Institute of Technology: H. L. Byerlay
*Lehigh University: D. E. Mode
Louisiana State University: Appointment later
*Louisville, University of: Appointment later
*Maine, University of: W. J. Creamer, Jr.
*Manhattan College: R. T. Weil, Jr.
*Maryland, University of: Appointment later
*Massachusetts Institute of Technology: E. A. Guillemin, W. H. Radford
McGill University: F. S. Howes
*Michigan State College: J. A. Strelzoff
*Michigan, University of: L. N. Holland
*Minnesota, University of: O. A. Becklund
*Missouri, School of Mines and Metallurgy: G. G. Skitek
*Missouri, University of: D. L. Waidelich

* Colleges with approved Student Branches.

# INSTITUTE REPRESENTATIVES IN COLLEGES (cont.)

*Nebraska, University of: F. W. Norris
Nevada, University of: I. J. Sandorf
*Newark College of Engineering: Solomon Fishman
New Hampshire, University of: W. B. Nulsen
*New Mexico, University of: W. H. Mullins
*New York, College of the City of: Harold Wolf
*New York University: Philip Greenstein
*North Carolina State College: W. T. Dickinson
*North Dakota, University of: Clifford Thomforde
Northeastern University: G. E. Pihl
*Northwestern University: A. H. Wing, Jr.
*Notre Dame, University of: H. E. Ellithorn
*Ohio State University: E. M. Boone
Oklahoma Agricultural and Mechanical College: H. T. Fristoe
*Oregon State College: A. L. Albert
Pennsylvania State College: C. R. Amerman
*Pennsylvania, University of: C. C. Chambers
*Pittsburgh, University of: J. F. Pierce
*Pratt Institute: E. A. Hertzler
*Princeton University: N. W. Mather
*Purdue University: R. P. Siskind
Queen's University: H. H. Stewart
Rensselaer Polytechnic Institute: H. D. Harris
*Rhode Island State College: J. L. Hummer
Rice Institute: M. V. McEnany
Rose Polytechnic Institute: H. A. Moench
*Rutgers University: J. L. Potter
*San Diego State College: D. C. Kalbfell
Santa Clara, University of: W. J. Warren
*Seattle University: Appointment later
*South Carolina, University of: J. C. Cosby
*South Dakota School of Mines and Technology: Appointment later
*Southern California, University of: G. W. Reynolds
*Southern Methodist University: E. J. O'Brien
*Stanford University: J. M. Pettit
*St. Louis University: G. L. Hollander
Stevens Institute of Technology: Carl Neitzert
*Syracuse, University of: R. P. Lett
*Tennessee, University of: E. D. Shipley
Texas Technological College: C. E. Houston
*Texas, University of: A. W. Straiton
*Toledo, University of: D. A. Powers
Toronto, University of: George Sinclair
Tufts College: A. H. Howell
Union College (N.Y.): R. B. Russ
Union College (Neb.): M. D. Hare
United States Military Academy: F. K. Nichols
United States Naval Post Graduate School: G. R. Giet
*Utah State Agricultural College: L. S. Cole
*Utah, University of: O. C. Haycock
*Virginia Polytechnic Institute: R. R. Wright
*Virginia, University of: L. R. Quarles
*Washington, University of: V. L. Palmer
Washington University: S. H. Van Wambeck
*Wayne University: M. B. Scherba
Western Ontario, University of: E. H. Tull
West Virginia University: R. C. Colwell
*Wisconsin, University of: Glenn Koehler
Witwatersrand, University of: G. R. Bozzoli
*Worcester Polytechnic Institute: H. H. Newell
*Wyoming, University of: R. G. Schaefer
*Yale University: H. J. Reich

* Colleges with approved Student Branches.

# INSTITUTE REPRESENTATIVES ON OTHER BODIES—1949

American Association for the Advancement of Science: J. C. Jensen
American Documentation Institute: J. H. Dellinger
ASA Standards Council: J. G. Brainerd, L. G. Cumming, alternate
ASA Conference of Staff Executives: G. W. Bailey
ASA Electrical Standards Committee: L. G. Cumming, F. B. Llewellyn, E. A. LaPort
ASA Sectional Committee (C16) on Radio: V. M. Graham, Chairman, J. G. Brainerd, L. G. Cumming, J. J. Farrell
ASA Sectional Committee (C18) on Specifications for Dry Cells and Batteries: H. M. Turner
ASA Sectional Committee (C39) on Electrical Measuring Instruments: Wilson Aull, Jr.
ASA Sectional Committee (C42) on Definitions of Electrical Terms: J. G. Brainerd, A. G. Jensen, Haraden Pratt
ASA Subcommittee (C42.1) on General Terms: J. C. Jensen
ASA Subcommittee (C42.6) on Electrical Instruments: J. H. Miller
ASA Subcommittee (C42.13) on Communications: J. C. Schelleng
ASA Subcommittee (C42.14) on Electronics: R. S. Burnap
ASA Sectional Committee (C60) on Standardization of Electron Tubes: L. S. Nergaard, C. E. Fay
ASA Sectional Committee (C61) on Electric and Magnetic Magnitudes and Units: S. A. Schelkunoff
ASA Sectional Committee (C63) on Radio-Electrical Co-ordination: C. C. Chambers
ASA Sectional Committee (C67) on Standardization of Voltages—Preferred Voltages—100 Volts and Under: A. F. Van Dyck
ASA Sectional Committee (Z10) on Letter Symbols and Abbreviations for Science and Engineering: H. M. Turner; (A. F. Pomeroy, alternate)
ASA Sectional Committee (Z14) on Standards for Drawings and Drafting Room Practices: Austin Bailey
ASA Sectional Committee (Z17) on Preferred Numbers: A. F. Van Dyck
ASA Sectional Committee (Z24) on Acoustical Measurements and Terminology: Eginhard Dietze, H. F. Olson
ASA Sectional Committee (Z32) on Graphical Symbols and Abbreviations for Use on Drawings: Austin Bailey; (A. F. Pomeroy, alternate)
ASA Subcommittee (Z32.9) on Communication Symbols: H. M. Turner
ASA Sectional Committee (Z57) on Standards for Sound Recording: S. J. Begun
ASA Subcommittee of Z57.1 on Magnetic Recording: W. J. Morlock
ASA Sectional Committee (Z58) on Standardization of Optics: E. D. Goodale (L. G. Cumming, alternate)
ASME Glossary Review Board: W. R. G. Baker
IRE, AIEE Committee on Noise Definitions: Stanford Goldman, Jerry Minter, Claude Shannon
IRE, RMA Problem No. 2: S. L. Bailey
Joint EEI, NEMA, RMA Co-ordination Committee on Radio Reception: C. E. Brigham
Joint IRE, ASA C42 Definitions Co-ordinating Committee: C. L. Dawes, A. G. Jensen, J. C. Schelleng
Joint IRE, AIEE, NEMA Co-ordination Committee on Commercial Induction and Dielectric Heating Apparatus: D. E. Watts
Joint RMA-IRE Co-ordination Committee: S. L. Bailey, Keith Henny
Joint Technical Advisory Committee: S. L. Bailey
National Electronics Conference Board of Directors: W. C. White
National Research Council, Division of Engineering and Research: F. B. Llewellyn
URSI (International Scientific Radio Union) Executive Committee: C. M. Jansky, Jr.
U. S. National Committee, Advisers on Electrical Measuring Instruments: Melville Eastham, H. L. Olesen
U. S. National Committee; Advisers on Symbols: L. E. Whittmore, J. W. Horton
U. S. National Committee of the International Electrotechnical Commission: L. G. Cumming, E. A. LaPort, F. B. Llewellyn

# What Kind of Engineers?*

J. D. RYDER†

THE EVOLUTIONARY theory teaches that modern man developed from some one-celled original form of living organism, through successive stages of improvement and specialization as water-living organisms, crustaceans and fishes, as amphibians, as land-living reptiles, and on into the present stage as a land-living mammal. It has been said that before birth a human embryo passes through a number of stages, each indicative of a phase in human evolution. While inaccurate, this statement implies a germ of truth—a human being, as a physical and mental assemblage of relatively worthless materials, is a product of all that has gone before in the history of life on this globe. Nature builds on experience and by experiments and, it is to be hoped, profits by her mistakes! However, some samples seem to indicate that only a small profit has been taken.

In the field of science we also build and profit on the lessons and experiences of the past. The difference between the accumulated experiences of the human animal and those of the human scientist may be proportional to the difference between one million years and 300 years, as the probable respective ages of the two. In considering the human animal, it is customary to state that we have come a long way from the early cave man; but perhaps in speaking of the human scientist we should say we have not yet come very far.

In such a discussion it is necessary to use the words "science" and "engineering" interchangeably, since, in the early days, what is now engineering was science, and what is now science will later be engineering. In order to decide where science or engineering now is and, therefore, what kind of engineers we should be turning out of our colleges at the present time, it is necessary to go back and scan the scientific progress.

It has been said that in the whole history of human endeavor going back about one million years there have been only four great inventions, or great developments which have radically altered the course of human history. These are considered to be: The art of making fire; the invention of the wheel; the invention of the alphabet; and the harnessing of electricity. It is interesting to note that we are now living in the period of time in which the fourth of these great changes is occurring. Is it any wonder that strife and turmoil exist? Is it not possible that those having the secret of fire were tormented, troubled, and attacked by the have-nots of that era? One can readily imagine the labor troubles arising if thousands of slaves carrying burdens on their backs were suddenly displaced by use of the roller or by carts with wheels. We talk of our modern technological and labor-saving advances, but is mankind in a situation really much different from that occurring at the time of the invention of the wheel? We continue to live as tribes, to regard nonmembers of our tribe as outlanders and possible enemies. We are working with much greater forces but our social problems continue to be much the same, and it appears that our social thinking processes (if any) have changed very little.

A visit to the cliff dwellings of Mesa Verde National Park may illustrate the point for anyone caring to follow it through. Those Stone-Age apartment dwellers of 800 years ago had a social organization and system very little different from ours—it was apparent that the social thinking in their village groups of 50 to 200 was much the same as now. They had their Elks and Masons and Knights of Pythias as men's clubs, with both religious and social aspects, and the women had their place for gossip at the community corn-grinding stone. They were banded together for mutual protection from marauders, and for a certain amount of labor saving and specialization in agriculture and the building trades. They had an "ever-normal granary" for beans and corn. It is reported that they finally departed from the area because of a 23-year drought, showing that their politicians were unable to make rain—even as ours.

The important difference between their civilization and ours was not social, but scientific; add science, research, and their results to that Late Stone-Age civilization, and you have US.

However, it should be noted that the added quantity, technology, has been acting on civilization for less than 300 years, perhaps most of us would say for only 100 years. We take the human mechanism after 1,000,000 years of social living, add a new ingredient, and in 100 years expect that mechanism to adapt itself to the new conditions!

About one million years ago man learned to kindle a fire. Ten thousand years ago someone invented the wheel, five thousand years ago iron was discovered, three thousand years ago the alphabet was invented and we began to write, five hundred years ago movable type was invented and we could turn out mass propaganda and the comic book, and finally only 70 years ago we began to harness electricity!

The engineer and scientist have been severely criticized because we have failed to change the social attitudes of the human race, as an accompaniment to our technological advances. The engineer's best answer to such criticism may lie in the time scale, since man's social reactions and attitudes have developed for a million years, and we are given one hundred years to change him! However, our scientific ability is such that I do not believe another million years will be required to adapt man to technology. In fact, good and noticeable progress may appear in the next thousand years.

As a result of this apparent disregard of the social implications of our scientific work, the engineering colleges have been severely criticized by engineers and nonengine and urged to include in their curric more "humanistic-social" courses. This tion is apparently based on the theory t with more humanistic-social courses the gineer becomes more socially conscious; develops a new machine to lay brick, only after considering the full and total cial implications of forcing 500 bricklay to find other jobs (where they will not able to earn $2.75 an hour), and civilizat will be much improved because the en neers are socially conscious! The doct lawyers, and sociologists should study a li more of their own field of human history realize that mankind has not changed a will not be changed in any short period; a that as we go through one of the gr change eras in the history of the world, harnessing of the electrical forces, there bound to be dislocations and disruptic This is not part of the old Industrial Revo tion, this is a new Era of the Electron o the Atom.

If study of humanistic-social subje would make the engineer better able to c verse and discuss social matters with doctors and lawyers, that would be a ga but it seems desirable that the doctors a lawyers come half-way and study a li science and engineering in order to disc such subjects with us, and to understa better many of their own problems.

A very real trouble with the engineer colleges is that they have alumni. Th alumni graduated from college 10, 20, 30 more years ago. Perhaps, as an example particular alumnus did not take account when he was in college. In his daily w since graduation he has found that it wo have been advantageous to know the fun mentals of accounting. He immediately jo a chorus urging the addition of account courses, or economics, speech, history, p chology, or doorbell pushing to the engine ing curricula. Does he look at a college ca log to see if courses in accounting are n required? No, that is too much trouble a besides nothing ever changes at Old Siwa When we went back for Homecoming l fall the ivy was still growing all over Kimpenpflueger Hall, wasn't it? And does Professor Hoffenpfesser still have his mo ing coffee at exactly 10:02 every mornir Nothing changes!

Actually, of course, he would disco the Old Siwash engineering program h radically changed, and he would find alrea included courses in most of the subjects now feels would be desirable. The difficu with the move for more liberalization engineering curricula is that the urge cor from men who base their criticism on wh was taught twenty or more years ago. C present curriculums may be good, but will not know for sure until our alumni us how bad they are twenty years hence!

In attempting to broaden the curricu if we are to meet at least partially the cr cism that has been directed at the engine ing schools, it is extremely important to t

* Decimal classification: R070. Original manuscript received by the Institute, April 25, 1949; revised manuscript received, May 12, 1949. Presented, IRE Cedar Rapids Section, January 19, 1949, Cedar Rapids, Iowa.

† Engineering Experiment Station, Iowa State College, Ames, Iowa.

note of certain fundamentals of the problem. In the first place, it is desirable to observe that generalized solutions to a subjective problem may be dangerous, that is, to group all students together and say that any one method of handling is best for all is to say that all students are alike, an obvious fallacy. Any solution to the enlarged engineering curriculum problem must allow for adequate variations to suit the needs of various types of students. In a narrow region, students may be assumed to have the same needs, but in an enlarged region differences appear. If students' characteristics were plotted as sets of curves, these curves could be matched and made to fall upon one another over a sufficiently narrow region. To assume from this that the curves are alike over the whole region is, of course, false. Water flowing in a narrow river is channeled and controlled, but water allowed the freedom of an ocean develops many cross currents. Broadened curricula should be planned to offer a wide field to the students, not a group of widely divergent, but individually narrow, channels.

A much more solid and desirable basis for planning of engineering curricula could be established if there were available the answer to a major question: "Does the engineering curriculum force engineers to a restricted field of interest, or does engineering attract a type of mind which would tend to narrow specialization in any field?" In other words, does the difficulty lie in the process, or the raw material? Lacking the results of research on this question, it is only possible to plan in a way that will straddle the issue, not necessarily an efficient solution.

While planning engineering curricula to include humanistic-social courses, the technical content should not be overlooked. In what way should the technical training of a young electrical engineer be oriented? We have said that the present is an era of change —the harnessing of electrical forces. It is only natural while science and the world are going through this transition that teaching in the engineering field should also be in a state of flux, which can be a very healthy condition. In fact, if one is not in motion, it may be that he is dead.

In this connection it is again of interest to go back and see what has happened, to rechart our past course, so as to improve our knowledge of our present position in science. After all, our location is pretty much a matter of dead reckoning, and that involves a knowledge of previous position, since as yet there are no loran or shoran methods of navigation in the sea of history.

It is usually considered that electricity was discovered by Thales of Greece, about 600 B.C. He was one of the seven sages of Greece, and in his writings mentioned that amber when rubbed attracted light bodies, such as particles of feathers. It happens that the Greek word for "amber" is "elektron" and so we have "electricity."

Nothing much was done about the general situation, people being interested in such things as the fall of Greece, the rise of the Roman Empire, the fall of the Roman Empire, the Dark Ages, the Renaissance, and a few other dates and pieces of history, until about 1580 when Dr. Gilbert, physician to Queen Elizabeth, investigated and discovered other materials besides amber which would attract light particles.

Then along came Ampere, Volta, Oersted, and finally Faraday, to discover the law of electromagnetic induction in 1831. In 1864 Maxwell told us that radio was possible, and Hertz proved in 1886 that Maxwell was right.

There are other fields in which the world has moved; in 1775 Washington took 12 days going by horse from New York to Boston to accept command of the Continental Army, and today we do it by plane in an hour. Bell invented the telephone in 1875 and we now have telephone communication with all parts of the world. Edison, in 1875, used five 125-horse power machines at Pearl Street to light his electric lamp, and today we have 250,000 horsepower in a single machine.

Technical progress has been fast. Most of our electrical progress dates from Faraday in a total of 118 years. It must be remembered that each new development contributed to the total of knowledge, each further development was in turn built on a broader base of knowledge. Thus we arrive at the unproven premise of those who would increase the number of years of a student in college: there is so much to learn that the time taken to learn it must be increased.

The increased accent on research is a second fundamental factor which must be considered in planning the college work of a young engineer. In order to develop an interest in our young graduate for such fundamental investigation, and to give him the basic tools with which to work, our engineering college courses need to provide considerable of the theoretical physical and mathematical bases of engineering.

The need is present because it can no longer be said that necessity is the mother of invention. Even if it were true, it seems a rather slipshod, unplanned, and unscientific way to get new devices invented. From an engineering standpoint it can be shown that very often invention is the mother of necessity, that one invention makes necessary a great many more inventions.

To refute the old saying, consider the invention of the first incandescent lamp by De La Rue in 1820. It used a platinum filament in a semi-evacuated space, much like the Edison lamp of 1900. It was not needed or necessary, in fact, the world was not yet ready for it. Using wet batteries as the only available electric power of the day, it was not practical or economical. The invention of the electric motor by Davenport in 1834 is another example of an invention ahead of the need, there being as yet no great mechanization of industry, no machines waiting to be driven, and the only electric power, that from batteries. Fifty years later, after invention of the electrical generator, the electric motor became practical and needed. The invention of the scanning disk by Nipkow was hardly a necessary invention in its day, but it made necessary other inventions that have followed and must still be made, to make television fully successful.

In fact, if we are to have real scientific progress of a continuous nature the basic invention must invariably be ahead of the need. Our present-day pure research is always of that nature, and more and more of our engineers are going into that work or into closely allied lines. Our colleges have not always trained engineers with that type of work as their intended vocation. It can be suspected that the goal of a great many of our engineering courses of 25 years ago was to train a man to take his place at a drafting board, in a design department where he could then learn to be an engineer, or to eventually place him as a salesman of electrical products. A rather superficial form of electrical engineering teaching had grown up at that time around the one-frequency idea of 60 cycles only. This superficiality was so firmly rooted, so few real fundamentals were taught or stressed, that the resulting graduate was not too satisfactory in really technical positions. In fact, the roots were so firm and thick that the tree could not be seen, and when radio made its entrance in the late 1920's electrical engineers were accused of over-specializing in the "narrow" field of radio.

It can now be seen in retrospect that the opposite was true, as radio and electronics have led to a return to true fundamentals, and the 60-cycle emphasis was actually the treatment of electrical engineering in a very narrow and specialized field. As a result, most men who came through our college electrical engineering departments, in the 60-cycle days, were not fully fitted for work under our present-day emphasis on research or in fundamentals. It is frequently said that you can make a power man out of a radio man, but not the reverse. The implications of that statement should be carefully thought out.

Why were the men not given more fundamental college work? The answer can be found in certain statistics, first, on the growth of research in industry in the United States as seen in Table I. In 1920, research was very small business in the United States, but it is not today, when it represents a $750,000,000 business anually. In 1920 industry did not demand training of graduates to fit them for research, but during the last two decades the picture has changed. Additional statistics, from a survey by E.C.P.D., support the argument that the present demand is for better fundamental training than was formerly given. This information is presented in Table II, and does not fully include the radio engineering group which would probably raise further the higher percentages. Other comparative figures in Table III further illustrate the trend and show the tendency toward more advanced degrees—these degrees being in almost all cases indicative of highly technical work.

TABLE I

GROWTH OF RESEARCH IN THE UNITED STATES

| *Year* | *Laboratories* | *Employees* |
|---|---|---|
| 1915 | 100 | 3,000 |
| 1920 | 300 | 9,300 |
| 1940 | 2,300 | 70,000 |
| 1946 | 2,500 | 133,500 |

Another factor which has increased the demand for higher technical excellence of our engineering graduates is that some of our engineering fields are approaching a point of increased difficulty. That is, they have

TABLE II

DIVISION OF ELECTRICAL ENGINEERING GRADUATES ACCORDING TO FIELD—1946

| | *per cent* |
|---|---|
| Tech. Adm. and Mgt. | 33.9 |
| Design. Research, Development | 36.7 |
| Mfg. and Production | 10.9 |
| Sales | 7.2 |
| Consulting | 7.0 |
| Teaching | 4.3 |

approached so closely to par figures that an increased amount of technical work is required for each small gain achieved.

It might not be too difficult, in terms of practice, for some engineers to take 3 strokes off their golfing averages, but for a ranking professional to take 3 strokes off his average would require phenomenal effort. As an example, consider the matter of the development of time-measuring devices, simple clocks.

TABLE III

COLLEGE DEGREES AMONG ENGINEERING EMPLOYEES

| *Degree* | *1934 per cent* | *1946 per cent* |
|---|---|---|
| Ph.D. | 0.6 | 3.7 |
| M.S. | 5.2 | 15.4 |
| B.S. | 72.4 | 63.8 |
| Incomplete college | 13.2 | 13.0 |
| No college training | 8.6 | 4.1 |

The first clock was probably the simple rising and the setting of the sun, a mere yes-or-no sort of accuracy. There are evidences that crude forms of sundials existed about 6,000 years ago for interpolating the yes-or-no answers. These were of use only when the sun shone and were, of course, in error at different times of the year, unless properly installed. Thirty-five hundred years ago there came into use water clocks of many designs. These involved the realization that a leaky bucket, always originally filled to the same level, took practically uniform increments of time to empty. If a slave were added to refill the bucket each time it became empty, and mark the fact by ringing a gong, there appears the stone-age Swiss movement. Someone then realized that fluids other than water might be used, and in the desert where they had little water, sand was used, the result being the common egg-timer or sand glass. Burning candles or oil lamps were also forms of hour markers and such devices were the best to be had, with an ultimate accuracy of 5 per cent, if the slave stayed awake. Such a condition persisted until 1360.

In that year the escapement was invented, using power derived from falling weights. Galileo described the pendulum in 1578, but since he spent a great part of his time in jail, he was not enough interested in the measurement of time to build the pendulum into a clock, and left that for Huygens to do in 1657. The pendulum was good, so good that after much development it is still used in our very best clocks. It has been superseded for laboratory use by the quartz crystal clock, and in fact the quartz crystal has been used to show up previously undiscovered variations in the rate of pendulum clocks. These are due to the daily lunar cycle or tidal effects and amount to a few tenths of a millisecond.

Now to summarize the point. The clock has been under development for 6,000 years. The present best clock is an electrical or electronic device, and of interest to radio engineers. What sort of limits are we facing in attempts to develop further improvements in the measurement of time? The sand glass was accurate to 5 per cent, or an error of about one second in every twenty. The escapement at the limit of its development had reduced this error to one second in 8 days. The modern best pendulum chronometer is accurate to one second in two years. The quartz crystal clock may have an error of one second in fifteen years. All this while the earth itself is only consistent to one second in three years. Certainly in the measurement of time, as in many other fields, we are at the point where each new step forward becomes harder to take and entails a higher level of excellence in our work, but good engineers prefer it that way.

Now what have the colleges done? How have they reconciled the conflicting demands on a student's time from those wishing to increase the humanistic-social content of the courses, from those insisting that the student know "more," and from those with demands for a higher technical level of accomplishment? Various schools have come up with different answers. Certain colleges, only a few, have gone to so-called "five-year plans," to gain time. Others are thinking about the matter, but it can readily be said there will be no stampede.

It appears possible to state a philosophy which might be followed in the development of college engineering curricula. Simply stated, this could be: *To meet modern needs, the engineering college should teach fundamentals only, and should teach those fundamentals thoroughly and well.*

As a corollary to that it is also possible to state the belief: *If the fundamentals are well taught, then the applications encountered in professional work will follow easily.*

Such a program is in line with the desires of certain industries which prefer to do further teaching in the applicational field in their own programs. Of course, there is room for discussion here as to where the dividing line comes between fundamentals and applications, but experience seems to indicate that the colleges usually are the better judges in the matter.

To carry out such a philosophy it is desirable that existing curricula be scrutinized closely. All curricula develop fringes, and dark corners with musty odors. Some dean, feeling that the course which he formerly taught was very good and extremely important, orders it included for all students. Then the dean becomes busy and no longer teaches the course, the teaching level and interest drops, the course deteriorates, the dean moves on, but the course remains. Other courses are attached to the curriculum because at one time they were thought important—electrical design, electric traction, telephones—to mention a few—and they carry on long past their prime. These should be carefully examined to determine if they are really fundamental. One enlightening question which may be asked concerning any such course is: How many men in a given graduating class will use that material in their future work? Then it is advisable to ask: Can a course be justified for that number?

Wartime curricula and teaching gave engineering teachers an excellent opportunity for research in details of curricular problems if advantage were taken of the situation thrust upon the colleges, and if questions were asked and studies were made. From such experience in research covering several such programs at the collegiate level, two basic principles were found to lead to more efficient use of a student's time, namely:

1. Four, but never more than five major courses in any one quarter or semester.
2. Courses should be given in concentrated doses, six credit hours in one semester being more efficient than three hours in each of two semesters.

In one of the wartime programs, students were assigned seven or eight courses in a given semester, resulting in a scattering of student interests and failure to do good work. Courses which are spread too thinly, meeting possibly twice a week, lose much of the value of a lecture and class discussion occurring on one day, because of the time elapsing before the student takes the book out of the corner to study for the second meeting of the week. By daily meetings today's class discussion and tomorrow's study are brought together.

By dropping nonessential and outdated courses, sufficient time may be found to include a number of humanistic-social courses such as additional English, psychology, history, economics, and biology. At the same time, because of the increased efficiency obtained through teaching courses in concentrated doses, it should be possible to teach more technical fundamental material in the same number of technical hours.

Graduates are now better paid when they leave college than was true twenty years ago, and they are worth more. It follows that their time in college is more valuable. Thus a college must increase the efficiency with which it utilizes a student's time in accordance with the increased value of this time, or it is failing in its duty to the student and to those who pay the college bills. Increases in utilization efficiency will require careful investigation by the faculty of their methods, and of the course contents, and this should stimulate the faculty along the lines of wholesome advancement.

It has been said that a college is a collection of buildings with ivy creeping around on the outside and with the faculty creeping around on the inside.

In a modern engineering school that cannot be true.

# Electronics Applied to the Betatron*

THEODORE W. DIETZE† AND THEODORE M. DICKINSON‡, ASSOCIATE, IRE

*Summary*—There are several phases of operation of the betatron, used as a source of X rays, which require the application of electronic circuits. This paper discusses the problems of electron injection, electron ejection, and X-ray monitoring. It reviews a set of electronic circuits which have been found satisfactory in solving these problems.

## I. Introduction

IT IS THE PURPOSE of this paper to review the electronic circuit components of the betatron, or induction electron accelerator, used as a source of X radiation.

The theory and development of the betatron have been discussed by others,[1–4] and its use as an X-ray equipment described.[5,6] These will not be treated in detail here.

The betatron accelerates electrons around a circular path or equilibrium orbit by means of magnetic induction. The electrons are accelerated by a radially symmetrical time-varying magnetic flux existing between two poles of a magnet. The space distribution of the flux, as determined by the profile of the magnet poles, is such that the electrons are both accelerated by the potential gradient due to the time variation of the flux, and constrained to move in a circular orbit of constant radius by the flux's force on them due to their motion. That portion of the flux which links the equilibrium orbit is called the accelerating flux, and that in the immediate vicinity of the orbit, the guiding flux. The relation between these fluxes has been shown to be

$$\Delta\phi = 2\pi r^2 \Delta B, \qquad (1)$$

in which

$\Delta\phi$ = change in accelerating flux

$\Delta B$ = change in flux density at the equilibrium orbit of radius $r$,

regardless of the shape of the flux versus time wave. Therefore, for constant orbit radius, the proportionality of $\Delta\phi$ and $\Delta B$ must remain constant. The time variation of the flux is usually sinusoidal, and the electrons are accelerated to their maximum energy once each cycle during a certain fraction of the increasing half-cycle of the flux. The flux may have a steady or dc component, in which case the betatron is said to be biased.[7]

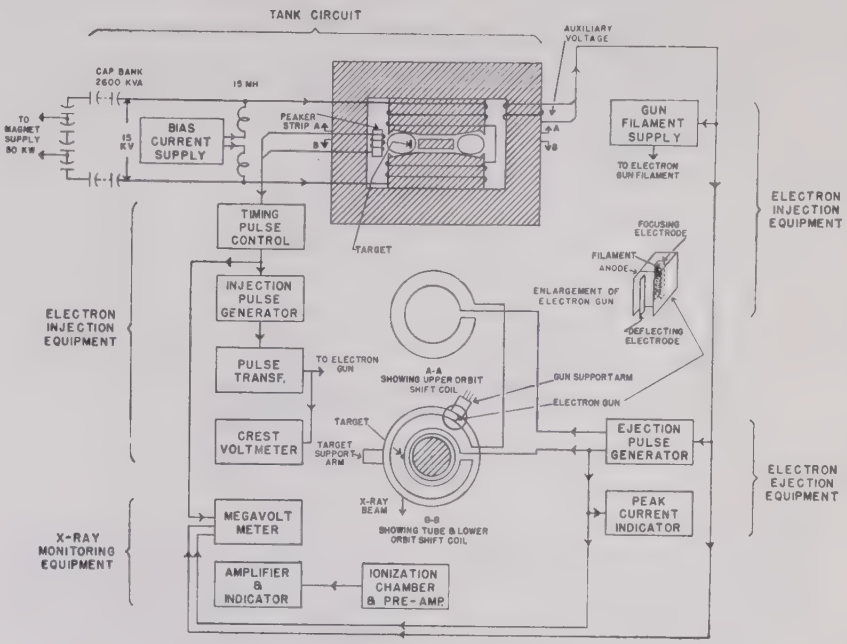


Fig. 1—Block diagram of biased open-core betatron.

The electrons are accelerated in a toroidal evacuated tube and, after reaching a desired energy, are caused to deflect or shift from their equilibrium orbit to strike a metal target. The rapid deceleration the electrons undergo as they strike the target gives rise to a fairly sharply defined *X*-ray beam projected in the direction the electrons were traveling at the instant they struck the target.

There are three phases of betatron operation which require the use of specialized electronic circuits.

Referring to Fig. 1, a block diagram showing a biased open-core betatron, these three phases of betatron operation are: (1) those concerned with injecting electrons into the equilibrium orbit; (2) those concerned with deflecting or ejecting electrons from the equilibrium orbit; and (3) those concerned with monitoring the resulting X-ray output.

## II. Electron Injection Equipment

The components in this group are:

a. Electron source, or gun
b. Gun filament supply
c. Gun accelerating voltage supply (injection pulse generator, pulse transformer, and crest voltmeter)
d. Timing-pulse control circuit.

These act to inject electrons into the equilibrium orbit once each cycle near the time the guiding flux passes through zero in an increasing direction (at *A* in Fig. 2). A timing reference is obtained from a "peaker strip" placed across the gap between the magnet pole pieces. The peaker strip is a laminated permalloy bar of small cross section on which a coil is closely wound. It is saturated by the magnetomotive force across the gap, except for a short interval of time near guiding flux zero. During this short interval, the rapid flux reversal in the peaker strip as it unsaturates and resaturates in the opposite direction induces a voltage pulse of short duration in the coil. Two such pulses are produced for each cycle of guiding flux and, since they are of opposite sign, the one produced at the zero-increasing guiding flux point can be selected.

This pulse is applied to the timing-pulse control circuit, which then generates a triggering pulse delayed the proper interval after guiding flux zero. This triggering pulse fires the injection pulse generator which, acting through the pulse transformer, applies the high accelerating injection voltage pulse to the elements of the electron gun.

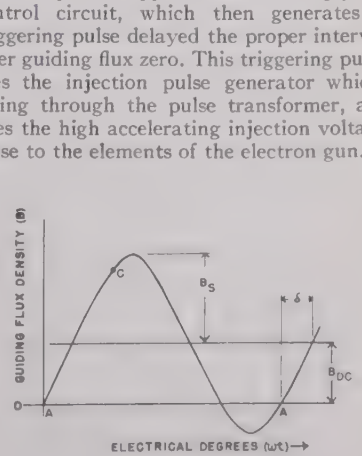


Fig. 2—Guiding flux density in a biased betatron.

* Decimal classification: 621.375.623. Original manuscript received by the Institute, June 3, 1949.

† Tulane University, New Orleans, La., and General Electric Company, Schenectady, N. Y.

‡ Cornell University, Ithaca, N. Y., and General Electric Company, Schenectady, N. Y.

[1] M. Steenbeck, U. S. Patent 2,103,303, December 28, 1937.

[2] D. W. Kerst, "The acceleration of electrons by magnetic induction," *Phys. Rev.*, vol. 60, pp. 47–53; July, 1941.

[3] D. W. Kerst and R. Serber, "Electronic orbits in the induction accelerator," *Phys. Rev.*, vol. 60, pp. 53–58; July, 1941.

[4] D. W. Kerst, "The betatron," *Amer. Jour. Phys.*, vol. 10, p. 219; 1942

[5] W. F. Westendorp and E. E. Charlton, "A 100-million volt induction accelerator," *Jour. Appl. Phys.*, vol. 16, pp. 581–593; October, 1945.

[6] G. D. Adams, "Radiography with the betatron," *Ind. Radiography*, vol. 4 pp. 23–30; 1946.

[7] W. F. Westendorp, "Use of direct current in induction electron accelerators," *Jour. Appl. Phys.*, vol. 16, pp. 657–660; November, 1945.

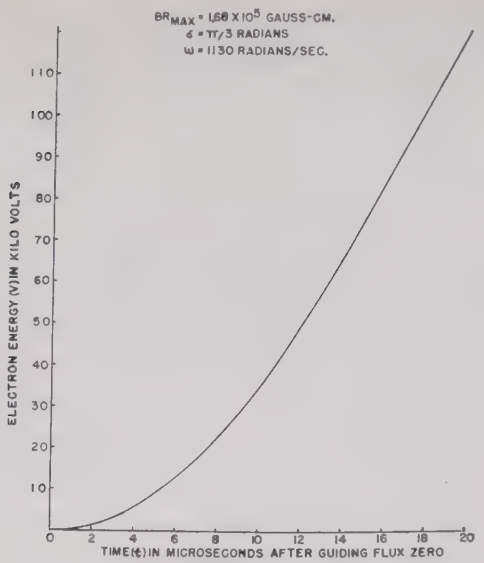
$Br_{MAX}$ = 1.68 X $10^5$ GAUSS-CM.
δ = π/3 RADIANS
ω = 1130 RADIANS/SEC.
ELECTRON ENERGY (V) IN KILO VOLTS
TIME(t) IN MICROSECONDS AFTER GUIDING FLUX ZERO

Fig. 3—Electron injection matching voltage.

In practice, the anode of the gun is connected to ground and the filamentary cathode is pulsed negatively. To supply the heating power for the filament, the secondary of the pulse transformer consists of a bifilar winding, the low potential end of which is connected to the filament supply and the high potential end through a step-down transformer to the filament.

There are also provided a voltage-regulated gun filament supply and an injection crest voltmeter for measuring the negative pulse supplied from the pulse transformer to the gun filament.

The relation between guiding flux density and the energy of an electron in an equilibrium orbit of given radius determines fundamentally the operating constants of the electron injection components. This relation may be written

$$Br = \frac{10^4}{3}\sqrt{V(V+1.02)}, \qquad (2)$$

in which

$B$ = guiding flux density at equilibrium orbit in gauss

$r$ = equilibrium orbit radius in centimeters

$V$ = electron energy in million electron volts (Mev).

As shown in Fig. 2 for a biased betatron, $B$ comprises a sinusoidal component of peak value $B_s$ and a steady component $B_{DC}$ of magnitude less than that of $B_s$. From the figure, it can be written that

$$B = B_s[\sin\delta + \sin(\omega t - \delta)]. \qquad (3)$$

Substitution of (3) into (2) yields upon solving for $V$

$$V = \{0.26 + (3B_s r)^2[\sin\delta + \sin(\omega t - \delta)]^2 10^{-8}\}^{1/2} - 0.51, \qquad (4)$$

an expression which correlates energy of the electron in the equilibrium orbit, radius of the equilibrium orbit, guiding flux density, and time after guiding flux zero.

In order to enter and remain in the equilibrium orbit, electrons injected a time $t$ after guiding flux zero must have the energy (corresponding to the flux at that instant) given by this expression. This energy is referred to as the "matching voltage." If from then on (1) is satisfied, the electrons will continue in the equilibrium orbit.

It has been found, in practice, that a good value for $\delta$ is $\pi/3$. Fig. 3 shows a plot of (4) with $\delta = \pi/3$, $\omega = 1{,}130$ (for a 180-cycle supply), and $Br_{max} = 1.68 \times 10^5$ gauss-centimeters (which corresponds to a maximum electron energy of 50 Mev).

The following points may be observed:

1. If excessive voltages on the electron gun are to be avoided, electron injection must be completed within a few microseconds after guiding flux passes through zero.

2. At a given instant only electrons of a certain energy match the equilibrium conditions exactly. For ideal matching conditions, the energy of the electrons coming from the gun should increase with time during the injection pulse.

To these may be added the following:

3. Because there exist restoring forces on electrons which are out of the equilibrium orbit, there is a small range of energy about the ideal value given by (4) which an injected electron may have at a given time after guiding flux zero and still mateh the equilibrium orbit. This range is of the order of $\pm 1$ per cent of the ideal value given by (4) and, as the magnitude of the restoring forces increases with $t$, it is larger for large values of $t$ and smaller for small values. This puts definite limitations on the amount of jitter which can be present in the injecting pulse.

4. It is desirable to capture in the equilibrium orbit as many electrons as possible with a minimum of "lost" electrons, since these lost electrons increase space charge and upon hitting the tube walls cause overheating.

Keeping these observations in mind, the properties of the components of the electron injection equipment can be discussed.

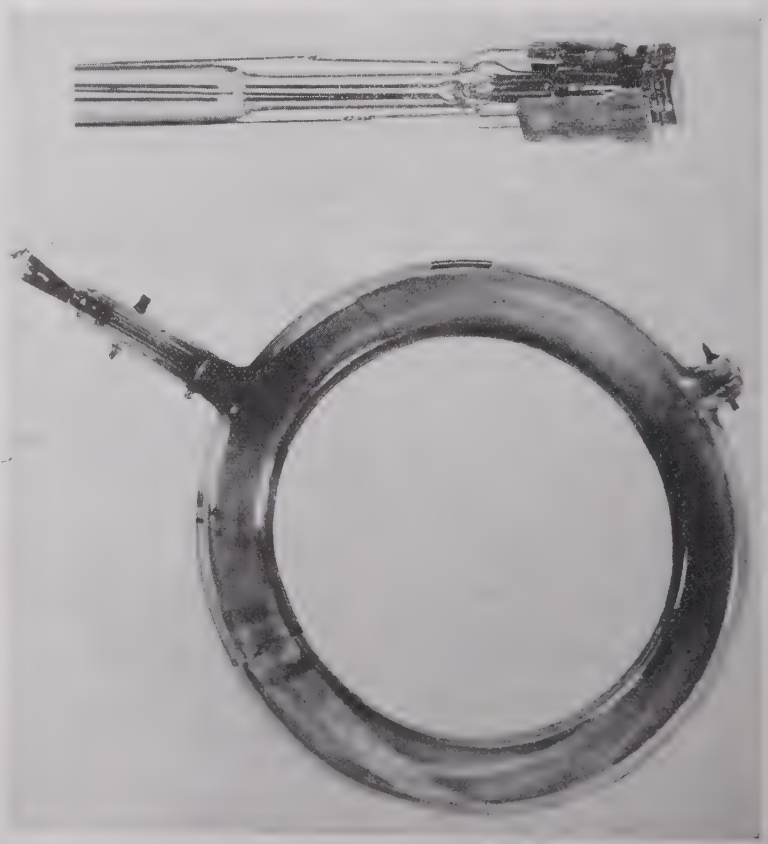

Fig. 4—Electron gun and tube for a 50-Mev betatron.

### *A. Electron Gun*

A 50-Mev betatron tube and electron gun are shown in Fig. 4. In order to achieve high gun emission and high percentage of electron capture in the equilibrium orbit, injection voltages should be high. This requirement has to be balanced against the spacing of the gun elements which is limited by the space available for the gun structure. For guns of size commensurate with available space, the maximum accelerating voltage pulse which can be applied to gun elements is around 70 kv peak. Reduction of the number of stray electrons hitting the tube wall can be helped in design of the gun by shaping the elements to produce a ribbon-like stream of electrons tangent to the equilibrium orbit. To avoid the necessity of close alignment of the gun structure and to insure tangency after it is mounted in the tube, a deflecting electrode is incorporated into the gun. In the gun shown, the filament and focusing electrode are connected together and pulsed negative with respect to the anode, while an adjustable proportional positive pulse is simultaneously applied to the deflector electrode. To prevent stray electrons from accumulating on the tube inside wall and building up a disturbing electrostatic field, the wall is covered with a grounded conducting coating of sufficiently high resistance to prevent excessive heating from the eddy currents induced by the alternating guiding flux.

The gun filament must be reasonably long-lived, capable of supplying about 2 amperes peak and 2 milliamperes average emission, and must be mechanically strong enough to withstand rather severe vibration.

### *B. Gun Filament Supply*

For steady X-ray output of the betatron, it is necessary that average gun emission be held quite closely to a constant value. This can be achieved by regulating the voltage of the gun filament supply, which, because the filament power is carried through the pulse transformer, is most conveniently an ac supply allowing use of a step-down transformer at the high end of the pulse transformer to keep the current through its bifilar winding low. The magnetic field resulting from the current flowing in the filament affects the output of the gun, and if the supply for the filament is not of the same frequency as the magnet flux, modulation of the X-ray output will result. Since there are not presently available non-electronic constant voltage supplies for frequencies other than 60 cps, an electronically regulated gun filament supply is required.

In Fig. 5 is shown the circuit employed for the gun filament supply. It is an adaptation of a circuit described by Ridenour and Lampson.[8]

The primary of transformer $T1$ is supplied through capacitor $C$ which has an appreciable impedance at the supply frequency. Diode $V1$ is operated emission limited such that anode current varies considerably with small changes in filament voltage. The anode of $V1$ is connected to the grid of $V2$, whose cathode is at a slightly higher positive potential. The anode of $V2$ is connected to the grids of the push-pull tubes $V3$ and $V4$ whose cathodes also are connected to a source of higher positive potential than that of their grids. The current drawn by these tubes through secondary $S2$, together with that drawn by the gun filament from secondary $S3$, cause a reduction in transformer voltage by virtue of the impedance drop through capacitor $C$. As supply voltage increases the increased emission in $V1$ causes considerable drop in its anode potential, which is amplified by $V2$ to produce a rise in grid potential of $V3$ and $V4$. The resulting increase in their anode current loads the transformer more heavily, and the increased impedance drop through $C$ maintains the transformer voltages essentially constant.

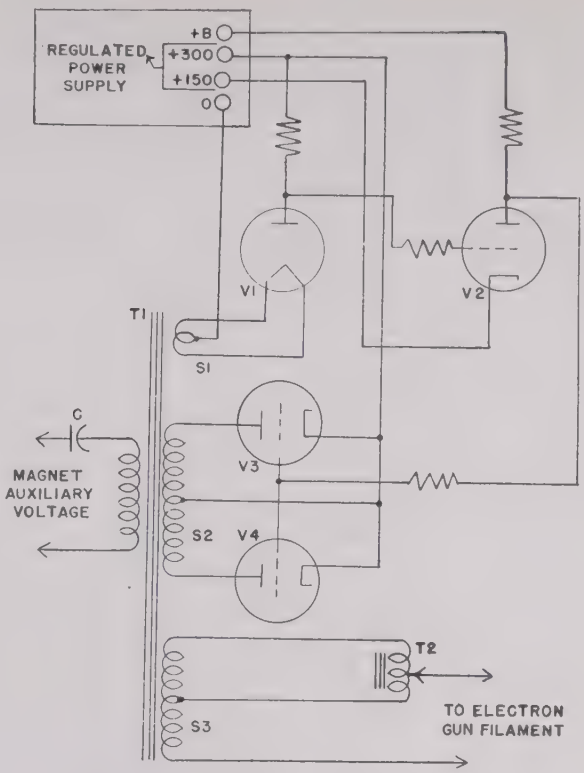


Fig. 5—Gun filament supply for a betatron.

Variable ratio auto transformer $T2$ allows adjustment of the gun filament voltage to any desired proportion of the regulated output voltage.

### *C. Gun Accelerating Voltage Supply*

Electrons will be captured in the equilibrium orbit only if they have at the instant of injection energies within about 1 per cent of that given by (4). Thus, recalling Fig. 3, the ideal wave shape of the pulse of injection voltage should be as shown in Fig. 6(a). It is not practically possible to obtain a pulse of exactly this shape; however, it has been found that by generating a square-wave pulse and applying it to the gun through a high turns-ratio pulse transformer, the resulting distorted secondary voltage pulse (which is roughly

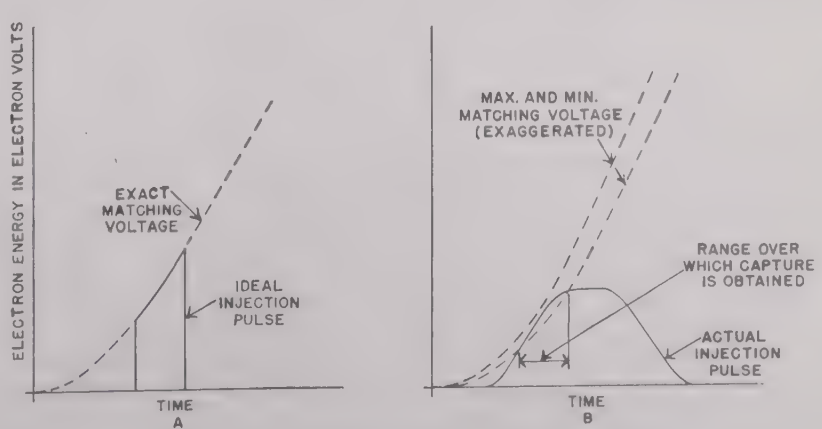


Fig. 6—Injection voltage pulses in the betatron.

[8] L. N. Ridenour and C. W. Lampson, "Thermionic control of an ionization gage," *Rev. Sci. Instr.*, vol. 8, p. 162; May, 1937.

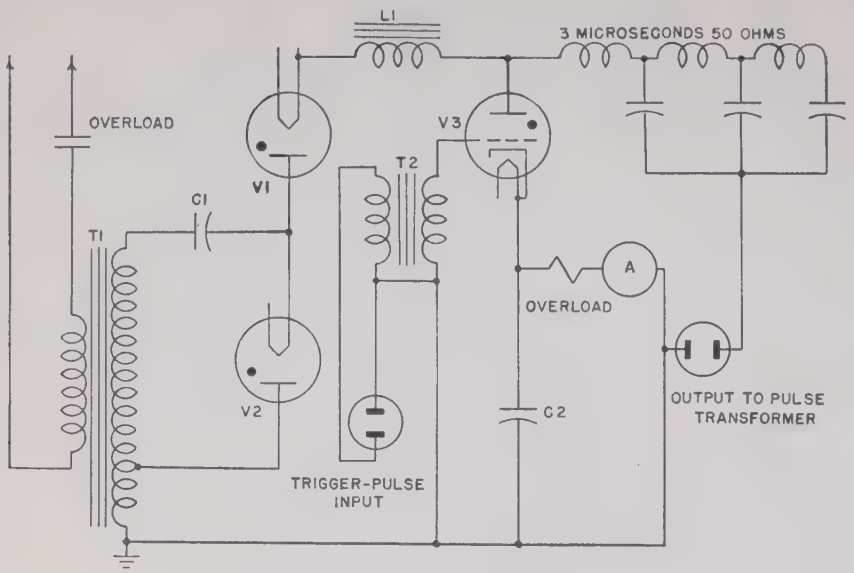


Fig. 7—Injection pulse generator for a betatron.

triangular in shape) falls within the capture range of matching voltage over a fair portion of time, as shown in Fig. 6(b), and provides good injection.

A typical injection pulse generator is shown in Fig. 7. It consists of a pair of 872 phanotrons $V1$ and $V2$ connected in a voltage-doubling circuit to charge a 3-microsecond, 50-ohm lumped-constant line to 8,000 volts. When the line is discharged through the 5C22 hydrogen thyratron $V3$ into a 50-ohm resistive load, a square wave of voltage of 4,000 volts and 3 microseconds duration is produced. A commutating voltage for the thyratron is provided by a tap on the supply transformer $T1$.

The 5C22 thyratron is chosen because of its high peak current rating and its short deionization time, allowing its use with betatrons operating at frequencies as high as 1,920 cps.

The pulse from the injection pulse generator is fed, as shown in Fig. 1, to a pulse transformer having a turns-ratio of $17\frac{1}{2}$ to 1. The secondary is loaded by the electron gun and its voltage divider to produce an equivalent load referred to the primary of 50 ohms. Ideally, the resulting 70-kv voltage appearing across the secondary terminals would be a square wave, but design limitations and unavoidable stray load capacitances produce the fortunately more desirable wave shape shown in Fig. 6(b).

The gun voltage divider is tapped at the proper points for supplying the gun elements and at 50 ohms from ground for supplying a low proportional voltage used in observing and measuring gun voltage with the injection crest voltmeter. This latter uses well-known circuits for measuring crest voltages, employing a diode rectifier which charges a capacitor to the crest voltage and a two-tube bridge voltmeter for measuring the capacitor voltage. An over-current relay is included in the output line to protect against arc-over of the gun.

According to (4), matching voltage is a function of guiding flux density; hence, in order to maintain correspondence between injection voltage and the matching voltage required by (4), the supply voltage for the injection pulse generator must not differ substantially from that supplying magnet excitation. In some circuits, such as the one shown in Fig. 1, the magnet exciting voltage is not constant and does not vary in the same manner as that of the magnet power supply. Therefore, best results are obtained by supplying the injection pulse generator from a source of voltage which is proportional to magnet flux. Such an auxiliary voltage supply may be had from several turns placed around a convenient section of the magnet core.

### *D. Timing-Pulse Control Circuit*

The essential function of the timing-pulse control circuit is to control the time phase of the gun acceleration voltage pulse with respect to magnet guiding flux zero. Three functions are required: (1) manual phase control to adjust initially the gun acceleration voltage pulse to the matching voltage; (2) automatic phase control to adjust for random variations of matching voltage; and (3) suppression of jitter in the gun acceleration voltage. These are provided by a circuit such as that shown in Fig. 8.

Manual phase control is achieved by the pipper and variable delay circuits, the details of which are given in Figs. 9 and 10. The peaker strip is biased by means of current flow resulting from the two sources of ac voltage as shown, such that its flux passes through zero before the magnet guiding flux. The voltage pulses from the peaker strip are applied to the pipper, Fig. 9, the input rectifiers of which are arranged to prevent a net direct current from being drawn through the peaker strip and to allow only negative pulses, Fig. 9(a), to reach $C1$. This capacitor, acting with the grid resistor $R3$ of tube $V1$, causes a voltage which is the derivative of the negative peaker pulse to appear at the grid of that tube (see Fig. 9(b)). $V1$ is a class-A amplifier which applies the amplified pulse shown by Fig. 9(c) to the grid of $V2$. The grid of this tube is over-driven so that the amplified pulse appears on the anode as shown by Fig. 9(d), which in turn is differentiated as shown in Fig. 9(e) by means of a small capacitor $C3$ and grid resistor $R7$. $V3$ is biased well below cutoff, so that only the narrow top of the differentiated wave causes plate current flow, and the resulting plate voltage pulse is as shown by Fig. 9(f). This pulse is applied to the positively biased $V4$ and is of sufficient value to drive this tube well below cutoff, producing the square topped wave shown by Fig. 9(g). $V4$ is a 6AG7, chosen for its high transconductance, which allows a small plate load resistor to be used. This keeps the time constant of the plate circuit low permitting a rapid rise of voltage upon cutoff which produces the desired steep wave front.

Refer now to the variable delay circuit, Fig. 10. In the normal condition, $V2$ is conducting because of its positive bias and $V1$ is held nonconducting by the negative bias developed across the common cathode resistor $R4$. The square-topped pulse from the

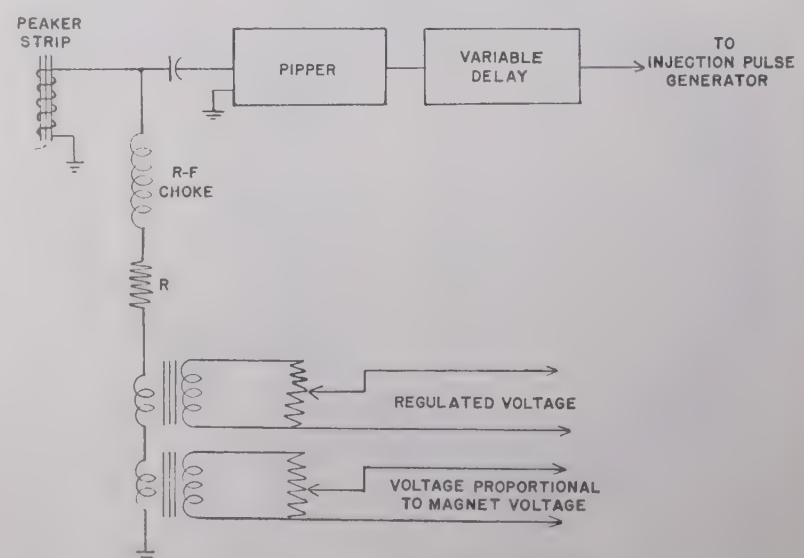


Fig. 8—Timing-pulse control circuit for a betatron.

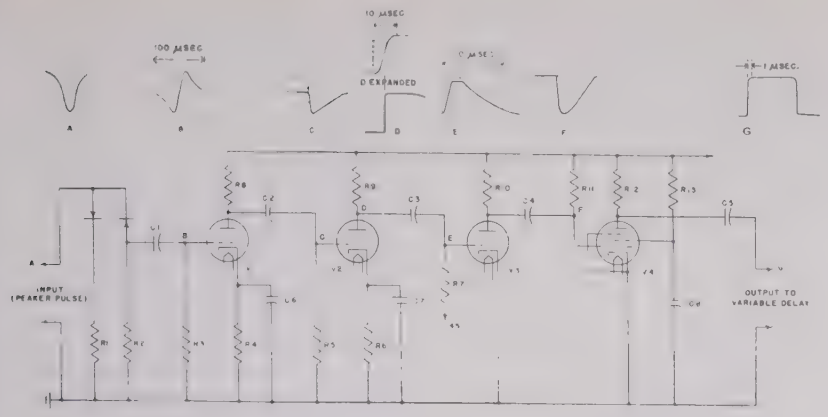


Fig. 9—Pipper circuit for a betatron.

pipper is applied to the input as shown in Fig. 10(a). This drives the grid of $V1$ positive, causing current to flow in the anode load potentiometer $P1$, and resulting in a fall of anode potential as shown by Fig. 10(b). Since the voltage across capacitor $C4$ cannot change instantly, the grid of $V2$ is driven negative as shown by Fig. 10(c) and the potential of its anode rises to supply voltage as shown by Fig. 10(d). The grid of $V1$ is then held positive by voltage divider action between $R14$ and the grid resistor $R2$. The voltage on $C4$ will slowly decay as shown by Fig. 10(c), as capacitor C4 discharges through resistor $R8$, allowing the grid voltage of $V2$ to rise to cutoff, at which point this tube starts to conduct. The fall of the anode voltage of $V2$ causes a fall of voltage on the grid of $V1$, causing a rise in the anode voltage of $V1$, which assists in the rise of grid voltage of $V2$. This results in a very rapid return to the original condition. The rapid fall of anode potential of $V2$ is differentiated by the small coupling capacitor $C5$ and grid resistor $R5$, producing a pulse at the end of the timing cycle on the grid of $V3$ as shown by Fig. 10(e). Since the grid is driven well below cutoff, the resulting pulse across the anode resistor $R13$ is square-topped as shown by Fig. 10(f). This pulse is applied to the grid of $V4$, a 6AS7 tube whose two sections are connected in parallel and biased to cutoff, and a 50-volt, 1-ampere pulse appears across the 50-ohm load at the end of a 50-ohm coaxial line in the cathode circuit. It is this pulse which fires the injection pulse generator. Manual control of the time delay between the input pulse and output pulses is determined by the setting of the potentiometer $P1$ in the anode of $V1$. This determines how far negative the grid of $V2$ is driven, which in turn determines the time required to rise to cutoff. The minimum time delay obtainable is equal to the width of the triggering pulse, and can readily be made only a few microseconds. In practice, the peaker strip bias is usually set ahead to allow full range of manual adjustment of the variable delay circuit. The variable delay circuit is then adjusted until gun accelerating voltage coincides sufficiently with the required matching voltage.

Automatic phase control is required because supplying the injection pulse generator from a source whose voltage varies linearly with the excitation voltage of the magnet does not eliminate entirely deviation of the gun accelerating voltage pulse from the value required for correspondence with the matching voltage. It may be observed from (2) that, for a given short time after guiding flux zero, matching voltage varies as the square of magnet excitation voltage. Thus if magnet excitation voltage increases slightly, the gun accelerating voltage should increase as its square, but, since the injection pulse generator supply voltage varies linearly with magnet excitation voltage, only a linear increase occurs. This means that gun accelerating voltage is too low. To correct for it, the time of injection must be advanced.

This is accomplished, as shown in Fig. 8, by that portion of the peaker strip bias current derived from the magnet voltage. As magnet voltage increases, more bias current is applied to the peaker strip, causing its flux to go through zero and produces the reference voltage pulse at an earlier time. The value of voltage supplied is such that the rate of change of voltage produces the correct rate of change in timing for the particular injection voltage being used. This voltage would normally result in an appreciable current through the peaker strip which would overheat the windings. Therefore, since it is only the change in current which is required for compensation, the initial current can be balanced out by a fixed opposing potential from a regulated source as shown. In the peaker bias circuit the rf choke prevents the high-frequency peak from being shunted out. The resistor $R$ (Fig. 8) is sufficiently large that the current flow from the ac bias supply is in phase with the voltage, such that its maximum value occurs at guiding flux zero when it is needed.

In order to suppress the jitter which appears in the gun acceleration voltage, it is necessary to eliminate the jitter at its source. One of the main sources of jitter may be due to the tolerance in input voltage which will fire the injection pulse generator thyratron. Consequently, for a given input pulse there will be a corresponding variation in the time at which the thyratron will fire. To minimize this time variation, it is necessary to use a large pulse of short build-up time to trigger the thyratron. Such a pulse is provided in the variable delay circuit by use of the high transconductance tubes ($V1$, $V2$, $V3$, in Fig. 10) working into low load resistors. Another source of jitter is pickup, which, if not suppressed, may trigger the thyratron before the desired time. Pickup can be minimized by careful shielding and the use of coaxial cables. A final source of jitter is variations in the timing circuit. This is eliminated by the use of high-quality components for $R8$ and $C4$ in the timing circuit (Fig. 10), and by using regulated voltage supplies.

## III. Electron Ejection Equipment

These circuits act to shift or eject the electrons from their equilibrium orbit and cause them to strike the metal target. As may be observed from (1), for electrons to remain in an orbit of constant radius during acceleration, the rate of change of accelerating flux with respect to guiding flux ($\Delta\phi/\Delta B$) must be constant. A deviation from this condition will cause a change in orbit radius; therefore, when it is desired to expand or contract the orbit to cause the electrons to strike the target, it is merely necessary to change one of either guiding or accelerating flux without changing the other.

In one form of the betatron, the core is so designed that its central portion saturates at the crest of the accelerating flux wave. This results in a deficiency of $\Delta\phi$, causing the orbit radius to reduce to maintain equilibrium, and the electrons spiral inward to strike the target. This simplified design produces X rays of only one maximum energy. A more flexible design incorporates "orbit-shift" coils mounted on the magnet

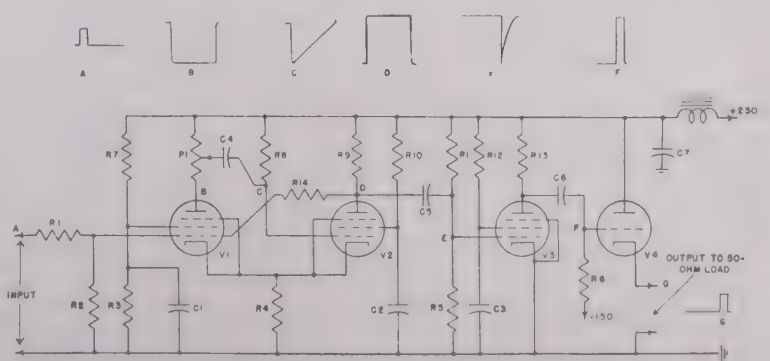


Fig. 10—Variable delay circuit for a betatron.

pole faces in the vicinity of the equilibrium orbit such that when current is passed through them, the guiding flux is strengthened or weakened and the orbit radius contracts or expands until the electrons hit the target. Current may thus be passed through these coils in a short pulse at any time after injection causing the electrons to strike the target with the production of X rays of any desired maximum energy up to the maximum for which the betatron is designed. Such a system is indicated in Fig. 1. The components in this group, designed to contract the orbit, are:

a. Orbit-shift coils
b. Orbit-shift coil supply (ejection pulse generator and peak current indicator).

*a. Orbit-Shift Coils:* The orbit-shift coils are mounted on the upper and lower magnet pole faces as shown in Fig. 1. At a point somewhere between guiding flux zero and guiding flux maximum, such as $C$ in Fig. 2, a pulse of current from the ejection pulse generator is sent through the coils in such a direction as to strengthen the guiding flux in the space between them.

The increase in guiding flux so obtained decreases the radius of the equilibrium orbit, and the electrons spiral inward striking the target with essentially the energy they had at $C$. Control of the time delay between guiding flux zero and the firing of the ejection pulse generator gives control of the location of point $C$, or, in other words, control of the maximum energy of the X rays produced by the betatron.

Design of the orbit-shift equipment is based on the positioning of the orbit-shift coils and the change in equilibrium orbit radius required to cause the electrons to strike the target. Assuming that the electron orbit is contracted rapidly without significant change in electron energy from one of radius $r_0$ to one of radius $r_t$ corresponding to the location of the target, the guiding flux density $B_t'$ at the target at the end of the orbit-shift pulse must be

$$B_t' = B_0 \frac{r_0}{r_t} \tag{5}$$

in which $B_0$ is the guiding flux density at the equilibrium orbit of radius $r_0$ at the beginning of the orbit-shift pulse.

In a betatron, the guiding flux density is a function of radial distance from the magnet polepiece center such that when no orbit-shift pulse is present, the guiding flux density $B_t$ at the radius $r_t$ is

$$B_t = B_0 \left(\frac{r_0}{r_t}\right)^n \tag{6}$$

in which $n$ is a number between zero and one, in present designs usually 3/4. Subtracting (6) from (5), the change $\Delta B_t$ in guiding flux density required to shift the orbit from one of radius $r_0$ to one of radius $r_t$ is:

$$\Delta B_t = B_0(A - A^n) \tag{7}$$

in which $A$ is the ratio $r_0/r_t$.

In order to shift the orbit from one of radius $r_0$ to one of radius $r_t$ it is necessary to change the flux through the entire area between $r_0$ and $r_t$. The coil configuration shown in Fig. 1 does this. For design purposes, it can be assumed that the orbit-shifting flux appears only in the volume between the upper and lower coils, and that the reluctance of the flux path in the magnet iron is negligibly small compared to that in air. Under these assumptions, the peak current required to shift the orbit is then

$$I_p = 0.795 \Delta B_t \frac{d}{N} \tag{8}$$

in which

$I_p$ = peak current in amperes
$\Delta B_t$ = orbit-shift flux pulse in gauss required by equation (7)
$d$ = average distance in centimeters between upper and lower orbit-shift coils
$N$ = total number of orbit-shift coil turns.

The inductance $L$ of the shift-coil configuration can be calculated or measured, and the peak energy $W_p$ required by the orbit-shifting flux pulse calculated from

$$W_p = \tfrac{1}{2} L I_p^2 \text{ joules.} \tag{9}$$

*b. Orbit-Shift Coil Supply:* A relatively simple way to obtain the flux pulse is to discharge a capacitor through the orbit-shift coils, the capacitor energy storage required being equal to that given by (9), or,

$$\tfrac{1}{2} C V^2 = \tfrac{1}{2} L I_p^2. \tag{10}$$

The value of capacitance chosen should be such that the time of rise of the current through the orbit-shift coils is small, compared to that of a cycle of the guiding flux. The practical limit is that of insulation for the higher voltages required to achieve shorter rise times.

A typical ejection pulse generator for supplying the orbit-shift pulse to a betatron is shown in Fig. 11.

Power for the orbit-shift coils is supplied through transformer $T1$ from turns on the magnet core. Capacitor $C1$ is charged through phanotron $V1$ to an energy given by (9) on the half-cycle of voltage preceding that during which the electrons are accelerated. When thyratron $V2$ is fired, $C1$ is discharged through the orbit-shift coils. $V2$ must be able to supply a peak current given by (8); further, it must have a deionization time which is short enough to enable the point of firing ($C$ in Fig. 2) to be moved close to guiding flux maximum, obtaining maximum energy ejected electrons while still allowing $V2$ to be deionized before $V1$ begins to conduct on the following charging half-cycle.

Bias for the thyratron is obtained from rectification of the voltage from one winding of $T2$ and the firing pulse from peaking transformer $T3$. $T3$ is fed from the phase-shifting network comprising $R1$ and $C2$, which is supplied from a second winding of $T2$. Since $T2$ is supplied from magnet voltage, this network determines the point $C$, Fig. 2, at which the ejection pulse occurs and hence the maximum energy of the X-ray output.

A voltage pulse for use in the megavoltmeter (to be discussed in the next section), and a peak current indicator is obtained from a current transformer $T4$ placed in series with the cathode of $V2$. The current transformer is loaded with a resistor $R2$ of sufficient value to produce a proportional voltage within its saturation rating. This voltage is applied to a crest voltmeter similar to that previously described, and serves to monitor the orbit-shift coil current.

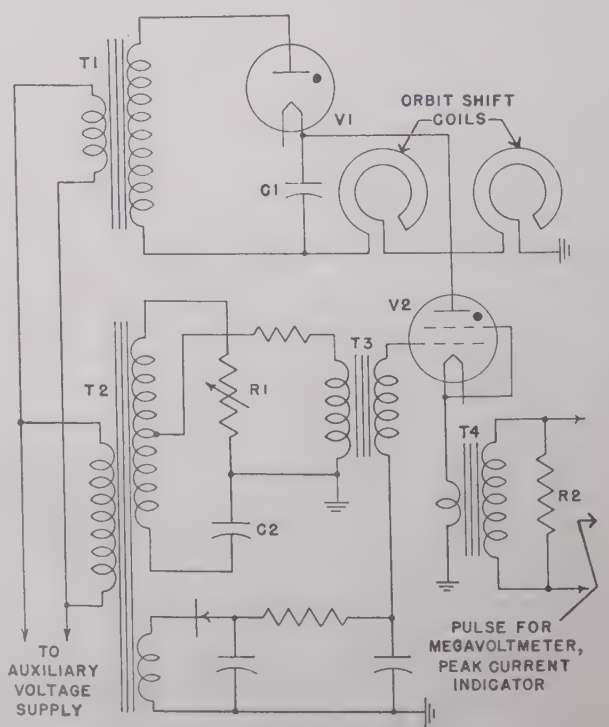


Fig. 11—Ejection pulse generator for a betatron.

## IV. X-Ray Monitoring Equipment

There are two components of monitoring equipment necessary

a. X-ray energy monitor (megavoltmeter)
b. X-ray intensity monitor (ionization chamber and associated amplifiers).

*a. X-Ray Energy Monitor:* As has been discussed previously, changing of the phase relative to guiding flux zero of the orbit-shifting current pulse changes the energy with which the electrons strike the target, and hence changes the maximum energy of the X rays produced by the betatron. It is necessary in many applications to know what the maximum X-ray energy is, and desirable to have a more or less direct way of measuring it, rather than depending on an indirect method such as calibrating the position of the phase shifting control $R1$ in the ejection pulse generator (Fig. 11).

As electron injection always occurs at essentially zero guiding flux density ($A$, Fig. 2), equation (1) may be rewritten

$$\Delta\phi = (2\pi r)Br. \tag{11}$$

It can be seen from (11) that the product $Br$ is proportional to the total change in accelerating flux over the time of acceleration; that is;

$$Br \approx \int_{\phi_0}^{\phi_1} d\phi \tag{12}$$

or

$$Br \approx \int_{t_0}^{t_1} \frac{d\phi}{dt}\, dt. \tag{13}$$

Since the instantaneous voltage $E$ induced around a loop enclosing the accelerating flux is proportional to the rate of change of that flux, it may be written

$$E \approx \frac{d\phi}{dt}. \tag{14}$$

Substituting (14) into (13):

$$Br \approx \int_{t_0}^{t_1} E dt. \tag{15}$$

The voltage $E$ may be integrated over the time of acceleration ($A$ to $C$ on Fig. 2) to obtain a quantity proportional to the value of $Br$ at the instant of ejection. From (2) the corresponding value of electron energy V can then be obtained.

A circuit (called a megavoltmeter) to accomplish the integration of $E$ over the time of acceleration has been described,[9] and is shown in Fig. 12. A voltage proportional to that induced within the equilibrium orbit ($E$ in (14)) is obtained from the auxiliary winding around the magnet core (Fig. 1). This is applied to thyratron $V1$, the anode of which is biased positively by an amount equal to the tube drop of approximately 15 volts. Thus, instantaneous current flow through the tube is proportional to $E$ divided by the series resistance $R1$ plus $R5$.

At guiding flux zero, the thyratron $V1$ is fired by the peaker strip voltage pulse and conduction starts. At the instant of ejection, a pulse of voltage from the orbit-shift circuit fires thyratron $V2$ whose cathode is connected to a dc potential more negative than the cathode of $V1$. This lowers the anode of $V1$ below its cathode potential causing conduction to cease. The ammeter $A$, in series with the anode of $V1$, measures the average current through that thyratron. Since this current is proportional to the integrated value of $E$, it is also proportional to the product $Br$. Knowing the constants of the betatron, it is then possible to substitute in (2) and obtain corresponding values of $V$ for each value of $Br$, and thus mark the scale of ammeter $A$ to be direct reading in maximum X-ray energy. The variable resistor $R5$ is provided to calibrate the ammeter initially to agree with the scale markings.

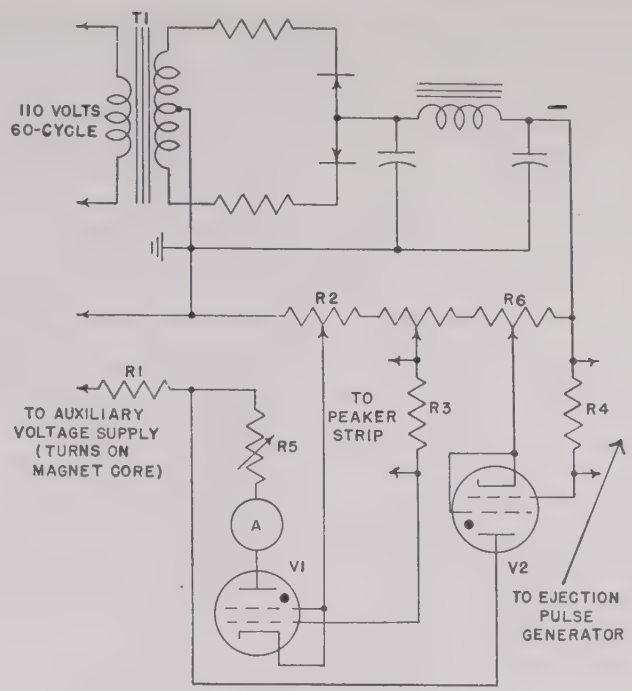


Fig. 12—Megavolt meter for a betatron.

*b. X-Ray Intensity Monitor:* The unit used in measuring the amount of X radiation passing by a point in space is called the roentgen (after the discoverer of X rays) and is symbolized by the letter $R$. It is defined by the ionization produced in a unit volume of air by the radiation at the point in question. Numerically, it is that quantity of radiation which will produce ions bearing one electrostatic unit of charge, of one sign, per cubic centimeter of dry air at standard temperature and pressure. In the practical system of units, then

$$1R \equiv 3.33 \times 10^{-10} \text{ coulombs/cc.} \tag{16}$$

The unit most commonly used in measuring intensity of X radiation is the roentgen per minute. Thus, X-ray intensity at a point may be measured by measuring the charge per minute produced in a unit volume of air at that point.

A practical form of intensity monitor consists of a thin walled metallic chamber filled with air in which is placed an insulated electrode connected to a source of direct potential. When an X-ray beam passes through the chamber, the resulting ionization allows current to flow between the electrode and the chamber walls. This current is a measure of the time rate of ionization produced in the chamber and hence, with the volume of the chamber known, is a direct measure of the average intensity of X radiation through it.

There are several factors dictating the design of an "ionization chamber" which have been discussed elsewhere.[10] Since the movement of ions through the air to the electrode is relatively slow (of the order of 1 centimeter per second per volt per centimeter gradient), it is desirable to have the spacings small and the potentials high to speed up the collection of ions, and thus minimize the occurrence of recombinations which will reduce the collected current. On the other hand, if the potential gradient is too high, the velocity of the simultaneously produced electrons becomes sufficiently great to cause ionization of additional gas molecules, causing an increase in collected current which can lead to a runaway condition once ionization is started. Therefore, in the design of an ionization chamber for direct reading of the relatively intense radiations of a betatron, the spacings are kept small in order that high speed of collection may be attained without excessive electron velocities.

One form of ionization chamber consists of three parallel circular plates spaced a small distance apart and placed directly in and perpendicular to the X-ray beam (see Fig. 13). These plates are made of a thin lightweight material, such as aluminum, and offer small absorption to the beam. The outer plates are connected to a source of potential of the order of 1,000 volts and the

[9] W. F. Westendorp, "A megavoltmeter for induction electron accelerators," *Rev. Sci. Instr.*, vol. 17, p. 215–217; June, 1946.

[10] Serge A. Korff, "Electron and Nuclear Counters," D. Van Nostrand Company, Inc., New York, N. Y. 1946.

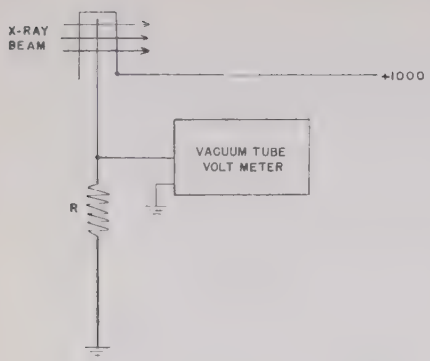


Fig. 13—Functional diagram of a high-level X-ray intensity monitor.

central plate through a high resistance to ground. The potential drop in this resistor caused by the current flow due to the ions produced by the X-ray beam is measured on a tube voltmeter, and the indication of the voltmeter taken as a measure of the intensity of X radiation through the chamber.

In a typical case, an ionization chamber having a 200 cubic centimeter volume placed in an X-ray beam of 60 rpm (1 rps, a minimum usable betatron output) will produce according to (16) a current of

$$(3.33 \times 10^{-10}) \times 200 \times 1 = 6.67 \times 10^{-8}$$

coulombs per second, or amperes, which through the 10-megohm resistor will produce 0.67 volt, which offers no problem in measurement.

In some cases where it is undesirable to remove the low energy component of the X-ray beam by the filtration of an "in-the-beam" ionization chamber, it is necessary to place the chamber to the side of the beam and pick up the "stray" radiation. By means of comparisons with measurements obtained by instruments placed in the beam, a calibration is obtained. Such positioning receives radiation of intensity many orders of magnitude less than one in the beam and requires a higher electrode resistor and a dc amplifier to operate an indicating instrument. Such a circuit is shown in Fig. 14. It is usually necessary to place the first stages of amplification at the location of the chamber, which is often a considerable distance from the point at which readings may be observed. The circuits must be shielded against relatively strong stray magnetic fields of guiding flux frequency and against vibration of frequency the first several integral multiples of guiding flux frequency.

Refering to Fig. 14, to minimize drift and increase stability in general, the pre-amplifier and amplifier are arranged for 100 per cent negative feedback and supplied from a closely regulated power supply. To avoid high voltages to ground, the power supply provides both a positive and negative bus.

The input signal from the ionization chamber is developed across a 5,000-megohm input resistor; the output signal is developed from the cathode of the last stage of the amplifier to ground. A switch for checking the output instrument reading with no current flowing through the input resistor and balance controls (acting on the cathode potential of the first stage of the pre-amplifier) for adjusting the output meter to read zero with zero input are provided.

The first stage of the pre-amplifier, which contains three stages, is a 954-pentode connected as a space-charge grid electrometer tube. This tube is operated at reduced filament and anode potentials to minimize grid current. It is followed by one stage of amplification and a cathode follower stage. All filament currents come from the regulated supply.

The amplifier contains sufficient stages to give a net feedback loop gain of about 50,000. The final stage is a cathode follower, the output of which energizes the output instrument.

## V. Conclusion

In this paper we have endeavored to present in some detail the electronic circuit components of the betatron. All electronic aspects of the device have not been touched upon, for a complete treatment would include design of the betatron tube, the magnet, and power control circuits; however, solutions to the main electronic circuit problems have been given.

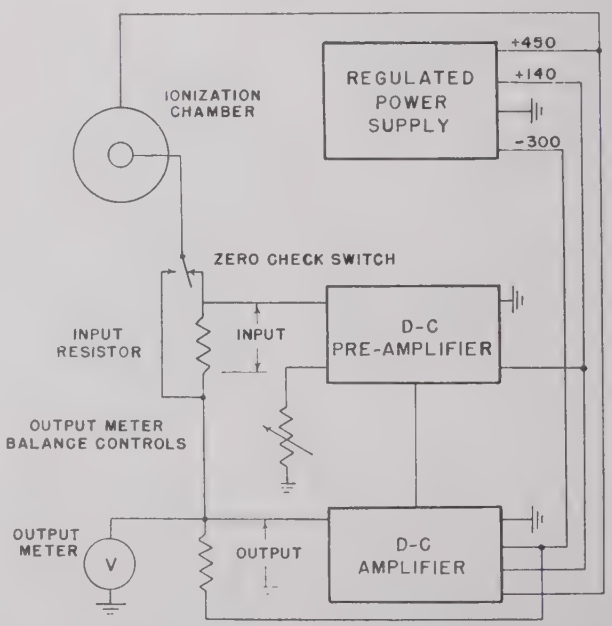


Fig. 14—Functional diagram of low-level X-ray intensity monitor.

# Correction

M. G. Morgan, author of the paper, "A Modulator Producing Pulses of $10^{-7}$ Second Duration at a 1-Mc Recurrence Frequency," which appeared on pages 505–509 of the May, 1949, issue of the Proceedings of the I.R.E., has called the following error to the attention of the editors.

In the computation on the lower left of page 507, the two plus signs should be multiplication signs, to read:

$$e = E(1 - \epsilon^{-t/RC})$$

$$R = \frac{t}{C \ln \frac{E}{E - e}} = \frac{\frac{1}{2} \times 10^{-7}}{125 \times 10^{-12} \ln \frac{5{,}000}{5{,}000 - 3{,}000}}.$$

$$= 437 \text{ ohms.}$$

# The Influence of UHF Allocations on Receiver Design*

JOHN D. REID†, FELLOW, IRE

The appearance of this paper in the PROCEEDINGS OF THE I.R.E. is the result of the activities of the IRE Broadcast Engineers Group.

*Summary*—**The principle of affording protection to receivers from adjacent channel interference by alternate channel assignments has been universally accepted. It is shown that approximately 20 db added protection between receivers from local oscillator radiation can be obtained by alternate channel assignments and receiver intermediate frequency standardization. There is also developed a square assignment plan in which added protection is provided for image interference, the picture image station being spaced 1.4 times the adjacent channel station and the co-channel station 2 times the adjacent channel station. It is shown that 41.25 is the optimum value of intermediate frequency for joint vhf-uhf usage.**

## Introduction

IN CONSIDERING the allocation of a new television band, it would seem justified to consider receiver design problems which affect the performance and cost of receivers in the allocation problem.

It is proposed that an intermediate frequency be standardized that is satisfactory for both very-high frequency and ultra-high frequency bands and that the uhf assignments be made in a manner to afford a degree of protection to receivers from oscillator radiation and image response, and so that local oscillator frequencies will come out in whole numbers divisible by a common integer.

## I. IF Requirements for Receiver Protection from Local Oscillator Radiation

Table I shows where the local oscillator frequency will fall as the if frequency is varied. From this Table it can be seen that an if between 36 and 42 Mc will place the local oscillator an odd number of channels above (assuming the local oscillator is above the signal frequency). The higher the beat that is produced with the picture the better, but caution should also be observed that the oscillator interference does not fall too close to a sound carrier.

In Table I where the oscillator interference is such as to interfere with sound or picture carrier an even number of channels above, the beat that is produced is italicized. Fig. 1 shows the preferred location for local oscillator interference to fall. The round top curves show the receiver susceptibility to interference which is a maximum at the picture carrier frequency, and falls off sharply on the low side and less sharply on the high-frequency side.

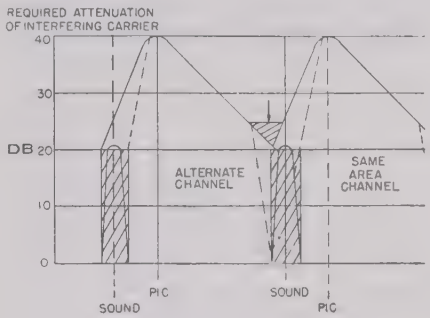


Fig. 1—Preferred location of oscillator interference.

This figure indicates that the best compromise would be reached if the local oscillator interference fell in an alternate channel and was approximately 3.8 Mc above the picture carrier of that alternate channel. This, of course, will not eliminate the problem of oscillator interference but merely means that some 20 db of added protection is afforded, or, stated another way, some 10 times increase in local oscillator voltage present on the receiver terminals can be tolerated.

From the standpoint of local oscillator radiation, it can be seen that an if of 41.3 Mc would afford optimum protection. If's ±12 Mc or multiples thereof would afford the same protection. However, −12 Mc puts us in the 10-meter amateur band and +12 Mc in television channel 2. It should be noted that an if above 36.6 Mc affords complete protection for the vhf channels which have a maximum block of 7 channels.

## II. IF Requirements in Relation to Image Response

As we go higher in signal frequency, radio frequency preselection becomes increasingly difficult to obtain, and the use of uhf rf stages ahead of crystal converters will generally result in a reduction in signal-to-noise ratio. The rf selectivity which can be obtained from two circuits in the uhf band is most unsatisfactory when considering the image rejection requirement predicated upon using if's below the vhf band. An if in the neighborhood of 400 Mc would minimize the image problem, but such an if is not practical today from gain and selectivity standpoints. It is, of course, highly desirable that a common if be used for combined vhf-uhf receivers.

Further consideration of this problem indicates that by careful design and the use of two tuned circuits in the preselector, an average image attenuation of 10 to 15 db can be expected in the uhf band in conjunction with a 41-megacycle if. This average figure would be approximately double at the low end of the band and approximately half at the high end of the band.

Table II shows the image interference which would result in respect to if's between 36 and 42 Mc. Figs. 2, 3, and 4 diagram the information contained in this Table. The curves of receiver susceptibility are drawn in an inverted position in Fig. 2, and the distance they are placed above the base line indicates the amount of receiver image attenuation required. In this diagram, the assumption is made that the image interference will be down 15 db in respect to the local station. These figures illustrate the

TABLE I

Oscillator Radiation

| IF | Osc. Falls | Beat with Pic. | Beat with Sound | Beat with Adj. Pic. or Sound |
|---|---|---|---|---|
| 21.25 | *4 Channels Above* | *1,750 Above Pic.* | OK | OK |
| 21.9 | *4 Channels Above* | *2,400 Above Pic.* | OK | OK |
| 30.4 | *6 Channels Above* | *1,100 Below Pic.* | OK | 400 Above Sound |
| 32.8 | *6 Channels Above* | *1,300 Above Pic.* | OK | OK |
| 36.4 | 7 Channels Above | 1,100 Below Pic. | OK | *400 Above Sound* |
| 36.6 | 7 Channels Above | 900 Below Pic. | OK | OK |
| 36.775 | 7 Channels Above | 725 Below Pic. | OK | OK |
| 41.20 | 7 Channels Above | 3,700 Above Pic. | OK | OK |
| 41.25 | 7 Channels Above | 3,750 Above Pic. | OK | OK |
| 41.75 | 7 Channels Above | 4,250 Above Pic. | 250 Below Sound | *1,500 Below Pic.* |

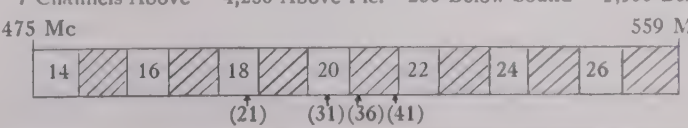


* Decimal classification: R583.5×R007.1. Original manuscript received by the Institute, June 13, 1949. Presented, Third Annual Spring Conference, Cincinnati, Ohio, April 23, 1949.

† Crosley Division, Avco Manufacturing Corporation, Cincinnati, Ohio.

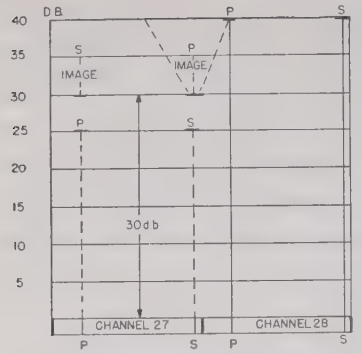


Fig. 2—Image of channel 14 with 36.775-Mc intermediate frequency.

case for the first channel of the uhf band (channel 14).

In Fig. 2 it will be seen that an if of 36.775 Mc would cause the image to fall 13 channels above channel 14, or in channel 27 with the picture image falling exactly on the sound frequency of channel 27 and the sound image falling exactly on the picture frequency of channel 27. In this instance, assume the carriers in channel 27 were down 15 db from the carriers of channel 14, or from the carriers of channel 28 which might be another local station. Then, in order to obtain a 40-db favorable ratio for the desired picture, the receiver image attenuation required would be 25 db. The inverted receiver susceptibiiity curve shows that, for equal protection from channel 28 picture carrier, 30-db receiver attenuation would be required.

Similarly, Fig. 3 shows that if an if of 41.25 Mc were used, the image attenuation required of the receiver would be between 18 and 24 db. Eighteen db would take care of the channel-29 picture carrier, while 24-db attenuation would be required for the channel-28 sound. If, as is likely, channel 28 is in an adjacent area to channel 14, then an additional 6-db. protection or more would be afforded and channel 29 picture would be the limiting interference. Fig. 4 illustrates that an if of 41.65 looks to be the optimum in that the receiver attenuation required would be between 12.5 and 18.5 db.

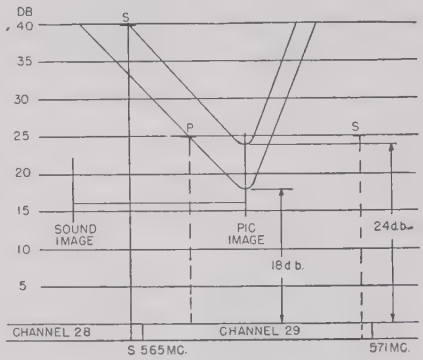


Fig. 3—Image of channel 14 with 41.25-Mc intermediate frequency.

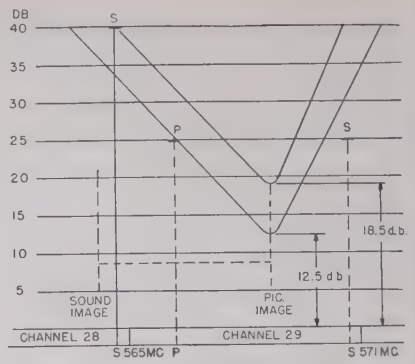


Fig. 4—Image of channel 14 with 41.65-Mc intermediate frequency.

TABLE II

IMAGE INTERFERENCE

| IF | Pic. Image | Sound Image |
|---|---|---|
| 36.4 | 13 Channels Above<br>*700 Below Sound*<br>*1,900 Below Pic.*<br>3,800 Above Pic. | 13 Channels Above<br>700 Below Pic. |
| 36.6 | 13 Channels Above<br>*300 Below Sound*<br>*1,500 Below Pic.*<br>4,200 Above Pic. | 13 Channels Above<br>*300 Below Pic.* |
| 36.775 | 13 Channels Above<br>*0 Beat with Sound*<br>1,250 Below Pic.<br>4,500 Above Pic. | 13 Channels Above<br>*0 Beat with Pic.* |
| 41.25 | 15 Channels Above<br>*3,000 Above Sound*<br>*1,500 Above Pic.*<br>3,000 Below Sound | 14 Channels Above<br>3,000 Above Pic.<br>1,500 Below Sound |
| 41.65 | 15 Channels Above<br>3,800 Above Sound<br>*2,300 Above Pic.*<br>2,200 Below Sound | 14 Channels Above<br>700 Below Sound |

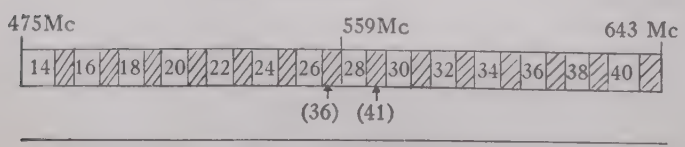


### III. Optimum IF for Combined VHF-UHF Usage

The RMA R-4 Committee considered various if's between 21 and 42 Mc for vhf usage and chose 41.2 Mc as first choice for proposed standardization. Re-examining the factors entering into a choice of 41.2, we find that the second harmonic of the sound if falls 850 kc below channel-6 picture. 41.65, as indicated by image requirements for the uhf band, would put this second harmonic within 50 cycles of channel-6 picture, and is therefore undesirable. 41.3, as indicated by uhf local oscillator radiation requirements, would put this second harmonic 650 below, channel-6 picture, which could probably be tolerated. However, there is another consideration which should enter into the final choice of the exact if frequency. It would be highly advantageous in respect to future developments where local oscillator frequencies might be obtained by multiplication and/or addition, that the local oscillator frequency be even integers. With this requirement in mind, 41.25 Mc seems to be the best compromise in respect to all of the preceding factors, and in that it gives us a series of local oscillator frequencies starting with 522 Mc and increasing in 6-Mc steps, all of which are divisible by 6.

### IV. Theoretical Allocation Plans

The ideal allocation plan, from a standpoint of conservation of spectrum, would be one which used adjacent channels in the same area. If all local areas had the same requirements for channels, we could use an alternate channel assignment basis with the same efficiency. Since areas do not have equal channel requirements, there is a sacrifice in spectrum usage from an alternate channel assignment basis, but this is recognized as necessary in order that receiver design is not unduly complicated. Present regulations provide at least 6-db protection to a transmitter's service area in respect to adjacent channel interference. This requires approximately a 100-mile separation between adjacent channel stations. Cochannel interference requires some 40 db protection, and may be obtained by spacing cochannel stations approximately 200 miles apart. Image interference in the uhf band will be a serious problem, and certainly one of equal if not greater importance than adjacent channel interference, in respect to receiver design.

Therefore it is logical that we should obtain as much or more protection for image interference in the allocation plan as we are now providing for adjacent channel interference. To do this, the image channel stations should be spaced in excess of the 100-mile separation provided for adjacent channel stations, and, if spaced by 150 miles, would afford approximately 15-db protection.

Circular, equilateral, triangular, and square allocation plans were investigated, and the square plan seemed to offer the greatest promise of providing image protection without increasing the number of channels required. Making the sides of the square equal to the adjacent channel spacing gives the diagonal of the square equal to 1.4 times the side or for 105 miles adjacent channel spacing, the diagonal will be 148 miles. Therefore, if the image channels are kept on the diagonals, the desired image channel separation will be obtained. The cochannel spacing will automatically be twice the adjacent channel spacings.

Fig. 5 shows a block of 28 6-Mc channels. This block is divided into half giving two groups of 14 channels. In the first group, alternate channels are designated $A$ and $B$, and in the second group, $C$ and $D$. Considering an if of 41.25 Mc, this will place the image of channels $A$ in channels $D$, and the image of channels $B$ in channels $C$. This gives us four types of stations to fit our square allocation plan. (There are only two basic types, as channels $C$ are an extension of $A$, and channels $D$ an extension of $B$.)

Fig. 6 illustrates the square assignment plan with channels $A$, $B$, $C$, and $D$ at the corners of a square and the image channels separated by the diagonals of the square.

A transparent grid of this basic pattern can be laid over a map as a guide in allocation. Consideration of the basic square assignment shows a large middle area without any guidance as to which type channel would be best to assign. This can be rectified by breaking the block assignment into 8 blocks rather than 4. Each type channel is split into two giving $A_1$, $B_1$, $A_2$, $B_2$, $C_1$, $D_1$ $C_2$, $D_2$, as illustrated in Fig. 5.

Channels $A_1$ will have their image (pic) in channels $D_1$.
Channels $A_2$ will have their image (pic) in channels $D_2$.
Channels $B_1$ will have their image (pic) in channels $C_1$.
Channels $B_2$ will have their image (pic) in channels $C_2$.

The above blocks allow 3 or 4 stations of one type in a given locality, whereas the former plan permitted 7 of each type.

We can then fill in the middle areas of our squares by displacing $A_2$, $B_2$, $C_2$, $D_2$ uniformly from $A$, $B$, $C$, and $D$, as illustrated in Figure 6.

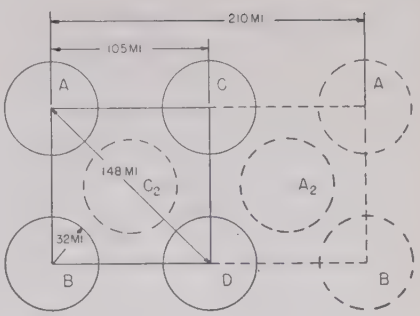


Fig. 6—Adjacent channel—105 miles (6 db). Image channel—148 miles (15 db). Cochannel—210 miles (40 db).

This plan still maintains our 210-mile cochannel, 105-mile adjacent channel, and 148-mile image channel separation.

This plan as illustrated for 28 channels could be repeated if double the number of stations per area were required.

Wherever possible, however, all stations in one area should be grouped. The assignment of stations in blocks for a given area is highly desirable from the standpoints of receiver performance and user convenience. The receiver performance will be improved by increased antenna efficiency and the possibility of improving the tracking of rf circuits over a limited portion of the band. The use of bandpass acceptor or rejector circuits would be facilitated. The user would find it convenient to have his local stations groups within a small area of the tuning dial.

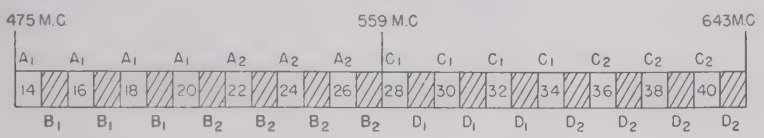


Fig. 5—Block of 28 6-Mc channels in the ultra-high-frequency band.

## CORRECTION

J. H. Mulligan, Jr., author of the paper, "The Effect of Pole and Zero Locations on the Transient Response of Linear Dynamic Systems," which appeared on pages 516–530 in the May, 1949, issue of the PROCEEDINGS OF THE I.R.E., has brought to the attention of the editors the following errors:

Page 517, equation (6): The upper limit $g$ in the second term of the denominator should be replaced by $q$.

Page 521, last line, left-hand side: "sin $(\beta_1 t-\lambda)$" should be "sin $(\beta_1 t+\lambda)$."

Page 521, third line from bottom of page, right-hand side: "$B_k$" should be $\beta_k$."

Page 522, first line, right-hand side: "$B_k$" should be "$\beta_k$."

Page 522, line 14, right-hand side: $D_{s1}{}^1$, $D_{s1}{}^2$ should be $D_{s1}^1$, $D_{s1}^2$.

Page 522, line 28, right-hand side: a parenthesis should be added between "poles" and "except."

Page 525, line 4, left-hand side: The line should read "the approximation $1-M_2 \csc \psi_2 \epsilon^{-\alpha_2 t} \sin(\beta_2 t+\lambda_2+\psi_2)$."

Page 525, equation (40): "$\lambda_{1'}$" should be "$\lambda_1'$."

Page 525, line 8: "$\pi_{1h}$" should be "$\gamma_{1h}$."

Page 525, equation (41): "$\log_\epsilon|\gamma_{1h}$" should be "$\log_\epsilon|\gamma_{1h}|$"; "cos $\psi_1$" should be "cot $\psi_1$"; "$\lambda_{1'}$" should be "$\lambda_1'$."

Page 526, equation (44): "$\lambda_{1'}$" should be "$\lambda_1'$."

Page 527, line 43: "$-\xi_1 \pm j\gamma_1$" should be added to the left of the equal sign.

Page 527, line 45: "$-\xi_2 \pm j\gamma_2$" should be added to the left of the equal sign.

Page 527, line 47: "$-\xi_3 \pm j\gamma_3$" should be added to the left of the equal sign.

# Electrodes for Vacuum Tubes by Photogravure*

MARSHALL P. WILDER†, ASSOCIATE, IRE

*Summary*—**An improved method of photogravure is described which is particularly suited for making up small lots of electrode parts for vacuum tubes. Complicated designs and configurations can be cut with a minimum of effort, and frequent changes prior to final tooling involve little time and expense. Its principal utility is in the flexibility introduced by this improved process enabling precise parts to be made for new experiments in vacuum-tube structures.**

## Introduction

THE WELL-KNOWN photomechanical process of photogravure has been used for many years to transfer variations in tone of a photographic image to variations in depth or area on a metal plate. This plate, properly inked, is used to reproduce the original image by all varieties of the printing art. Photogravure provides an inexpensive method whereby complicated vacuum-tube electrodes of 0.002 to 0.015 inch thick sheet, such as nickel, iron, or stainless alloys, may be produced in an easily reproducible form and in a wide variety of shapes. Resolution of the order of 40 lines per millimeter has been done with fair results; however, for such fine work, thin copper 0.002 inch thick is required. In general, vacuum-tube electrodes do not require definition much greater than 15 lines per millimeter. With reasonable care, this is readily accomplished. Electrolytic etching is used for all tube parts except for very fine screens 500 to 1,000 holes per linear inch. This method is faster and undercuts much less than more conventional ferric chloride etching procedures. (See Fig. 1.)

The photoengraving process consists of applying to the metal a light sensitive coating which becomes less water soluble when exposed to light. This coating, therefore, is referred to as a "resist." On exposure to light of the plate covered by a negative, the areas protected by the dark lines on the plate remain soluble and can be washed off with water, leaving the light struck portions of the coating intact. The resist is then soaked in a solution of ammonium dichromate, dried, and baked to further insolubilize the resist.

The unprotected portions of the metal can then be etched. It is necessary to completely etch through the metal plate and preferable to etch through simultaneously from both sides; therefore, exposure of both sides of the metal plate is accomplished by using an envelope negative. Duplicate negatives of the design required are placed together so that the images match and three edges are sealed together, while the fourth is left open for insertion of the metal plate. (The term "negative," as used in this paper, refers to what is called a positive transparency in the usual photographic terminology.) Considerable difficulty is encountered in etching the metal by ferric chloride because material formed in the cut slows down the etching process and the time required to completely etch through results in lifting of the resist. Electrolytic etching was developed as a procedure, using solutions of acids and acid salts, and resulted in reducing the etching time to less than a tenth of that otherwise required.

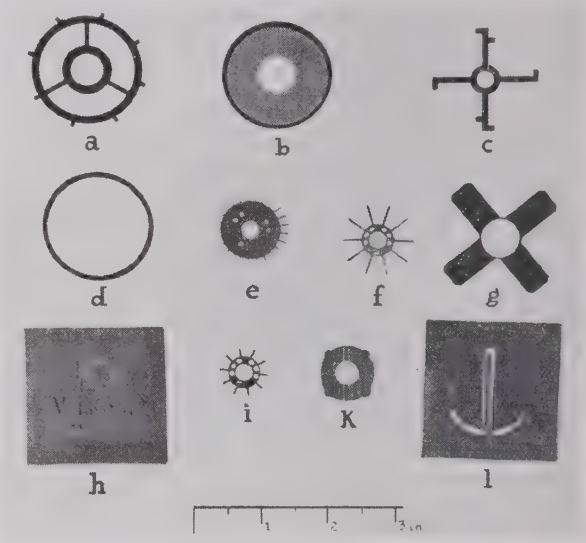


Fig. 1—A selection of parts made by the photogravure process: (a) dynode support, (b) dynode, (c) cathode support, (d) grid mesh support, (e) electrode, (f) electrode, (g) spring support, (h) spray stencil, (i) electrode, (k) grid collar blank, (l) spray stencil.

## Detailed Procedure

### *Preparation of Negatives*

The lines in the art work should be approximately $\frac{1}{8}$ inch wide when the work is to be reduced photographically approximately 5 to 1. The work is reduced to actual size by photography and sufficient positives made so that an envelope can be formed registering the pieces carefully under a miscrocope if necessary and cementing three sides of the envelope. (See Fig. 2.)

When it is desired to etch out areas more than about 0.040 inch across, it is usually preferable to prepare the original drawing in such a way that only the boundary of the area has to be etched, allowing the inside to drop out rather than etching the entire area. It is also desirable to avoid extremely fine lines on the envelope negative such as those under 0.002 inch.

* Decimal classification: R331×R720. Original manuscript received by the Institute, February 24, 1949; revised manuscript received, June 10, 1949.

† Laboratory for Advanced Research, Remington Rand, Inc., South Norwalk, Conn.

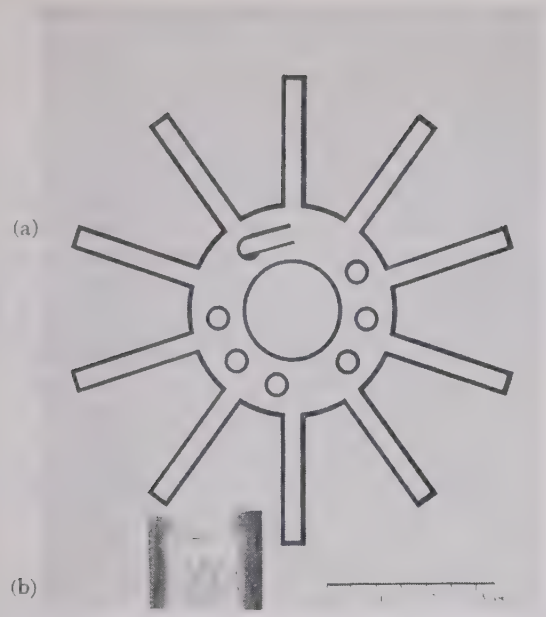


Fig. 2—(a) Original drawing (Scale 8:1) and, (b) envelope made from this drawing for exposing photosensitive coating of the metal plate.

*Preparation of Metal Plates*

The metal plates should be free from scratches, pits, or other deep surface imperfections. Some difficulty was encountered in using metal in which bubbles were left in the sheets after rolling.

The plates of metal suitably cut and flattened are cleaned by boiling in a solution of 5 per cent sodium hydroxide containing about 0.3 per cent Tergitol Penetrant 08. They are then rinsed, boiled in distilled water, and kept in distilled water until ready for use. This procedure usually gives sufficiently clean plates, as evidenced by a continuous water film. If a continuous water film is not obtained by this method alone, electrolytic cleaning in an alkaline cleaner should precede the above cleaning operation.

*Resist Coating*

The resist is prepared in two steps. A stock albumen solution is made up first, and this is combined with glue and more ammonium dichromate as detailed below:

Stock Albumen Solution:

| | | |
|---|---|---|
| 57 | gms. | Egg Albumen |
| 240 | ml. | Water |
| 0.1 | ml. | Chloroform |
| 4 | drops | Ammonium Hydroxide (Sp. Gr. 0.90) |

This is allowed to stand overnight and filtered through absorbent cotton. After addition of 30 ml. of ammonium dichromate solution (22 gms. per 100 ml. of solution), the stock solution is diluted to 280 ml. with water.

Resist Solution:

| | | |
|---|---|---|
| 54 | gms. | Photoengravers Glue (Rogers) |
| 22.4 | ml. | Albumen Stock Solution |
| 41 | ml. | Ammonium Dichromate Solution (22 gms. per 100 ml. solution) |
| 100 | ml. | Water |

The ammonium dichromate solution is diluted with the water before addition of the glue and albumen. The entire solution is diluted to 300 ml. with water.

The solutions should be protected from light during storage and may not work satisfactorily if more than a week old. The protein material becomes less soluble in water on aging, with the result that the unexposed parts of the image are not completely free from resist after development. Higher temperatures of storage increase the rate of aging.

The resist solution is filtered through absorbent cotton in a funnel into the container to be used for dipping immediately before use. The end of the stem of the funnel should touch the side of the container to eliminate bubbles. The plates are dipped in the resist held horizontal for five seconds, then immediately redipped and held horizontal for 20 seconds. They are then hung vertically by one corner to drain and partially dry. After about one hour, they are again dipped in the same manner as before. After draining, the drop of solution at the lower corner should be wiped off. The plates are allowed to dry until no longer tacky. The plates should be dipped and dried where they will be exposed to a minimum of light, particularly direct light.The coated plates can be kept in the dark for 24 hours without harm, but if kept for longer periods, particularly where warm, they may be difficult to develop satisfactorily.

*Exposure and Development*

The dried plates are inserted in the envelope negative previously described and exposed to light in a printing frame. The simple type of printing frame can be used for very flat, flexible plates, but a photoengraver's vacuum printing frame is preferable. This frame consists of a ribbed rubber blanket with a connection for attaching a vacuum line, and a piece of $\frac{1}{4}$-inch thick plate glass, as shown in Fig. 3. These frames are available from photoengraving supply houses. One No. 2 photoflood bulb in a 10-inch aluminum reflector held about $5\frac{1}{2}$ inches above the work produces sufficient light on a 30-second exposure. The usual printing cabinets do not give nearly as much light, with the result that excessively long exposures are required. This has the disadvantage of overheating the negative and plate, as well as being time consuming. After the exposure, the negative with the plate is reversed, being careful not to move the plate in the envelope, and the reverse side exposed similarly.

The exposed plate is developed by sweeping it back and forth in water at room temperature (20 to 30°C) for one minute and rinsing in clean water. The developed plate is then immersed for three minutes in a 3 per cent ammonium dichromate solution in water. After a rinse in clean water, it is now ready for drying and baking. This is accomplished by heating to about 300°C for 8 minutes to harden and further insolubilize the resist. The image should be readily visible, but the resist should be a very pale golden color. The plate can now be stored for extended periods of time without deterioration. Before etching, the edges should be coated with a lacquer such as a 5 per cent nitrocellulose solution to reinforce the resist. The times and temperatures given above are not critical.

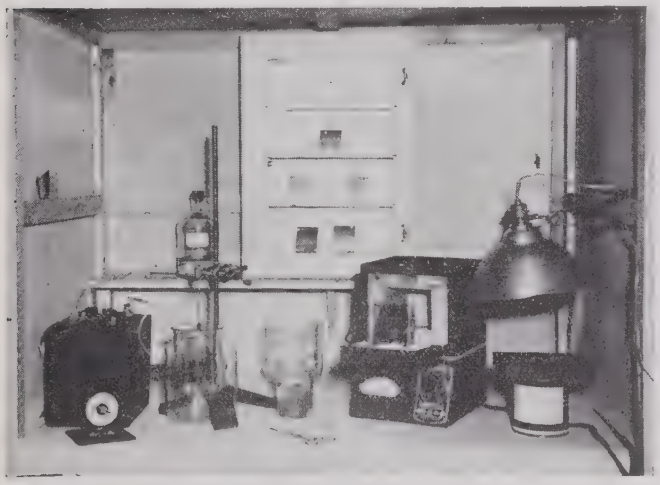

Fig. 3—Work table and equipment for photogravure, showing etching bath with battery, furnace for baking resist, photoflood light, and printing frame for exposing photosensitive coating.

*Etching*

Ferric chloride solutions of 32 to 44 per cent consentrations are commonly used for commercial photoengraving, but are slow in action and not particularly satisfactory in hand operations. Electrolytic etching with acid salts, such as ferric chloride and sodium acid sulfate, or with acids such as sulfuric acid, were found much more rapid and gave much better results than simple immersion in ferric chloride. Sulfuric acid solution containing 50 per cent acid by weight is particularly satisfactory. This solution can be used several times and has been discarded only when it became so dark from dissolved salts that it was difficult to see the work.

The electrolytic cell consists of a suitable container in which two flat iron or steel electrodes exceeding the length and width of the plates to be etched by at least ½ are held vertically and parallel. The distance between them may be from 2 to 4 inches for plates up to 3 inches square. Make the work the anode. A current density of the order of 15 amperes per square inch of actual surface to be etched has been found satisfactory. The area to be etched will, of course, be the surface area not protected by the resist, and is independent of the total area of the plate. A voltage of 3 to 4 volts measured between the anode and cathode of the cell is sufficient for etching small areas totaling about ½ square inch. (See Fig. 4.)

The temperature of the etching solution is of importance primarily because of its effect on the resist coating. The coating is less rapidly affected by the acid solution at temperatures below 20°C than at 30°C. Plates of Nichrome V with a thickness up to 0.006 inches are rapidly etched, requiring only 5 to 10 minutes at temperatures up to 20°C. Nickel of the same thickness requires about 50 per cent more time, and is best carried out at lower temperatures, under 20°C. Temperature has little or no effect on the rate of etching.

*Removal of Resist*

The resist coating can be readily removed from the etched work by boiling in the same caustic solution used for cleaning the metal plates originally.

## Conclusions

The photogravure method is suitable for making up small lots of electrode parts for vacuum tubes. Rather complicated shapes and designs can be cut out and, later, formed by drawing and bending into a desired shape. The possibility of saving time and money, particularly where frequent changes in design may become necessary prior to the final tooling, makes this method a valuable tool in vacuum-tube research and production.

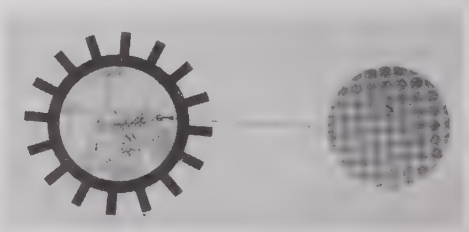

Fig. 4—Etched copper screen, 0.0003-inch thick, 1,000 holes per linear inch.

## Acknowledgment

The writer wishes to acknowledge the very valuable help and contributions made by Earle S. Bidgood of this Laboratory. Electrolytic etching and the additional hardening of the developed resist coating by soaking in ammonium dichromate were suggested and developed by him. Fine mesh screens (Fig. 4) were prepared employing similar procedures by Buckbee Mears Company of St. Paul, Minn.

# Short Antenna Characteristics—Theoretical*

LYNNE C. SMEBY†, SENIOR MEMBER, IRE

*Summary*—**The experimental data obtained by Smith and Johnson on short antennas top-loaded by an umbrella were analyzed mathematically. The theory developed therein is within practical agreement with the measurements. It shows that, for single-tower operation, the horizontally polarized radiation is negligible. In addition, it is shown that with the optimum length of umbrella, the vertical radiation characteristic is the same as it would be from the radiator without top loading. The paper provides a tool for further investigation of other top-loading arrangements.**

## Introduction

DURING THE WAR, the performance of short antennas, on the order of 36° or $\lambda/10$ high, was scrutinized.[1] Smith and Johnson investigated experimentally in Cleveland the performance of a vertical tower top-loaded by an umbrella of various lengths. This paper was prepared in an endeavor to explain theoretically the measurements made at Cleveland and to suggest a possible better arrangement.

## Discussion

The first arrangement tried by Smith and Johnson was an "umbrella" loading such as shown in Fig. 1(a). The angle $\Delta$ used was $-40°$.[2] In order to simplify computation, it was assumed that the top-load consisted of a perfectly conducting cone as shown in Fig. 1(b).

This will be called "cone" loading to distinguish the theoretical from the measured.

In the Appendix is shown the derivation of the formulas used to compute the radiation from the cone. As may be seen from the formulas in the Appendix, computation is greatly simplified if the angle in Fig. 1(b) is chosen as $-45°$. Therefore, this angle was used rather than the $-40°$-angle used in Cleveland. In Fig. 1(b), the current was assumed to be zero at the periphery of the cone. Radiation from the vertical lead to the apex of the cone was computed from the conventional formula for a vertical antenna with a nonradiating top load.

It was assumed that the cone was opaque to the radiation from the vertical. Mechanical integration and comparison with a "standard" $\lambda/4$ antenna was used to obtain the resistances of the various arrangements.

The second arrangement tried in Cleveland had a skirt at the end of the umbrella wires referred to as "umbrella with skirt" as shown in Fig. 2(a). Again in order to compute the performance of this arrangement, a cone was substituted for the wires and a nonradiating load was placed at the periphery of the cone to simulate the loading due to the skirt as shown in Fig. 2(b). The theoretical arrangement will be called "loaded-cone" top loading.

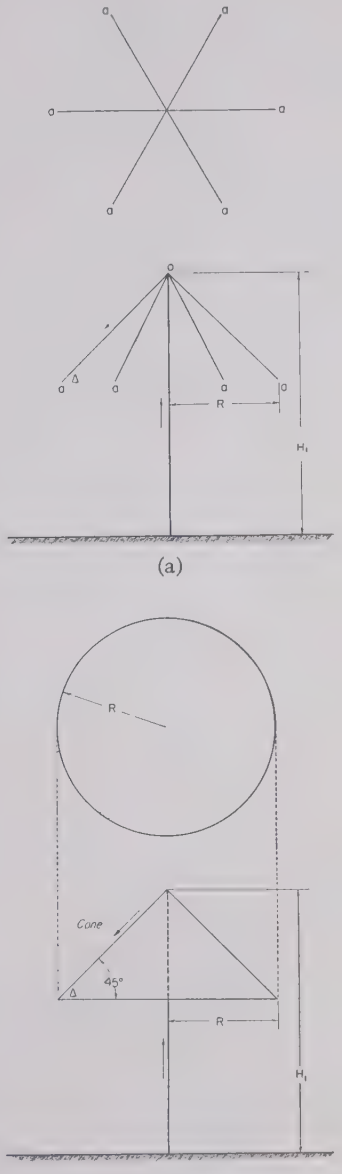


(a)

(b)

Fig. 1—Top-loaded vertical antenna; (a) umbrella loading and (b) cone loading.

A third arrangement, called "folded umbrella" that was not tried at Cleveland, suggested itself to the author subsequently and is shown in Fig. 3(a). In this arrangement, the umbrella wires are connected at the outer periphery by a skirt but the alternate wires have an insulator at the top of the antenna. The simulated

* Decimal classification: R326.612×R120. Original manuscript received by the Institute, January 10, 1949; revised manuscript received, April 25, 1949.

† Consulting Radio Engineer, Washington, D. C.

[1] C. E. Smith and E. M. Johnson, "Performance of short antennas," PROC. I.R.E., vol. 35, pp. 1026–1038; October, 1947.

[2] The negative sign is used because the angle is opposite in sign to that used in the development shown in the Appendix.

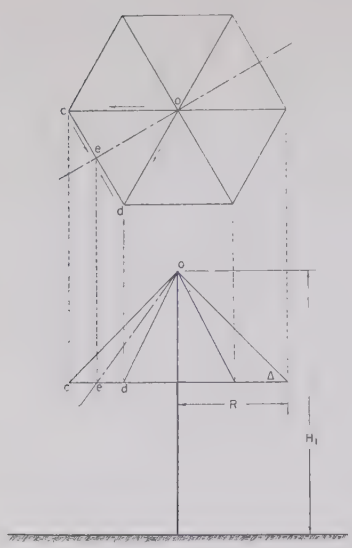


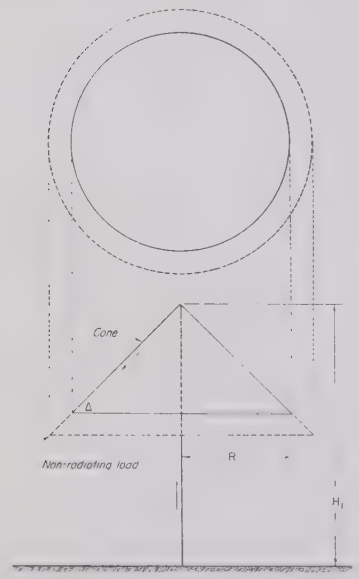


Fig. 2—Top-loaded vertical antenna; (a) umbrella with skirt loading and (b) cone with nonradiating load at periphery.

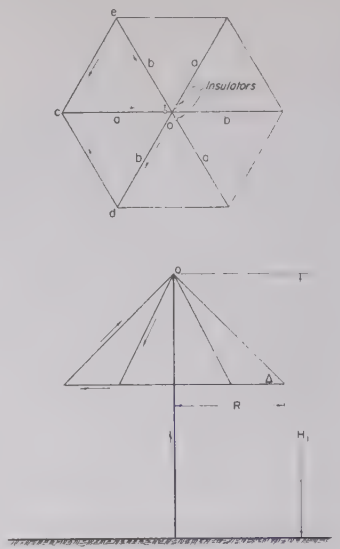


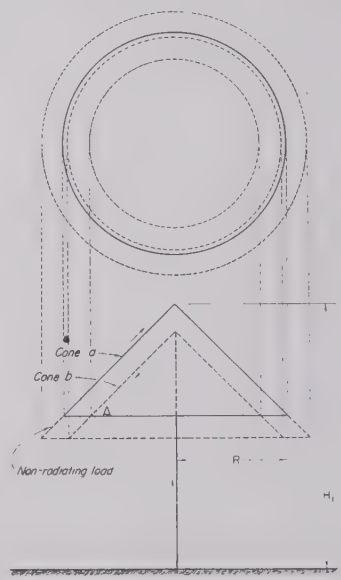


Fig. 3—Top-loaded vertical folded-back umbrella; (a) folded-umbrella loading and (b) double-cone top loading.

theoretical arrangement is shown in Fig. 3(b) and is called "double-cone" top loading.

The computed base resistance for the three arrangements is shown in Fig. 4 plotted for various radii of the cone. Also plotted in Fig. 4 is the Smith-Johnson experimental data for the condition where the Cleveland tower was $\lambda/10$ high. It is to be noted that the base resistance at the zero radius is somewhat different for the measured and the computed. Two factors contribute mainly to this. The first is that the Cleveland tower had a considerable cross section compared to the wavelength and, therefore, the velocity of the propagation on it was lower than the speed of light assumed in the computations. This would lower the measured base resistance. Secondly, the large base shunt capacitance of the tower would tend to lower the measured resistance. As can be seen from Fig. 4, as the radius of the cone was expanded out from zero, the measured resistance increased more rapidly with increase of radius than did the computed values. Again there are two principal reasons for this.

In the Smith-Johnson experiments, the first increment of top loading added included the "hat" on the WHK tower. It can be seen from Figs. 1, 2, and 3 that there is radiation from the "umbrella" and the "umbrella with skirt" that is out of phase with the radiation from the vertical. Mechanically, the "hat" is substantially horizontal and, therefore, contributes practically nothing to the field at the same time producing a large "capacitance" to load. This would then

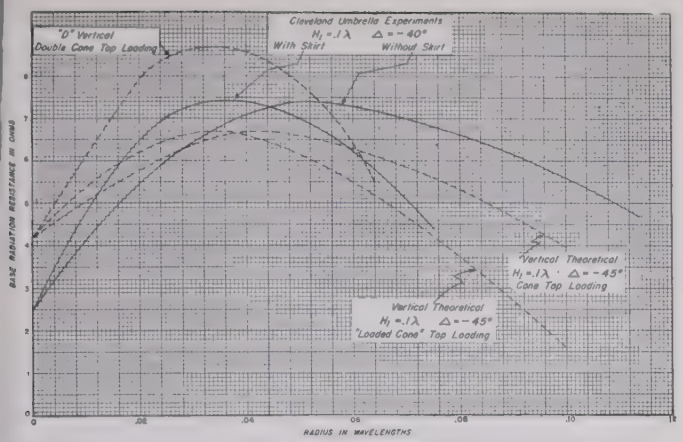


Fig. 4—Various top-loadings base radiation resistances.

make the measured resistance rise more rapidly than the computed resistance. Secondly, the Cleveland umbrella was at a flatter angle and, therefore, for any given length of wires the vertical currents which are out of phase with the current in the vertical thus producing an out of phase field would be less than in the computed arrangements. Therefore, as the radius of the top-load was increased from zero, the measured resistance should increase more rapidly than the computed.

It is to be noted that the "umbrella with skirt" came up to the same maximum base resistance as the "umbrella" but at a lesser radius. The computed arrangements show the same thing. It may be that, in practice, the skirt wires are undesirable mechanically in view of the fact that the same effect can be obtained with an "umbrella" of slightly greater radius. The performance of a "double cone" (in practice a "folded umbrella") top-load as shown in Fig. 4 indicates that this arrangement may have enough merit to warrant using a skirt. It is expected that a considerably higher base resistance may be obtained at a somewhat smaller radius.

In the Appendix, it is shown that the radiation from the cone is entirely vertically polarized. Referring to Fig. 2(a), if the system of wires is viewed from any point in a plane perpendicular to the ground and the plane containing any wire and its complement wire at azimuth 180° or viewed from any point in a plane drawn through the apex of the umbrella and bisecting the angle between two of the wires, that the viewer is looking at a symmetrical mechanical arrangement of wires such that each horizontal component of current on any wire has an equal but opposite component elsewhere at the same distance from the viewer. Therefore, in these six planes, there is no horizontal radiation. If all the possible planes are inserted there will be an azimuth angle of 22.5° between planes. The angle of greatest dissymmetry will be midway between planes; i.e., 11.25° to any given plane. Viewed from any point in a plane placed thusly, there is very little dissymmetry and, therefore, the horizontal radiation is extremely small compared to the vertical radiation. A similar reasoning applied to the "folded umbrella" shown in Fig. 3 leads to the conclusion that the horizontally polarized radiation is also small in this arrangement. Therefore, in many applications, the top loadings discussed herein are satisfactory on the score of magnitude of horizontal radiation.

The vertical form factors for the individual components as well as the total system of a "double-cone" top-loaded antenna of $\lambda/10$ height were computed for a radius of 0.04 $\lambda$ for the cone and are shown in Fig. 5. For comparison purposes, the vertical form factors, for a zero height, a $\lambda/4$ height, and for the $\lambda/10$ height top-loaded, assuming the top loading were nonradiating antennas, are shown in Fig. 5. The form factor for a $\lambda/10$ height without any top loading conforms almost exactly with the radiation from the total antenna and is, therefore, not plotted. This indicates that the improvement in radiated field, as observed by Smith and Johnson, was due almost entirely to reduction in ground losses and not to an improvement in the vertical form factor.

Loop-radiation resistances were computed for the various elements and for the total system of a "double-cone" top-loaded antenna and are shown in Fig. 6. This shows that if the optimum top loading could be effected without it contributing to the radiation field, a $\lambda/10$ antenna would have a loop-radiation resistance of 14.9 $\Omega$ as compared with 1.46 $\Omega$ for the same height without any top loading. The base resistance in each case would be higher. Unfortunately, in the arrange-

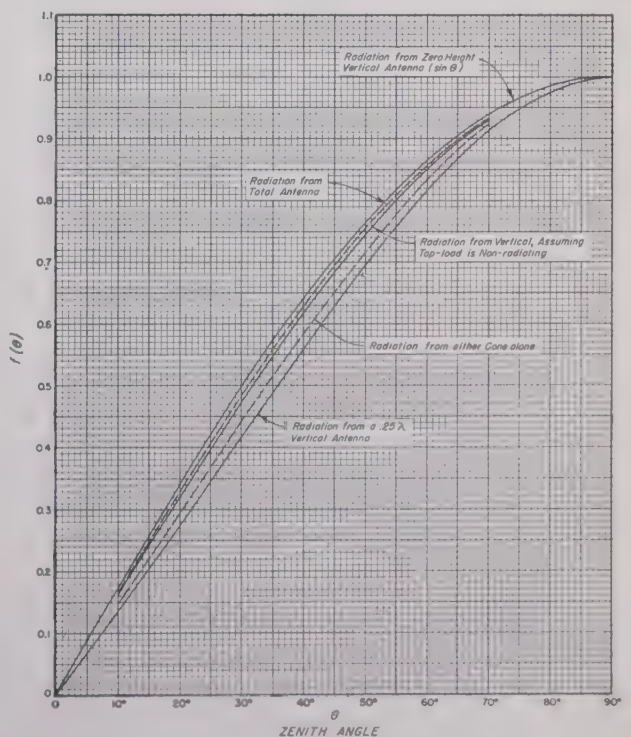
Radiation from Zero Height Vertical Antenna ($\sin\theta$)
Radiation from Total Antenna
Radiation from Vertical, Assuming Top-load is Non-radiating
Radiation from either Cone alone
Radiation from a .25$\lambda$ Vertical Antenna
$f(\theta)$
$\theta$
ZENITH ANGLE

Fig. 5—Double-cone-loaded vertical antenna, vertical radiation pattern $f(\theta)$; $H_1 = 0.1\lambda$, $\Delta = -45°$, $R = 0.04\lambda$, and $K_1 = 1.04$.

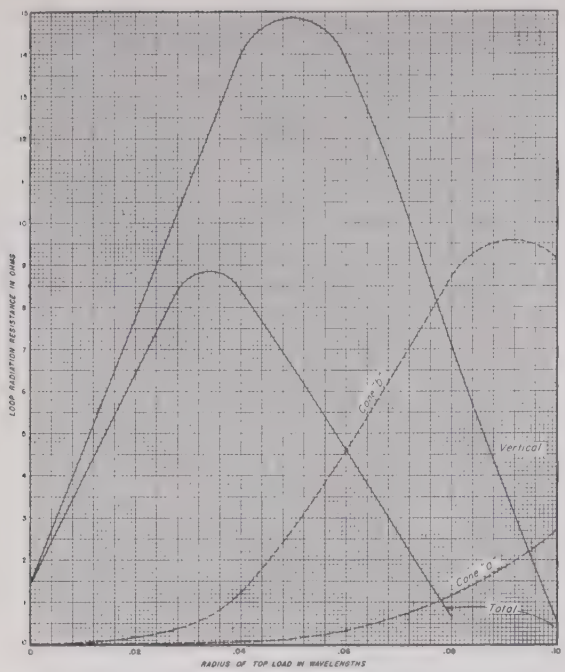


Fig. 6—Vertical double-cone top-loading loop-radiation resistances, $H_1 = 0.1\lambda$ and $\Delta = -45°$.

ments under discussion as the radius is increased, the radiation from the top-load which is 180° out of phase with the radiation from the vertical, increased rapidly. This is shown by the increase in radiation resistance of cone "*b*" with increase in radius of the cone, the radiation from which is out of phase with the radiation from the vertical as shown in Fig. 6.

As a side light to the theme of this paper, Fig. 6 is interesting in regard to the radiation from "hats" as they have been used on broadcast station towers. Cone "*a*" at a radius of 0.044 λ or 15.84° has a loop resistance of 0.1 Ω. In the case of a "hat," the mechanical arrangement in the vertical plane is flatter than the computed cone and, therefore, would have a still lower loop-radiation resistance. On the other hand, in broadcast applications the "hat" is at a greater height, usually on the order of 120° which would raise the resistance. It is, therefore, reasonable to assume that the radiation resistance of the "hat" as used in broadcasting, is only a fraction of an ohm. Therefore, the intrinsic radiation from the "hat" is negligible in view of the much higher loop-radiation resistance of the tower. Due to symmetry of the mechanical arrangement, as viewed from any distant point, there can be no horizontally polarized radiation from a "hat" as used in broadcasting.

## Conclusions

The observations made by Smith and Johnson have been explained theoretically. Certain assumptions were used in the analysis, however, it is believed that they have been justified in the paper. A refinement of the Smith-Johnson arrangements has been suggested which promises to effect a worthwhile improvement.

# APPENDIX

## Radiation from a Cone Antenna

### Introduction

The vertical plane component, for all zenith angles, of the electric-field intensity is computed for a sinusoidally varying current flowing from the periphery to the apex of a perfectly conducting cone antenna over perfectly conducting earth.

The first step in determining the electric-field intensity from the cone antenna is to divide the area of the cone into infinitesimal areas. The current passing through each infinitesimal area is next determined and then the electric-field intensity due to each element of current. Finally, the total electric-field intensity due to the cone is determined by adding, vectorially, all the individual components.

### General Radiation Formula

The increment of the electric-field intensity due to current flowing in an infinitesimal antenna in vacuum and sufficiently accurate in air is[3]

$$\delta(E_0) = \frac{\eta j k}{4\pi r'} I_0 \sin \tau \, \epsilon^{-jkr'} f(\delta r_1). \tag{1}$$

The mks system of practical units is used where

$E_0$ = the electric-field intensity in volts per meter at a distant point $P$
$\delta r_1$ = the infinitesimal length of the infinitesimal antenna
$f(\delta r_1)$ = the scalar component of $\delta r_1$ whose normal component to $r'$ contributes to the field at point $P$
$I_0$ = the current in amperes flowing in the infinitesimal element $\delta r_1$
$r'$ = the distance in meters from $\delta r_1$ to the point $P$
$k = 2\pi/\lambda$
$\lambda$ = the operating wavelength in meters
$\tau$ = the angle between $f(\delta r_1)$ and $r'$
$\epsilon^{-jkr'}$ = the retarded vector
$j$ = the operator $\sqrt{-1}$
$\eta = 120\pi$.

Ramo and Whinnery derived (1) by taking the curl of the vector potential due to a sinusoidally varying current flowing in an infinitesimal element. A similar development is used by others, such as Skilling.[4]

### Infinitesimal Areas on Cone

Referring to Fig. 7, the surface of the cone is divided radially into rings of infinitesimal width $\delta r_1$ such as shown at a distance $r_1$ in meters from the apex of the cone or at a radius $r$ in meters.

[3] S. Ramo and J. R. Whinnery, "Fields and Waves in Modern Radio," John Wiley and Sons, New York, N. Y., 1944; p. 431. Note that their $\theta$ has been changed to $\tau$; $r$ to $r'$, and $h$ to $f(\delta r_1)$. This is for convenience.

[4] H. H. Skilling, "Fundamentals of Electric Waves," John Wiley and Sons, Inc., New York, N. Y., 1942.

Each ring is, in turn, divided into infinitesimal segments. At any angle $\phi$; an increment of angle $\delta\phi$, is added such as shown in Fig. 7. The length of an arc on

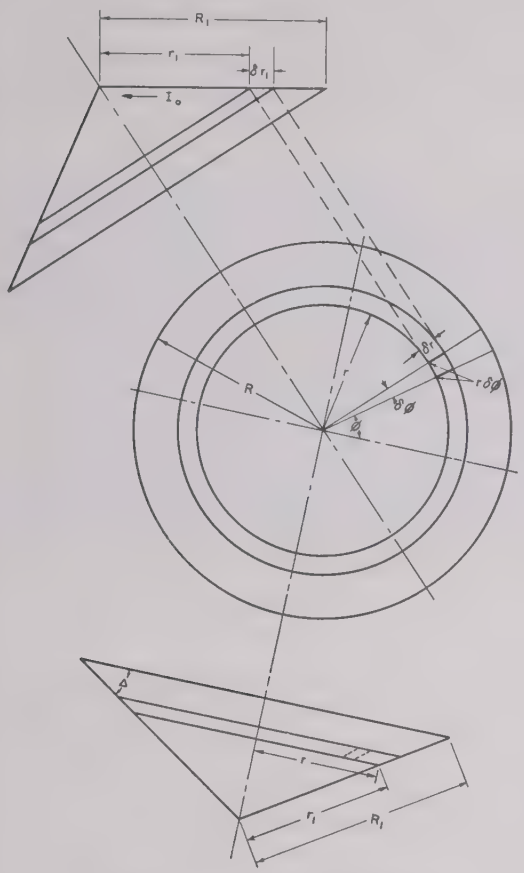


Fig. 7—Cone antenna dimensions.

a circle equals the radius times the angle of arc in radians. The arc length of the segment of the ring is then $r\delta\phi$ long. By selecting successively the proper values of $r_1$ and $\phi$ and adding the increments $\delta r$ and $\delta\phi$, the area of the cone is divided into infinitesimal areas of size $(\delta r_1)(r\delta\phi)$.

## Current Distribution

The rigorous solution for the current distribution on a cone can be obtained by the use of principles set forth by Hallen[5] or Schelkunoff.[6-7]

The rigorous solution is involved and requires a great deal of labor even for a single case. Therefore, an approximation was sought which would be acceptable. It is known that as the diameter of a cylindrical or the diameter of the base of a conical antenna is increased, the phase velocity of propagation decreases. King and Harrison[8] have made solutions for the current distribution on cylindrical antennas of practical diameters.

Schelkinoff[6] also has made semirigorous solutions for the current distribution on cylindrical antennas of practical diameters. On page 504 of footnote reference 6, Schelkunoff said, "In practice, precise knowledge of current distribution is of lesser importance than knowledge of the input impedance. This is because the directive gain of antennas and their radiation patterns are not very sensitive to the changes in the current distribution. Radiation patterns will be affected seriously only in those directions in which radiation is small."

Harrison and King[9] said, "The results of the present analysis indicate that for purposes of computing the shape of the pattern of the distant field, even for relatively thick antennas, a simple sinusoidal distribution is entirely adequate if it is understood that sharp zeros are rounded off."

Both of these comments are applicable to cylindrical antennas of practical dimensions on the order of height to radius ratios of 50 to 1 or greater. To how much smaller ratios they can be trusted will be left to the mathematicians.

Where cones are treated in this paper, practically a limited number of wires may replace the solid cone surface in many applications. Therefore, carrying the solution for the cone beyond the first approximation, as is done in this paper, may not be justified.

At the apex of a cone, the diameter of the conductor is zero and, therefore, the velocity of propagation is the velocity in free space. As the diameter increases toward the periphery, the velocity gradually decreases.

Schelkunoff[10] has given the following approximate formula for the current on a cylindrical antenna[11]

$$\frac{I_0(r)}{I_0} = \left(\sin \beta(l-r) + \frac{F(L)}{K}\cos\beta(l-r)\right) - j\frac{G(L)}{K}\cos\beta(l-r) \qquad (2)$$

where

$l$ = total length of the antenna
$r$ = distance from the base to a point of interest
$I_0(r)$ = current at point $r$
$I_0$ = loop current
$\beta = 2\pi/\lambda$
$j = \sqrt{-1}$

$l$, $r$, and $\lambda$ are measured in the same units.
$F(L)$, $G(L)$, and $K$ as defined in Schelkunoff's article.[6]

[5] E. Hallen, "Theoretical investigations into the transmitting and receiving qualities of antennas," *Nova Acta, Roy. Soc. Sci.* (Uppsala), vol. 11, pp. 1–44; March, 1938.
[6] S. A. Schelkunoff, "Theory of antennas of arbitrary size and shape," Proc. I.R.E., vol. 29, pp. 493–521; September, 1941.
[7] S. A. Schelkunoff, "Electromagnetic Waves," D. Van Nostrand Co., Inc., New York, N. Y., 1943.
[8] C. W. Harrison, Jr., and R. King, "The distribution of current along a symmetrical center-driven antenna," Proc. I.R.E., vol. 31, pp. 548–567; October, 1943.
[9] C. W. Harrison Jr., and R. King, "The radiation field of a symmetrical center-driven antenna of finite cross section," Proc. I.R.E., vol. 31, p. 697; December, 1943.
[10] See p. 504 of footnote reference 6.
[11] The symbols used in the text from the beginning of (2) to the beginning of (6) are not necessarily the same as in the rest of the paper because Schelkunoff's symbols have been used.

If the differential of (2) in respect to $r$ is taken and set equal to zero, the points of maximum and minimum current may be determined by solving for $r$. Performing this operation

$$\tan 2\beta(l - r) = \frac{2KF(L)}{F^2(L) + G^2(L) - K^2}. \quad (3)$$

Referring to Fig. 8, the distance from the periphery

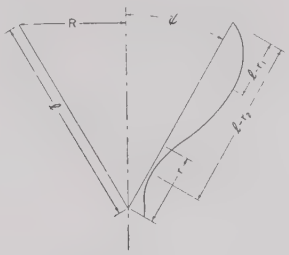


Fig. 8—Determination of velocity factor for a cone.

to the first maximum $(l-r_1)$ would be $\lambda/4$ if the velocity were that in free space. The apparent velocity is then proportional to

$$V_{max} = \frac{4(l - r_1)}{\lambda}. \quad (4)$$

Similarly the distance from the periphery to the first minimum $(l-r_2)$ would be $\lambda/2$ if the velocity were that in free space. The apparent velocity is then proportional to

$$V_{min} = \frac{2(l - r_2)}{\lambda}. \quad (5)$$

Using a length equal to $\lambda/2$ and varying the radius $R$ of the cone the apparent velocity factor was computed from (3), (4), and (5), and is shown in Fig. 9.

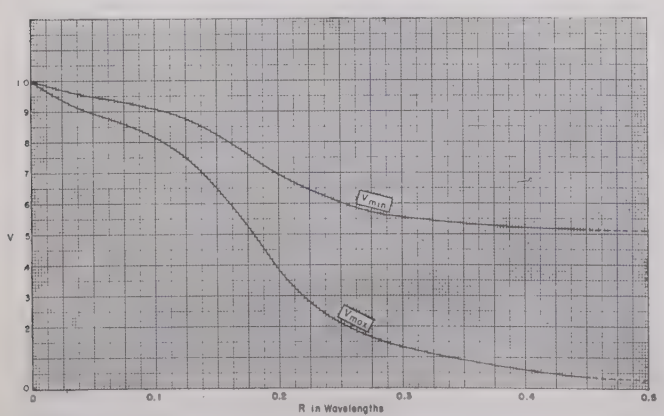


Fig. 9—Apparent velocity factor of propagation on a cone.

Curve $V_{max}$ is the apparent velocity factor using (4), and curve $V_{min}$ is the apparent velocity factor using (5).

In all cases, the free-space distance from the maximum to the minimum, turns out to be $\lambda/4$. This is due to the approximations used in deriving (3) and indicates that the development is not rigorous.

This current distribution development has been fraught with assumptions to the extent that $V_{max}$ showed a supposedly unreasonable inclination to approach zero at a radius of $0.5\lambda$.

It is believed that the shape of the curves in Fig. 9 should have a uniform trend rather than three trends.

The inverse of $V_{min}$ is plotted in Fig. 10. Also plotted

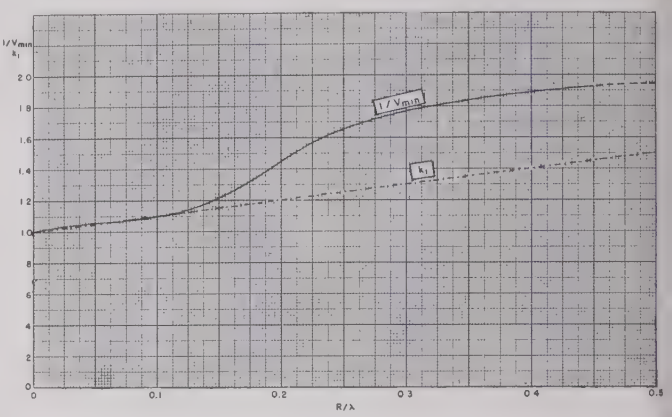


Fig. 10—Velocity factors.

is a straight line labeled $k_1$ that approximates the inverse of $V_{min}$ at small values.

Arbitrarily "velocity factors" in accordance with $k_1$ of Fig. 10 will be used. The formula is[11]

$$k_1 = \text{velocity factor} = 1.0 + R/\lambda \quad (6)$$

where

$R$ = the radius of the cone

$\lambda$ = the free-space operating wavelength.

The way $k_1$ is used in the subsequent development, it is assumed that the velocity of propagation is the same over all of the cone.

No mention has been made of the fact that the current has a complex character nor have the mutual effects been commented on except as they bear on the comments quoted earlier from Schelkunoff, and King and Harrison.

In this development, the current distribution will be assumed to be a sinusoidal distribution modified by the velocity factor $k_1$.

### Current Passing through an Infinitesimal Arc $r\delta\phi$

Let

$I_r$ = the total current in amperes flowing through any given ring such as shown in Fig. 7.

$I_0$ = the current in amperes flowing through the infinitesimal arc segment $r\delta\phi$.

Then

$$I_0 = \frac{I_r \delta\phi}{2\pi}. \quad (7)$$

Referring to Fig. 11, it is assumed that the current $I_r$ has a sinusoidal distribution. In setting up the formula for the current distribution, the cone dimensions such as $R_1$ and $r_1$ will be multiplied by the velocity factor $k_1$ as given by (6). The electrical length of the cone will be greater than the physical length by the factor $k_1$.

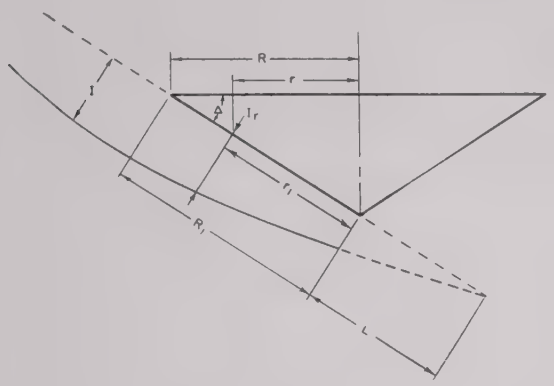


Fig. 11—Physical cone-antenna current distribution.

It is also assumed that there is a nonradiating top-load $L$ in meters at the apex of the cone as shown in Fig. 11.

Referring to Fig. 11, at any distance $r_1$ from the apex of the cone the current $I_r$ is

$$I_r = I \sin \frac{2\pi}{\lambda}\left(L + \frac{k_1 r}{\cos \Delta}\right) \tag{8}$$

where $I$ is the loop current in amperes.

Substituting (8) in (7)

$$I_0 = I \sin \frac{2\pi}{\lambda}\left(L + \frac{k_1 r}{\cos \Delta}\right)\frac{\delta\phi}{2\pi}. \tag{9}$$

### Determination of $f(\delta r_1)$

Referring to Fig. 12 a set of co-ordinates $X'$, $Y'$, and $Z'$ have been selected such that the $X'Y'$ plane is parallel to the ground plane and the $X'Z'$ plane is perpendicular to the ground plane.

Because the cone is symmetrical, the electric-field intensity from the cone is the same in all directions at any given distance $r'$ and at any given zenith angle $\theta$. It is, therefore, only necessary to derive the electric-field intensity in one direction. The direction will be chosen such that a line drawn from any current element of interest to the distant point $P$ will lie in the $X'Z'$ plane or a colinear plane. $P$ is a point at sufficient distance from the cone so that only the radiation field is important and so that lines drawn from all points on the cone to $P$ may be considered parallel.

$\delta r_1$ is a current element lying in the cone at distance $r_1$ from the apex. Let $\delta r_1$ be expressed as a vector in terms of three vectors in the $X'$, the $Y'$, and the $Z'$ directions as shown in Fig. 12.

Then

$$\delta r_1 = i' A_{X'} + j' A_{Y'} + k' A_{Z'} \tag{10}$$

where

$i'$ = a unit vector in the $X'$ direction,
$j'$ = a unit vector in the $Y'$ direction,
$k'$ = a unit vector in the $Z'$ direction.

An examination of Fig. 12 reveals that each $A_{Y'}$ component has an equal and opposite component elsewhere on the cone at the same distance from $P$. The retarded vector potentials for the two components are, therefore, equal and opposite at $P$ and, hence, this component of the electric field is zero. The $A_{Y'}$ components are, therefore, of no interest. This is not true of the $A_{X'}$ and the $A_{Z'}$ components. The components of $\delta r_1$ of interest, therefore, lie in the $X'Z'$ plane and the colinear planes.

Let $\delta r_{X'Z'}$ represent the $X'Z'$ component of $\delta r_1$. Then from (10)

$$\delta r_{X'Z'} = i' A_{X'} + k' A_{Z'}. \tag{11}$$

From Fig. 12, it is seen that

$$i' A_{X'} = O_1' P_1' = i' \delta r_1 \cos \Delta \cos \phi \tag{12}$$

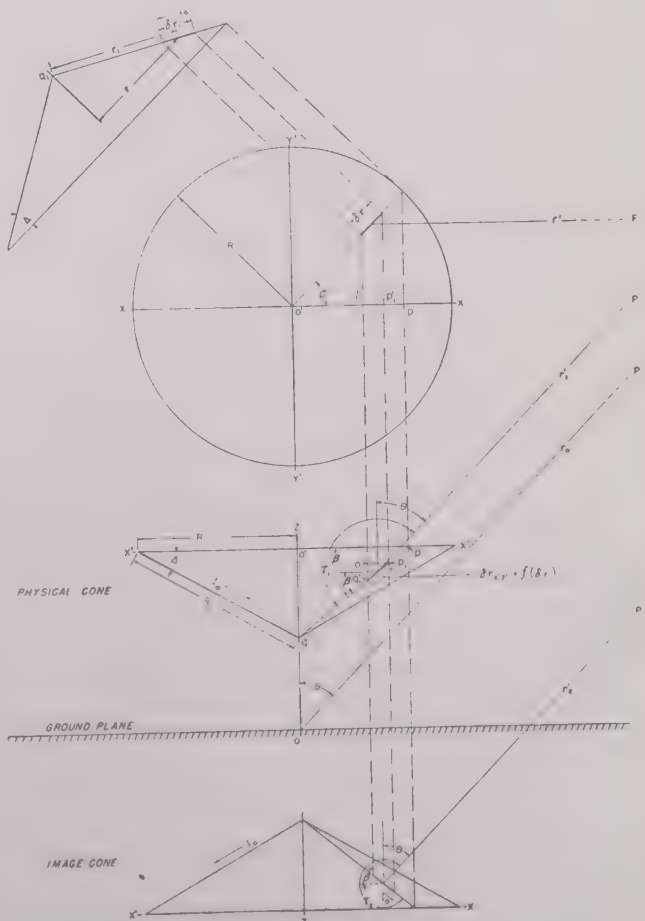


Fig. 12—Distribution of current components in a cone antenna.

and

$$k'A_{Z'} = O_1'Q_1' = k'\delta r_1 \sin\Delta = k'\delta r_1 \cos\Delta \tan\Delta. \quad (13)$$

Substituting (12) and (13) in (11)

$$|\delta r_{X'Z'}| = \delta r_1 \cos\Delta\sqrt{\cos^2\phi + \tan^2\Delta}. \quad (14)$$

Since (14) expresses the $X'Z'$ scalar component of the current element length $\delta r_1$ and since only the $X'Z'$ components are of interest, then (14) equals $f(\delta r_1)$ in (1).

Therefore

$$f(\delta r_1) = \delta r\sqrt{\cos^2\phi + \tan^2\Delta}. \quad (15)$$

### Sin $\tau$ for "Physical-Cone" Element

The total electric-field intensity at $P$ is due to the contribution made by the "physical cone" and its image referred to as "image cone." The discussion so far applies equally to both the "physical cone" and the "image cone."

The radiation due to the "physical cone" will now be determined. In (1), the only two parameters undefined so far are $\sin\tau$ and $\epsilon^{-jkr'}$.

Referring to Fig. 12, the component of $f(\delta r_1)$ normal to $r'$ is the only component contributing to the field at $P$. The term $\sin\tau$, therefore, appears in (1). $\tau$ is the angle between $f(\delta r_1)$ and $r'$.

Referring to Fig. 12, for the "physical cone," keeping in mind that the current $I_0$ flows from the periphery to the apex

$$\tau_1 = \theta + 90 + \beta.$$

Then

$$\sin\tau_1 = \sin(\theta + 90^\circ + \beta) = \cos\theta\cos\beta - \sin\theta\sin\beta. \quad (16)$$

After some manipulation

$$\sin\tau_1 = \frac{\cos\theta\cos\phi - \sin\theta\tan\Delta}{\sqrt{\cos^2\phi + \tan^2\Delta}}. \quad (17)$$

### "Physical-Cone" Element Retarded Vector $\epsilon^{-jkr'}$

The retarded vector $\epsilon^{-jkr'}$ will now be determined for the "physical-cone" element. This vector indicates the effect on the field at the distant point $P$ due to the time difference between the flow of current in $\delta r_1$ and the effect at $P$. The phase of all the infinitesimal antennas will be referred to a common point $O$ as shown in Fig. 13. The distance from $O$ to $P$ is designated as $r_0$.

From Fig. 13 for the "physical cone"

$$r_1' = r_0 - W_1 - Y_1 - X_1 \quad (18)$$

where

$$W_1 = (H - H_3)\cos\theta = (H - R\tan\Delta)\cos\theta$$
$$Y_1 = H_2\cos\theta = r\tan\Delta\cos\theta$$
$$X_1 = (O''P'')\sin\theta = r\cos\phi\sin\theta.$$

Multiplying (18) by $k$ and substituting

$$kr_1' = \frac{2\pi}{\lambda}[r_0 - (H - R\tan\Delta)\cos\theta - r\tan\Delta\cos\theta - r\cos\phi\sin\theta] \quad (19)$$

where

$$k = \frac{2\pi}{\lambda}.$$

Let

$$a = \frac{2\pi r_0}{\lambda}$$

$$b = \frac{2\pi}{\lambda}(H - R\tan\Delta)\cos\theta$$

$$c = \frac{2\pi}{\lambda}(r\tan\Delta\cos\theta)$$

$$d = \frac{2\pi}{\lambda}(r\cos\phi\sin\theta).$$

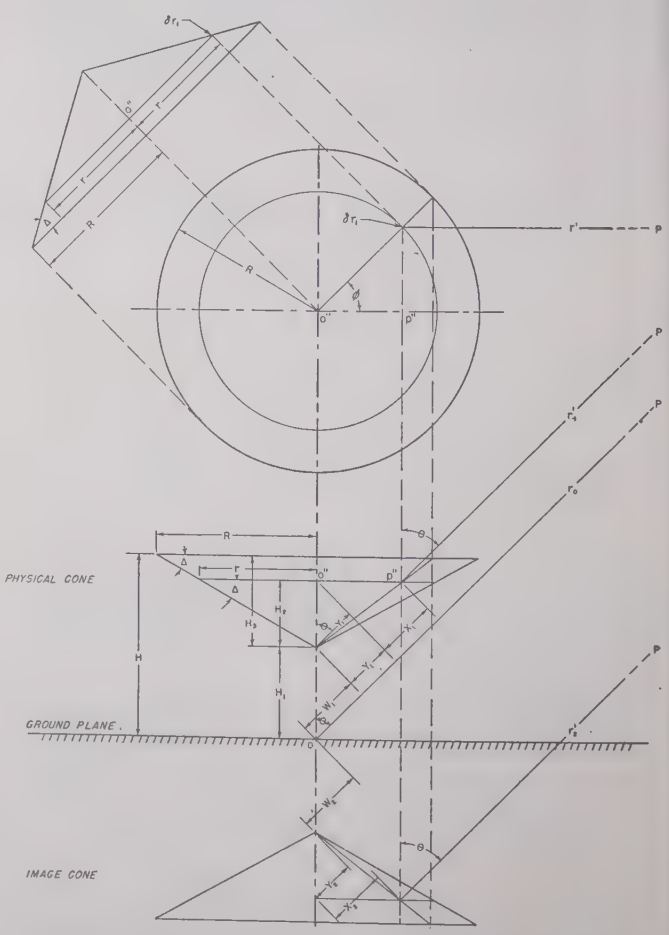


Fig. 13—Determination of retarded vector from a cone antenna.

Then (19) becomes

$$kr_1' = a - b - c - d. \quad (20)$$

Hence, the retarded vector is

$$\epsilon^{-jkr_1'} = \epsilon^{j(-a+b+c+d)} = \epsilon^{-ja}\epsilon^{j(b+c+d)}. \quad (21)$$

### Increment of the Electric-Field Intensity for the "Physical-Cone" Element

All of the parameters have now been defined for the "physical-cone" element.

Let

$E_0'$ = the electric-field intensity due to the "physical cone"

$E_0''$ = the electric-field intensity due to the "image cone"

$E_0 = E_0' + E_0''$ = the total electric-field intensity due to the cone antenna.

Substituting from (9) for $I_0$; (17) for $\sin \tau$; (21) for $\epsilon^{-jkr'}$ and (15) for $f(\delta r_1)$ in (1), the result is

$$\delta(E_0') = \frac{\eta j \frac{2\pi}{\lambda}}{4\pi r_1'}\left[I \sin \frac{2\pi}{\lambda}\left(L + \frac{k_1 r}{\cos \Delta}\right)\frac{\delta\phi}{2\pi}\right] \cdot \left[\frac{\cos\theta \cos\phi - \sin\theta \tan\Delta}{\sqrt{\cos^2\phi + \tan^2\Delta}}\right] \cdot \left[\epsilon^{-ja}\epsilon^{j(b+c+d)}\right]\left[\delta r\sqrt{\cos^2\phi + \tan^2\Delta}\right]. \quad (22)$$

Let

$$e = \frac{2\pi L}{\lambda}$$

$$f = \frac{2\pi k_1 r}{\lambda \cos \Delta}.$$

Then (22) becomes

$$\delta(E_0') = \frac{30j\epsilon^{-ja}I}{r_1'\lambda}\{\sin(e+f) \cdot \epsilon^{j(b+c+d)}(\cos\theta\cos\phi - \sin\theta\tan\Delta)\}\delta r\delta\phi. \quad (23)$$

### "Image-Cone" General Discussion

The vertical plane electric-field intensity distribution due to the "image cone" will now be determined.

It should be remembered that the ground was assumed to be a flat perfect conductor. The current term $I_0$ and the $X'Z'$ component $f(\delta r_1)$ are both the same for the "physical-cone" element and the "image-cone" element. $I_0$ as given in (9) and $f(\delta r_1)$ as given in (15) may, therefore, be used for these two terms in determining $E_0''$. The development for the "physical cone" may be used up through (15) for the "image cone."

### Sin $\tau$ for "Image-Cone" Element

By a process similar to that used in deriving (17)

$$\sin \tau_2 = -\frac{\cos\theta\cos\phi + \sin\theta\tan\Delta}{\sqrt{\cos^2\phi + \tan^2\Delta}}. \quad (24)$$

### "Image-Cone" Element Retarded Vector $\epsilon^{-jkr'}$

By a process similar to that used in deriving (21)

$$\epsilon^{-jkr_2'} = \epsilon^{j(-a-b-c+d)} = \epsilon^{-ja}\epsilon^{j(-b-c+d)}. \quad (25)$$

### Increment of the Electric-Field Intensity for the "Image-Cone" Element

Substituting from (9) for $I_0$; (24) for $\sin \tau$; (25) for $\epsilon^{-jkr'}$ and (15) for $f(\delta r_1)$ in (1) and after some manipulation

$$\delta(E_0'') = \frac{30j\epsilon^{-ja}I}{r_2'\lambda}\{\sin(e+f) \cdot \epsilon^{j(-b-c+d)}(-\cos\theta\cos\phi - \sin\theta\tan\Delta)\}\delta r\delta\phi. \quad (26)$$

### Increment of the Electric-Field Intensity for the Cone Element

The increment of the total electric-field intensity for the cone-antenna element is the sum of (23) and (26).

The distance $r_1'$ in the denominator of (23) and $r_2'$ in the denominator of (26) may be set equal to $r_0$ with negligible error.

The term $\epsilon^{-ja}$ in (23) and (26) is a constant phase function and may be set equal to unity.

Therefore

$$\frac{30j\epsilon^{-ja}I}{r_1', r_2'\lambda} = \frac{30jI}{r_0\lambda}.$$

Let

$$E = \frac{30jI}{r_0\lambda}. \quad (27)$$

Then combining (23) and (26), substituting (27) for its equivalent and rearranging

$$\delta(E_0) = E\sin(e+f)\{\cos\theta\cos\phi\epsilon^{jd}[\epsilon^{j(b+c)} - \epsilon^{-j(b+c)}] - \sin\theta\tan\Delta\epsilon^{jd}[\epsilon^{j(b+c)} + \epsilon^{-j(b+c)}]\}\delta r\delta\phi. \quad (28)$$

Equation (28) is the increment of the electric-field intensity for the cone-antenna element.

### The Internal Equation

Indicating the integration of (28) and setting the limits of integration

$$E_0 = E\int_0^R\int_0^{2\pi}\sin(e+f)\{\cos\theta\cos\phi\epsilon^{j(2\pi/\lambda)(r\sin\phi\cos\phi)} \cdot [\epsilon^{j(b+c)} - \epsilon^{-j(b+c)}] - \sin\theta\tan\Delta\epsilon^{j(2\pi/\lambda)(r\sin\phi\cos\phi)}[\epsilon^{j(b+c)} + \epsilon^{-j(b+c)}]\}d\phi dr. \quad (29)$$

### Integration in Respect to $\phi$

The solution of the first term containing $\phi$ is[12]

$$\int_0^{2\pi}\cos\phi\epsilon^{j(2\pi/\lambda)(r\sin\phi\cos\phi)}d\phi = j2\pi J_1\left(\frac{2\pi r}{\lambda}\sin\theta\right). \quad (30)$$

The solution of the second term containing $\phi$ is[13]

[12] N. W. McLachlan. "Bessel Functions for Engineers," Oxford University Press, London, England, 1934; example (10a), p. 51.

[13] See example (19) p. 43 of footnote reference 12.

$$\int_0^{2\pi} \epsilon^{j(2\pi/\lambda)(r\sin\phi\cos\phi)}d\phi = 2\pi J_0\left(\frac{2\pi r}{\lambda}\sin\theta\right). \quad (31)$$

Substituting (30) and (31) in (29)

$$E_0 = E\int_0^R \sin(e+f)\left\{\cos\theta\left[j2\pi J_1\left(\frac{2\pi r}{\lambda}\sin\theta\right)\right]\cdot\left[\epsilon^{j(b+c)} - \epsilon^{-j(b+c)}\right] - \sin\theta\tan\Delta\left[2\pi J_0\left(\frac{2\pi r}{\lambda}\sin\theta\right)\right]\cdot\left[\epsilon^{j(b+c)} + \epsilon^{-j(b+c)}\right]\right\}dr. \quad (32)$$

After manipulation and rearrangement

$$E_0 = \frac{30jI}{r_0}\int_0^R \{-2[\pi\cos\theta J_1(qr/\lambda)][\sin A\sin p_1 r/\lambda + \sin B\sin p_2 r/\lambda - \cos A\sin p_1 r/\lambda + \cos B\cos p_2 r/\lambda] + 2j[j\pi\sin\theta\tan\Delta J_0(qr/\lambda)][\sin A\cos p_1 r/\lambda - \sin B\cos p_2 r/\lambda + \cos A\sin p_1 r/\lambda + \cos B\sin p_2 r/\lambda]\}\frac{dr}{\lambda} \quad (33)$$

where

$$A = (b+e) = \frac{2\pi}{\lambda}[(H - R\tan\Delta)\cos\theta + L]$$

$$B = (b-e) = \frac{2\pi}{\lambda}[(H - R\tan\Delta)\cos\theta - L]$$

$$P_1 = \frac{f+c}{r/\lambda} = \frac{2\pi(k_1 + \sin\Delta\cos\theta)}{\cos\Delta}$$

$$P_2 = \frac{f-c}{r/\lambda} = \frac{2\pi(k_1 - \sin\Delta\cos\theta)}{\cos\Delta}$$

$$q = 2\pi\sin\theta.$$

In (33) the electric-field strength $E_0$ is expressed in volts per meter at a distance of 1 meter for 1 loop-ampere.

Converting to millivolts per meter at 1 mile for 1 loop-ampere

$$-\frac{30jI}{r_0} = -18.64jI. \quad (34)$$

For convenience the variable will be changed. Let

$$z = \frac{qr}{\lambda} = \frac{2\pi r\sin\theta}{\lambda}.$$

Substituting

$$E_0 = -j18.64I\int_0^z \{\cot\theta[\sin A\sin n_1 z J_1(z) + \sin B\sin n_2 z J_1(z) - \cos A\cos n_1 z J_1(z) + \cos B\cos n_2 z J_1(z)] + \tan\Delta[\sin A\cos n_1 z J_0(z) - \sin B\cos n_2 z J_0(z) + \cos A\sin n_1 z J_0(z) + \cos B\sin n_2 z J_0(z)]\}dz \text{ mv/m/mi/loop-ampere} \quad (35)$$

where

$$n_1 = \frac{k_1 + \sin\Delta\cos\theta}{\sin\theta\cos\Delta}$$

and

$$n_2 = \frac{k_1 - \sin\Delta\cos\theta}{\sin\theta\cos\Delta}.$$

The expression "mv/m/mi/loop ampere" is used to denote millivolts per meter at a distance of 1 mile for 1 loop-ampere.

The expressions containing $z$ in (35) may be integrated by several methods. For each expression, either the circular or the Bessel function or both may be expanded and the result integrated term for term. The expressions may also be integrated by parts, considering either the circular or Bessel function first. The methods all lead to an answer that is a series of series and, therefore, numerical computation is long and tedious.

Solutions derived for the author by Smith[14] yields answers that make the burden of numerical computation much less than it is with any of the author's derivations.

Following Smith's solutions

$$\int \sin nz J_0(z)dz = \frac{-2}{\sqrt{n^2-1}}\{F(n,z)\cos nz + \phi(n,z)\sin nz\} \quad (36)$$

$$\int \cos nz J_0(z)dz = \frac{2}{\sqrt{n^2-1}}\{F(n,z)\sin nz - \phi(n,z)\cos nz\} \quad (37)$$

$$\int \sin nz J_1(z)dz = \frac{2n}{\sqrt{n^2-1}}\{F(n,z)\sin nz - \phi(n,z)\cos nz\} - \sin nz J_0(z) \quad (38)$$

$$\int \cos nz J_1(z)dz = \frac{2n}{\sqrt{n^2-1}}\{F(n,z)\cos nz + \phi(n,z)\sin nz\} - \cos nz J_0(z) \quad (39)$$

where

$$F(n,z) = 1/2J_0(z) - k_n^2 J_2(z) + k_n^4 J_4(z)\cdots$$

$$\phi(n,z) = k_n J_1(z) - k_n^3 J_3(z) + k_n^5 J_5(z)\cdots$$

$$k_n = n - \sqrt{n^2-1}.$$

Taking $n$ equal to $n_1$ or $n_2$, as the case may be, (35) may be evaluated by using (36) through (39).

[14] The author is indebted to Prof. V. G. Smith, Department of Electrical Engineering, University of Toronto, Toronto, Ontario, Canada, for the derivation of the integrals in (35).

# Diffraction of High-Frequency Radio Waves Around the Earth*

M. D. ROCCO† AND J. B. SMYTH†

*Summary*—**This paper reports nonoptical height-gain measurements on a remarkably uniform desert link at frequencies of 25, 53, 170, 520, 1,000, 3,300, and 9,375 Mc using horizontal polarization. It has been shown[1,2] that when the index of refraction of the atmosphere is a linear function of elevation, the problem of refraction and diffraction may be represented approximately by a problem in diffraction alone. Data taken under linear and slightly nonlinear index of refraction gradients are compared with fields predicted by standard diffraction theory. A mechanism other than diffraction is required to explain the higher-frequency fields observed under standard[3] meteorological conditions.**

## I. Introduction

THERE ARE FEW PROBLEMS which have received the theoretical attention that has been given the investigation of the propagation of radio waves around the earth;[4–7] and yet, quantitative data sufficiently accurate to compare with theory are very meager at the higher frequencies. It is not expected that the ionosphere will affect the higher-frequency fields near the earth, only diffraction around the earth together with reflection, refraction, absorption, and scattering in the lower troposphere must be considered in explaining nonoptical fields. This paper compares experimental data with diffraction theory, particular interest being centered on investigating the validity of replacing the problem in diffraction and refraction by one in diffraction alone for: (a) standard meteorological conditions, and (b) nonstandard meteorological conditions. The data presented are for horizontal polarization. However, numerous checks showed identical results for vertical polarization.

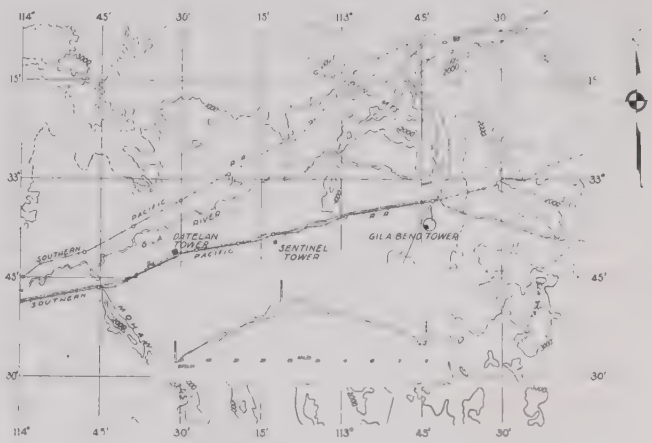


Fig. 1—Contour and profile of desert link. The vertical scale is indicated by 200-foot tower markers.

## II. Experimental Site

The data presented in this paper were obtained at the Navy Electronics Laboratory's experimental station located in the Gila Valley in southern Arizona. Fig. 1 is a contour map of the region and shows the location of

Fig. 2—Photograph of a typical desert terrain.

* Decimal classification: R112.14. Original manuscript received by the Institute, December 13, 1948; revised manuscript received, April 18, 1949.

† U. S. Navy Electronics Laboratory, San Diego 52, Calif.

[1] J. C. Schelleng, C. R. Burrows, and E. B. Ferrell, "Ultra-short-wave propagation," PROC. I.R.E., vol. 21, pp. 427–463; March, 1933.

[2] C. L. Pekeris, "Accuracy of the earth-flattening approximation in the theory of microwave propagation," *Phys. Rev.*, vol. 70, pp. 518–522; October, 1946.

[3] If the index of refraction near the earth is a linear function of elevation, decreasing at the rate of $1.18\times10^{-8}$ per foot, the refracting property of the atmosphere is defined as standard. Refraction is taken into account in the diffraction problem by increasing the earth's radius by a factor of $k$[1]. For the standard atmosphere, $k=1.33$.

[4] K. A. Norton, "The calculation of a ground-wave field intensity over a finitely conducting spherical earth," PROC. I.R.E., vol. 29, pp. 623–639; December, 1941.

[5] B. van der Pol and H. Bremmer, "The diffraction of electromagnetic waves from an electric point source round a finitely conducting sphere, with applications to radiotelegraphy and the theory of the rainbow," *Phil. Mag.*, vol. 24, part I, pp. 141–176; July, 1937; part. II, pp. 825–864, November, 1937.

[6] T. L. Eckersley, "Ultra-short-wave refraction and diffraction," *Jour. IEE* (London), vol. 80, pp. 286–304; March, 1937.

[7] G. N. Watson, "The diffraction of electric waves by the earth," *Proc. Roy. Soc.* (London), vol. 95, pp. 83–99; October 7, 1918; and pp. 546–563; July, 1919.

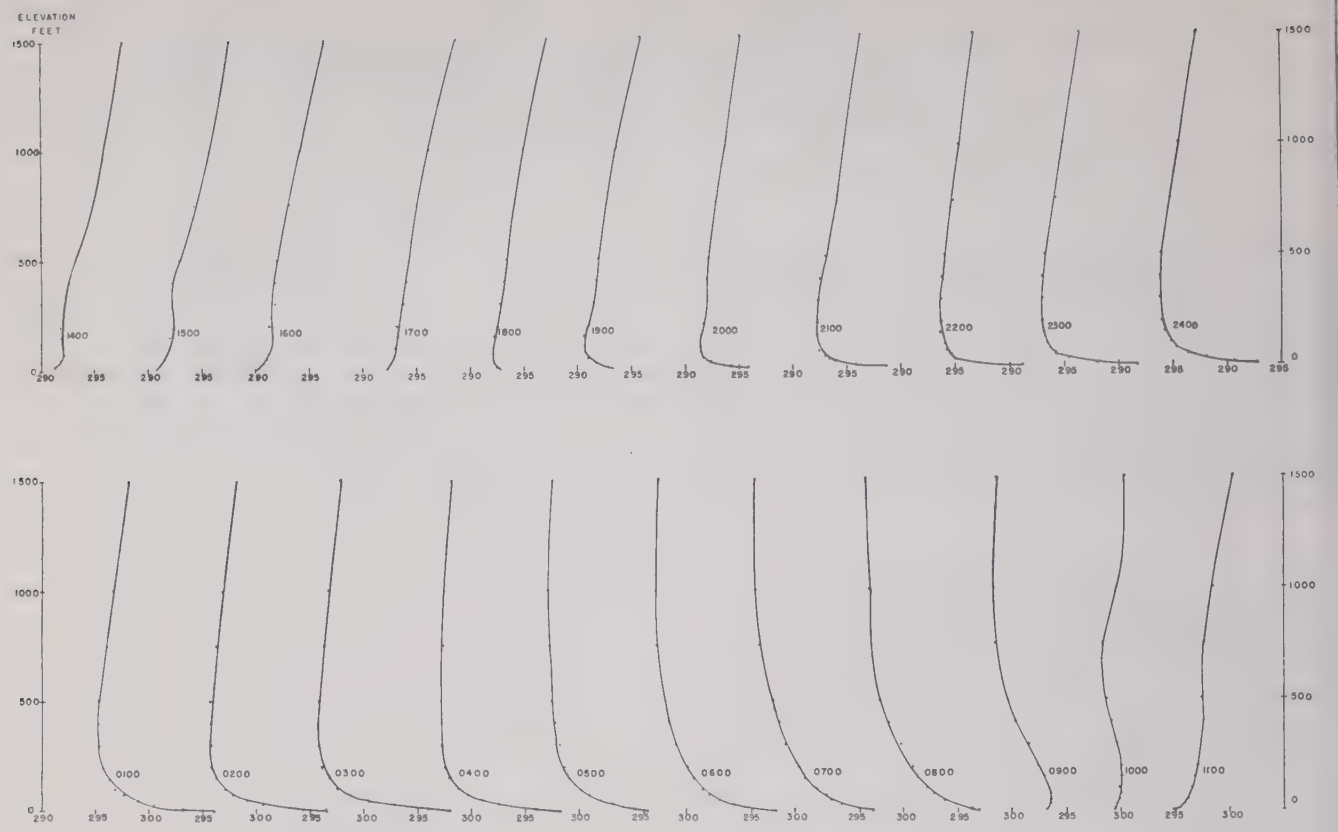


Fig. 3—A time sequence of the vertical distribution of the index of refraction for February 5 and 6, 1946. $B=n+\alpha h$, where $\alpha=1.18\times10^{-6}$/foot.

the three 200-foot towers on which elevator cabs were installed for hoisting radio antennas and associated equipment. The insert in Fig. 1 is a profile of the radio link, the vertical scale is indicated by the 200-foot tower markers. Transmitters were located at Gila Bend airfield and receivers at Datelan, 47 miles west along the valley. Fig. 2 is a photographic view of the path taken from atop the Gila Bend tower.

The receiver cab made continuous excursions measuring the vertical field distribution associated with successive transmitter cab elevations of 1, 25, 50, 100, and 190 feet. About 15 minutes was required to take a complete set of data which included a height-gain run for each of the 5 transmitter cab locations. Measurements were made over a number of 24-hour periods. The meteorology of the lower atmosphere in the region is characterized by a large diurnal variation in the temperature of the air near the ground. Fig. 3 gives a time sequence of index of refraction[8] versus elevation covering a typical 24-hour period. Each curve is the average of data taken at 6 stations approximately equally spaced along the propagation path. In the daytime, the index of refraction increases with elevation through the lower 6 feet of the atmosphere, producing a substandard condition in this region.

## III. Standard Propagation[3]

The measured fields are plotted in decibels versus the receiver height multiplied by the wavelength raised to the minus two-thirds power. This is a convenient representation which allows the data to be shown on one graph for direct comparison with diffraction theory. Fig. 4 is a typical height-gain run for the transmitter at 190 feet. The 4 plots show the same data compared with theory where different values of $k$ have been used. This does not affect the shape of the height-gain; the only change is the reference level for the various frequencies. If a sphere is drawn through the base of the towers at Gila Bend and Datelan, and the highest point at Sentinel, the value of $k$ appropriate to this geometry and the standard atmosphere would be 1.10. It will be noted that the majority of the data agree best with theory where a value of $k=1.33$ is chosen,[9] possibly showing

[8] L. J. Anderson, "Captive balloon equipment for low-level meteorological soundings," *Bull. Amer. Met. Soc.*, vol. 28, pp. 356–362; October, 1947.

[9] Free-space fields (i.e., attenuation as inverse distance) for the transmitter at 190 feet are obtained by subtracting the following decibels:

| frequency | 170 | 520 | 1,000 | 3,300 | 9,375 |
|---|---|---|---|---|---|
| db | 57.4 | 64.7 | 71.7 | 89.2 | 113.2 |

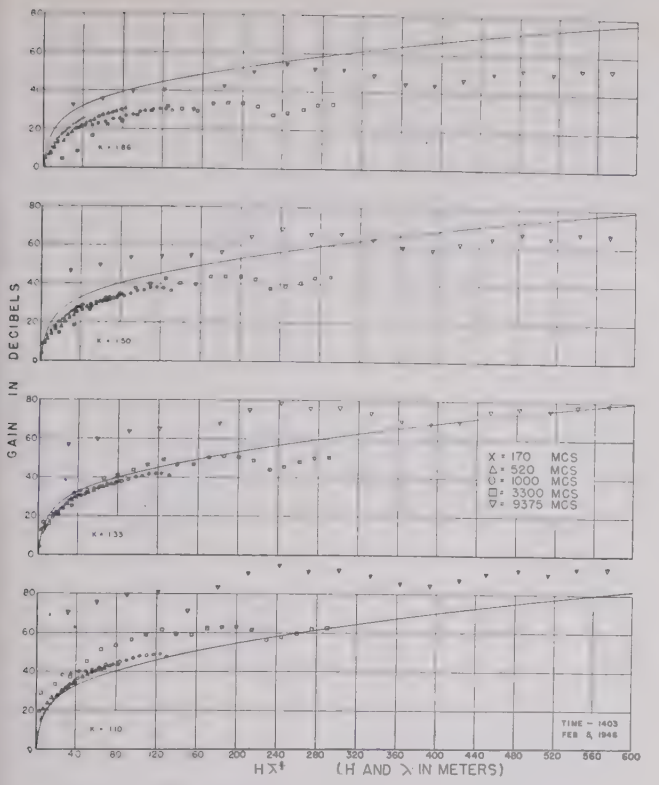


Fig. 4—Observed fields compared with theory (parameter *k* varied as specified).

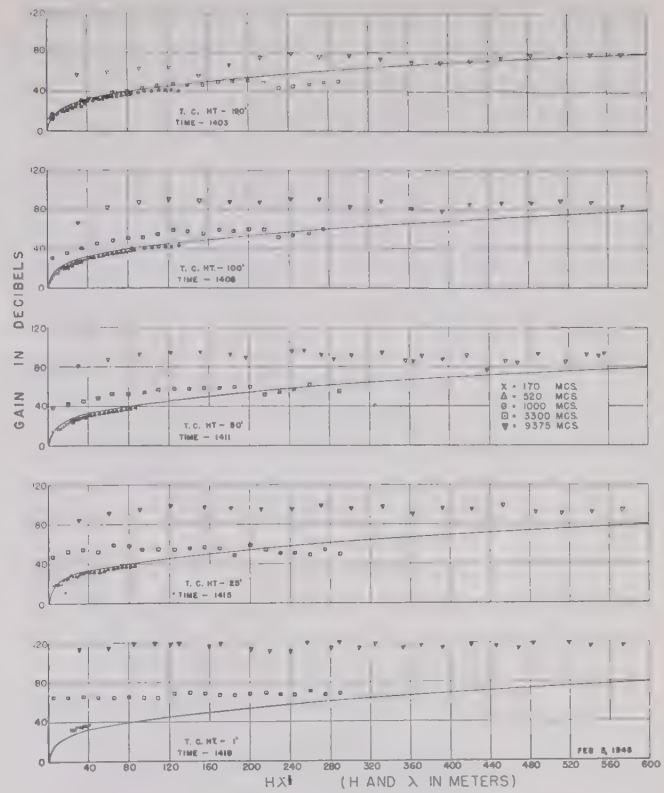
GAIN IN DECIBELS
T. C. HT – 190'
TIME – 1403
T. C. HT – 100'
TIME – 1408
T. C. HT – 50'
TIME – 1411
T. C. HT – 25'
TIME – 1415
T. C. HT – 1'
TIME – 1418
X = 170 MCS
Δ = 520 MCS
○ = 1000 MCS
□ = 3300 MCS
▽ = 9375 MCS
FEB 8, 1946
HX^½ (H AND λ IN METERS)

Fig. 6—The effect of transmitter elevation on nonoptical fields.

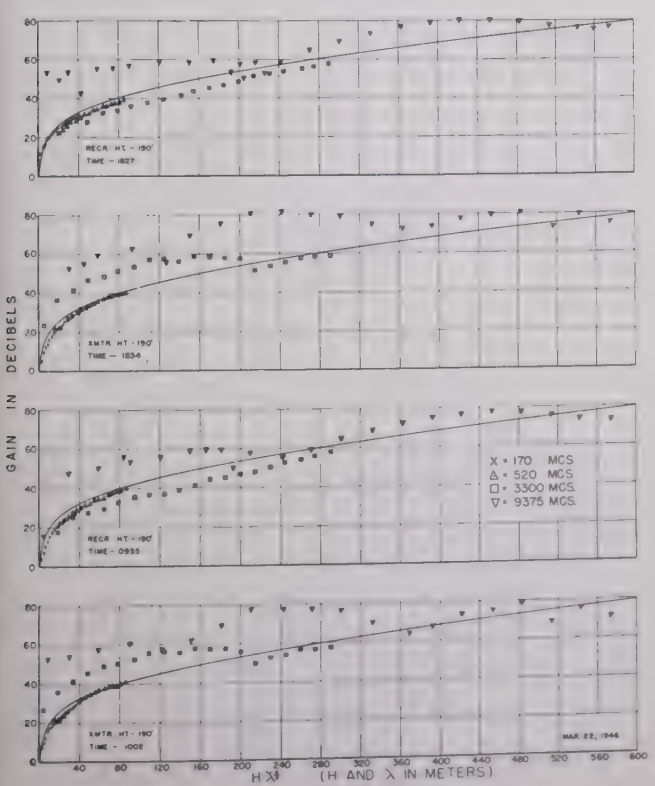


Fig. 5—The effect of local terrain near the link terminals.

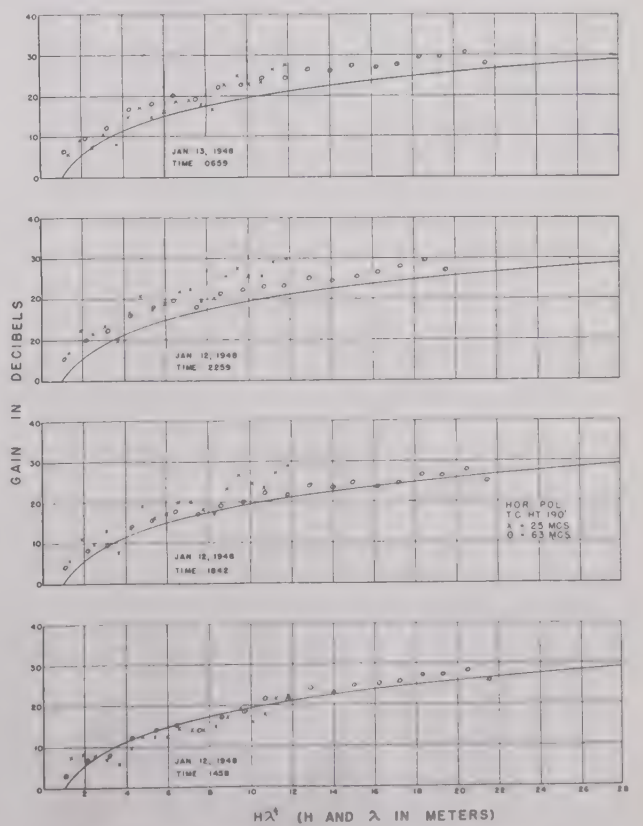


Fig. 7—25- and 63-Mc fields compared with theory.

that the earth's curvature; i.e., the local topography, near the transmitter and receiver is more important than the small hill at Sentinel, which is the only portion of the path that deviates much from a sphere with the earth's radius (Fig. 1).

Fig. 5 shows the local effect in another way. Height-gain data obtained by placing the receiver at 190 feet and lowering the transmitter cab are compared with data taken in the usual manner. At the higher frequencies, there is a marked difference between the data taken by the two methods.

Height-gain data for the various transmitter heights are shown in Fig. 6. As the antenna elevations are decreased, the agreement with theory becomes poorer the higher the frequency. When both the receiving and transmitting antennas approach the ground, the higher frequency fields fluctuate and the gain in field with height disappears. Both of these facts are at variance with predictions based on standard diffraction theory and will be discussed more fully in the last section.

## IV. Nonstandard Propagation

In reality, the so-called standard index gradient is the anomaly. The meteorological situation which is standard for one frequency may markedly affect nonoptical fields[10,11] on other frequencies. A comparison of the lowest with the highest frequency signals in Fig. 6 clearly shows this effect. The 25- and 63-Mc data presented in Fig. 7 show no consistent time variation which can be attributed to the low-level modification of the air.[12]

Fig. 8 shows how the nonoptical fields on the higher frequencies are affected by various degrees of modification of the refractive index gradient near the earth's surface (Fig. 3). The data presented here might be interpreted as confirmation for the waveguide type of propagation.[13,14] Such an interpretation of the data is being investigated; the present paper is limited to a description of the data by considering the problem as one in diffraction alone. If a value of $k=1.81$ is chosen, the data taken at 1808 and 2313 with the transmitter at 190 feet are moderately well predicted by diffraction alone, as demonstrated in Figs. 9 and 10.[15] This value of $k$

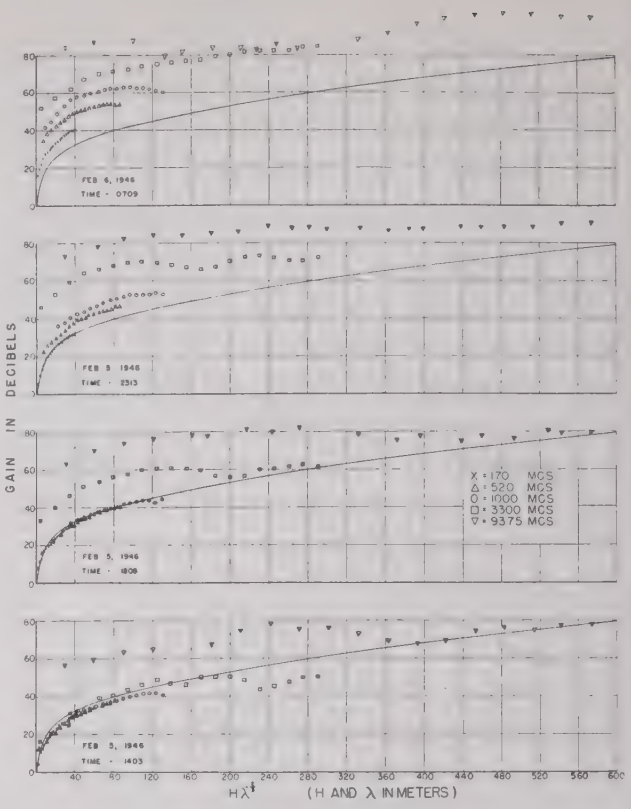


Fig. 8—The effect of low-level modification of the air on nonoptical fields. Transmitter cab height = 190 feet.

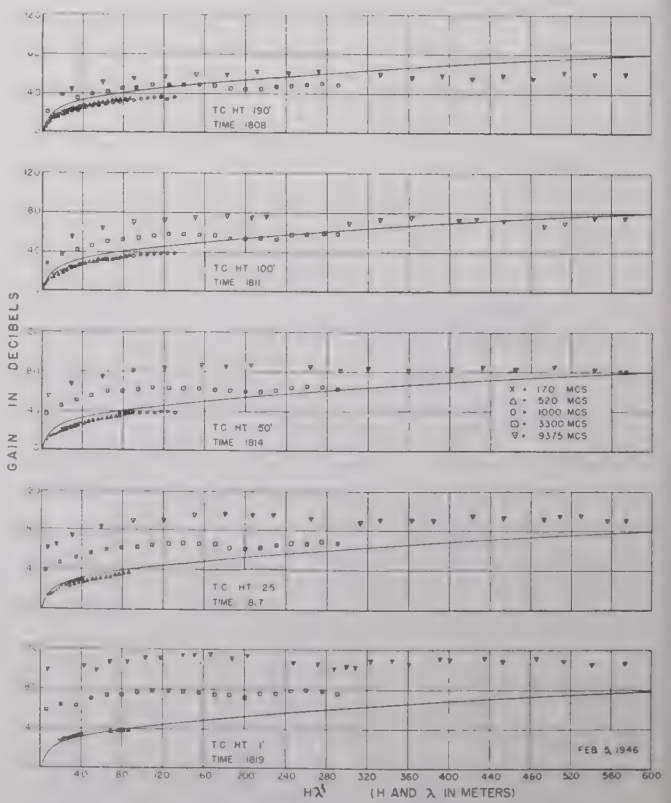


Fig. 9—Diffracted fields under nonstandard meteorological conditions ($k=1.81$).

[10] Martin Katzin, R. W. Bauchman, and William Binnian, "3- and 9-centimeter propagation in low ocean ducts," Proc. I.R.E., vol. 35; pp. 891–905; September, 1947.

[11] H. T. Friis, "Radar reflections from the lower atmosphere," Proc. I.R.E., vol. 35, pp. 494–495; May, 1947.

[12] Free-space fields for a transmitter elevation of 190 feet are obtained by subtracting 52.4 db and 54.6 db, respectively, from the 25- and 63-Mc levels.

[13] H. G. Booker and W. Walkinshaw, "The mode theory of tropospheric refraction and its relation to wave-guides and diffraction," Meteorological Factors in Radio-Wave Propagation, The Physical Society of London, pp. 80-127; April, 8, 1946.

[14] C. L. Pekeris, "Perturbation theory of the normal modes for an exponential $M$-curve in non-standard propagation of microwaves," *Jour. Appl. Phys.*, vol. 17, pp. 678-684; August, 1946.

[15] Free-space fields for a transmitter elevation at 190 feet are obtained by subtracting the following decibels:

| frequency | 170 | 520 | 1,000 | 3,300 | 9,375 |
|---|---|---|---|---|---|
| db | 53.4 | 58.7 | 62.7 | 78.2 | 94.2 |

makes the 1,000-Mc height-gain data taken at 2313, with the transmitter cab at 190 feet, approach closely the theoretical curve. The comparison of experience with theory under these conditions is certainly no less favorable than the similar comparison under meteorological conditions approaching standard.

Fig. 11 is an actual height-gain record taken under a meteorological condition approaching standard. Fig. 12 is a similar record obtained during nonstandard conditions.

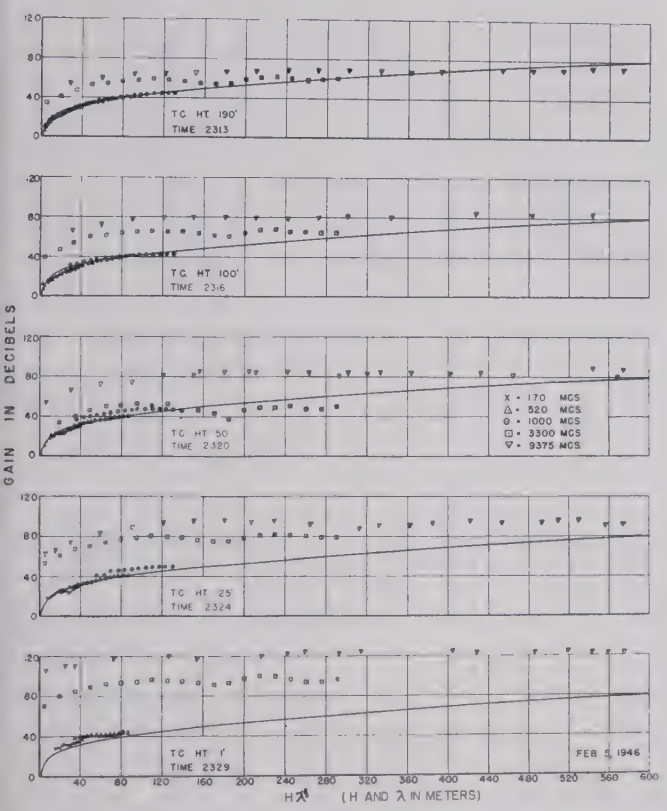


Fig. 10—Diffracted fields under nonstandard meteorological conditions ($k = 1.81$).

## V. Signal Fluctuations

Nonoptical fields recorded during the daytime (meteorological conditions approaching standard) yield moderately steady signals for the lower frequencies at all heights and for the higher frequencies when the antennas are high. Figs. 13 and 14 are photographs of the recording tape showing the signal fluctuations at various receiver elevations under standard and nonstandard conditions. During the daytime, the maximum signals observed at the frequencies of 9,375 and 3,300 Mc for low antenna heights are well above the fields associated with diffraction under standard conditions. With the transmitter at 1 foot, the 9,375-Mc field is stronger, relative to the free-space level, than the 3,300-Mc field; the index of refraction gradient during this time is substandard near the earth.

Scattering in the lower atmosphere would appear to be a plausible process that might produce variable nonoptical fields on the higher frequencies which are stronger than can be accounted for by diffraction. In order to make a detailed investigation of the signal fluctuations, the 3,300-Mc pulses displayed on an oscilloscope were recorded photographically. Fig. 15 is a frequency distribution of received pulses compared with a Rayleigh distribution.[16] The chi-squared test[17] for goodness of fit was near the 20 per cent level, possibly indicating that the observed nonoptical signal might be produced by incoherent scattering in the lower atmosphere.

The authors are indebted to W. C. Hoffman and R. F. Arenz for the analysis leading to Fig. 15.

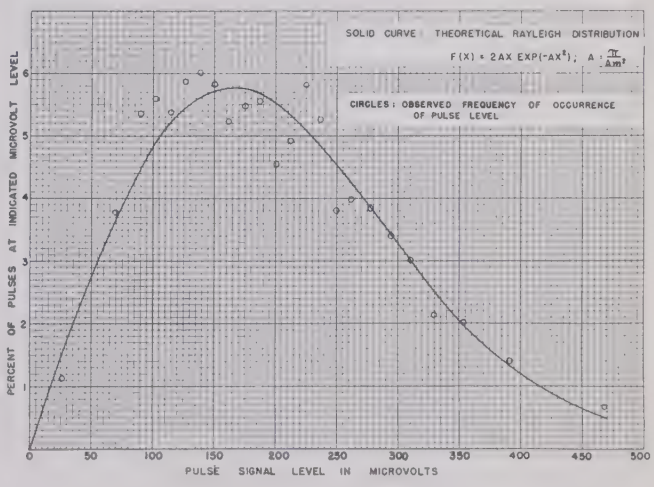
SOLID CURVE: THEORETICAL RAYLEIGH DISTRIBUTION
F(X) = 2AX EXP(-AX²); A = π/Δm²
CIRCLES: OBSERVED FREQUENCY OF OCCURRENCE OF PULSE LEVEL
PERCENT OF PULSES AT INDICATED MICROVOLT LEVEL
PULSE SIGNAL LEVEL IN MICROVOLTS

Fig. 15—Frequency distribution of 3,300-Mc pulse signal levels.

## VI. Conclusions

The lower frequency fields received on the nonoptical link under the meteorological conditions encountered, are amply described by diffraction alone.

The fields observed at the higher frequencies for low terminal heights were considerably stronger than standard diffraction theory would predict, even under meterological conditions which were definitely substandard near the ground. These strong fields were characterized by rapid time variations and no apparent variation with height. The frequency distribution of the signal fluctuations agrees with a Rayleigh distribution.

[16] Lord Rayleigh, "Theory of Sound," Dover Publishers; New York, N. Y., 1945; vol. 1, sec. 42(a).
[17] P. G. Hoel, "Introduction to Mathematical Statistics," John Wiley and Sons, New York, N. Y., 1947; pp. 134, 186.

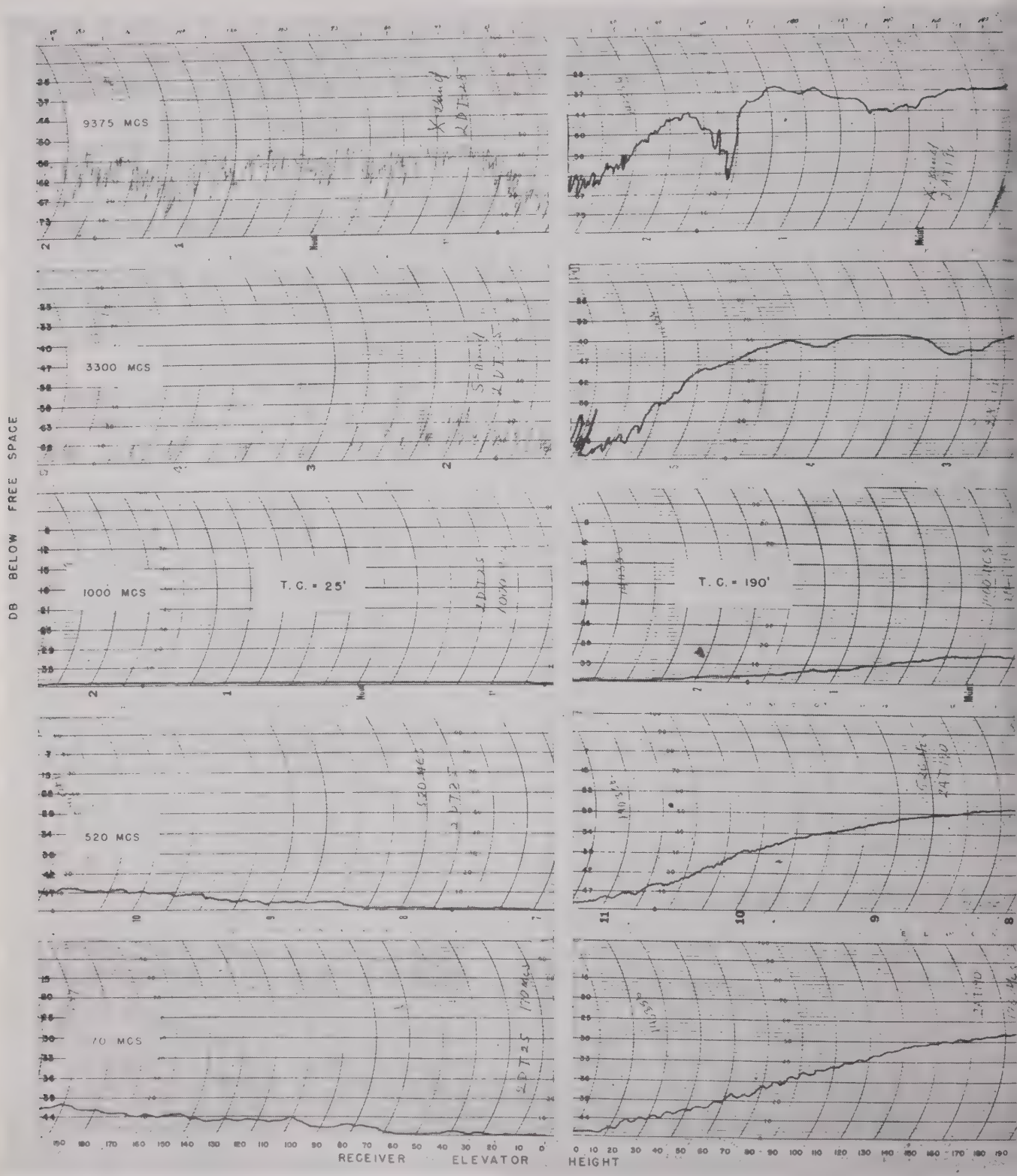


Fig. 11—Height-gain record under standard meteorological conditions.

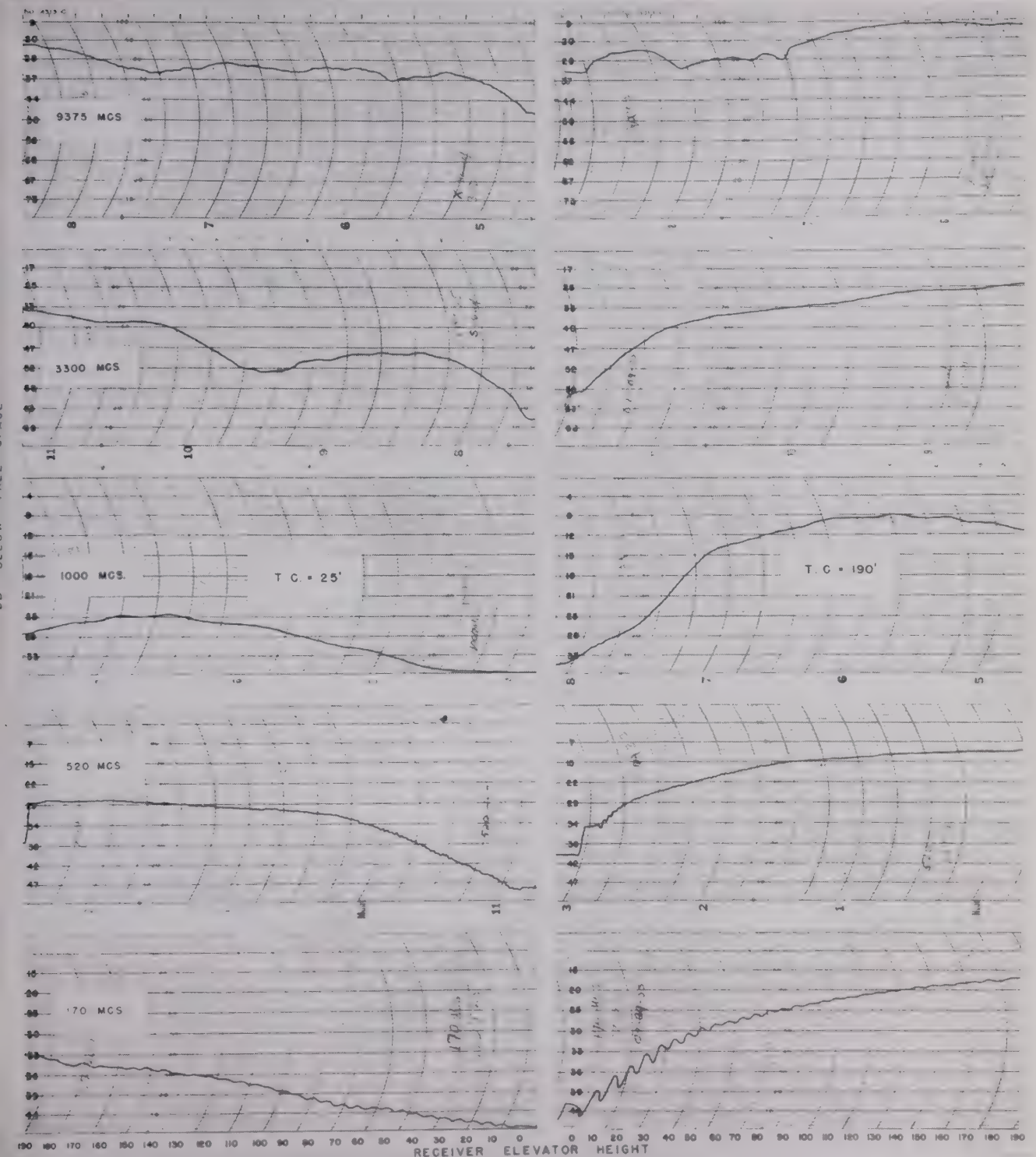


Fig. 12—Height-gain record under nonstandard meteorological conditions.

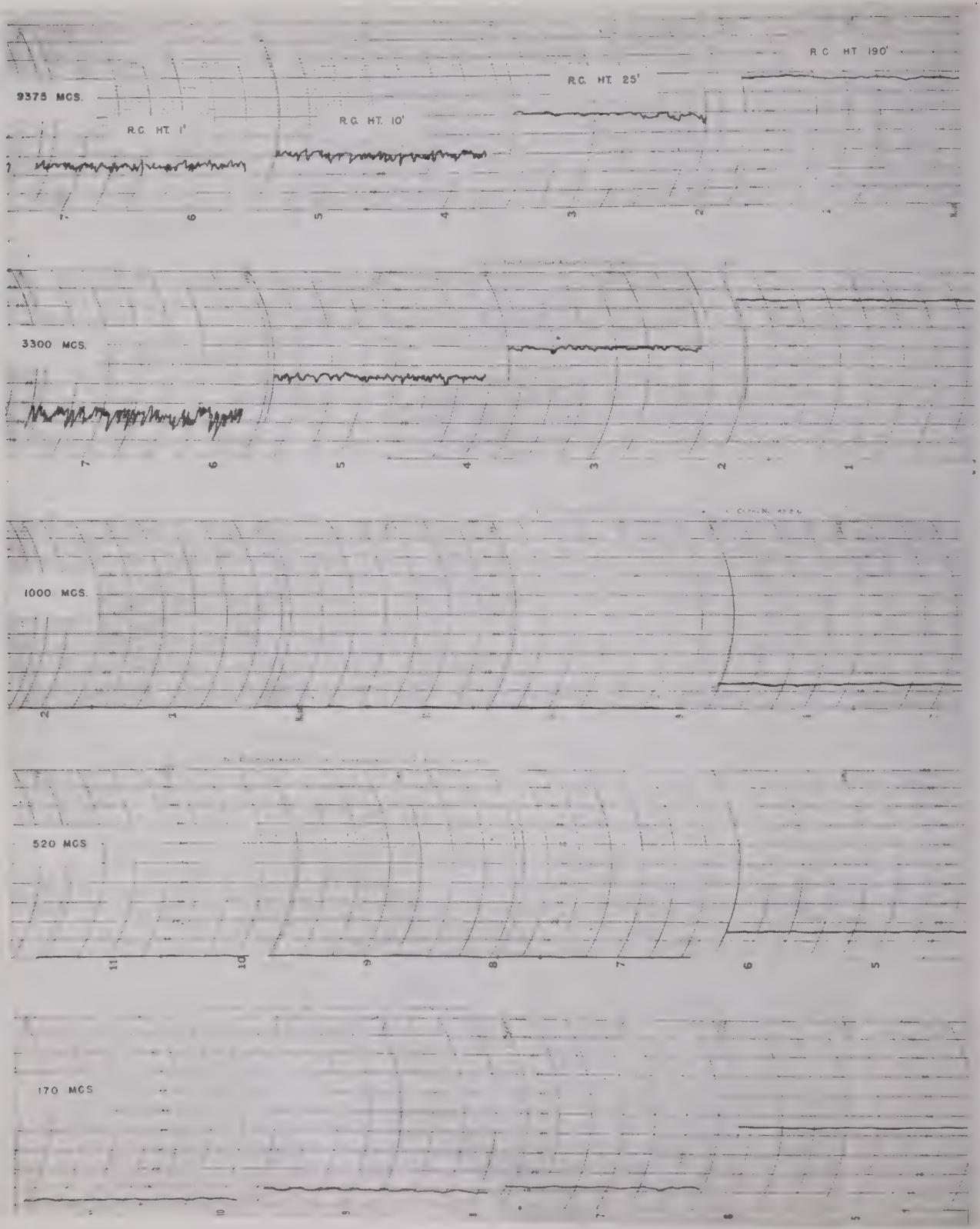


Fig. 13—Time variation in received signal (at elevation indicated) under standard meteorological conditions. Elevation of transmitting antennas = 190 feet. Time : 5:30 p.m.

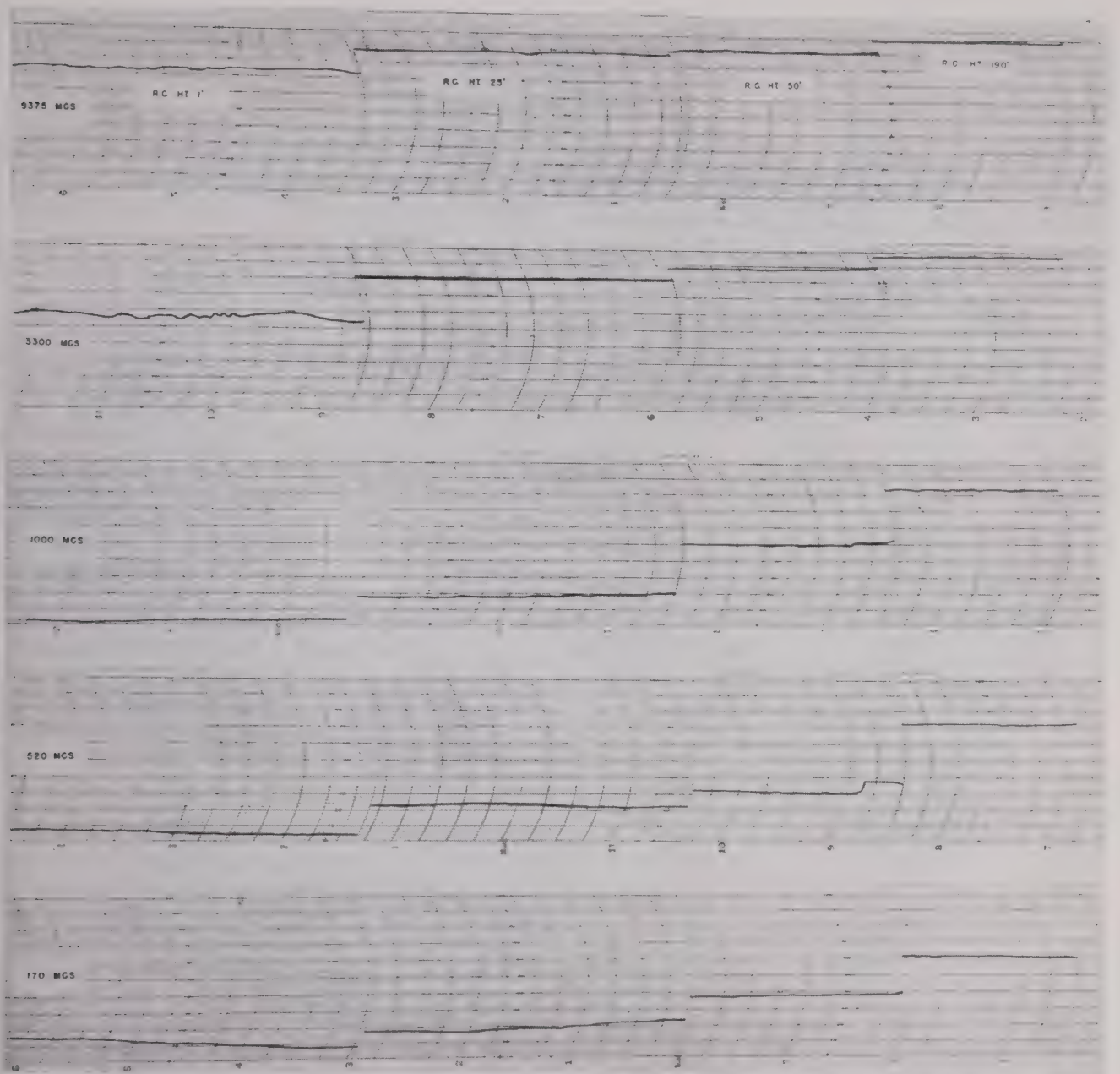


Fig. 14—Time variation in received signal (at elevation indicated) under nonstandard meteorological conditions. Elevation of transmitting antennas = 190 feet. Time: 7:30 a.m.

# Calculator and Chart for Feedback Problems*

JEAN H. FELKER†, ASSOCIATE, IRE

*Summary*—**This paper describes a chart and a mechanization of the chart in the form of a calculator that will simplify the calculation of the effects of feedback. When the magnitude and phase of the feedback are put into the calculator, figures are obtained at each frequency point for the magnitude and phase shift of the transfer characteristic with the feedback loop closed.**

## I. The Mu-Beta Effect

THE CHART and calculator are based on the "mu-beta" effect, which is defined by use of the fundamental feedback equation:

$$G = \frac{\mu}{1 - \mu\beta} \tag{1}$$

where

$\mu$ = the voltage amplification of the amplifier with the feedback loop open

$\beta$ = the fraction of the output voltage of the amplifier that is fed back to the input

$G$ = voltage amplification of the amplifier with the feedback loop closed.

Equation (1) can be rewritten in the form

$$G = -\frac{1}{\beta}\left(\frac{-\mu\beta}{1 - \mu\beta}\right), \tag{2}$$

from which it is seen that, when $\mu\beta$ is large, the response is given approximately by

$$G \doteq -\frac{1}{\beta}$$

and is independent of the $\mu$ or gain circuit. Since amplifying devices always have a finite bandwidth, there will be frequencies at which $\mu\beta$ is not large, and at these frequencies account must be taken of the second factor of (2), which can be anything from 0 to $\infty$.

The departure of the amplifier response from $-1/\beta$ has been described as the "mu-beta" effect, because it results from the noninfiniteness of $\mu\beta$.[1] Accordingly, the $\mu\beta$ effect is defined as a complex number

$$\gamma\angle\phi = \frac{-|\mu\beta|\angle\theta}{1 - |\mu\beta|\angle\theta} \tag{3}$$

$\gamma$ = modulus or magnitude of mu-beta effect

$\phi$ = argument or phase of mu-beta effect

$|\mu\beta|$ = modulus or magnitude of $\mu\beta$

$\theta$ = argument or phase of $\mu\beta$ (which is equal to the phase shift around the $\mu\beta$-loop).

Substitution of (3) in (2) gives

$$G = \frac{|1|}{|\beta|}\gamma\angle 180° + \phi - \psi \tag{4}$$

from which it is seen that the magnitude of $G$ in decibels[2] is $\gamma$ in decibels minus the magnitude of $\beta$ in decibels, while the phase of $G$ is 180° plus $\phi$ minus $\psi$ (the phase of $\beta$).

A plane can be visualized in which the vector from the origin to any point represents the $\mu\beta$ effect at that point. For a given $\mu\beta$ effect there can correspond only one value of $\mu\beta$. One might label each point with the corresponding values of $|\mu\beta|$ and $\theta$, or one might plot contours of constant $|\mu\beta|$ and $\theta$ on such a plane. Such a representation would be useful when $\gamma < 1$, since this region is confined within a unit circle. The lower half of such a plane is shown in the lower half of Fig. 1.

For values of $\gamma$ between 1 and $\infty$, an inverse plane might be imagined in which the distance from the origin represents the inverse of the $\mu\beta$ effect. The mirror image of such a plane is shown in the top half of Fig. 1.

## II. Use of the Calculator

The chart of Fig. 1 can be made into a calculator[3] by cutting out the scale at the bottom of the figure and attaching it at the center of the chart as a rotatable arm. To find the $\mu\beta$ effect corresponding to a particular pair of values for $|\mu\beta|$ and $\theta$, first locate the intersection of the appropriate $|\mu\beta|$ and $\theta$ contours, and then rotate the calculator arm until the edge of the scale on it crosses the intersection. Read the magnitude ($\gamma$) of the $\mu\beta$ effect off the scale on the arm, and the phase ($\phi$) at the point where the arm crosses the semicircular phase scale at the top of the calculator.

Since the calculator shows only one-half of the direct and inverse $\mu\beta$-effect planes, only angles between 0 and 180° can be represented. This represents no real difficulty, since any angle greater than 180° can be represented as a negative angle less than 180°. To permit the use of the calculator for both negative and positive angles, no signs have been attached to the $\theta$ contours. The only rule that need be remembered to avoid angle

* Decimal classification: R078×R363.23. Original manuscript received by the Institute, October 21, 1948; revised manuscript received, January 25, 1949.

† Bell Telephone Laboratories, Inc., New York, N. Y.

[1] H. W. Bode, "Network Analysis and Feedback Amplifier Design," D. Van Nostrand Co., Inc., New York, N. Y., p. 33; 1945.

[2] The term "in decibels" is employed herein to refer to 20 $\log_{10}$ of the absolute value of a quantity. (The quantities dealt with are ratios of linear quantities; voltages or currents, rather than power.)

[3] This calculator is commercially available as advertised in this issue.

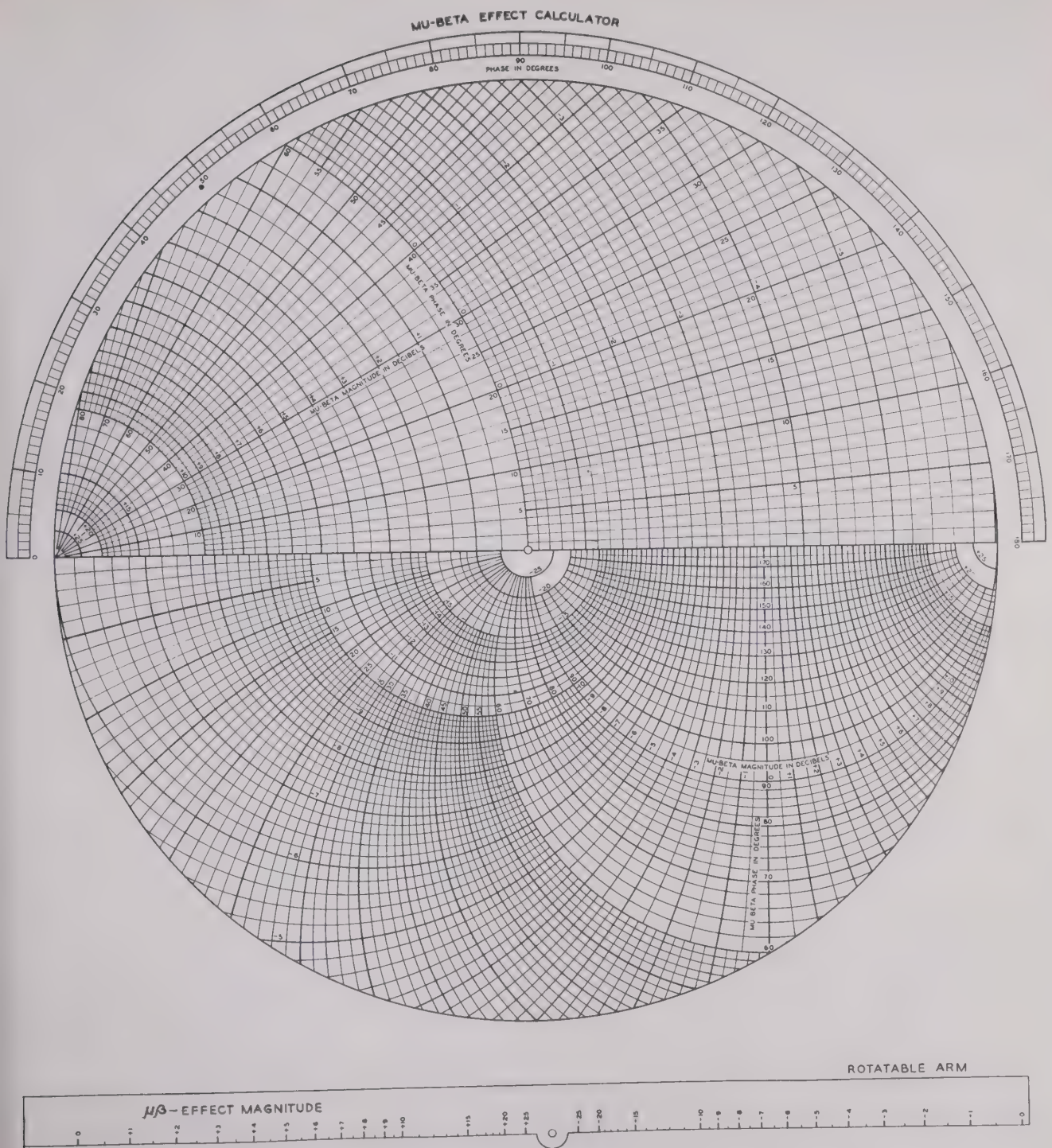


Fig. 1—The $\mu\beta$-effect chart.

ambiguity is that the sign of $\phi$ will always be the negative of $\theta$. If, for example, $|\mu\beta|$ is 10 db and $\theta$ is 30°, $\gamma$ is +2.6 db and $\phi$ is −12°, while if $\theta$ were −30° (or 330°), $\phi$ would be +12°.

Note that the positive half of the calculator arm has been made longer than the negative half, with the result that the phase of the $\mu\beta$ effect can be determined only when the positive half of the arm is in the top half of the calculator. Thus no special effort is required to insure that the correct sign is attached to the decibel value of $\gamma$.

## III. A Sample Problem

The characteristic of the $\mu\beta$ loop of a servo is shown in Fig. 2. Since $\beta$ in a servo is −1, the $\mu\beta$ effect is the

TABLE I

| $\omega$ | $\lvert\mu\beta\rvert$ (db) | $\theta$ | $\gamma$ (db) | $\phi$ |
|---|---|---|---|---|
| 1.5 | 17 | 37° | +1 | −5.5° |
| 2 | 13 | 44° | +1.4 | −10.5° |
| 4 | 5 | 56° | +1.6 | −34.5° |
| 10 | −4 | 57° | −2.5 | −84° |
| 30 | −15 | 23° | −13.5 | −151° |

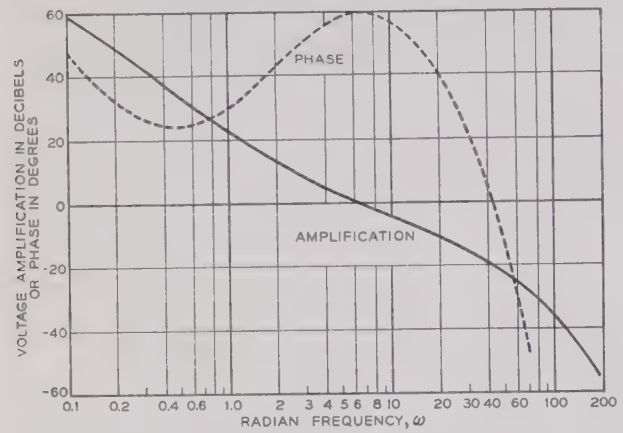


Fig. 2—$\mu\beta$ characteristic of a servo.

transfer characteristic (see (4)). To permit checking by the reader, $\lvert\mu\beta\rvert$, $\theta$, and the resulting values of $\gamma$ and $\phi$, as obtained from the calculator, are tabulated in Table I for several frequencies. These values of $\gamma$, as well as the values corresponding to $\mu$ variations of +12, +6, −6 and −12 db, are plotted in Fig. 3 to illustrate the comprehensive results that are readily obtainable from the calculator.

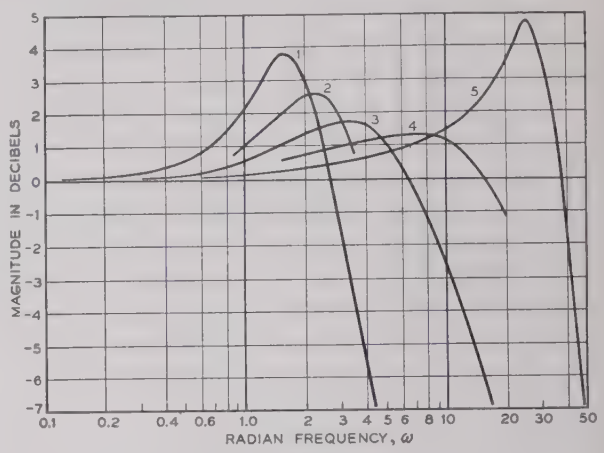


Fig. 3—Transfer characterictic of the servo with gain varied.
1—Gain down 12 db.
2—Gain down 6 db.
3—Gain at nominal value.
4—Gain up 6 db.
5—Gain up 12 db.

# The High-Frequency Response of Cylindrical Diodes*

EDWARD H. GAMBLE†

THIS ABSTRACT includes the results of an investigation into the response of cylindrical diodes to the application of voltages which contain high-frequency components. In particular, the response to "large" signals has been determined, where the term "large signal" refers to the condition that the amplitudes of the time-varying components are comparable to that of the constant polarizing voltage.

The problem has been studied as a quasi-stationary one since the applied signal may be assumed to change only slightly in the time required for an electromagnetic wave to propagate the interelectrode space. The three basic postulates upon which this theory is built are Poisson's equation, Newton's equation, and the continuity equation.

The complete solution of the cylindrical diode under general space-charge conditions is found to be more complicated than the associated planar case. The method of integral equations has been adopted. The solution for the trajectory of the electrons or the radial distance $R(t, \tau)$ is the most difficult problem since the integral equation for $R(t, \tau)$ involves the reciprocal of $R(t, \tau)$ under the integral sign. A method of successive approximations has been adopted for each specific form of applied voltage. In general, only approximate solutions can be found for the cylindrical diode under various space-charge conditions. Nevertheless, the derived relationships between the fundamental physical quantities do afford one insight into the inner workings of the cylindrical thermionic diode.

The simplifying assumptions which must be made to reduce the general space-charge relations to those which describe the space-charge-limited operation and temperature-limited operation have been pointed out.

Numerical solutions have been determined for a wide variety of signal voltages for both space-charge-limited and temperature-limited operation. These should prove of considerable help to the tube designer. The variations in the important physical variables which occur as the amplitude of the voltage signal increases from that referred to as "small" to the "large" signals are determined and graphically shown. These numerical solutions check the integral equation relationships to an accuracy of about 2 per cent.

Under large signal conditions, considerable modulation of the electric field, and the velocity and trajectory of the electrons occur. In some cases, the electrons are returned to the cathode or caused to oscillate radially in the interelectrode space.

When the radii of both the cathode and anode are large, the solutions reduce to those which are found for the planar diode configuration.

The first approximation for the numerical solutions was determined by setting the nonlinear differential equation of motion of the electrons into an electronic analogue computer. Analytic formulas which matched the numerical solutions were determined. These analytic expressions were substituted for the variables in the integral equations and found to satisfy them within the accuracy of the numerical solution.

* Decimal classification: R134×R362.21. Original manuscript received by the Institute, February 15, 1949; abstract received. May 18, 1949.

† Curtiss-Wright Corp., Columbus, Ohio.

# Response of *RC* Circuits to Multiple Pulses*

DANIEL LEVINE†, MEMBER, IRE

*Summary*—The voltage across the capacitor in a pulsed *RC* circuit can be found without difficulty, if the change in the base-line is known as a function of the number of pulses. This paper derives the necessary equations for this transient effect, using only the well-known charge discharge functions for a direct-current circuit. The results can be extended immediately to the voltage across the resistor.

THE VOLTAGE variation across a component in a resistor-capacitor circuit upon applying a rectangular voltage wave is treated adequately in many textbooks;[1,2] however, the effect of applying several pulses in succession generally is left as an exercise for step-by-step solution. This paper generalizes the step-by-step process for any number of pulses.

The case for $n$ pulses, where $n$ may have any value, is of practical concern in some circuit design, and may be solved exactly by finding the voltage before the start of the $n$th pulse. An equivalent statement is that we want to find functions that describe the maximum and minimum envelopes for a finite number of pulses.

Initially, we shall consider the voltage variation across the capacitor in Fig. 1. Starting the rectangular wave at

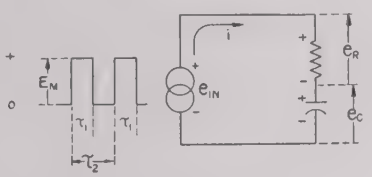


Fig. 1—Pulsed *RC* circuit.

time $t=0$, when the capacitor has a voltage denoted by $e_C(0)$, causes a change in voltage of

$$\Delta e_C(t) = [E_m - e_C(0)](1 - e^{-t/T_1}), \tag{1}$$

where $T_1=R_1C_1$, and $E_m$ is the magnitude of the rectangular wave. The total voltage across the capacitor, therefore, is

$$e_C(t) = e_C(0) + [E_m - e_C(0)](1 - e^{-t/T_1}). \tag{1a}$$

At the end of the pulse the time is equal to the pulse duration $\tau_1$, so that the voltage is

$$\begin{aligned} e_C(\tau_1) &= e_C(0) + [E_m - e_C(0)](1 - e^{-\tau_1/T_1}) \\ &= e_C(0) + a_1[E_m - e_C(0)], \end{aligned} \tag{2}$$

where

$$a_1 = 1 - e^{-\tau_1/T_1}. \tag{2a}$$

The voltage variation for $t>\tau_1$ is given by

$$e_C(t) = \{e_C(0) + a_1[E_m - e_C(0)]\}e^{-(t-\tau_1)/T_2}$$

where $T_2=R_2C_2$. (In many sweep generators the time constant during discharge is different from that during charge. In order to develop equations having the broadest application, this type of condition is covered by introducing $T_2$.)

The start of the second pulse is at time $t=\tau_2$, where $\tau_2$ is the pulse repetition period; the initial voltage is

$$e_C(\tau_2) = e_C(\tau_1)e^{-(\tau_2-\tau_1)/T_2} = a_2e_C(\tau_1) \tag{3}$$

where

$$a_2 = e^{-(\tau_2-\tau_1)/T_2}. \tag{4}$$

In a similar manner we obtain for the second pulse interval

$$\begin{aligned} e_C(\tau_2 + \tau_1) &= e_C(\tau_2) + a_1[E_m - e_C(\tau_2)] \\ &= a_1E_m + a_2(1 - a_1)e_C(\tau_1), \end{aligned} \tag{5}$$

and

$$e_C(2\tau_2) = a_2e_C(\tau_2 + \tau_1).$$

When this procedure is extended to cover additional pulses, we find that the voltage expressions may be represented by the following progression:

| *Pulse* | *Voltage at* $t = (m-1)\tau_2 + \tau_1$ | | |
|---|---|---|---|
| 1. | $b$ | $b = e_C(\tau_1)$ | (6) |
| 2. | $a + br$ | $a = a_1E_m,\ r = a_2(1 - a_1)$ | (7) |
| 3. | $a + (a + br)r$ | $= a + ar + br^2$ | |
| . . . | . . . . . | . . . . . | |
| $m$. | $a + ar + ar^2 + \cdots + ar^{m-2} + br^{m-1}$ | | |
| | $= \dfrac{a}{1-r}\left[1 - r^{m-1}\left(1 - \dfrac{b}{a} + \dfrac{b}{a}r\right)\right]$. | | (8) |

Therefore, the voltage at the termination of the $m$th pulse is obtained by substituting the values for $a$, $b$, and $r$ (given in equations (6) and (7)) into equation (8):

$$\begin{aligned} e_C[(m-1)\tau_2 + \tau_1] &= \frac{a_1E_m}{1 - a_2(1 - a_1)}\left\{1 - [a_2(1 - a_1)]^{m-1}\right. \\ &\quad \left.\cdot\left[1 - \frac{e_C(\tau_1)}{a_1E_m}[1 - a_2(1 - a_1)]\right]\right\}. \end{aligned} \tag{9}$$

As $m$ becomes very large, the factor containing $r^{m-1}$ approaches zero, since the ratio factor $r$ is less than unity; therefore

* Decimal classification: R140. Original manuscript received by the Institute, December 29, 1948; revised manuscript received, April 5, 1949.

† Aircraft Radiation Laboratory, Air Matériel Command, Dayton, Ohio.

[1] Ernst A. Guillemin "Communication Networks," Vol. I, John Wiley and Sons, Inc., New York, N. Y., 1931, pp. 30–40.

[2] For the steady-state solution, see Nathan Marchand, "The response of electrical networks to non-sinusoidal periodic waves," PROC. I.R.E., vol. 29, pp. 330–333; June, 1941.

$$\lim_{m\to\infty} e_c[(m-1)\tau_2+\tau_1] = \frac{a_1E_m}{1-a_2(1-a_1)}. \quad (10)$$

Equation (9) expresses the variation of the envelope as a function of the number of pulses, while (10) gives the asymptotic value of the envelope.

In order to obtain corresponding values for the end of the pulse period, which is equivalent to finding the baseline upon which the signal is superposed, it is necessary to multiply (9) and (10) by the decay factor $a_2$:

$$e_C(m\tau_2) = \frac{a_1a_2E_m}{1-a_2(1-a_1)}\left\{1-[a_2(1-a_1)]^{m-1}\cdot\left[1-\frac{e_C(\tau_1)}{a_1E_m}[1-a_2(1-a_1)]\right]\right\} \quad (11)$$

and

$$\lim_{m\to\infty} e_C(m\tau_2) = \frac{a_1\,a_2\,E_m}{1-a_2(1-a_1)}. \quad (12)$$

The steady-state pulse amplitude, obtained as the difference between (10) and (12), is given by

$$\frac{a_1E_m(1-a_2)}{1-a_2(1-a_1)}. \quad (13)$$

Since the amplitude of the first pulse is $a_1[E_m-e_C(0)]$, the ratio of the first pulse amplitude to the steady-state amplitude is

$$\frac{[E_m-e_C(0)]\cdot[1-a_2(1-a_1)]}{E_m(1-a_2)}. \quad (14)$$

The voltage across the resistor in the $RC$ circuit does not require a separate analysis, since the sum of the resistor and the capacitor voltages is equal to the applied voltage.

The wave forms in Fig. 2 illustrate the application of these equations to the problem of a square wave applied to a circuit having no initial charges, and a time constant 0.721 times the period.

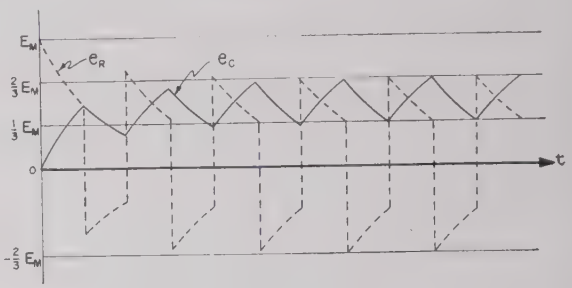


Fig. 2—Instantaneous voltages across capacitor and resistor.

# Impedance Measurements with Directional Couplers and Supplementary Voltage Probe*

B. PARZEN†, ASSOCIATE, IRE

*Summary*—**Impedance measurements may be made at very-high frequencies and above with the impedometer, consisting of two oppositely connected directional couplers and a voltage probe in a short transmission line. An experimental model for frequencies between 50 and 500 Mc is described.**

## Introduction

DIRECTIONAL COUPLERS have been used to determine the magnitude of the reflection coefficient (and hence SWR) of impedances referred to a given transmission line.[1] The addition of a voltage probe permits the phase angle and magnitude of the reflection coefficient to be determined from which the real and imaginary components of the impedance may be obtained.

The essential components of the equipment are shown in Fig. 1. The impedance $Z_L$ to be measured is connected by a short length of transmission line to a generator, preferably through an attenuating pad. Two directional couplers are inserted anywhere in the line. One, giving an output $E_2$, is directed to the reflected wave and the other, of output $E_3$, to the forward wave. A voltage probe, giving an output $E_1$, is inserted in the line at electrical degrees $\theta_1$ from $Z_L$.

The attenuating pad maintains $E_3$ substantially independent of the load $Z_L$, and is not required if the internal impedance of the generator is equal to the characteristic impedance of the line.

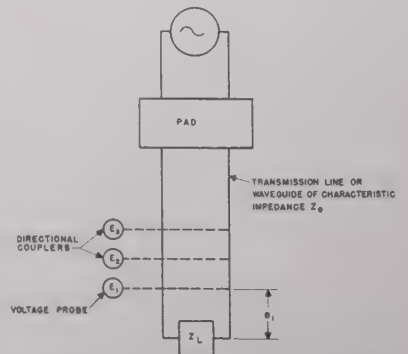


Fig. 1—Essential components of impedometer.

## Theory of Operation

What the equipment directly measures is the reflection coefficient $K$ and not the impedance. The relations

* Decimal classification: R244.224. Original manuscript received by the Institute, September 7, 1948; revised manuscript received, February 7, 1949. Presented, 1948 IRE National Convention, New York, N. Y., March 24, 1948.

† Federal Telecommunication Laboratories, Inc., Nutley, N. J.

[1] B. Parzen and A. Yalow, "Theory and design of the reflectometer," *Elec. Commun.*, vol. 24, pp. 94–100; March, 1947.

at any point $\alpha$ on the line between the reflection coefficient $K_\alpha$ and the normalized impedance $z$, equal to the actual impedance $Z_\alpha$ divided by the characteristic impedance of the line $Z_0$, are given by

$$z_\alpha = r_\alpha + jx_\alpha = \frac{1}{y_\alpha} = \frac{1}{g_\alpha + jb_\alpha} = \frac{1 + K_\alpha}{1 - K_\alpha}, \tag{1}$$

$$K_\alpha = |K| \epsilon^{j\delta_\alpha} = \frac{z_\alpha - 1}{z_\alpha + 1} = \frac{1 - y_\alpha}{1 + y_\alpha}. \tag{2}$$

From well-known transmission-line and directional-coupler theory, we have

$$E_1 = C_1 \underrightarrow{E_1}(1 = K_1), \tag{3a}$$

$$E_2 = C_2 \underrightarrow{E_2} K_2, \tag{3b}$$

$$E_3 = C_3 \underrightarrow{E_3},$$

where $C_1$, $C_2$, and $C_3$ are constants and $\underrightarrow{E}$ indicates the forward components of the voltage wave in the transmission line.

After making $C_1$, $C_2$, and $C_3$ equal to each other, we obtain from (2) and (3)

$$|e_1| = \left|\frac{E_1}{E_3}\right| = |1 + K_1|$$

$$= |1 + |K| \cos \delta_1 + j |K| \sin \delta_1|, \tag{4}$$

$$|e_2| = \left|\frac{E_2}{E_3}\right| = |K|. \tag{5}$$

From (1), (2), (4), and (5) result

$$\cos \delta_1 = \frac{|e_1|^2 - |e_2|^2 - 1}{2|e_2|}, \tag{6}$$

$$\frac{1}{z_\alpha} = y_\alpha = g_\alpha + jb_\alpha = \frac{1 - K_\alpha}{1 + K_\alpha}$$

$$= \frac{1 - |K|^2 - 2j|K| \sin \delta_\alpha}{1 + |K|^2 + 2|K| \cos \delta_\alpha}, \tag{7}$$

$$|e_1|^2 = |1 + K_1|^2 = \frac{4}{(1 + g_1)^2 + b_1^2}, \tag{8}$$

$$|e_2|^2 = |K|^2 = 1 - \frac{4g_1}{(1 + g_1)^2 + b_1^2}. \tag{9}$$

From (5) and (6), the magnitude $|K|$ and phase angle $\delta_1$ of the reflection coefficient at the point of the voltage probe may be calculated. We can calculate the angle $\delta_L$ at the load from the relation

$$\delta_L = \delta_1 + 2\theta_1. \tag{10}$$

If $2\theta_1$ is not known, it may be found easily as follows: (1) Short the end of the line for which load $|e_2| = 1$ and $\delta_L = 180°$, and read $e_1$, (2) calculate $\delta_1$ from (6), and (3) $2\theta_1 = 180 - \delta_1$.

Equation (6) is incomplete in that it permits the determination of only the magnitude of $\delta_1$ and not its sign since, in general, $\cos \delta = \cos(-\delta)$. An additional component is, therefore, added to obtain the sign of $\delta_1$. For convenience, the component consists of a capacitive susceptance $jb$ at the point of the voltage probe. The susceptance is normally out of the line and is inserted into the line and its effect noted after $E_1$, $E_2$, and $E_3$ have been measured. Equations (7), (8), and (9) show that $|e_1|$ increases and $|e_2|$ decreases when $\delta_1$ is positive and conversely when $\delta_1$ is negative. Thus, by noting the change in $|e_1|$ and/or $|e_2|$, the sign of $\delta_1$ is determined. Equations (8) and (9) also indicate that the effective change in $|e_1|$ is greater when the reflection coefficient is large and the change in $|e_2|$ is greater when the reflection coefficient is small. In every case, the change in either $|e_1|$ or $|e_2|$ will be sufficient to fix the sign of $\delta_1$ positively.

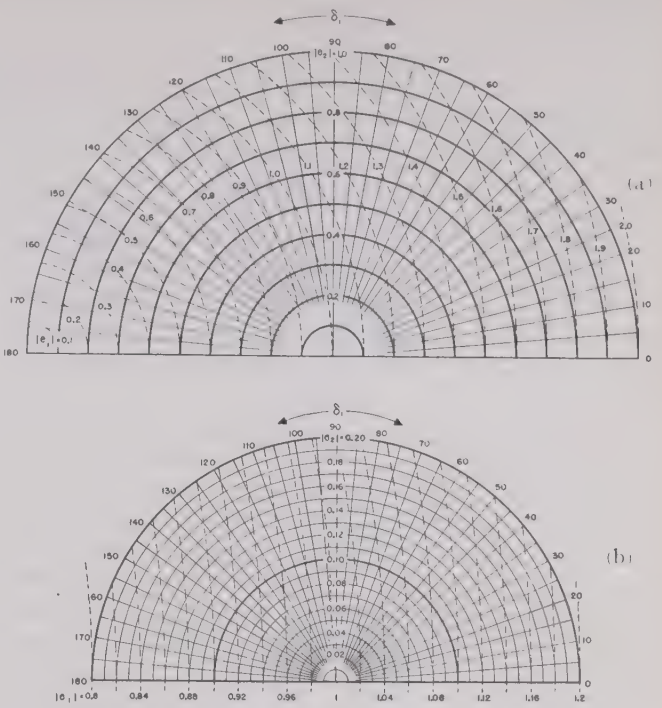


Fig. 2—Plot of $|e_1|$, $|e_2|$, and $\delta_1$, in (a) for $|e_2| = 0.2$ to 1 and in (b) for $|e_2| = 0.01$ to 0.2.

The procedure to be followed in measuring an impedance is (1) connect the unknown impedance to the equipment, (2) read $E_1$, $E_2$, and $E_3$, (3) find the sign of $\delta$, by inserting the susceptance and noting the change in readings, (4) calculate $|K|$ from (5) and $\delta_1$ from (6), (5) add $\delta_1$ to $2\theta_1$ and obtain $\delta_L$ (if $2\theta_1$ is not known, it is found as described above), (6) calculate $z$ from (7), using Smith or equivalent impedance charts.

To minimize labor in calculating $\delta_1$ from (6), that equation has been plotted in Fig. 2. It may be noted that (6) is but an expression of the cosine law for triangles.

This method is practical at *all* frequencies, since all the components (directional couplers, voltage probe, variable capacitive susceptance, and short section of transmission line) have been built at *all* radio frequen-

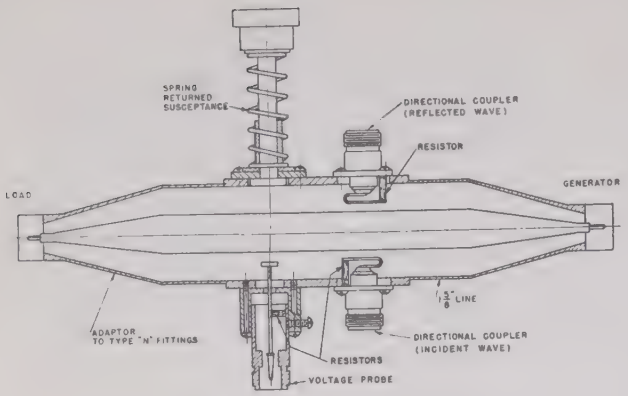


Fig. 3—Cross-sectional view of impedometer.

cies. The method is particularly useful for measurements between 50 and 500 Mc in view of the absence of other good methods for this frequency region.

## Experimental Model

A cross-sectional view of an impedometer for use from 50 to 500 Mc is shown in Fig. 3 and a photograph in Fig. 4. It consists of a short section of $1\frac{5}{8}$-inch coaxial line with adapters for type *N* fittings. In this line, are placed two wide-band directional couplers, a capacitive voltage probe, and a variable susceptance made up of a high-capacitance probe that can be inserted by a spring-returned push button. The length of the active portion is 5 inches and the total length, including the adapters, is 15 inches.

Each coupler consists of a resistor, capacitor, and loop. They differ only in the orientation of the loop with respect to the line. Their theory of operation has been fully covered in the referenced paper.

The coupler characteristics are as follows.

### *Internal Impedance*

The internal impedance is approximately 50 Ω.

### *Directivity*

The directivity is approximately 40 db. By directivity is meant the value of $|e_2|^2$ expressed in db when the line is terminated by $Z_0$. The directivity is important as it fixes the lowest value of reflection coefficient that can be measured. Thus, a directivity of 40 db corresponds to a minimum reflection coefficient of 0.01, which is equivalent to a VSWR of 1.02. For the type of couplers shown, a directivity of 35 db and better can be readily obtained.

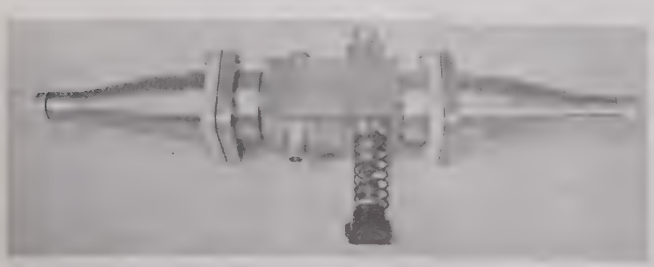

Fig. 4—Experimental model of impedometer.

### *Coupling*

The coupling is approximately −40 db at 100 Mc. The coupling decreases 6 db as the frequency decreases by an octave. By coupling is meant the ratio in db of the power obtained from the $E_3$ coupler to the power absorbed by the impedance being measured, when the impedance is equal to $Z_0$. The coupling should be as small as possible, for as it increases, so do the distortion of the field within the line and the measurement errors. It will be noted that the impedometer as presently constructed has a coupling of −25 db at 500 Mc. However, the coupling can be easily decreased by reducing both the inductive and capacitive couplings.

### *Voltage Probe*

The voltage probe consists of a small capacitance in series with a low resistance. The degree of coupling is adjusted by moving the probe in or out to vary the capacitance. When properly adjusted, the internal impedance and attenuation characteristics of the probe are identical to those of the couplers. Thus, correct probe adjustment at *any* frequency insures correct adjustment at all frequencies.

### *Transmission Line*

The transmission line has a characteristic impedance of 53 Ω. For maximum accuracy, the impedometer should be used without the adapters. The VSWR of the impedometer with both adapters is 1.05.

### *Adjustable Susceptance*

The adjustable susceptance consists of a grounded variable-capacitance probe, which can be inserted into the line by a spring-returned mechanism. On inserting the probe, both $E_1$ and $E_2$ change. As previously explained, the change in $E_2$ is greater when the VSWR is low and the change in $E_1$ is greater when the VSWR is high. In every case, the change in either $E_1$ or $E_2$ is sufficient to fix positively the sign of $\delta_1$.

On initial use of the impedometer, the following should be checked:

$E_1 = E_3$ when the load is equal to $Z_0$,
$E_2 = 0$ when the load is equal to $Z_0$,
$E_2 = E_3$ when the load is a short circuit.

When these conditions are established, we can be certain of the correct operation of the impedometer. The impedometer possesses fair accuracy when the reflection coefficient of the impedance being measured has a magnitude between 0.02 and 0.95 at any phase angle.

## Impedance Measurements

Impedance measurements made with the impedometer at 100 Mc have been found to be within 5 per cent

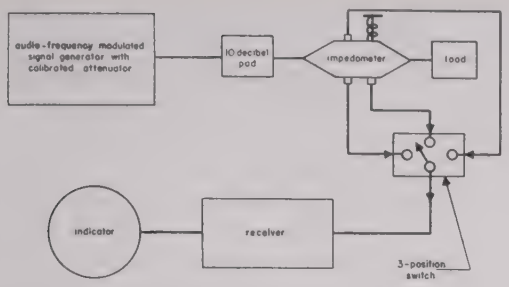


Fig. 5—Block diagram for impedance measurements.

of those obtained with a slotted line. At this frequency, the required minimum length of the slotted line is 60 inches compared with the 5-inch active length of the impedometer.

The equipment arrangement illustrated in Fig. 5 and the following procedure makes indicators having precise amplitude calibrations unnecessary.

(1) A standard-signal generator having a maximum calibrated output of 100,000 $\mu$v was used. The attenuator was accurately calibrated over a range from +40 to −10 db referred to 1,000 $\mu$v. The modulation was at 400 cps.

(2) The detector was a standard communications receiver, having sufficient selectivity so that generator harmonics are not troublesome.

(3) A 10-db resistive attenuator was inserted between the generator and the impedometer to insure constancy of $E_3$ regardless of the impedance being measured.

(4) The impedance to be measured was connected to the impedometer, and the attenuator was set to 1,000 $\mu$v. The output of the receiver was noted when it was connected to the $E_3$ probe. The values of the attenuator settings required to yield the identical receiver output when connected to the $E_1$ and $E_2$ probes determine the magnitude of $E_1$ and $E_2$.

(5) The impedance is then calculated in the manner previously described. The accuracy is thus determined almost entirely by the quality of the impedometer probes and by the calibration of the signal-generator attenuator; fairly accurate measurements are, therefore, not too difficult to achieve.

Although the impedometer has been specifically designed for the frequency band of 50 to 500 Mc, it is usable at much lower frequencies, being limited only by the attenuation of the coupler, which increases 6 db per octave decrease in frequency. Where sufficiently powerful signal generators and sufficiently sensitive receivers are available, this limitation is not serious. For example, at 3 Mc, a generator having a maximum output of 1 volt and a receiver sensitivity of 5 $\mu$v will be suitable.

To summarize, the basic principles of the impedometer are applicable at all frequencies. However, the availability of good bridges at frequencies below 50 Mc, restrict its application to the higher frequencies. It is particularly useful between 50 and 500 Mc as (1) it covers a very-wide frequency band, (2) it is a low-cost instrument, (3) except for the slotted line, no other simple instrument is available, and (4) slotted lines for this frequency region are too bulky and expensive.

# Bilinear Transformations Applied to the Tuning of the Output Network of a Transmitter*

K. S. KUNZ†, ASSOCIATE, IRE

*Summary*—**The literature on the proper tuning of the output network of a class-C power amplifier inductively coupled to a load is surprisingly meager[1-3] and, in general, there seems to exist considerable confusion concerning the relation between the following three conditions:**

**(a) Resonance of the secondary circuit**

**(b) Maximum-minimum point of average plate current**

**(c) Maximum coupled circuit efficiency.**

**This state of affairs is probably due in large part to the complexity of mathematics involved in a straightforward analysis of the circuits involved. In this paper we have employed the powerful theory of bilinear transformations in a complex plane, for which circles are transformed into circles, to determine the actual value of the secondary capacitance for a maximum-minimum of average plate current and for maximum coupled circuit efficiency.**

**The results of this investigation show that (b) and (c) differ widely from (a)—except for the case of a series load in the secondary circuit. Moreover, although (b) may differ considerably from (c), these two conditions are indistinguishable if the $Q$ of the primary coil is large, and the coefficient of coupling is very small.**

* Decimal classification: R141.2×R355.7. Original manuscript received by the Institute, November 29, 1948; revised manuscript received, March 22, 1949. The research reported in this document was made possible through support extended Cruft Laboratory, Harvard University, jointly by the Navy Department (Office of Naval Research), the Signal Corps of the U. S. Army, and the U. S. Air Force, under ONR Contract N5-ori-76, T. O. I.

† Computation Laboratory, Harvard University, Cambridge, Mass.

[1] One of the few completely reliable discussions of the factors to be considered in designing and tuning the output network of a class-C amplifier is given in "Applied Electronics," MIT Electrical Engineering Staff, Technology Press, 1943; pp. 584–592. There, however, only the simplest case of a series load neglecting distributed capacitance of the secondary is considered. Moreover, even for this case, series resonance is assumed rather than derived.

[2] "Electronic Circuits and Tubes," Cruft Laboratory Electronics Staff, McGraw-Hill Book Co., New York, N. Y., 1947; pp. 454–462.

[3] "Fundamentals of Radio," W. L. Everitt, editor, Prentice-Hall, Inc., New York, N. Y., 1942; pp. 374–379.

## Introduction

THE OUTPUT circuit of a class-C amplifier that acts as the final stage of a transmitter (see Fig. 1) is usually considered to be properly tuned if any

change in the plate circuit capacitor $C_1$ increases the plate current, and any change in the secondary circuit capacitor $C_2$ decreases it.[4] In other words, one often adjusts $C_1$ for minimum and $C_2$ for maximum plate current. It should be pointed out that in Fig. 1 the load is included in the four-terminal network $A$.

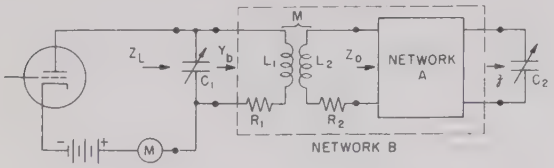


Fig. 1—Class-C amplifier inductively coupled to a load.

Parker,[5] in investigating the use of such an inductively coupled class-C amplifier for rapid determination of an unknown load impedance in the secondary circuit, noted that, contrary to what is often implied, the maximum-minimum tuning referred to above did not coincide with resonance of the secondary circuit. In fact, for a load in shunt with $C_2$, this maximum-minimum tuning was obtained when the secondary was not even in the neighborhood of resonance.

The following paper is an outcome of the author's efforts to determine theoretically the conditions for a maximum-minimum of average plate current and for maximum coupled circuit efficiency. Ordinary methods of determining maxima and minima by differentiation proved inadequate, due to the complexity of the circuits.[6] However, the theory of bilinear transformations as applied to networks turns out to be a very powerful tool for this purpose. When adapted to this problem, it makes possible the determination of the tuning of $C_1$ and $C_2$ for a maximum-minimum condition of plate current for even the most complex secondary circuit, one in which the network $A$ of Fig. 1 is any assemblage of passive linear elements,[7,8]

Since the tuning of $C_1$ that makes $Z_L$ a pure resistance also makes this impedance a maximum, it is generally agreed that, for minimum plate current, $C_1$ is tuned for resonance, i.e., $Z_L = R_L$ (pure resistance).[9] This tuning insures that the plate voltage is least when the pulse of plate current flows through the tube. It is then only the tuning of the capacitor $C_2$ for maximum plate current that leads to serious mathematical complexity, when treated by elementary methods. In fact, we shall assume that $C_1$ is at all times adjusted for resonance, and confine our attention to finding the value of $C_2$ for maximum plate current.

It is clear that, since $C_1$ is adjusted for resonance, the tube sees only the real part of the admittance $Y_b = G_b - jB_b$; hence, $C_2$ is to be adjusted for maximum value of $G_b$. If one considers the four-terminal network $B$ (see Fig. 1), the problem may be considered as follows. As $C_2$ is varied, the load impedance for network $B$ varies along a straight line, the imaginary axis of the complex plane. The input admittance $Y_b$, as $C_2$ is varied, will also describe some path in the complex plane. It remains only to find the value of load impedance for network $B$ that corresponds to the point in the locus of $Y_b$ that is farthest to the right.

That the locus of $Y_b$ is a circle results directly from the following general theorem of network theory:

*Theorem I:*

*If a variable impedance is applied to the output of a linear four-terminal network and the locus of the points in the complex plane representing the variation of this impedance is either a circle or a straight line, then the locus of the points in the complex plane representing the input impedance (or admittance) is a circle* (or in some cases a straight line).[10]

In part I we shall review briefly the subject of bilinear transformations and the basis of the general network theorem stated above, and then demonstrate how the maximum-minimum tuning can be expressed in terms of the constants of network $B$. In part II, we shall consider the three important special choices for network A given

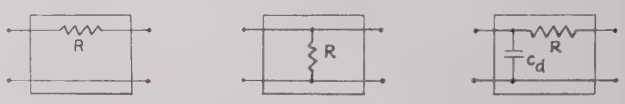


(a) (b) (c)

Fig. 2—Special choices for network $A$ of Fig. 1.

in Fig. 2. In each case $R$ is the load resistance. Thus, described in the ordinary way, the three cases considered are:

(a) Series load, neglecting distributed capacitance of the secondary
(b) Parallel or shunt load
(c) Series load as influenced by the distributed capacitance $C_d$ of the secondary.

Part III will include an alternative graphical treatment of the problem that has considerable merit as a conceptual aid in visualizing the requirement for maximum-minimum tuning. In part IV we shall determine the proper tuning of $C_2$ for maximum coupled circuit efficiency and relate this tuning to the maximum-minimum tuning.

[4] "Electronic Circuits and Tubes," Cruft Laboratory Electronics Staff, McGraw-Hill Book Co., New York, N. Y., 1947; p. 458.
[5] Sam E. Parker, now at the U. S. Navy Electronics Laboratory, San Diego, Calif.
[6] Only for a series load (see Fig. 2(a)) was this method at all applicable.
[7] Previous use has been made of this method for solving other problems. For example, A. Hazeltine, "Current loci in the general linear A-C network," *Elec. Eng.*, vol. 56, pp. 325–330, 1937.
[8] A. C. Seletzky, "Cross potential of a 4-arm network," *Elec. Eng.*, vol. 52, pp. 861–867; 1933.
[9] P. H. Osburn, "A study of class-B and -C amplifier tank circuits," PROC. I.R.E., vol. 20, p. 817; May, 1932.
[10] The statement of this theorem is simplified if one considers a straight line as a special case of a circle, namely, one with an infinite radius.

## I. Bilinear Transformations and the General Conditions for Maximum-Minimum Tuning

A complex variable $w$ is said to be a bilinear function of another complex variable $z$ if

$$w = \frac{Az + B}{Cz + D}, \tag{1}$$

where $A$, $B$, $C$, and $D$ are constants (in general complex). If $C \neq 0$, (1) can be written

$$w = \frac{az + b}{z + d}. \tag{2}$$

If the real and imaginary parts of $z$ are represented by the $x$- and $y$-co-ordinates, respectively, of a point in a plane called the $z$ plane, then the possible values of $z$ are simply the two fold infinity of points in this plane. To each such point in the $z$ plane there corresponds a value of $w$ given by (1), and hence a point in a second plane, which we will call the $w$ plane.

*Lemma 1.* Any set of points lying on a circle in the $z$-plane is transformed by a bilinear transformation into a set of points lying on a circle in the $w$ plane, it being noted, however, that a straight line is to be considered as a special case of a circle (one with infinite radius).

Since a general proof of this lemma may be found in many standard books on the functions of a complex variable,[11] we shall not give this proof. However, a special case of the lemma, the one actually needed in our calculations, will be proved in the Appendix.

*Lemma 2.* The input impedance (or admittance) of a linear four-terminal network is a bilinear function of the impedance (or admittance) closing the other end.

The proof of this lemma is very simple and may be found in various books on network theory.[12]

The combination of Lemmas 1 and 2 leads at once to the proof of Theorem I.

From the discussion in the Introduction we have deduced the following conditions for maximum-minimum tuning:

1. $C_2$ is tuned for the maximum value of $G_b$, where $Y_b = G_b - jB_b$.
2. $C_1$ is tuned to cancel the imaginary part of $Y_b$, so that the tube seen a pure conductance $G_b$; therefore, $\omega C_1 = B_b$.

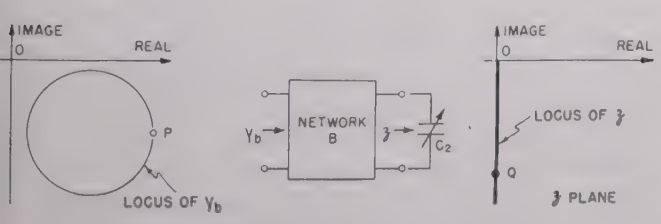


Fig. 3—Variation of $Y_b$ as $C_2$ is varied.

Also, we have shown that, as a consequence of Theorem I, the locus of $Y_b$ in the complex plane, as $C_2$ is varied, is a circle (see Fig. 3). The problem thus reduces to finding the point $P$ in the $Y_b$ plane that lies farthest to the right and the corresponding point $Q$ in the impedance plane of $C_2$ in terms of the constants of the network $B$.

Since $Y_b$ is a bilinear function of $z = -j/\omega C_2$ (see (2)),

$$Y_b = \frac{az + b}{z + d}, \tag{3}$$

where the complex constants $a$, $b$, and $d$ can be determined, once network $B$ is specified.

It is shown in the Appendix that the tuning of $C_2$ for maximum $G_b$ is given by the equation

$$\frac{1}{\omega C_2} = \frac{\text{Re}\,(Nd^*)}{\text{Im}\,(N)} \equiv \frac{\text{Real part of } Nd^*}{\text{Imaginary part of } N}, \tag{4}$$

where

$$N \equiv \sqrt{ad - b}, \tag{5}$$[13]

and $a$, $b$, and $d$ are the constants of the bilinear transformation (3). The complex conjugate of a quantity is indicated by an asterisk. The desired tuning of $C_2$ for the condition of a maximum-minimum of average plate current is therefore given by (4).

## II. Special Cases

In this part we shall determine the maximum-minimum tuning of $C_2$ for the three special cases mentioned in the Introduction. These correspond to the three choices of network $A$, of Fig. 1, given in Fig. 2.

### A. *Series Load Neglecting Distributed Capacitance of Secondary*

Network $B$ is then

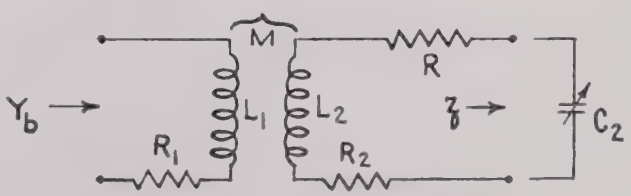


hence from the theory of coupled circuits

$$Y_b = \frac{Y_1 z + Y_1(Z_2 + R)}{z + (Z_2 + R + \omega^2 M^2 Y_1)} \tag{6}$$

where

$$\begin{aligned} Z_1 &= R_1 + j\omega L_1 = R_1(1 + jQ_1) \\ Z_2 &= R_2 + j\omega L_2 = R_2(1 + jQ_2). \end{aligned} \tag{7}$$

The constants of this bilinear transformation are (see (3) and (5))

$$\begin{aligned} d &= Z_2 + R + \omega^2 M^2 Y_1 \\ N &= \omega M Y_1. \end{aligned} \tag{8}$$

[11] T. M. MacRobert, "Functions of a Complex Variable," Macmillan Co., New York, N.Y., 1938; p. 9.

[12] See, for example, page 492 of "Electric Circuits," M.I.T. Engineering Staff, John Wiley and Sons, Inc., New York, N. Y., 1943.

[13] One may use whichever square root one chooses.

Substituting these constants into (4), one has

$$\frac{1}{\omega C_2} = \omega L_2 - \frac{1}{Q_1}\left[R + R_2 + \frac{\omega^2 M^2}{R_1}\right]. \tag{9}$$

This can be alternatively expressed as

$$\frac{1}{\omega C_2} = \omega L_2\left[1 - \frac{1}{Q_1 Q_e} - k^2\right], \tag{10}$$

where

$$Q_e \equiv \frac{\omega L_2}{R_2 + R} \tag{11}$$

$$k = \frac{M}{\sqrt{L_1 L_2}} \equiv \text{coefficient of coupling.} \tag{12}$$

Since at resonance $1/\omega C_2 = \omega L_2$, it is clear that the maximum-minimum tuning for $C_2$ given by (9) or (10) differs from resonance. Note that even when the coupling is reduced to a negligible amount, the secondary still differs from resonance by the term $-(R+R_2)/Q_1$

For actual circuits the latter term is apt to be very small, but the term depending on the coupling will usually be quite appreciable.

B. *Shunt Load*

For this case, the network $B$ is

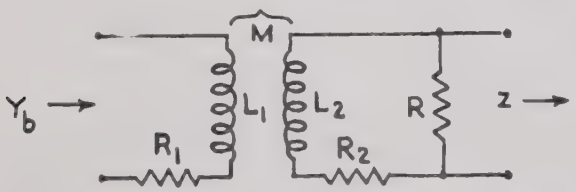


hence

$$Y_b = \frac{(Z_2 + R)z + RZ_2}{[Z_1(Z_2 + R) + \omega^2 M^2]z + (\omega^2 M^2 + Z_1 Z_2)R}. \tag{13}$$

This is a bilinear function of $z$ expressed in the form of (1). By dividing through by the coefficient $C$, it takes the form of (2). On applying (4) and simplifying, one obtains the equation,

$$\frac{1}{\omega C_2} = \omega L_2\left\{\frac{1 - \dfrac{1}{Q_1 Q_2} - k^2}{1 + \dfrac{R_2}{R}\left(1 + \dfrac{Q_2}{Q_1}\right)}\right\}. \tag{14}$$

This is the maximum-minimum tuning for $C_2$. Note that as long as the load resistance $R$ is large, compared to the resistance of the secondary coil, the tuning of $C_2$ is practically independent of the load.

The condition for resonance of the secondary circuit is decidedly different from (14). For one thing, it clearly does not depend on $R_2$, the resistance of the secondary coil, or on the coupling $k$. If we take these two factors to be zero, then (14) becomes $1/\omega C_2 = \omega L_2$, which is clearly independent of $R$. On the other hand, for resonance to occur at all, $R$ must be greater than the critical value $R = 2\omega L_2$, and for $R > 2\omega L_2$, there are two resonance tunings. If we choose the one that reduces to series resonance for $R = \infty$, then $1/\omega C_2 = \lambda \omega L_2$, where $\lambda$ varies from 1 at $R = \infty$ to 2 at the critical value of $R$.

C. *Series Load Taking into Account the Distributed Capacitance of Secondary*

Network $B$ for this case has the form

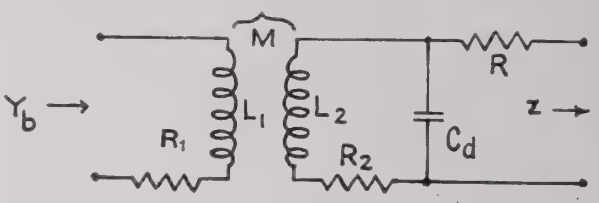


hence

$$Y_b = \frac{(Z_2 + Z_d)z + Z_2(Z_d + R) + Z_d R}{(Z_1(Z_2 + Z_d) + \omega^2 M^2)z + (Z_1 Z_2 + \omega^2 M^2)(Z_d + R) + Z_1 Z_d R},$$

where

$$Z_d = -j/\omega C_d.$$

Proceeding as in the foregoing case and making use of (4), one obtains the expression

$$\frac{1}{\omega C_2} = \omega L_2\left\{\frac{\left(1 - \dfrac{1}{Q_1 Q_e} - k^2\right) + \omega C_d R\left(\dfrac{1}{Q_1} + \dfrac{1}{Q_2}\right)}{1 - \omega C_d \omega L_2\left(1 - \dfrac{1}{Q_1 Q_2} - k^2\right)}\right\}, \tag{15}$$

where $Q_e$ is defined as in (11). As a check we observe that for $C_d = 0$, this equation reduces to that given by (10).

## III. Contours of Constant $G_b$ in the $Z_0$-Plane

An alternative treatment of the problem of maximum-minimum tuning can be had by determining how the contours of constant $G_b$ and $B_b$ appear in the $Z_0$-plane [$Z_0$ being the impedance attached to the secondary of the transformer, (Fig. 1)]. In the $Y_b$ plane, the input admittance plane, the contours of constant $G_b$ and $B_b$ are, of course, straight lines parallel to the axes. To obtain the contours of constant $G_b$ and $B_b$ in the $Z_0$ plane as given in Fig. 4, it is merely necessary to determine how the bilinear transformation expressing $Z_0$ as a function of $Y_b$ transforms these orthogonal straight lines.

Since from coupled-circuit theory (see Fig. 1),

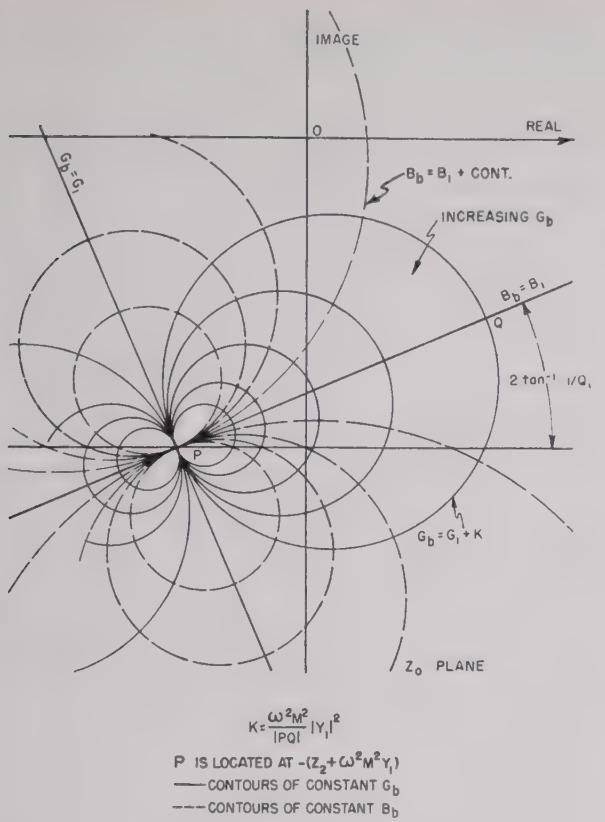


Fig. 4—Contours of constant primary conductance $G_b$ in the load impedance plane.

$$\frac{1}{Y_b} = Z_1 + \frac{\omega^2 M^2}{Z_2 + Z_0},$$

the bilinear transformation needed is

$$Z_0 = -Z_2 + \frac{\omega^2 M^2}{1/Y_b - Z_1} = \frac{(Z_1Z_2 + \omega^2M^2)Y_b - Z_2}{-Z_1Y_b + 1}. \quad (16)$$

Now the contours of constant $G_b$ and $B_b$ in the $Y_b$ plane ($Y_b = G_b - jB_b$) all pass through the point at infinity, and since this point is transformed into the point $Z_0 = -Z_2 - \omega^2M^2/Z_1$ by (16), the circles representing contours of constant $G_b$ and $B_b$ in the $Z_0$ plane must all pass through this point. Similar considerations will verify the fact that these latter contours form the system of orthogonal circles shown in Fig. 4.

As $C_2$ is tuned in Fig. 1, the impedance $Z_0$, which is the input impedance of network $A$, must by Theorem I vary along a circle or straight line. Since the maximum-minimum tuning requires that $C_2$ be adjusted for maximum value of $G_b$, it is clear that this required tuning is represented by the point of tangency of the circle or straight line representing the locus of $Z_0$ with the family of circles of constant $G_b$ shown in Fig. 4.

To illustrate the use of Fig. 4, consider the case of a series load, where

$$Z_0 = R - j\frac{1}{\omega C_2}. \quad (17)$$

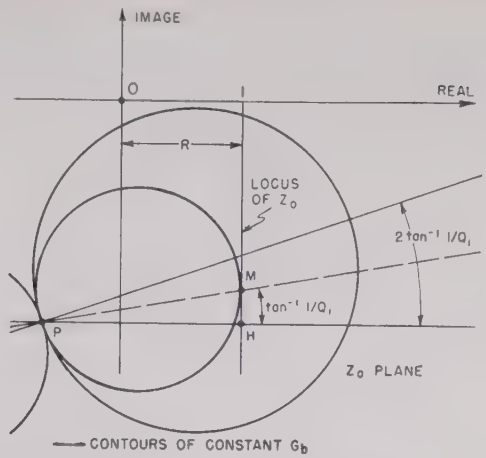


Fig. 5—Determination of the maximum-minimum tuning for a series load.

As $C_2$ is varied the locus of $Z_0$ is the vertical straight line shown in Fig. 5. Since the circles of constant $G_b$ have their centers on a line having a slope of $2\tan^{-1} 1/Q_1$, it can easily be proved geometrically that the point of tangency $M$ of the locus of $Z_0$ with these circles lies on a line passing through $P$ and making an angle of $\tan^{-1} 1/Q_1$ with the horizontal. This point $M$, being the point on the locus of $Z_0$ yielding the maximum value of $G_b$, is the value to which $Z_0$ is adjusted when $C_1$ and $C_2$ are tuned for maximum-minimum of plate current.

The imaginary part of $Z_0$ at the point $H$ is equal to the imaginary part of $Z_0$ at $P$, and hence

$$Z_0 \text{ at } H = R - j \text{ Im } (Z_2 + \omega^2M^2Y_1) = R - j(\omega L_2 - \omega^2M^2B_1).$$

Since

$$|MH| = \frac{1}{Q_1}|PH| = \frac{1}{Q_1}[R + \text{Re } (Z_2 + \omega^2M^2Y_1)]$$
$$= \frac{1}{Q_1}[R + R_2 + \omega^2M^2G_1], \quad (18)$$

we have

$$Z_0 \text{ at } M = R - j\left[\omega L_2 - \frac{R+R_2}{Q_1} - \omega^2M^2G_1\left(Q_1 + \frac{1}{Q_1}\right)\right].$$

Therefore, by the use of (17) and the fact that

$$G_1 = \frac{1}{R_1(1 + Q_1^2)},$$

we obtain the formula for the tuning of $C_2$,

$$\frac{1}{\omega C_2} = \omega L_2 - \frac{1}{Q_1}\left(R + R_2 + \frac{\omega^2M^2}{R_1}\right). \quad (19)$$

This is the same tuning as given by (9).

The reason for maximum-minimum tuning of $C_2$ given by (19) differing from resonance is here seen to be due to two factors. The *first* is due to coupling, and results in the term $-\omega^2M^2B_1$ being added to the imaginary part of $Z_0$ at $P$ (or at $H$). This is just the impedance that would be reflected into the secondary circuit if the pri-

mary circuit were short-circuited. The *second* factor is due to the resistance in the primary circuit and results in the contours of constant $G_b$ being rotated through an angle of $2 \tan^{-1} 1/Q_1$ about the point $P$. This necessitates a correction equal to $|MH|$, given by (18), in the reactance of $C_2$.

## IV. Tuning for Maximum Coupled-Circuit Efficiency

Perhaps the most important consideration in the determination of the proper tuning of the secondary capacitor $C_2$ of an inductively coupled output amplifier such as that diagrammed in Fig. 1 is that of coupled-circuit efficiency. This is defined as the fraction of the power that the tube delivers to its load impedance that reaches the secondary circuit. One should, therefore, investigate how well the maximum-minimum tuning agrees with the condition of maximum coupled-circuit efficiency.[14]

It is convenient to take account of the secondary circuit, in the following investigation, by the impedance $Z_r = \omega^2 M^2/(Z_2+Z_0)$ that is reflected into the primary circuit. Thus the equivalent circuit for Fig. 1 is that

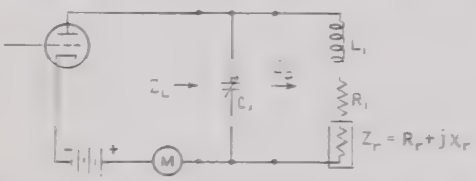


Fig. 6—Equivalent plate circuit for amplifier of Fig. 1.

given in Fig. 6. The power transferred to the secondary circuit is accounted for in this equivalent circuit by the power dissipated in $R_r$, the resistive part of reflected impedance. The coupled-circuit efficiency $\eta$ is thus seen to be

$$\eta = \frac{R_r}{R_r + R_1}.$$

Since $R_1$ is fixed, the maximum value of $\eta$ occurs when $R_r$ is a maximum or the equivalent, $R_b$ a maximum. *Thus the condition for maximum coupled-circuit efficiency is that $C_2$ be tuned for maximum value of the real part of $Z_b$, the input impedance of the transformer and hence of network B.* This is completely parallel to the condition for maximum-minimum tuning, except that $Z_b$ now replaces $Y_b$. Accordingly, we need only apply formulas (4) and (5) to the bilinear transformation connection $z = -j/\omega C_2$ to the impedance $Z_b$, namely the transformation

$$Z_b = \frac{Az + B}{Cz + D} = \frac{\alpha z + \beta}{\gamma z + \delta}. \tag{20}$$

We shall consider the same three special cases treated in Part III of this paper.

### A. *Series Load*

From (6),

$$Z_b = \frac{Z_1 z + Z_1(Z_2 + R) + \omega^2 M^2}{z + Z_2 + R} \tag{21}$$

By reference to (20),

$$\beta = Z_2 + R$$

$$N = \sqrt{ad - c} = j\omega M.$$

Therefore by (4)

$$\frac{1}{\omega C_2} = \frac{\mathrm{Re}\,(Nd^*)}{\mathrm{Im}\,(N)} = \omega L_2 \tag{22}$$

Thus (for maximum coupled-circuit efficiency) the secondary is tuned to resonance.

### B. *Shunt Load*

From (13)

$$Z_b = \frac{[Z_1(Z_2 + R) + \omega^2 M^2]z + (Z_1 Z_2 + \omega^2 M^2)R}{(Z_2 + R)z + Z_2 R}; \tag{23}$$

Therefore by (4)

$$\frac{1}{\omega C_2} = \omega L_2 \left(1 - \frac{R_2}{R + R_2}\right) \tag{24}$$

Thus when $R \ll R_2$ the tuning of $C_2$ for maximum coupled-circuit efficiency is almost independent of $R$, which is not the case for resonance of the secondary. It more nearly approximates the maximum-minimum tuning given by (14); however, the latter depends on the coupling and the $Q$ of the primary and secondary coils as well as on the ratio of $R_2$ to $R$.

### C. *Series Load Taking into Account the Distributed Capacitance of the Secondary Coil*

For this case

$$Z_b = \frac{[Z_1(Z_2 + Z_d) + \omega^2 M^2]z + (Z_1 Z_2 + \omega^2 M^2)(Z_d + R) + Z_1 Z_d R}{(Z_2 + Z_d)z + Z_2(Z_d + R) + Z_d R}. \tag{25}$$

Dividing numerator and denominator by $Z_2+Z_d$ and applying (4),

$$\frac{1}{\omega C_2} = \omega L_2 \frac{1 + \frac{1}{Q_2} C_d R}{1 - \omega^2 L_2 C_d} \tag{26}$$

[14] The maximum considered in this paper is that obtained for a fixed value of coupling. A better criterion of the proper tuning of $C_2$ would be obtained by maximizing the coupled-circuit efficiency under the condition that the load presented to the tube is constant. This can be done by letting the coupling vary.

This is the tuning of $C_2$ for maximum coupled-circuit efficiency; clearly if $C_d$ is zero, this equation reduces to (22).

Note that in all three cases the tuning for maximum coupled circuit efficiency is independent of the coupling. If in (10), (14), and (15) for maximum-minimum of average plate current one sets $k=0$ and $Q_1=\infty$, these equations reduce respectively to (22), (24), and (26), the equations giving the tuning of $C_2$ for maximum coupled circuit efficiency.

*Practical Considerations*

The design of the output network of a transmitter depends on several considerations besides that of maximum coupled circuit efficiency;[1] however, once the network is built, the primary factor in tuning the secondary capacitor is to achieve maximum efficiency of power transfer from the plate circuit to the antenna.[15] The plate circuit efficiency of the tube is not to be considered, since it depends only on the load presented to the tube, which presumably can be adjusted to its optimum value by changing the coupling and adjusting the plate capacitor for unity power factor.

One sometimes uses the dc milliammeter of the plate circuit as an indicator for the proper tuning of the output circuit. This is done by alternately tuning the plate and antenna capacitors. Proper tuning is then usually taken to be that for maximum-minimum average plate current, the plate capacitor being tuned for minimum and the antenna capacitor for maximum current.

In this paper it is shown that the above maximum-minimum tuning yields maximum coupled circuit efficiency only if the $Q$ of the plate tank circuit is large and the coupling is very small.[16] Moreover, only for a series load, neglecting distributed capacitance, does the adjustment of the antenna capacitor for resonance of the secondary circuit occur near the adjustment for maximum coupled circuit efficiency—or, for that matter, near the adjustment for maximum-minimum of average plate current.

## APPENDIX

### Derivation of Equation (4)

Equation (3) can be written

$$Y_b = a + \frac{b - ad}{z + d} = a + \frac{b - ad}{z + d + z^* + d^*}\left(1 + \frac{z^* + d^*}{z + d}\right), \tag{27}$$

where the star indicates the complex conjugate of a number. Since $z^*+z=0$,

$$Y_b = a + \frac{b - ad}{d + d^*}(1 + e^{j\theta}), \tag{28}$$

where

$$e^{j\theta} = \frac{z^* + d^*}{z + d}.$$

Variation of $z$ thus causes only a change in $\theta$ in (28); therefore the locus of $Y_b$ is a circle with center at

$$a + \frac{b - ad}{d + d^*} \tag{29}$$

and radius

$$R = \frac{|b - ad|}{d + d^*}. \tag{30}$$

The value of $Y_b$ having the greatest real part $G_b$, i.e., that corresponding to the point $P$ in Fig. 3, is as, seen from (28),

$$\overline{Y}_b = a + \frac{b - ad}{d + d^*} + \frac{|b - ad|}{d + d^*}. \tag{31}$$

Letting $\bar{z}$ be the corresponding value of $z$, i.e., that represented by the point $Q$ in Fig. 3, we have from (27) and (31) and the fact that $\bar{z}^*+\bar{z}=0$,

$$\bar{z} = \frac{d^*(b - ad) - d|b - ad|}{b - ad + |b - ad|}. \tag{32}$$

If $d$ is written as $d=d_1+jd_2$,

$$\bar{z} = d_1\frac{b - ad - |b - ad|}{b - ad + |b - ad|} - jd_2.$$

It is convenient to introduce a constant $N=N_1+N_2j$, defined as one of the square roots of $ad-b$; that is

$$-N^2 = -N_1^2 + N_2^2 - 2N_1N_2j = b - ad.$$

Our equation then simplifies to

$$\bar{z} = -j\omega C_2 = \frac{-N_1}{N_2}d_1j - d_2j = \frac{-(N_1d_1 + N_2d_2)j}{N_2}.$$

This can be written

$$\bar{z} = -j\frac{\text{Real part of } Nd^*}{\text{Imaginary part of } N} \equiv -j\frac{\text{Re}\,(Nd^*)}{\text{Im}\,(N)},$$

or, in terms of $C_2$,

$$1/\omega C_2 = \frac{\text{Re}\,(Nd^*)}{\text{Im}\,(N)}. \tag{33}$$

This is a surprisingly simple equation for maximum-minimum tuning of $C_2$, for any network in which a single capacitor $C_2$ is used to tune the secondary circuit.

[15] This efficiency of power transfer is the product of the coupled circuit efficiency and the secondary circuit efficiency. In this paper we consider only the first. Notice, however, that for a series load the secondary circuit efficiency is fixed by the design of the circuit and is independent of the tuning of $C_2$.

[16] More precisely, the requirements in the three cases studied are:
Case (a) $k^2<<1$, $Q_1Q_2>>1$
(b) $k^2<<1$, $Q_1Q_2>>1$, $Q_1>>Q_2$.
(c) $k^2<<1$, $Q_1Q_2>>1$, and for sizeable $C_d$, $Q_1>>Q_2$.

# Contributors to Waves and Electrons Section

T. M. Dickinson (A'29–VA'39) was born on September 21, 1905, at Chicago, Ill. He received the E.E. degree and commission in the Signal Corps Reserve from Cornell University in 1927. He was employed in the electrical construction section of the Revere Copper & Brass Corporation, Rome, N. Y. Division, from 1927 to 1928, and since that time he has been with General Electric Company in Schenectady, N. Y.

T. M. Dickinson

Mr. Dickinson joined the vacuum tube department on tube design and application, remaining until 1936 when he joined the General Engineering and Consulting Laboratory to work in the field of high-frequency measurements. From 1941 to 1946 he served as an officer in the Signal Corps, and upon return to the General Electric Company he was assigned to the high voltage and nucleonics division of the General Engineering and Consulting Laboratory to work on particle accelerators. At present he is project engineer for cyclotrons.

Mr. Dickinson is an associate of the American Institute of Electrical Engineers, a member of the National Society of Professional Engineers, and the author or joint author of several papers on measurements and tube design.

❖

T. W. Dietze was born on March 25, 1921, at New Orleans, La. He received the E.E. degree from Tulane University in 1942. Immediately after graduation, Mr. Dietze joined the General Electric Test Course, where he worked in motors and generators, control, transformers, turbines and other divisions at Schenectady, Lynn, Pittsfield, and Fort Wayne. During the war his major activities were in connection with the Manhattan District Project. He joined the General Engineering and Consulting Laboratory in 1944 and was assigned to the high voltage and nucleonics division, where his activities are concerned with the design and construction of particle accelerators. He is at present project engineer for betatrons.

T. W. Dietze

Mr. Dietze is an associate member of the American Institute of Electrical Engineers, a member of the National Society of Professional Engineers, and an associate of the Louisiana Engineering Society.

Jean H. Felker (A'46) was born in 1919 at Centralia, Ill. In 1941 he received the B.S. degree in electrical engineering from Washington University, in St. Louis, Mo. After graduation he was associated with the Emerson Electric Co., and later he instructed at a Naval Training School in St. Louis, Mo. In 1942 he joined the U. S. Army, and served as a radar maintenance officer attached to the Royal Artillery in Great Britain, as a member of the Electronics Training Group. Later he returned to this country as an Army publications officer.

Jean H. Felker

Since 1945, Mr. Felker has been a member of the technical staff of the Bell Telephone Laboratories, and is currently working on computer circuits.

❖

Kaiser S. Kunz (A'43) was born in New Middletown, Ind., on October 16, 1915. He received the A.B. degree in physics from Indiana University in 1936; the A.M. degree in 1937, and the Ph.D. degree in 1939 in theoretical physics from the University of Cincinnati. The next three years he served as instructor in mathematics in the engineering college of the latter University. From 1942 to 1945 he was a member of the staff of the Officer's Training School (pre-radar) at Harvard University. In 1945 he entered the research program set up at Harvard University under Division 13 of the Office of Scientific Research and Development, his field of investigation being a study of slot antennas for high-speed aircraft.

Kaiser S. Kunz

Early in 1946, Dr. Kunz received an appointment as Research Fellow in communications at the Electronics Research Laboratory of Harvard University. One of his chief researches during this period was a mathematical study of the radiation from the open end of waveguides. In 1947 he was appointed lecturer in applied mathematics at the Computation Laboratory of Harvard University. His field of interest has been the development of finite difference methods for solving problems in applied mathematics. He is a member of Phi Beta Kappa, Sigma Xi, and the American Physical Society.

Daniel Levine (S'44–A'47–M'47) was born in New York, N. Y., on July 21, 1920. He received the B.S. degree from the University of Michigan in 1941, majoring in chemistry. The following year, during which he served as laboratory assistant in electrochemistry at the same University, he received the M.S. degree. In 1948, he received the M.S. degree from Ohio State University, with a major in electronics. In 1942 he entered the Army Air Corps, and attended radio and radar schools at Sioux Falls, S. D., Harvard, and Massachusetts Institute of Technology. Following these courses he went into countermeasures work, and was engaged in Ferret activities in the Pacific Theater at the end of the war.

Daniel Levine

Upon his return to the United States in 1945, Mr. Levine was assigned to the radar laboratories at Wright Field, Ohio, and continued his project work at that laboratory following his separation from the armed forces. His research interests have included radar systems design, propagation, and television transmitter problems.

❖

Benjamin Parzen (A'47) was born in Poland on April 5, 1913. He received the B.S. degree in engineering from the College of the City of New York in 1936. From 1939 to 1943, he did postgraduate work in electrical engineering at the Polytechnic Institute of Brooklyn.

Benjamin Parzen

From 1936 to 1937, Mr. Parzen was a radio inspector for the Federal Communications Commission. He served as a civilian electrical engineer for the United States Navy from 1938 to 1944. Mr. Parzen joined Federal Telecommunication Laboratories in 1944, where he is now employed as a senior project engineer in the radio and radar components division.

Mr. Parzen is an associate member of the American Institute of Electrical Engineers, and is a licensed professional engineer of New York State.

❖

# Contributors to Waves and Electrons Section

John D. Reid, (A'41–M'44–SM'46–F'49) was born on March 18, 1907, in Morristown, N. J. He attended the University of Pennsylvania from 1923 to 1929. The period 1926–1927 was spent with the Arcturus Radio Tube Company, where he was engaged in circuit application work. He joined the Norden Hauck Radio Manufacturing Company as chief engineer in 1929. From 1930 to 1940 he was employed by the RCA Manufacturing Corporation as a radio and television development engineer.

John D. Reid

In 1940 Mr. Reid joined the Crosley organization, heading an advance development group. During the war he was in charge of Crosley's development work on the proximity fuze, for which he was awarded the Naval Ordnance Development Award, and the President's Certificate of Merit. Since the war he has been manager of research for the Crosley Division, AVCO Manufacturing Corporation. He is a member of the Engineering Society of Cincinnati, and of the Acoustical Society of America. The IRE awarded him the Fellow grade for "his developments in radio-frequency circuits." He has served on the Professional Groups, Papers Review, and Board of Editors IRE committees, and was Chairman of the Papers Procurement group in 1948–1949. Mr. Reid was also Chairman of the Cincinnati Section during 1946–1947.

❖

M. D. Rocco was born on March 16, 1910, at New Haven, Conn. He received the B.S.R.E. from Tri-State College in 1937. Mr. Rocco was employed in the consulting section of the radio division at the Naval Research Laboratory, in Washington, D. C., from 1938 to 1945.

M. D. Rocco

He transferred to the U. S. Navy Electronics Laboratory, San Diego, Calif., in 1945 and is currently engaged in radio-wave propagation studies.

❖

J. D. Ryder was born in 1907 in Columbus, Ohio. He received the B.E.E. degree in 1928 and the M.S. degree in 1929 from Ohio State University, where he was Robinson Fellow. In 1944 he was awarded the Ph.D. degree in electrical engineering by Iowa State College.

J. D. Ryder

From 1929 to 1931 he was associated with General Electric Company. He joined the Bailey Meter Company of Cleveland, Ohio, in 1931, as supervisor of the electrical and electronic section of the Research Laboratory. He holds twenty-four patents on this work, covering temperature-recording and automatic control applications of electronics. He was appointed assistant professor of electrical engineering at Iowa State College in 1941, was made professor in 1944, and in 1947 assumed his present position of assistant director of the Iowa Engineering Experiment Station. He is the author of two textbooks on electronics and networks, and of other technical papers.

Dr. Ryder is a member of the American Institute of Electrical Engineers, American Association for the Advancement of Science, Tau Beta Pi, Eta Kappa Nu, and Sigma Xi.

❖

Lynne C. Smeby (A'27–M'42–SM'43) was born in Alden, Minn., on September 1, 1903. He received the B.E.E. degree from the University of Minnesota in 1928. From then until 1939 he was successively chief engineer of WDGY, Minneapolis; WRHM, now WTCN, Minneapolis; KSTP, St. Paul; and the Michigan Radio Network including WXYZ in Detroit and WOOD in Grand Rapids. During 1939 to 1942, he was director of engineering for the National Association of Broadcasters. During the war, he was deputy director, under Dr. W. L. Everitt, of the Operational Research Staff, Office of the Chief Signal Officer, at Washington.

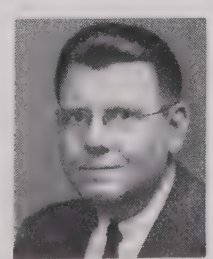

L. C. Smeby

Mr. Smeby is a member of the Board of Editors of The Institute of Radio Engineers. He was Chairman of the Detroit Section for 1939 and Chairman of the Washington Section for 1947. He was a member of the original Professional Groups Committee of the Institute. He is a member of the Board of Advisors of the Cleveland Institute of Radio Electronics and is a registered professional engineer in the State of Ohio.

Mr. Smeby was co-author of the textbook "Fundamentals of Radio" of which Dr. W. L. Everitt was editor. He has extensively participated in the proceedings of industry committees, such as the Board of War Communications, the Radio Technical Planning Board, and the National Television Systems Committee. He was the "father" of the move to formulate recording and reproducing standards and was chairman of the original committee that prepared the first 16 standards. Mr. Smeby is a charter member of the Engineer's Club of Washington, and since May, 1946, has been in private practice as a consulting radio engineer in Washington.

❖

J. B. Smyth was born in Pembroke, Ga., on June 8, 1914. He received the B.S. degree in 1934 and the M.S. degree in 1937 from the University of Georgia, and the Ph.D. degree in 1942 from Brown University. From 1937 to 1938, he was on the technical staff of the Tennessee Eastman Corporation.

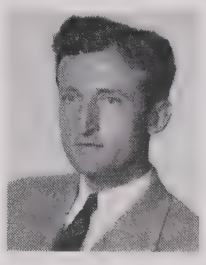

J. B. Smyth

Since 1942, he has been engaged in electromagnetic-wave propagation studies at the U. S. Navy Electronics Laboratory, in San Diego, Calif.

❖

Marshall P. Wilder (A'28) was born in New York, N. Y., on September 8, 1906. He attended the Massachusetts Institute of Technology. He also attended the Berlin Technische Hochschule and the Stevens Institute of Technology for graduate work in 1937 and 1939, respectively. In 1936 Mr. Wilder was associated with the Kenrad Radio and Tube Corporation in Owensboro, Ky., leaving in 1937 to join the National Union Radio Tube Company in Newark, N. J., where he was a cathode-ray tube engineer. During the period 1939 to 1941 he was affiliated with the National Broadcasting Company in New York City, in the television development group. The following eight years were spent as chief engineer in the vacuum-tube section of Remington Rand, in South Norwalk, Conn. Mr. Wilder is still with this company, as chief engineer and manager of the picture tube division.

M. P. Wilder

# Abstracts and References

Prepared by the National Physical Laboratory, Teddington, England, Published by Arrangement with the Department of Scientific and Industrial Research, England, and *Wireless Engineer*, London, England

NOTE: The Institute of Radio Engineers does not have available copies of the publications mentioned in these pages, nor does it have reprints of the articles abstracted. Correspondence regarding these articles and requests for their procurement should be addressed to the individual publications and not to the IRE.

Acoustics and Audio Frequencies..... 1220
Antennas and Transmission Lines..... 1220
Circuits and Circuit Elements..... 1221
General Physics ..... 1224
Geophysical and Extraterrestrial Phenomena..... 1225
Location and Aids to Navigation..... 1225
Materials and Subsidiary Techniques. 1225
Mathematics..... 1226
Measurements and Test Gear..... 1226
Other Applications of Radio and Electronics..... 1228
Propagation of Waves..... 1229
Reception..... 1229
Stations and Communication Systems. 1230
Subsidiary Apparatus..... 1231
Television and Phototelegraphy..... 1231
Transmission..... 1231
Vacuum Tubes and Thermionics..... 1231
Miscellaneous..... 1232

The number in heavy type at the upper left of each Abstract is its Universal Decimal Classification number and is not to be confused with the Decimal Classification used by the United States National Bureau of Standards. The number in heavy type at the top right is the serial number of the Abstract. DC numbers marked with a dagger (†) must be regarded as provisional.

**The Institute of Radio Engineers has made arrangements to have these Abstracts and References reprinted on suitable paper, on one side of the sheet only. This makes it possible for subscribers to this special service to cut and mount the individual Abstracts for cataloging or otherwise to file and refer to them. Subscriptions to this special edition will be accepted only from members of the IRE and subscribers to the PROC. I.R.E. at $15.00 per year. The Annual Index to these Abstracts and References, covering those published from January through December 1948, may be obtained for 2s. 8d. postage included from the *Wireless Engineer*, Dorset House, Stamford St., London S. E., England.**

## ACOUSTICS AND AUDIO FREQUENCIES

534.21 2415
**On the Calculation of the Sound Field of Circular Membranes in a Rigid Wall**—H. Stenzel. (*Ann. Phys.* (Lpz.), vol. 4, pp. 303–324; March 1, 1949.) Three developments in series are obtained, each with particular advantages for a certain portion of the field. A method is used involving characteristic functions which can be calculated by means of differential operators and which can be applied to radiation fields in general, including both acoustic and electromagnetic fields. Practical examples are given.

534.232:621.316.727:621.396.677 2416
**Applications of Phase Devices**—Thiede. (*See* 2454.)

534.26 2417
**The Diffraction of Two-Dimensional Sound Pulses incident on an Infinite Uniform Slit in a Perfectly Reflecting Screen**—E. N. Fox. (*Phil. Trans.*, vol. 242, pp. 1–32; May 25, 1949.)

534.61 2418
**Application of Miniature-Circuit Techniques to the Sound Level Meter**—H. H. Scott, H. Chrystie, and E. G. Dyett, Jr. (*Proc. N.E.C.* (Chicago), vol. 4, pp. 33–45; 1948.) Engineering and production problems are considered for a meter small enough for a coat pocket, but meeting all American Standards Association requirements.

534.833 2419
**Absorption by Sound-Absorbent Spheres**—R. K. Cook and P. Chrzanowski. (*Jour. Res. Nat. Bur. Stand.*, vol. 42, pp. 219–223; March, 1949.) See 2123 of September.

534.862.4:621.383 2420
**A New Reproducing Device for Scanning Optical Sound-Tracks**—J. Fassbender. (*Funk und Ton*, vol. 3, pp. 261–264; May, 1949.) Description of apparatus using a special photo cell consisting of a single crystal of CdS, of dimensions about $10\times1\times0.1$ mm. The conductivity spectrum of this cell extends from about 5,100 Å into the short-wave ultraviolet and its general properties make it particularly suitable for this application.

621.395.625.2:621.392.52 2421
**Crossover Filter for Disc Recording Heads**—Roys. (*See* 2470.)

621.395.625.3 2422
**Magnetic Recording Tapes**—M. Camras. (*Trans. AIEE*, vol. 67, part 1, pp. 503–506; 1948.) Magnetic properties, frequency response, signal-to-noise ratio, output level, sensitivity, and ease of erasure are considered for various tapes. A new coated material, Type 140-A, developed by the Armour Research Foundation, is found specially suitable for high-quality recording.

621.395.625.3:621.395.813 2423
**An Evaluation of the Application of New and Old Techniques to the Improvement of Magnetic Recording Systems**—L. C. Holmes. (*Proc. N.E.C.* (Chicago), vol. 4, p. 46; 1948.) Summary only. Discussion of various factors contributing to high quality in such systems, and of data showing the performance characteristics obtainable under the most favorable operating conditions.

621.396.8:621.396.44 2424
**Channels of Equal Acoustic Quality with Different Frequency-Response Characteristics and Different Bandwidths**—P. V. Anan'ev. (*Radiotekhnika* (Moscow), vol. 4, no. 1, pp. 16–26; January and February, 1949. In Russian.) The necessary bandwidth and the permissible deviations in the frequency characteristic for a wire broadcasting system are discussed. Experimental curves and results are given.

## ANTENNAS AND TRANSMISSION LINES

621.392.26† 2425
**Closed- and Open-Ridge Waveguide**—T. G. Mihran. (PROC. I.R.E., vol. 37, pp. 640–644; June, 1949.) Expressions are derived for the voltage-current and voltage-power impedance, allowing for the discontinuity capacitance. Simplifying approximations and the conditions of their validity are discussed. A preliminary result can be obtained by using Cohn's curves (23 of 1948).

621.392.26† 2426
**Channel Section Waveguide Radiator**—A. L. Cullen. (*Phil. Mag.*, vol. 40, pp. 417–428; April, 1949.) The transmission characteristics are studied theoretically and the phase constant and attenuation coefficient are calculated. Simple approximate formulas are deduced; the validity of these has been verified by experiment. The use of the device as a radiator is limited because the attenuation rate is too great for narrow beams to be obtainable, and the angle between the emergent beam and the normal to the array is rather large.

621.392.26† 2427
**A Set of Second-Order Differential Equations Associated with Reflections in Rectangular Wave Guides—Application to Guide Connected to Horn**—S. O. Rice. (*Bell Sys. Tech. Jour.*, vol. 28, pp. 136–156; January, 1949.) When a bent waveguide is conformally transformed into a straight guide filled with nonuniform medium, propagation may either be studied by an integral equation method (2428 below) or by a more general method based upon a certain set of ordinary differential equations. The latter method is here developed and applied to determine the reflection produced at the junction of a straight guide and a sectoral horn; this problem cannot be solved by the integral equation method. The *WKB* approximation, discussed for a single second-order differential equation by Schelkunoff (1570 of 1946), is extended to a set of equations and approximate expressions for the reflection coefficient are derived.

621.392.26†:517.54 2428
**Reflection from Corners in Rectangular Wave Guides—Conformal Transformation**—S. O. Rice. (*Bell Sys. Tech. Jour.*, vol. 28, pp. 104–135; January, 1949.) Approximate expressions are obtained for the reflection coefficients for sharp corners by using a conformal transformation which replaces the bent guide by a straight guide filled with a nonuniform medium. The reflection coefficient for the transformed system can be expressed in terms of the solution of an integral equation, which may be solved approximately by successive substitutions. An explicit expression for the reflection coefficient can be obtained when the corner angle is small and the corner is not truncated. The method can be applied to other types of irregularities in rectangular waveguides. See also 2427 above.

621.392.26†:621.3.09 2429
**The Effect of Openings in the Walls of Metal Waveguides on the Wave Propagation—**

G. Klages. (*Arch. Elek.* (Übertragung), vol. 3, pp. 85–92; March, 1949.) Theory of propagation in a lossless line in series with an attenuating line is applied to discussion of the effect of openings of various sizes. By analogy with the theory of reflection from optically absorbing plates, the theory of an attenuating line is extended by the introduction of capacitance and inductance variations. Small openings in waveguide walls have no effect either on the propagation or on the attenuation, but with wide slits, the wavelength inside the guide is increased and energy is radiated from the slits. The results of measurements with slits of different widths in different positions in both closed- and open-ended rectangular waveguides are shown graphically and discussed. The effects of parasitic waves are also considered.

621.392.26†:621.3.09 2430

**Propagation of $TE_{01}$ Waves in Curved Wave Guides**—W. J. Albersheim. (*Bell Sys. Tech. Jour.*, vol. 28, pp. 1–32; January, 1949.) "$TE_{01}$ waves transmitted through curved wave guides lose power by conversion to other modes, especially to $TM_{11}$.

"This power transfer to coupled modes is explained by the theory of coupled transmission lines. It is shown that the power interchange between coupled lines and their propagation constants can be derived from a single coupling discriminant.

"Earlier calculations of $TE_{01}$ conversion loss in circular wave guide bends are confirmed and extended to *S*-shaped bends.

"Tolerance limits for random deflections from an average straight course are given."

621.392.26†:621.3.09 2431

**A Waveguide with Phase Velocity $v<c$ for the $E_{10}$ Wave**—E. Kettel. (*Frequenz*, vol. 3, pp. 73–75; March, 1949.) Propagation theory for a cylindrical waveguide with equally spaced annular partitions. A formula for the phase velocity is derived.

621.392.26†:621.396.67 2432

**Open-Ended Waveguide Radiators**—R. E. Beam, M. M. Astrahan, and H. F. Mathis. (*Proc. N.E.C.* (Chicago), vol. 4, pp. 472–486; 1948.) Attempts were made to broaden the radiation pattern of open-ended $\frac{1}{2}\times 1$ inch waveguide, operating at 9,375 Mc, by changing the shape of the opening. A 90° pointed end gave the widest pattern, but also gave a large amount of backward radiation. The effect of reflecting disks at various distances from the open end, and of polystyrene slugs and prisms within the end of the waveguide, was also investigated.

621.392.26†:621.396.671 2433

**Some Properties of Radiation from Rectangular Waveguides**—J. T. Bolljahn. (Proc. I.R.E., vol. 37, pp. 617–621; June, 1949.) Exact relationships between the radiation pattern and impedance characteristics are developed for a waveguide with walls of infinitesimal thickness. The ratio of the radiation intensities in certain preferred directions to the power gain in those directions is simply related to the coefficient of reflection inside the waveguide.

621.392.3 2434

**Directional Couplers**—W. W. Mumford. (Proc. I.R.E., vol. 37, p. 625; June, 1949.) Correction to 2007 of 1947.

621.396.67 2435

**A High-Gain Cloverleaf Antenna**—P. H. Smith. (*Proc. N.E.C.* (Chicago), vol. 4, pp. 497–504; 1948.) Design is discussed. Laboratory tests on a 1/10-scale model show that power gains of the order 10 to 12 can be obtained. The antenna is suitable for omnidirectional radiation of horizontally polarized waves, as required for FM broadcasting.

621.396.67 2436

**Microwave Antennas and Dielectric Surfaces**—R. M. Redheffer. (*Jour. Appl. Phys.*, vol. 20, pp. 397–411; April, 1949.) Discussion of the effect of placing a dielectric sheet in front of an antenna for the following cases: (a) receiving antenna and plane sheet, (b) transmitting antenna and plane sheet, (c) transmitting antenna and cylindrical shell. In case (a), results are explained in terms of an equivalent antenna reflection; phase, arbitrary incidence, and elliptical polarization are considered. In case (b) there is inverse-instance attenuation for a distant sheet; the effect of initial antenna mismatch is investigated. In case (c), reflection varies with angle according to the secondary power pattern. Formulas are given for the reflection from a circular cylinder, a narrow strip, a corrugated surface, or a series of strips, used with a paraboloid antenna. Applications to radomes and to the design of pressurizing seals are discussed. All results are verified experimentally.

621.396.67 2437

**New Principle for Broad Band Antennas**—M. W. Scheldorf and J. F. Bridges. (*Tele-Tech.*, vol. 8, pp. 43–44; June, 1949.) Discussion of the characteristics of antennas consisting of several similar elements, which may be of different lengths, arranged in the form of a fan and fed from a common source. A bandwidth of over 10 per cent was obtained with a symmetrical arrangement of 6 elements, the 3 pairs being of different lengths.

621.396.671 2438

**Radiation Resistance of Loaded Antennas**—R. C. Raymond and W. Webb. (*Jour. Appl. Phys.*, vol. 20, pp. 328–330; April, 1949.) Short cylindrical antennas were loaded by cylindrical or conical dielectric sheaths or by metal end-disks so as to resonate at frequencies below the normal values. Measured resonance resistances are compared with values calculated by the Poynting vector method for assumed uniform or sinusoidal current distribution. For a given current distribution at resonance, the antenna radiation resistance depends only on the antenna length. Particular loading methods alter the current distribution. Those which give more nearly uniform current distributions yield higher radiation resistances. See also 2439 below.

621.396.671 2439

**Current Distributions on some Simple Antennas**—W. Webb and R. C. Raymond. (*Jour. Appl. Phys.*, vol. 20, pp. 330–333; April, 1949.) A method of measurement is described and measured distributions are compared with some frequently assumed curves. Some distributions were integrated numerically to determine the driving-point impedances. Deviations from curves usually assumed are significant, but do not bring about large errors in the calculated impedances. See also 2438 above.

621.396.671 2440

**Measured Impedance of Vertical Antennas over Finite Ground Planes**—A. S. Meier and W. P. Summers. (Proc. I.R.E., vol. 37, pp. 609–616; June, 1949.) For a ground plane of dimensions small compared with $\lambda$, the impedance is a damped oscillating function of $\lambda$ and the ground-plane dimensions. Impedance variations of $-5$ to $-20$ per cent were found with a circular ground plane; the corresponding variations for a square ground plane were about half as great, except when the ground plane was small. Impedance is relatively independent of antenna thickness.

At microwave frequencies, measurements were made by a modified Chipman method (1618 of 1939) the merits of which are compared with those of the conventional slotted-line standing-wave method.

621.396.674:621.317.34 2441

**Measurements on Frame Aerials**—E. Roeschen. (*Funk und Ton*, vol. 3, pp. 271–277; May, 1949.) The dependence of the effective height of a frame antenna on the number of turns of the winding and on the frequency is discussed. Measurements on tuned antennas, with and without screens, are tabulated. Screening increases the damping by about 15 per cent.

621.396.677 2442

**Directional Characteristics and Radiated Power of Directive Aerials**—(*Frequenz*, vol. 3, pp. 152–153; May, 1949.) Long summary of paper abstracted in 1861 of 1948 (Saxton).

621.396.677:534.232:621.316.727 2443

**Applications of Phase Devices**—Thiede. (*See* 2454.)

## CIRCUITS AND CIRCUIT ELEMENTS

538.1:621.392.26†:621.396.611.4 2444

**Narrow Gaps in Microwave Problems**—W. R. Smythe. (*Rev. Mod. Phys.*, vol. 20, p. 472; July, 1948.) Correction to 2149 of September.

621.3(083.74) 2445

**Standardization in the Armed Forces**—L. J. Tatom and H. E. Bernstein. (*Tele-Tech*, vol. 8, pp. 22–23, 57; June, 1949.) An account of the work of ASESA (Armed Services Electro Standards Agency), with examples of economies effected, such as the replacement of 350 different crystal holders by 3 standard types, the reduction of 10,000 different sizes and shapes of transformer cases to 22 standard types, etc. In collaboration with the Radio Manufacturers Association, ASESA is responsible for the preparation of "Jan" (Joint Army-Air-Navy) specifications for standard components.

621.314.25 2446

**A Cross-Coupled Input and Phase Inverter Circuit**—J. N. Van Scoyoc. (*Radio and Telev. News, Radio-Electronic Eng. Supplement*, vol. 11, pp. 6–9; November, 1948.) The basic circuit is discussed. Advantages include low input capacitance, low sensitivity to hum and to anode supply-voltage variations, and a large dynamic range of input signals. Application to a balanced amplifier for a cro, a dc tube voltmeter, af amplifiers and tone control are considered.

621.314.3† 2447

**An Analysis of Interlinked Electric and Magnetic Networks with Application to Magnetic Amplifiers**—D. W. ver Planck, M. Fishman, and D. C. Beaumariage. (*Proc. N.E.C.* (Chicago), vol. 4, p. 426; 1948.) Summary only. A general system of nonlinear equations is developed and applied to determine the steady-state behavior of 6 types of magnetic amplifier without feedback. The relationship between current and time is determined for given applied voltages and circuit and core parameters. Results are confirmed experimentally. Amplifiers using two separate magnetic cores have important advantages over those using a single three-legged core. See also 2448 below.

621.314.3† 2448

**An Analysis of Magnetic Amplifiers with Feedback**—D. W. ver Planck, M. Fishman, and D. C. Beaumariage. (*Proc. N.E.C.* (Chicago), vol. 4, p. 436; 1948.) Summary only. Two methods of obtaining feedback are discussed, namely (a) external feedback, for which a bridge rectifier and separate coils for the feedback current are used, and (b) self feedback, for which two rectifier elements are arranged so that separate feedback windings are not required. The general system of equations discussed in 2447 above is applied; wave shapes and the magnitudes of the currents

resulting from given applied voltages are obtained, and results are confirmed experimentally. The two methods of obtaining feedback have certain very similar characteristics.

621.314.3† 2449
**Effect of Core Materials on Magnetic Amplifier Design**—A. O. Black, Jr. (*Proc. N.E.C.* (Chicago), vol. 4, pp. 427–435; 1948.)

621.314.3† 2450
**The Transductor**—H. B. Rex. (*Instruments*, vol. 20, pp. 1102–1109; December, 1947.) Discussion of (a) the transductor without self-excitation, (b) the self-excited transductor under various conditions of feedback and (c) the transductor with constrained magnetization. The article is based on papers by T. Buchhold in *Arch. Elektrotech.*, 1942 to 1944, noted in 3547 of 1942, 363 of 1943, and 55 of 1944. See also 2451 below.

621.314.3†:016 2451
**Bibliography on Transductors, Magnetic Amplifiers, etc.**—H. B. Rex. (*Instruments*, vol. 21, pp. 332, 362; April, 1948.) A list of 213 references, with brief notes indicating the scope of many of the papers.

621.314.63 2452
**A Practical Approach to Calculating Optimum Performance of Semiconductor Rectifiers**—E. D. Wilson. (*Trans. AIEE*, vol. 67, part 1, pp. 640–642; 1948. Discussion, p. 642.) By applying Kirchhoff's laws to a conventional 4-arm rectifier bridge, an expression is derived for efficiency in terms of the reverse $R$, forward $F$, and load $L$ resistances. Maximum efficiency is obtained when $L^2 = R \cdot F$; the forward and reverse losses are then equal. Efficiency versus temperature curves are given for various current densities.

621.316.722.4 2453
**Controlled Voltage Divider**—S. Freedman. (*Radio and Telev. News, Radio-Electronic Eng. Supplement*, vol. 11, pp. 7–9, 29; October, 1948.) The basic circuit is discussed for a device whose output depends only upon the ratio of two separate voltages applied to the input, and not on the actual values of these voltages. The principle is applied in an AM-FM detector in which the undesired AM signal is eliminated during FM reception, and vice versa.

621.316.727:621.396.677:534.232 2454
**Applications of Phase Devices**—H. Thiede (*Funk und Ton*, vol. 3, pp. 249–255; May, 1949.) Arrangements are described for obtaining directional acoustic or radio beams from a number of radiators spaced uniformly in a straight line. The phases of the voltages applied to consecutive transmitters differ by an amount $\delta$ which determines the direction of the beam relative to the line of radiators. Circuits including $n$ crossed-coil variometers, each connected to two of the $2n$ radiators, permit cyclical variation of the phase difference $\delta$ so that the beam can be swept through a prescribed angle without varying the position of the radiators. Typical directional characteristics obtained with 8 radiators in line are illustrated. Similar devices can be used for reception. See also 1873 and 2738 of 1948.

621.317.71 2455
**An Automatic Current Integrator**—M. J. Poole. (*Jour. Sci. Instr.*, vol. 26, pp. 113–114; April, 1949.) Circuit diagram and description of an instrument for measuring mean currents ranging from $2\times10^{-9}$ *A* to $10^{-6}$ *A*. Arrangements are included to enable counting apparatus recording nuclear disintegrations to be switched on or off at exact charge intervals.

621.318.572:512.99 2456
**The Synthesis of Two-Terminal Switching Circuits**—C. E. Shannon. (*Bell Sys. Tech. Jour.*, vol. 28, pp. 59–98; January, 1949.) A general discussion of the design of a 2-terminal network with given operating characteristics. Boolean algebra is explained and used.

621.318.572:539.16.08 2457
**An Improved Quench Circuit for Geiger Counters**—E. H. Cooke-Yarborough, C. D. Florida, and C. N. Davey. (*Jour. Sci. Instr.*, vol. 26, pp. 124–125; April, 1949.)

621.319:679.5 2458
**The Electret**—F. Gutmann. (*Rev. Mod. Phys.*, vol. 20, pp. 457–470; July, 1948. Bibliography, pp. 471–472.) A comprehensive discussion of properties, methods of production, and various theories.

621.385.832:535.767 2459
**Cathode-Ray Presentation of Three-Dimensional Data**—O. H. Schmitt. (*Jour. Appl. Phys.*, vol. 18, pp. 819–829; September, 1947.) IRE 1947 Convention paper. By means of simple transformations easily performed electrically, isometric projections or true perspective views can be obtained. The observer's viewpoint can be changed at will by turning range, elevation, and azimuth controls. A similar but more elaborate arrangement permits the presentation of separate pictures which are stereoscopically correct. See also 2984 of 1948 (Iams, Burtner, and Chandler).

621.392 2460
**Use of a Mechanical Harmonic Synthesizer in Electrical Network Analysis**—S. L. Brown and C. M. McKinney. (*Jour. Appl. Phys.*, vol. 20, pp. 316–318; April, 1949.)

621.392 2461
**The Synthesis of Electric Networks According to Prescribed Transient Conditions**—M. Nadler. (Proc. I.R.E., vol. 37, pp. 627–630; June, 1949.) A network function yielding a prescribed transient response may be determined by means of Laplace transforms. The procedure is based directly on the prescribed function of time, without consideration of amplitude or delay as a function of frequency. An example is given in which the Poisson-Stieltjes integral is used for the physical realization of a network function involving a transcendental term. The limitations of existing mathematical technique are briefly discussed.

621.392 2462
**Synthesis of *RC*-Networks**—E. A. Guillemin. (*Jour. Math. Phys.*, vol. 28, pp. 22–42; April, 1949.) The nature of the transfer characteristic of such networks is considered, and a method whereby any given transfer characteristic may be approached closely by means of a physically realizable passive *RC* network is discussed in detail. The synthesis procedure is illustrated by examples.

The physical realization of the required network is always possible in an unbalanced form suitable for operation between conventional tubes. High-quality network performance does not necessarily require high-quality coils, provided that one can compensate for constant loss.

621.392 2463
**Active Networks and the General Locus Criterion for Stability**—F. Strecker. (*Frequenz*, vol. 3, pp. 78–84; March, 1949.)

621.392.4 2464
**Graphical Method of Computation for Two-Terminal Networks with Nonlinear Resistances**—G. I. Nikonov. (*Avtomatika i Telemekhanika*, vol. 10, pp. 149–156; March and April, 1949. In Russian.)

621.392.41:518.43 2465
**Method of Integration by Successive Points (Step-by-Step Method) Applied to Electrical Circuits**—G. Gillon. (*Rev. Gén. Élec.*, vol. 58, pp. 192–198; May, 1949.) A method allowing simple calculation of transients in circuits comprising resistance, inductance, and capacitance. The approximation is good enough for plotting current and voltage curves and can be applied to circuits whose elements are variable or to complex circuits of the multiple-reactance type which lead to characteristic equations of high order.

621.392.43 2466
**Broad-Band Dissipative Matching Structures for Microwaves**—H. J. Carlin. (Proc. I.R.E., vol. 37, pp. 644–650; June, 1949.) Microwave network functions are studied by means of interpolation in the complex plane. A rational function can thus be found which approximates to a given network function over a specified bandwidth. A lumped-circuit approximation for a microwave structure can be deduced and used for the synthesis of matching networks. Where dissipative devices are involved, the poles of the rational approximating function may satisfy special conditions, in which case the ideal lumped matching network can be realized and transformed into a suitable microwave structure. Applications of this method and experimental results are given for the synthesis of a new type of broad-band coaxial "chimney" attenuator.

621.392.5 2467
**Foundations of the General Theory of the Linear Quadripole**—E. V. Zelyakh. (*Avtomatika i Telemekhanika*, vol. 10, pp. 135–148; March and April, 1949. In Russian.)

621.392.52:537.228.1 2468
**Crystal Filters Using Ethylene Diamine Tartrate in Place of Quartz**—E. S. Willis. (*Trans. AIEE*, vol. 67, part 1, pp. 552–556; 1948.) Performance is comparable to that of quartz filters. See also 2215 of 1948, for which the above Universal Decimal Classification is preferable, and 2529 below.

621.392.52:621.392.26† 2469
**Analysis of a Wide-Band Waveguide Filter**—S. B. Cohn. (Proc. I.R.E., vol. 37, pp. 651–656; June, 1949.) A rectangular waveguide structure consisting of a series of constrictions and cavities is shown to have the properties of a wide-band filter. The lower cutoff frequency of the lowest-frequency pass band is due to the cutoff property of the waveguide itself. The upper cutoff frequency of this band is due to the discontinuities. Exact equations for the image parameters are derived, assuming no dissipation in the filter sections; full allowance is made for the discontinuities and their interaction. Formulas are incidentally obtained for the equivalent circuits of cavities formed (a) by two changes in height, (b) by an increase in height followed by a short-circuiting wall, and for the hypothetical case of a cavity in which an increase in height is followed by an open-circuiting wall. The analysis for (b) can be used to obtain an improved solution for a ridged waveguide.

621.392.52:621.395.625.2 2470
**Crossover Filter for Disc Recording Heads**—H. E. Roys. (*Audio Eng.*, vol. 33, pp. 18–21; June, 1949.) Description of a practical device designed to compensate for variations in cutter characteristics, both at the transition frequency and at the high-frequency end of the spectrum.

621.392.52:621.396.65 2471
**Filters for a 150-Kc Carrier System**—R. C Taylor. (*Trans. AIEE*, vol. 67, part 1, pp. 583–588; 1948.) Description of the filters used in the system discussed in 2637 below.

621.396.611.1 2472
**Conditions for the Reproducibility of Properties and Parameters of Oscillatory Systems**—M. Päsler. (*Frequenz*, vol. 3, pp. 76–78; March, 1949.)

621.396.611.1:621.317.6:621.396.645 2473

**The Response of a Tuned Amplifier to a Signal Varying Linearly in Frequency**—W. H. Hamilton. (*Proc. N.E.C.* (Chicago), vol. 4, pp. 377–396; 1948.) A mathematical analysis using the solution obtained from a differential analyzer for the integral

$$U(2m,n)=\frac{2}{\pi}\int_0^n e^{2my}\cos y^2\,dy$$

and a similar integral involving sin $y^2$. A response versus time curve is obtained for various values of the parameter $\gamma = t\times$bandwidth, $t$ being the interval during which the frequency of the input signal is within the half-power bandwidth of the tuned circuit. A curve of signal-to-noise ratio as a function of $\gamma$ is included. Results for a 456-kc amplifier are shown graphically. See also 670 of March (Barber and Ursell) and 671 of March (Hok).

621.396.611.21 2474

**The Theory of a Self-Oscillator with a Quartz Crystal**—S. I. Evtyanov. (*Radiotekhnika* (Moscow), vol. 4, pp. 27–40; January and February, 1949. In Russian.) The quartz crystal is connected between the grid and filament. A vector method is used in the analysis. The condition for self-excitation is established and formulas are derived for determining the amplitude of steady-state oscillations and the frequency change corresponding to a change in the tuning of the anode circuit. The stability of steady-state operation is examined; when the tuning of the anode circuit is altered a hysteresis effect takes place in the oscillatory process.

621.396.611.3:621.396.619.13 2475

**The Application of Coupled Systems with Distributed Constants to Frequency Modulation in the Ultra-High-Frequency Range**—V. A. Tolstikov. (*Radiotekhnika* (Moscow), vol. 4, pp. 69–74; March and April, 1949. In Russian.) Modern FM methods for meter waves require manifold frequency multiplication even for sound broadcasting and it is doubtful whether these methods can be used at higher frequencies. Experiments were, therefore, conducted to show the effect of a secondary system with distributed constants on the frequency and amplitude of oscillations in a self-exciting system with distributed constants (Fig. 1). These experiments are discussed. It is possible, in principle, to obtain direct modulation of the carrier of sufficient depth without using frequency multiplication.

621.396.611.4:621.392.26† 2476

**Tunable Waveguide Cavity Resonator for Broadband Operation of Reflex Klystrons**—W. W. Harman. (*Proc. N.E.C.* (Chicago), vol. 4, pp. 233–252; 1948.) A study of the design of broad-band resonators (2 to 1 tuning range) for use with reflex klystrons of the external-cavity type. Two groups are considered: (a) $\lambda/4$ or fundamental-mode resonators, whose high-frequency limit is set by the physical size of the tube envelope, (b) $3\lambda/4$ resonators, which allow operation up to the electronic limit of the tube.

621.396.611.4.029.64/.65† 2477

**Modified Cavity Oscillator for the Generation of Microwaves**—G. G. Bruck. (*Jour. Appl. Phys.*, vol. 18, pp. 843–844; September, 1947.) The cavity consists of two coaxial cylinders and two end-plates. The inner cylinder has $n$ longitudinal slots. Electrons can be made to describe circular orbits between the cylinders by applying a positive potential to the inner one. No magnetic field is required. Because of progressive sorting, $n$-electron clouds are formed. The cathode and accelerating grid are both parallel to the cylinder axis. The voltage on the accelerating grid is so related to the potential difference between the cylinders that orbits are initially circular. Microwave power is extracted from the inner cavity. High output should be obtainable at frequencies above 30 kMc; this type of oscillator is thought capable of working at 100 kMc or higher.

621.396.615 2478

**An Extremely Wide Range Electronically Deviable Oscillator**—M. E. Ames. (*Proc. N.E.C.* (Chicago), vol. 4, pp. 397–405; 1948.) For another account see 2177 of September.

621.396.615 2479

**Single-Sideband Generators**—E. L. Watkins. (*Radio and Telev. News, Radio-Electronic Eng. Supplement*, vol. 11, pp. 7–9, 31; December, 1948.) A pair of balanced modulators in a phase rotation system can be used to give single-sideband output.

621.396.615.029.64 2480

**The Self-Excitation of a Triode Oscillator Loaded by a Line with Distributed Constants, at Microwave Frequencies**—V. A. Zore. (*Zh. Tekh. Fiz.*, vol. 19, pp. 570–577; May, 1949. In Russian.) The theory of Gvozdover and Zore (999 of May) is applied to the case of a triode oscillator loaded with a length of coaxial or 2-wire transmission line (Fig. 1). The operation of the oscillator is discussed and formulas (8) and (9) determining respectively the frequency and the condition of self-excitation are derived. The effect of the transit time of electrons on the condition for self-excitation is examined in detail and methods are indicated for determining the minimum wavelength that can be generated by the oscillator.

621.396.615.17 2481

**An Improved Regenerative Frequency Standard Application**—F. E. Wyman. (*Proc. N.E.C.* (Chicago), vol. 4, pp. 406–413; 1948.) This arrangement uses two tuned circuits in the mixer. It has a high division ratio (10 to 1), requires no voltage-regulated power supply, and has satisfactory self-starting and locking qualities.

621.396.619 2482

**Contribution to the General Theory of Modulation and Demodulation for Any Type of Characteristic**—O. Heymann. (*Arch. Elek.* (Übertragung), vol. 3, pp. 73–79; March, 1949.) The given characteristic is represented by a Fourier double integral; the tube output voltage can then be obtained directly as a Fourier series. The coefficients of this series are definite integrals whose integrands are given by the characteristic itself and two additional elementary functions. The form of the constant term of the series is particularly simple. This fact is very important in applications of the theory, since it enables the low-frequency behavior to be presented clearly and facilitates numerical evaluation. Two examples illustrate the usefulness of the general formulas.

621.396.621 2483

**Wideband Frequency-Discriminator Design**—V. C. Rideout. (*Proc. N.E.C.* (Chicago), vol. 4, pp. 414–424; 1948.) An analysis of the ordinary transformer-coupled frequency discriminator for the shunt-loaded case. For a slightly modified form of discriminator, the response can be calculated even for cases where the bandwidth is a large percentage of the center frequency. The output voltage passes through zero at a frequency above the transformer mid-frequency; improvement in linearity can, therefore, be better effected by detuning than by overcoupling of the transformer.

621.396.645 2484

**A Concise Theory of Aperiodic Amplifiers**—B. A. Khanov. (*Radiotekhnika* (Moscow), vol. 4, pp. 57–68; March and April, 1949. In Russian.) In studying the operation of a low-frequency amplification stage, it is customary to consider three different equivalent circuits corresponding respectively to the lower, middle and upper frequencies of the bandwidth and to derive three separate equations for the frequency and phase characteristics of the stage. A single formula is here derived containing a minimum number of generalized parameters and describing in the simplest manner the characteristics of the main types of amplification circuits. The results obtained are tabulated.

621.396.645 2485

**The Chain Amplifier**—H. Feigs. (*Funk und Ton*, vol. 3, pp. 291–301; May, 1949.) The principles and mode of operation of distributed-amplification circuits are considered. The grid-to-cathode capacitances of the amplifier tubes on the one hand, and the anode-to-cathode capacitances on the other hand, form the cross capacitances of balanced transmission lines and are uniformly distributed along their length. The amplification and frequency characteristics of this type of amplifier are calculated from transmission-line theory; they are not subject to the limitations of the usual type of amplifier. A uniform frequency-response curve can be obtained from 0 to 200 Mc, using ordinary tubes. The upper frequency limit is determined solely by the unavoidable grid loading of the tubes. See also 3375 of 1948 (Ginzton *et al.*).

621.396.645 2486

**A New Type of High-Frequency Amplifier**—J. R. Pierce and W. B. Hebenstreit. (*Bell Sys. Tech. Jour.*, vol. 28, pp. 33–51; January, 1949.) Amplification is obtained by means of an electromechanical interaction within the electron flow, which consists of two streams with different average velocities. When the currents or charge densities of the two streams are sufficient, the streams interact to give an exponentially increasing wave. Conditions for and the gain of an increasing wave are determined for a particular geometry of flow.

Advantages include: (a) the electron flow need not pass close to complicated circuit elements, (b) for a sufficiently great length of electron flow, amplification can be obtained even though input and output circuits have very low impedance or poor coupling to the electron flow, and (c) close synchronism between an electron velocity and a circuit-wave velocity is not essential. See also 2487 below.

621.396.645 2487

**Experimental Observation of Amplification by Interaction between Two Electron Streams**—A. V. Hollenberg. (*Bell Sys. Tech. Jour.*, vol. 28, pp. 52–58; January, 1949.) Discussion of the construction and performance of the amplifier used, which has identical input and output helices connected identically to a coaxial line several wavelengths long between the helices. Concentric tubular electron streams originate at the ring-shaped emitting surfaces of the two cathodes, pass through their respective control grids, and then through a common accelerating grid. An axial magnetic field of about 700 gauss is applied to maintain the definition of the streams. The gain produced depends on a difference in velocity between the two streams. The signal is impressed on the inner stream by the helix when its velocity is that at which traveling-wave amplifier interaction between the stream and helix occurs. The outer stream travels at a lower velocity. A gain of 33 db at a center frequency of 255 Mc was observed, with bandwidth of 110 Mc between 3-db points. The gain at 240 Mc estimated from theory is 40 db. The theory of Pierce and Hebenstreit (2486 above) is thus qualitatively confirmed, though the actual conditions in the amplifier differ from the theoretical assumptions.

621.396.645 2488

**Theory of the Superregenerative Amplifier**

—L. Riebman. (PROC. I.R.E., vol. 37, p. 608; June, 1949.) Corrections to 1627 of July.

621.396.645 2489

**Transient Response of Cathode Followers in Video Circuits**—B. Y. Mills. (PROC. I.R.E., vol. 37, pp. 631–633; June, 1949.) The effect of irregular radar or television video signals on cathode-follower circuits is analyzed. The maximum signal amplitude which can be handled by a cathode follower may be reduced if it has a capacitive load. A general formula determining the reduction is given and its bearing on design procedure is discussed.

621.396.645 2490

**New Developments in Preamplifiers**—C. J. LeBel. (*Audio Eng.*, vol. 33, pp. 9–12, 35; June, 1949.) A comprehensive discussion of the advantages of subminiature design techniques.

621.396.645:621.317.72 2491

**D.C. Amplifier Stabilized for Zero and Gain**—Williams, Tarpley, and Clark. (*See* 2563.)

621.396.645:621.385.029.63/.64 2492

**A Note on Filter-Type Traveling-Wave Amplifiers**—Pierce and Wax. (*See* 2668.)

621.396.645:621.392.52 2493

**Single-Circuit and Optimally Coupled Band Filters in Amplifiers**—A. Lennartz. (*Funk und Ton*, vol. 3, pp. 265–270; May, 1949.) Discussion shows that, in general, the symmetrical 2-stage band filter with optimum coupling is preferable, giving the greater amplification.

621.396.645:621.392.53 2494

**Investigations on Path-Time Distortion in Carrier-Frequency Amplifiers**—G. Schaffstein. (*Frequenz*, vol. 3, pp. 125–135; May, 1949.) Theoretical discussion and experimental results for directly transmitted signals show that the distortion can be largely reduced by the use of linear compensation networks with cross-connected members. Conditions for carrier transmission with a low degree of modulation resemble those for direct transmission, and similar compensation methods can be used. With a high degree of modulation, however, the resulting nonlinear distortion can only be eliminated by special methods. A circuit is described which, in spite of the relatively small bandwidth of the carrier-frequency amplifier, possesses a good frequency characteristic without path-time distortion, so that in pulse transmission, a symmetrical output pulse can be obtained without appreciable broadening at the base.

621.396.645.37 2495

**Single-Stage Feedback A.C. Amplifier**—W. Geyger. (*Funk und Ton*, vol. 3, pp. 278–285; May, 1949.) Discussion of the cathode-follower circuit with (a) current feedback, (b) voltage feedback, and (c) mixed current and voltage feedback, with formulas for the load current, output voltage, and gain.

621.396.828 2496

**Circuit Design for Reduction of Hum**—A. F. Dickerson. (*Proc. N.E.C.* (Chicago), vol. 4, p. 425; 1948.) Summary only. The chief sources of hum are electromagnetic fields, electrical leakage, badly arranged input-circuit wiring, and cathode-heater leakage current. Hum in high-frequency local oscillators is also discussed. Practical remedies are suggested, but no single device can eliminate all types of hum.

## GENERAL PHYSICS

537.1:512.9 2497

**Tensors and Electricity**—Bouthillon. (*See* 2541.)

537.52:538.569.029.5/.6 2498

**Experimental Investigations on the High-Frequency Discharge**—M. Chenot. (*Ann. Phys.* (Paris), vol. 3, pp. 277–373; May and June, 1948. Bibliography, pp. 373–375.) A comprehensive research. Evidence is given of the existence of wave-propagation phenomena in the motion of charged particles in discharge tubes; the propagation velocity is determined from measurements of the standing waves obtained with suitable excitation. A tentative theory of the observed effects is discussed.

Results are given for the voltage at which a discharge suddenly occurs in $H_2$, using frequencies from 1 to 75 Mc and pressures from $10^{-1}$ mm to 1.5 mm Hg. The curves extend the results of other workers concerning the existence of abrupt variations of the sudden-discharge voltage. The dimensions and arrangement of the electrodes are of fundamental importance. Empirical relations are established between the various factors determining the amplitude of the abrupt voltage variation; a possible explanation of the effect is suggested. See also 1932 Abstracts, *Wireless Eng.*, p. 217 (Gutton and Beauvais).

537.523.3 2499

**Point-to-Plane Impulse Corona**—D. B. Moore and W. N. English. (*Jour. Appl. Phys.*, vol. 20, pp. 370–375; April, 1949.) Corona characteristics were investigated for both positive and negative square pulses of 1 or 2 μsec. duration, voltage up to 12 kv, and repetition frequency 50 to 2,000 per second. Typical photographs are included and results discussed. See also 2225 of 1948 (Loeb and English).

537.525 2500

**Starting Potentials of Electrodeless Discharges**—E. W. B. Gill and A. von Engel. (*Proc. Roy. Soc. A*, vol. 197, pp. 107–124; May 11, 1949.) Discussion of measurements of the starting field at pressures between 0.2 mm and 350 mm Hg in H, N, Ne, D, and He at wavelengths between 5 meters and 2 km in vessels of different sizes and of different types of glass. The starting field rises slowly and continuous.y with λ until a kind of cutoff occurs, caused by the growing amplitude of electron oscillations and the corresponding rise of wall losses. In N, H, and D, the sharp cutoff persists up to the highest pressure used. The cutoff extends over a considerable wavelength range in Ne at pressures above 0.2 mm Hg and in He above 0.5 mm Hg. Part 1, 1906 of 1948.

537.533.8 2501

**Secondary Electron Emission**—H. Salow. (*Fernmeldetech. Z.*, vol. 2, pp. 161–165; June, 1949.) Discussion of fundamental phenomena, dependence on the physical condition of metal surfaces, emission powers of compounds (including semiconductors, insulators, and aggregated layers), and angular energy distribution with a qualitative explanation of the experimental results.

538.541.029.64 2502

**Effect of Surface Roughness on Eddy Current Losses at Microwave Frequencies**—S. P. Morgan, Jr. (*Jour. Appl. Phys.*, vol. 20, pp. 352–362; April, 1949.) The power dissipation in a metallic surface having regular parallel grooves whose dimensions are comparable to the eddy-current skin depth is investigated theoretically.

538.566.2 2503

**Reflection and Transmission of Electromagnetic Waves by a Spherical Shell**—H. B. Keller and J. B. Keller. (*Jour. Appl. Phys.*, vol. 20, pp. 393–396; April, 1949.) Exact explicit expressions are obtained for the field of a radiating periodic point-dipole located in medium 1 at the center of a spherical shell of medium 2, which is bounded by medium 3. The values of $\epsilon$, $\mu$, $\sigma$, and the shell radii are arbitrary. The reflected and transmitted fields are examined for various special cases and results compared with those of other workers.

538.569.4:543/545 2504

**Microwave Spectra and Chemical Analysis**—B. P. Dailey. (*Anal. Chem.*, vol. 21, pp. 540–544; May, 1949.) The relevant principles of molecular dynamics are discussed. The relative merits of the microwave spectrometer, the mass spectrometer, and infrared instruments for chemical analysis are considered.

538.569.4.029.64+537.226.2]:546.212 2505

**Absorption of 12.5-mm Wave-Length Electromagnetic Radiation in Supercooled Water**—J. A. Saxton and J. A. Lane. (*Nature* (London), vol. 163, pp. 871–872; June 4, 1949.) Measurements have been made for layers of various thicknesses up to several millimeters; the lowest water temperature so far reached is −7° C. The water completely filled a cylindrical waveguide 24 mm in diameter over a portion of its length and the resulting attenuation was measured, using only the $H_{11}$ wave. The waveguide was lined inside with glass and the probe covered with a glass sheath. The absorption-coefficient versus temperature curve is shown. See also 1913 and 1914 of 1948 (Saxton).

548.0:537:539.16.08 2506

**Crystal Counters: Part 1.**—R. Hofstadter. (*Nucleonics*, vol. 4, pp. 2–27; April, 1949. Bibliography, p. 27.) A comprehensive review. The theory of operation is outlined; important parameters are evaluated and the effect of impurities and faults in crystals is examined. Polarization effects, including those due to β-particles and penetrating radiation, are considered. Materials known to be capable of detecting single ionization events are AgCl, AgBr, C (diamond), ZnS, TlBr-TlI, CdS, and solid and liquid Ar. Some relevant characteristics are given. No alkali halide has yet been successfully used as a counter.

Experimental techniques for the production of crystals and for their use as counters are described.

Advantages claimed for crystal counters are: (a) small size, (b) high stopping power, (c) low resolving time, and (d) better conversion of ion pairs than in a gas. At present, difficulties are encountered due to crystal strains, polarization effects, variations in counting efficiency in different regions within the same crystal, annealing procedures, and the requirements for operation at low temperatures. Part 2, 2507 below.

548.0:537:539.16.08 2507

**Crystal Counters: Part 2**—R. Hofstadter. (*Nucleonics*, vol. 4, pp. 29–43; May, 1949. Bibliography, p. 43.) Two fundamental quantities for crystal counters are (a) the electron mobility of the crystal, (b) the energy per ion pair. Experimental measurements of (a) can be compared with theory, but this is not yet possible for (b). Experimental results concerning polarization for various types of counter material are discussed. No general criterion can yet be formulated to distinguish materials which can be used as counters from those which cannot. Some crystals which appear to be single are actually mosaic; this together with various properties briefly discussed, may explain the behavior of particular crystals. The high stopping power of crystal counters leads to good linearity, especially for energetic particles. At present the bulky and complicated apparatus required for use with large silver or thallium halide crystals, which require low temperatures and annealing, is a serious disadvantage, but the discovery of a new room-temperature counting material would radically change the situation. For small detectors, little improvement upon diamond or CdS is to be expected. Part 1, 2506 above.

## GEOPHYSICAL AND EXTRATERRESTRIAL PHENOMENA

523.53:621.396.9 2508

**The Diffraction of Radio Waves from Meteor Trails and the Measurement of Meteor Velocities**—J. G. Davies and C. D. Ellyett. (*Phil. Mag.*, vol. 40, pp. 614–626; June, 1949.) Automatic equipment, using pulse technique, is described for recording photographically the reflected amplitude of radio waves from meteor trails in time intervals of the order of milliseconds. Fluctuations in reflected amplitude like those associated with the diffraction of light at a straight edge are expected theoretically. Such fluctuations are associated with many meteor echoes, and the velocity of individual meteors can be deduced from the experimental results. Velocity measurements for meteors from known showers agree with earlier photographic and visual measurements. See also 3101 of 1948.

523.72+523.854]:621.396.822 2509

**Radio Astronomy**—C. R. Burrows. (*Sci. Mon.*, vol. 68, pp. 299–304; May, 1949.) Elementary discussion of: (a) the frequencies at which rf astronomical observations are possible, (b) the main differences in the requirements for radio telescopes and for communication receivers, (c) the variation of solar apparent temperature with frequency, and (d) galactic radiation, and the location of its chief sources.

523.72:621.396.822 2510

**Some Observations on Solar Noise**—Chief Engineer's Branch, General Post Office, Wellington. (*N.Z. Jour. Sci. Tech.*, vol. 29, Section B, pp. 140–141; November, 1947.) Discussion of observations made at Awarua during a period of high sunspot activity in February, 1946, at frequencies between 6.7 and 25.6 Mc. Simultaneous direction-finding observations prove conclusively the solar origin of the noise. Some of the noise surges lasted as long as one minute and reached high signal intensities.

523.72.029.63:523.746:621.396.822 2511

**Relation between Decimetre-Wave Solar Radiations and Sunspots**—J. F. Denisse. (*Compt. Rend. Acad. Sci.* (Paris), vol. 228, pp. 1571–1572; May 16, 1949.) The correlation coefficient between sunspots and the 10.7-cm solar radiations observed by Covington (2513 of 1948) shows a progressive increase according as comparison is made with (a) the relative sunspot number $N$, (b) the sum $\Sigma A$ of the areas of the spots, and (c) the daily index $\Sigma H_0\sqrt{A}$, where $H_0$ is the maximum magnetic field of a spot of area $A$. The correlation coefficients are respectively (a) 0.53, (b) 0.76, and (c) 0.87.

523.75 2512

**Solar Flares and their Terrestrial Effects**—M. A. Ellison. (*Nature* (London), vol. 163, pp. 749–753; May 14, 1949.) Substance of lecture to the Cavendish Laboratory Radio Section. Flares occur within a radius of $10^5$ km of a visible sunspot, and most frequently between the leading and following elements of a bipolar group. The largest flares sometimes obscure the largest sunspots. An intense flare usually occurs as a brief flash of radiation followed by a slow decay. The development curve of such a flare is correlated with the corresponding observations of radio noise. Immediate effects, due mainly to ultraviolet radiations, include geomagnetic crochets, fading of short-wave signals, and anomalous changes in the phase of long waves due to changes in $D$-layer ionization. Delayed effects, due to particles, include geomagnetic storms and abnormal cosmic radiation. The theoretical work of Giovanelli (2230 of 1948 and 376 of March) and of Unsöld (2217 of September) is briefly mentioned.

551.510.5:621.396.9 2513

**Radar as an Aid to the Study of the Atmosphere**—Jones. (*See* 2526.)

551.510.52:538.566 2514

**On the Internal Reflection of Electromagnetic Waves in a Stratified Medium. Application to the Troposphere**—Eckart and Kahan. (*See* 2605.)

551.510.535 2515

**The Reliability of Ionospheric Height Determinations**—L. A. Manning. (Proc. I.R.E., vol. 37, pp. 599–603; June, 1949.) Continuation of 725 of 1948. Uncertainties in determinations of electron distribution based on virtual-height data are discussed. The effect of an assumed distribution between two layers upon the upper-layer form is investigated. A method is given for evaluating the maximum error in height determination.

551.510.535 2516

**Critical-Frequency Difference Variations and the Poynting Vector in the Ionosphere**—J. C. W. Scott. (*Nature* (London), vol. 163, p. 993; June 25, 1949.) The variations in the $f^z$–$f^0$ critical frequency difference noted in 717 of April can be explained in terms of a diurnal expansion and contraction of the $F$ layer.

551.510.535 2517

**Short-Period Variations in the Ionosphere**—G. H. Munro. (*Nature* (London), vol. 163, pp. 812–814; May 21, 1949.) Correlation of $(h', f)$ records with the observations noted in 1664 of July establishes that the effects in question are due to local fluctuations in $F$-layer ionization, which show both a downward vertical and a horizontal progression. Results obtained on June 22, 1948, are shown graphically and discussed.

551.510.535 2518

**The Ionosphere over Mid-Germany in March 1949**—Dieminger. (*Fernmeldetech. Z.*, vol. 2, p. 157; May, 1949.) Continuation of 1661 of July and 1934 of September. On various specified dates, the limiting frequencies were from 10 to 35 per cent below the normal value. See also 2519 below.

551.510.535 2519

**The Ionosphere over Mid-Germany in April 1949**—Dieminger. (*Fernmeldetech. Z.*, vol. 2, p. 172; June, 1949.) Continuation of 2518 above. In April, the change from winter to summer ionosphere conditions was completed. Disturbances and abnormal values of critical frequency are noted.

551.510.535:621.396.11 2520

**The Analysis of Ionospheric Reflections: Part 2**—de Voogt. (*See* 2606.)

551.594:523.78"1949.04.28" 2521

**Observations of the Atmospheric Electric Field during the [partial] Solar Eclipse of 28th April 1949**—J. Rouch. (*Compt. Rend. Acad. Sci.* (Paris), vol. 228, pp. 1547–1549; May 16, 1949.) Field measurements in Monaco with a Wulf bifilar electrometer before, during, and after the eclipse are plotted, together with results for the same period on the following day. Before the eclipse started, the field strength was about normal for the season, with a value of 100 to 200 volts per meter. In the three-quarter hour before the eclipse started, the field increased to 720 volts per meter. It remained high during the whole of the eclipse, with a peak reading $>850$ volts per meter; after the eclipse, it oscillated around 550 volts per meter. On the following day, there was a fairly regular increase from 200 volts per meter to 500 volts per meter. The mean value for the month of April is 300 volts per meter and no values as high as 600 volts per meter were reached. A marked increase of the electric field was also observed during the eclipse of April 8, 1921. The random variations of the field are, however, so frequent and sometimes so large that it is possible for the large field increases observed, both in 1949 and 1921, to be chance coincidences.

551.594.5 2522

**Auroral Displays at Saskatoon**—W. Petrie, P. A. Forsyth, and E. McConechy. (*Nature* (London), vol. 163, p. 774; May 14, 1949.) Brief description of intense displays observed during the nights of January 24 and 25, 1949, and February 21 and 22, 1949. All auroral forms were present at some time during both displays. A large sunspot group passed the solar meridian on January 22, 1949, and was present, though reduced in size, on February 21, 1949.

## LOCATION AND AIDS TO NAVIGATION

534.88:623.96 2523

**An Electroacoustical System**—E. A. Walker. (*Trans. AIEE*, vol. 67, part 1, pp. 35–40; 1948. Discussion, pp. 40–41.) The location of torpedoes lost in firing tests is discussed. An ultrasonic generator is fitted in the torpedo and the signal is detected by a portable hydrophone capable of giving the approximate bearing and depth of the source. The simple magnetostriction generator is driven by two 3Q5-GT tubes, used as master oscillator and power amplifier, and produces a signal audible above background noise at 1,000 yards. Power is obtained from storage batteries.

621.396.9 2524

**Radar**—E. G. Schneider. (*Bull. Schweiz. Elektrotech. Ver.*, vol. 39, pp. 192–196, 251–256, 290–291, 313–316, and 343–344; March 20 to May 15, 1948.) Translation into German of an article noted in 3285 of 1946.

621.396.9:523.53 2525

**The Diffraction of Radio Waves from Meteor Trails and the Measurement of Meteor Velocities**—Davies and Ellyett. (*See* 2508.)

621.396.9:551.510.5 2526

**Radar as an Aid to the Study of the Atmosphere**—F. E. Jones. (*Jour. R. Aero. Soc.*, vol. 53, pp. 433–442; May, 1949. Discussion, pp. 442–448.) Radar is being used to investigate precipitation, to detect clouds dangerous to flying, and to measure cloud height and wind velocity. Techniques are being developed for measuring pressure, temperature, humidity, and atmospheric density in the upper air.

621.396.933(94) 2527

**Operational Trials of the Australian Distance-Measuring Equipment and Multiple-Track Radar Range**—J. G. Downes. (Proc. I.R.E. (Australia), vol. 9, pp. 10–21; April, 1948. Discussion, pp. 21–23.) The desirable features of short-range navigational aids for civil aircraft are discussed. The two equipments are briefly described. The DME is a beacon interrogator operating on 200 Mc and the presentation is on a meter with scales of 0 to 12 and 0 to 120 miles. The MTR is a hyperbolic navigation system using two synchronized pulse transmitters, operating on 212 Mc and a relatively short distance apart, so that the hyperbolic track system is nearly radial. The presentation consists of track numbers indicated on a meter.

The results of operational tests during regular flights between Melbourne and Sydney are fully described. Three ground stations were used, but the coverage was not complete over the 450-mile path.

## MATERIALS AND SUBSIDIARY TECHNIQUES

531.788.7 2528

**An Investigation on Hot-Wire Vacuum**

**Gauges: Part 3**—H. von Ubisch. (*Ark. Mat. Astr. Fys.*, vol. 36, part 1, Section A, 14 pp.; January 21, 1949. In English.) Part 1, 436 of 1948. Part 2, 731 of April.

537.228.1 2529

**Design and Performance of Ethylene Diamine Tartrate Crystal Units**—J. P. Griffin and E. S. Pennell. (*Trans. AIEE*, vol. 67, part 1, pp. 557–560; 1948.) A general discussion, including comparison with corresponding quartz crystal units. See also 740 of 1948 (Mason) and 2468 above.

537.228.1:548.5 2530

**Growing Crystals of Ethylene Diamine Tartrate**—A. C. Walker and G. T. Kohman. (*Trans. AIEE*, vol. 67, part 1, pp. 565–570; 1948. Discussion, p. 570.) A general account of the apparatus used and of the process of growth.

537.312.62 2531

**Properties of CbN at Radio Frequencies**—J. V. Lebacqz and D. H. Andrews. (*Proc. N.E.C.* (Chicago), vol. 4, pp. 11–23; 1948.) When modulated rf signals are applied across a strip of CbN at its transition temperature, an af voltage at the modulation frequency appears at the terminals. Experimental apparatus is described and results are discussed. A partial explanation based on the rapid change of resistance with current at certain temperatures is given. See also 3853 of 1947 (Andrews and Clark) and 3135 of 1948 (Lebacqz).

546.212–16:621.3.011.5.029.64 2532

**The Dielectric Properties of Ice at 1.25 cm Wavelength**—J. Lamb and A. Turney. (*Proc. Phys. Soc.*, vol. 62, pp. 272–273; April 1, 1949.) The permittivity remains approximately constant at 3.18 between 0° C and −200° C. The value of tan $\delta$ falls continuously with decreasing temperature. Any further dipole relaxation, apart from that giving a loss maximum at about $10^5$ cps is unlikely. A large atomic polarization may account for the high value of the permittivity.

546.431.82 2533

**Barium Titanates as Circuit Elements**—A. I. Dranetz, G. N. Howatt, and J. W. Crownover. (*Tele-Tech*, vol. 8, pp. 29–31, 55, 28–30, 57 and 36–39, 53; April to June, 1949.) Discussion of the dielectric and piezoelectric properties of $BaTiO_3$ ceramics, modern production methods, and applications.

546.431.82 2534

**High Indices of Refraction of Barium Titanate and other Heteropolar Titanium Compounds**—J. H. van Santen and F. de Boer. (*Nature* (London), vol. 163, pp. 957–958; June 18, 1949.) A tentative explanation in terms of molecular structure and electronic polarization.

621.315.61:621.396.662.029.64 2535

**Attenuator Materials, Attenuators and Terminations for Microwaves**—G. K. Teal, M. D. Rigterink, and C. J. Frosch. (*Trans. AIEE*, vol. 67, part 1, pp. 419–428; 1948.) A similar but shorter paper was abstracted in 1691 of July.

621.315.612 2536

**Ceramic Materials with a High Dielectric Constant**—E. J. W. Verwey and R. D. Bügel. (*Philips Tech. Rev.*, vol. 10, pp. 231–238; February, 1949.) Theoretical reasons are given for the high value of the dielectric constant $\epsilon$ of $TiO_2$ (rutile). The effect of impurities in reducing the value of $\epsilon$ and varying its temperature coefficient is discussed. Admixture of MgO in suitable proportion gives a material for which $\epsilon$ is 12 to 18, temperature coefficient $\alpha$ is practically zero and tan $\delta$ is $10^{-4}$ at 1,000 cps. For a mixture of 85 per cent $CeO_2$ and 15 per cent $TiO_2$, $\epsilon \approx 40$, $\alpha$ is roughly zero and $\tan\delta \approx 8\times10^{-4}$ at 1,000 cps. $ZrO_2$ can also be used to obtain a material with $\alpha$ about zero. As with other mixtures, the values of $\epsilon$, $\alpha$ and tan $\delta$ depend on the proportion of $ZrO_2$.

621.315.612.011.5 2537

**Development and Properties of Some Ceramic Dielectrics**—G. R. Shelton, E. N. Bunting, and A. S. Creamer. (*Proc. N.E.C.* (Chicago), vol. 4, pp. 24–31; 1948.) The dielectric constant and its temperature coefficient and the reciprocal of the power factor are studied as functions of composition for various binary and ternary systems. Stability after storage for 6 months or more is also considered. See also 3551 of 1947 and 3441 of 1948.

621.318.322:621.384.612.1† 2538

**Soft Iron for the Electromagnet of a Cyclotron**—J. J. Went. (*Philips Tech. Rev.*, vol. 10, pp. 246–254; February, 1949.) The iron for electromagnets should have high saturation flux density, relatively high remanence and low coercive force. The iron used for the 200-ton magnet of the Institute for Nuclear-Physical Research, Amsterdam, has a remanence 70 per cent of the saturation value.

621.385.2.032.216 2539

**Testing Cathode Materials in Factory Production**—Acker. (*See* 2674.)

621.385.2.032.216 2540

**A Standard Diode for Electron-Tube Oxide-Coated Cathode-Core-Material Approval Tests**—McCormack. (*See* 2675.)

## MATHEMATICS

512.9:537.1 2541

**Tensors and Electricity**—L. Bouthillon. (*Bull. Soc. Franç. Élec.*, vol. 9, pp. 212–234; May, 1949.) A detailed tensor theory of electrostatics, magnetostatics, and electromagnetism. Scalar and pseudoscalar quantities, polar and axial entities, the various products corresponding to the scalar and vector products of vector rotation, and the derivatives corresponding to the divergence, gradient, curl, and Laplacian, can all be represented simply.

512.99:621.318.572 2542

**The Synthesis of Two-Terminal Switching Circuits**—Shannon. (*See* 2456.)

517.727:518.12:621.392.52 2543

**Numerical Computation of the Elliptic Function sn($mK/n$), where $m$ and $n$ are Integers**—J. C. Stewart. (*Commun. Rev.*, vol. 1, pp. 24–29; March, 1948.) $K$ is the real quarter-period. The values of the function are required in the design of filters of the Tchebycheff type.

518.5 2544

**Electro-Mechanical and Electronic Calculating Devices**—R. Davis-Berry. (*Trans. S. Afr. Inst. Elec. Eng.*, vol. 40, part 3, pp. 55–73; March, 1949. Discussion, pp. 73–75.) The fundamental circuits and general principles of operation of punched-card machines are fully discussed, with detailed diagrams. Simple electronic counters are briefly considered. The automatic sequence controlled calculator (noted in 461, 468, and 787 of 1947) is described in detail. Limiting factors in the applications of such equipment to scientific and mathematical problems are examined.

518.5 2545

**Design and Operation of the IBM Selective-Sequence Electronic Calculator**—R. R. Seeber, Jr. (*Proc. N.E.C.* (Chicago), vol. 4, p. 288; 1948.) Summary only.

518.5 2546

**A Large-Scale General-Purpose Electric Analog Computer**—E. L. Harder and G. D. McCann. (*Trans. AIEE*, vol. 67, part 1, pp. 664–673; 1948.) Description of the Westinghouse and California Institute of Technology computers, which only differ in minor matters. Accuracy is, in general, within 1 to 5 per cent for the type of engineering problems to be solved.

518.5 2547

**Analysis of Rototrol Voltage Regulators by Electrical Analogy**—J. T. Carleton. (*Proc. N.E.C.* (Chicago), vol. 4, pp. 272–278; 1948.) Discussion of the principles of operation of the ANACOM, an analogue computer, made by the Westinghouse Electric Corp.

518.5:512.37 2548

**Root-Solver for Tenth-Degree Algebraic Equations**—J. F. Calvert, H. R. Johnston, and G. H. Singer, Jr. (*Proc. N.E.C.* (Chicago), vol. 4, pp. 254–271; 1948.) Theory and design of a proposed analogue computer are discussed. The coefficients in the equation may be complex.

## MEASUREMENTS AND TEST GEAR

531.761+621.3.018.4(083.74) 2549

**The Atomic Clock**—H. Lyons. (*Instruments*, vol. 22, pp. 133–135, 174; February, 1949.) See 1983 of August.

621.3.011.4(083.74) 2550

**A Standard of Small Capacitance**—C. Snow. (*Jour. Res. Nat. Bur. Stand.*, vol. 42, pp. 287–308; March, 1949.) A formula is derived for the capacitance of a parallel-plate capacitor with coplanar guard, the circular face of the electrode being at the bottom of a cylindrical hole in the guard. The analogous two-dimensional arrangement is also considered; an exact formula is obtained by conformal transformation and is used to determine the errors in certain general approximate formulas. With certain restrictions, easily fulfilled in practice, the resultant error is less than 0.05 per cent.

621.3.018.41(083.74) 2551

**Absolute Accuracy. Primary Frequency Standard**—H. B. Meahl. (*Proc. N.E.C.* (Chicago), vol. 4, pp. 446–450; 1948.) The sources of probable error in a primary frequency standard of the quartz-crystal-controlled oscillator type are analyzed. Attempts to determine the long-term constancy of the rotation of the earth are discussed. Although quartz-crystal-controlled oscillators of special design have very good frequency stability and their frequencies can be compared with great precision, the absolute accuracy with which their frequencies are known is considered to be only within 1 part in $10^7$.

621.3.018.41(083.74) 2552

**Microwave Frequency Measurements and Standards**—B. F. Husten and H. Lyons. (*Trans. AIEE*, vol. 67, part 1, pp. 321–328; 1948.) Full paper; long summary abstracted in 1712 of July.

621.317.3:621.385.38 2553

**A Method for the Measurement of the Ionization and Deionization Times of Thyratron Tubes**—M. Birnbaum. (*Trans. AIEE*, vol. 67, part 1, pp. 209–214; 1948.) A circuit is described for generating rectangular pulses, with rise times less than 0.01 μsec., for measurement of ionization times. For deionization-time measurement, the thyratron is made to conduct and the anode voltage is then dropped below that of the cathode. At various intervals afterwards, anode voltage is suddenly reapplied; the maximum voltage which does not cause reignition is a measure of the degree of deionization. Results of measurements for various American thyratrons, including Types 2D21, 884, and 2050, are shown graphically. Circuit constants and methods of measurement

are discussed for each case. Accuracy is estimated to be within 0.01 μsec.

621.317.3.029.64 2554
**Centimetre-Wave Measurement Technique**—H. H. Meinke. (*Arch. Elek.* (Übertragung), vol. 3, pp. 3–11 and 46–54; January and February, 1949.) Discussion of general principles, energy sources and detectors, resistance measurement, loss-free 4-poles and 6-poles, directional couplers and power, frequency, and phase measurement.

621.317.323(083.74) 2555
**A Primary High-Frequency Voltage Standard**—M. C. Selby. (*Instruments*, vol. 22, pp. 318–319; April, 1949.) See also 2262 of September.

621.317.331:621.319.4.015.3 2556
**A Method of Measurement of the Internal Series Resistance of a Capacitor under Surge Conditions**—B. S. Melton. (Proc. I.R.E., vol. 37, pp. 690–693; June, 1949.) A ballistic method using a vacuum thermocouple and a galvanometer.

621.317.335.3.029.64†:621.315.611.011.5 2557
**Microwave Dielectric Measurements**—T. W. Dakin and C. N. Works. (*Jour. Appl. Phys.*, vol. 18, pp. 789–796; September, 1947.) The method of Roberts and von Hippel (178 of 1947) was used with 10-cm and 3-cm waves. A simplified procedure for calculating the dielectric properties from the measurements is given. Results are tabulated.

621.317.336 2558
**The Measurement of Antenna Impedance Using a Receiving Antenna**—D. G. Wilson and R. W. P. King. (*Proc. N.E.C.* (Chicago), vol. 4, p. 496; 1948.) Summary only. Energy from a remote transmitter was received by an antenna located above a large conducting plane and terminated in a slotted coaxial cavity. The combined phase and damping functions for the two ends of the cavity were determined by the resonance-curve method. Since the phase and damping due to the lower end could be measured independently, the phase and damping due to the upper end could be found and used to calculate the antenna impedance. Curves of impedance as a function of length of antenna were obtained for several antennas. The impedance of a dipole, as determined in this way, was in reasonable agreement with the value measured when using the same apparatus as a transmitting system.

621.317.336 2559
**Antenna Impedance Measurement by Reflection Method**—E. Istvánffy. (Proc. I.R.E., vol. 37, pp. 604–608; June, 1949.) The dipole whose impedance is to be measured is mounted on a small wooden carriage which can be moved along a track in front of transmitting and receiving parabolic reflectors mounted side by side. The amplitude of the received signal depends on the power reflected by the dipole, and the target distance for maximum power depends on the phase of the dipole impedance. Results obtained for dipoles of various lengths and diameters of 0.14, 0.48, 3, 13.6, and 40 mm are discussed.

621.317.373.029.64 2560
**A Method of Measuring Phase at Microwave Frequencies**—S. D. Robertson. (*Bell Sys. Tech. Jour.*, vol. 28, pp. 99–103; January, 1949.) One part of the output of a signal generator is modulated by an af signal in a balanced modulator. The resulting suppressed-carrier double-sideband signal is applied to the device to be measured, in which means are provided for sampling the signal at both input and output. The other part of the signal-generator output is fed through a calibrated phase shifter and applied to a crystal detector, to which the signal samples are then applied successively, the phase shifter being in each case adjusted for minimum af signal in the detector output. The difference between the two settings of the phase shifter gives the phase difference between the two samples. Compensation for amplitude inequalities of the two samples is thus unnecessary.

621.317.7.087/.088 2561
**Frequency Response Characteristics of Recording Instruments**—T. D. Graybeal. (*Trans. AIEE*, vol. 67, part 1, pp. 755–766; 1948.) Methods are discussed for determining the errors due to the dynamic limitations of instrument movements, and which appear in records. The ac steady-state response may be obtained by means of charts, given the undamped natural frequency and the relative damping. Test procedure is described for finding these two basic constants of a particular instrument. The importance of proper damping is emphasized; techniques are suggested whereby the frequency response may be made even better than that obtainable with optimum damping. A simplified analysis of servo-actuated recorders is included. Numerical examples are given.

621.317.71 2562
**An Automatic Current Integrator**—Poole. (*See* 2455.)

621.317.72:621.396.645 2563
**D.C. Amplifier Stabilized for Zero and Gain**—A. J. Williams, Jr., R. E. Tarpley, and W. R. Clark. (*Trans. AIEE* vol. 67, part 1, pp. 47–57; 1948.) An amplifier for dc measurements is described in detail. The zero is stabilized by means of a dc-ac converter vibrating at 60 cps. The over-all voltage gain is about $40\times10^6$. Great care is taken to ensure that no unwanted 60-cps component can affect the zero. Gain is stabilized within a small fraction of 1 per cent by the use of over-all dc feedback. Circuits are described for various measurements involving voltages of the order of 0.05 μ volt.

621.317.726:621.319.4 2564
**A Wide-Range Variable Capacitor**—G. W. Bowdler. (*Jour. Sci. Instr.*, vol. 26, pp. 117–119; April, 1949.) Description of a 3-terminal capacitor covering the range 0.01 to 10 pF. With a pair of Si rectifiers and a dc measuring instrument, it can be used as a rf peak volt meter for the range 1 to 10 kv at frequencies from 50 kc to 50 Mc.

621.317.733:621.317.794 2565
**A Direct Reading D.C. Bridge for Microwave Power Measurements**—H. J. Carlin and J. Blass. (*Trans. AIEE*, vol. 67, part 1, pp. 311–315; 1948.) A self-contained balanced bolometer bridge circuit suitable for field work is described in detail. The bridge uses two bolometer elements, a Wollaston wire for the range 0 to 1 milliwatt and a metallized-glass element for the range 10 to 100 milliwatts. The design of a built-in attenuator with a range of 0.03 to 3 db and maximum error 2.0 per cent is discussed.

621.317.733.029.64 2566
**A Microwave Impedance Bridge**—M. Chodorow, E. L. Ginzton, and F. Kane. (Proc. I.R.E., vol. 37, pp. 634–639; June, 1949.) A symmetrical 6-arm waveguide structure is described and its equivalent circuit is analyzed theoretically. The relation between the admittances of the various arms is exactly that of a Wheatstone bridge with shunting susceptances across each pair of terminals. A device of this sort for use at a wavelength of 10 cm has been found to behave as predicted.

With this bridge, any impedance can be measured to about the same accuracy as with a standing-wave detector. The standard impedances required are three variable reactances (movable shorting plungers) and a $Z_0$ termination. The positions of the plungers are measured. The device can be used as a 4-terminal lattice section for filter design or other applications; greater flexibility is obtained than with conventional tee or pi sections.

621.317.74.029.64 2567
**Microwave Slotted Sections**—S. A. Johnson. (*Proc. N.E.C.* (Chicago), vol. 4, pp. 222–232; 1948.) Instruments used to measure the magnitude and phase of standing waves in a transmission line or waveguide without introducing appreciable field disturbance. The electrical impedance of the line can be deduced. High mechanical precision is required in the construction of the slotted sections. Sections for use at frequencies up to 75 kMc are described. Tuners for matching the probe of the detector are considered.

621.317.755 2568
**A Cathode-Ray Oscillograph with 100-Megacycle Bandwidth**—M. M. Newman, R. P. Featherstone, and P. S. Christaldi. (*Proc. N.E.C.* (Chicago), vol. 4, p. 445; 1948.) Summary only.

621.317.755:621.317.791 2569
**A Polar Vector Indicator**—A. H. Waynick, P. G. Sulzer, and E. A. Walker. (*Proc. N.E.C.* (Chicago), vol. 4, pp. 279–286; 1948.) An electronic device for demonstration purposes, which displays and permits determination of the magnitudes and phase angles of as many as three voltages or currents of the same frequency. Frequency range is 15 to 300 cps, amplitude accuracy within ±10 per cent, phase accuracy within ±3°.

621.317.761 2570
**Contribution to the Technique of 'Dense' Standard-Frequency Spectra**—H. J. Griese. (*Fernmeldetech. Z.*, vol. 2, pp. 179–188; June, 1949.) The term "dense" is applied to spectra whose components are so close together in frequency that they can be separated from one another by means of simple electrical circuits and filters. Special technique is required in applications involving such spectra. Methods of generating dense spectra by the use of dc and ac pulses, and arrangements for frequency multiplication and for pulse modulation are described. Special equipment discussed includes (a) a generator providing standard frequencies at 10-kc intervals, with stronger signals at 100-kc intervals, for the calibration of receivers, (b) an interpolation frequency meter, (c) a direct-reading frequency meter, (d) apparatus for frequency stabilization, including a unit using a phase bridge. Direct and indirect methods of selecting a particular frequency from a dense frequency spectrum are also described.

621.317.772:621.396.67 2571
**Measurement of the Phase of Radiation from Antennas**—J. N. Hines and C. H. Boehnker. (*Proc. N.E.C.* (Chicago), vol. 4, pp. 487–495; 1948.) The equipment described consists of a signal generator, attenuator, probe antenna, a T-junction mixer, and receiving apparatus. Two signals are introduced into the T-junction which combine if in phase and cancel if out of phase. Phase contours thus measured for various antennas are shown. Prediction of amplitude and phase patterns of arrays by combining vectorially the patterns of individual antennas is discussed.

621.317.784.087.44 2572
**A Square-Law Power-Level Recorder**—W. R. Clark, W. R. Turner, and A. J. Williams, Jr. (*Proc. N.E.C.* (Chicago), vol. 4, pp. 132–146; 1948.) A recorder with a linear 40-db scale above a datum level of 0.0002 milliwatts. The error is less than 0.1 db between 20 cps and 200 kc. The operation of the recorder is described. See also 488 of 1941 (Clark).

621.317.79:621.396.615:621–526 2573
**Signal Generators for Servo System Measurements**—C. F. White. (*Proc. N.E.C.* (Chicago), vol. 4, pp. 59–71; 1948.)

621.317.79:621.396.615:621.396.619.11 2574
**A Low-Distortion A.M. Signal Generator**—E. S. Sampson. (*Proc. N.E.C.* (Chicago), vol. 4, pp. 147–157; 1948.) Special features are (a) the modulator, which uses af detection and feedback in the cathode circuit, (b) the cancellation amplifier, (c) the output amplifier, which includes a broad-band rf transformer, and (d) the exalted-carrier detector. Af distortion is $<0.1$ per cent at 100 per cent modulation.

621.317.79:621.396.615:621.396.93 2575
**Radio Direction Finder System Analyzer**—E. C. Jordan and J. J. Meyers. (*Proc. N.E.C.* (Chicago), vol. 4, pp. 462–471; 1948.) A test device consisting of a 175-kc signal source, which can be suitably modulated, and various phase shifters for simulating the voltages appearing at the antenna terminals of any direction-finding array. The present analyzer can simulate the effects of two rays arriving at an 8-element direction-finding array. Its use reduces the time required for the analysis of direction-finding systems, both old and new, and it could be useful for training purposes.

621.317.79:621.396.615.14 2576
**A Broad-Band Signal Generator**—T. P. Hahn, J. Ebert, and W. A. Lynch. (*Trans. AIEE*, vol. 67, part 1, pp. 316–320; 1948.) Design problems are discussed. Three internal-cavity reflex klystrons are used to cover the frequency range 4,000 to 10,000 Mc. Attenuator and wavemeter designs in coaxial rf cable are considered, as well as attenuator calibration and accuracy of power measurement. The method of applying impulses to the klystrons is described, with emphasis on ways of obtaining very short rise and decay times.

621.317.79:621.396.813 2577
**A Simple Method for Determining Distortion Factors**—F. Enkel. (*Fernmeldetech. Z.*, vol. 2, pp. 153–154; May, 1949.) A signal of frequency 800 cps is applied to the system to be tested, and the amplitude of the second and third harmonic in the output is measured, using in succession bandfilters tuned to 1,000 and 2,400 cps. The nonlinear distortion can then be calculated from simple formulas which are given. Curves show the variation of the quadratic and cubic terms of the distortion factor determined for (a) a triode amplifier, (b) a pentode amplifier, and (c) a magnetophone, as a function of the loading.

621.396.662(083.74) 2578
**A Standard of Attenuation for Microwave Measurements**—R. E. Grantham and J. J. Freeman. (*Trans. AIEE*, vol. 67, part 1, pp. 329–335; 1948.) Full paper; long summary abstracted in 1730 of July.

## OTHER APPLICATIONS OF RADIO AND ELECTRONICS

531.717.1:621.386 2579
**An X-Ray Thickness Gauge for Hot-Strip Rolling Mills**—C. W. Clapp and R. V. Pohl. (*Trans. AIEE*, vol. 67, part 1, pp. 620–626; 1948.)

531.717.1:621.386 2580
**X-Ray Thickness Gauge for Cold-Rolled Strip Steel**—W. N. Lundahl. (*Trans. AIEE*, vol. 67, part 1, pp. 83–90; 1948.) One photomultiplier pickup and two X-ray sources are used. Range is 5 to 50 mil; accuracy within 1 per cent.

536.58:621.316.7 2581
**Precision Photoelectric Control of High-Temperature Furnaces**—F. C. Todd. (*Proc. N.E.C.* (Chicago), vol. 4, pp. 289–297; 1948.)

539.16.08 2582
**The Scintillation Counter**—J. W. Coltman. (PROC. I.R.E., vol. 37, pp. 671–682; June, 1949.) A review of present knowledge regarding characteristics and operation of this type of counter.

539.16.08 2583
**Accurate Determination of the Deadtime and Recovery Characteristics of Geiger-Müller Counters**—L. Costrell. (*Jour. Res. Nat. Bur. Stand.*, vol. 42, pp. 241–249; March, 1949.) The relevant theory is briefly discussed. An electronic gating instrument for the determination of deadtime and recovery time within 1 per cent or 2 μsec. is described. The variation of these times with counter pressure and overvoltage is shown graphically.

539.16.08:548.0:537 2584
**Crystal Counters: Part 1**—Hofstadter. (*See* 2506 and 2507.)

539.16.08:621.318.572 2585
**An Improved Quench Circuit for Geiger Counters**—Cooke-Yarborough, Florida, and Davey. (*See* 2457.)

551.508.5:621.396.645.371 2586
**Application of a D.C. Negative-Feedback Amplifier to Compensate for the Thermal Lag of a Hot-Wire Anemometer**—P. G. Hubbard. (*Proc. N.E.C.* (Chicago), vol. 4, pp. 171–178; 1948.) Description of an instrument for measuring the instantaneous velocity of the air in wind tunnels, ducts, or free jets where small size and a very small time constant are essential. The use of feedback results in simple construction, improved stability, and greater freedom from undesirable noise and oscillations.

615.849 2587
**F.C.C. Diathermy Design for Low Harmonic Radiation and Good Frequency Stability**—E. W. Chapin, W. K. Roberts, and M. C. Mobley. (*Trans. AIEE*, vol. 67, part 1, pp. 42–46; 1948. Discussion, p. 46.)

621.317.083.7 2588
**A Faster Telemeter for Carrier-Current Channels**—E. E. Lynch, H. C. Thomas, and G. S. Lunge. (*Trans. AIEE*, vol. 67, part 1, pp. 288–294; 1948. Discussion, p. 294.) A current of frequency between 6 and 27 cps and directly proportional to the quantity to be measured is used to modulate carrier-current channels of conventional fixed-frequency types. The apparatus used is fully described, and compared with existing systems. Advantages claimed are: instantaneous response without overshoot, a high degree of accuracy and stability, absence of contacts and a minimum number of moving parts.

621.317.79:[531.787.9+531.718.4 2589
**Electronic Methods for Measurement of Pressure and Displacement**—A. Crossley and D. L. Elam. (*Proc. N.E.C.* (Chicago), vol. 4, pp. 158–170; 1948.) Description of (a) the pressuregraph-syncromarker, for measuring static or dynamic pressures in a chamber containing fluid or gas, (b) the dynamic micrometer, which measures movement of vibrating metal bodies within $\pm 0.1$ mil. See also 3214 of 1947.

621.365.003.12 2590
**Some Economic Aspects of Radio-Frequency Heating**—L. M. Duryee. (*Trans. AIEE*, vol. 67, part 1, pp. 105–112; 1948.)

621.38.001.8 2591
**Digests of Papers at Conference on Electron Tubes in Industry**—(*Elec. Eng.*, vol. 68, pp. 525–529; June, 1949.) Summaries of most of the papers presented at the AIEE conference on the Industrial Application of Electron Tubes, Buffalo, N. Y., April 11 and 12, 1949.

621.38.001.8:681.9 2592
**Fairchild Electronic Half-Tone Engraving Machine**—J. Boyajean. (*Proc. N.E.C.* (Chicago), vol. 4, pp. 330–336; 1948.)

621.383.001.8 2593
**Research on Reading Aids for the Blind**—V. K. Zworykin, L. E. Flory, and W. S. Pike. (*Jour. Frank. Inst.*, vol. 247, pp. 483–496; May, 1949.) Discussion of the system already mentioned in 3700 of 1946 and 3229 of 1947. An electronic method of letter recognition is also considered. Results so far achieved while not spectacularly successful, indicate possible approaches to the problem.

621.384.611.2† 2594
**A 70-Mev Synchrotron**—F. R. Elder, A. M. Gurewitsch, R. V. Langmuir, and H. C. Pollock. (*Jour. Appl. Phys.*, vol. 18, pp. 810–818; September, 1947.)

621.384.62† 2595
**The Design of Linear Accelerators**—J. C. Slater. (*Rev. Mod. Phys.*, vol. 20, pp. 473–518; July, 1948.) The relative merits of linear and orbital accelerators are discussed. The phase velocity in a waveguide can be reduced by loading so that the waves travel with the same speed as that of the particles to be accelerated. The loaded guide has band-pass filter characteristics. Formulas are derived for the amplitude of the accelerating field in standing-wave and traveling-wave accelerators respectively. The distance between successive feeds to the guide must not exceed the attenuation length, or distance in which the energy density of a traveling wave falls to $1/e$ of its initial value. Geometrical factors affecting acceleration are discussed. Group velocity is less than phase velocity; it is theoretically zero for the pi-mode tube used in the MIT accelerator, which has small attenuation length. The feeding of power into linear accelerators, tolerances in long accelerators, and particle dynamics for different types of accelerator, are considered.

621.385.832:[535+77 2596
**Cathode-Ray Tube Applications in Photography and Optics**—C. Berkley and R. Feldt. (*Proc. N.E.C.* (Chicago), vol. 4, p. 314; 1948.) Summary only.

621.385.833 2597
**On the Calculation, for an Immersion Objective with Axial Symmetry, of the Potential along the Axis and of Its Derivatives**—M. Duchesne. (*Compt. Rend. Acad. Sci.* (Paris), vol. 228, pp. 1407–1408; May 2, 1949.) The results of calculations for the objective of an electron telescope are in good agreement with values determined experimentally, using an electrolyte tank.

621.385.833 2598
**Use of the Electron Microscope in the Optical Industry**—J. Robillard. (*Rev. d'Optique*, vol. 28, pp. 129–145; March, 1949.) General discussion, with special reference to investigation of the characteristics of antireflection layers.

621.385.833:537.133 2599
**The Proton Microscope**—C. Magnan. (*Nucleonics*, vol. 4, pp. 52–66; April, 1949.) Aberrations are shown to limit the maximum theoretical resolving powers of optical, electrostatic, and electromagnetic electron microscopes to 170 mμ, 2.5 mμ, and 1 mμ respectively.

At the Collège de France, an electrostatic electron microscope is being converted to an electrostatic proton microscope. Suitable proton sources, lens systems, and object carriers are described. The maximum theoretical resolving power is 0.15 mμ. With photographic enlargement, a total magnification of 600,000 is expected.

621.386:621.396.9 2600
**The Application of Radar Techniques to a System for High-Speed X-Ray Motion Pictures**—D. C. Dickson, Jr., C. T. Zavales, and L. F. Ehrke. (*Proc. N.E.C.* (Chicago), vol. 4, pp. 298–313; 1948.)

621.391.63:526.9 2601
**An Optical Radar for Surveying**—W. W. Hansen. (*Trans. AIEE*, vol. 67, part 1, pp. 660–663; 1948.) For another account see 3211 of 1948.

## PROPAGATION OF WAVES

538.56 2602
**The Approximate Solution of One-Dimensional Wave Equations**—C. Eckart. (*Rev. Mod. Phys.*, vol. 20, pp. 399–417; April, 1948.) A general discussion, in terms of Hamiltonian functions, of the type of differential equation applicable to waves on a stretched string, sound waves in a tube of uniform cross section, the propagation of electric currents along a uniform wire, etc. The Fourier solution of the initial-value problem, group and phase velocity, the resolution of waves into spectra, wave fronts, and unresolved waves are considered. Particular attention is given to the method of stationary phase, which is the mathematical foundation for the Hamilton-Jacobi ray theory. Difficulties in the application of this method to a dissipative medium are considered but no definite conclusions are reached.

538.566 2603
**On Sommerfeld's "Radiation Condition"**—F. V. Atkinson. (*Phil. Mag.*, vol. 40, pp. 645–651; June, 1949.) Discussion of the uniqueness of solution in problems of wave motion involving an infinite medium. A set of conditions is formulated under which the solution is proved to be unique; these include Sommerfeld's "condition of finiteness" as well as his "radiation condition."

538.566 2604
**On the Propagation of Electromagnetic Waves in Stratified Media**—F. Abelès. (*Ann. Phys.* (Paris), vol. 3, pp. 504–520; July and August, 1948.) The media are assumed to be composed of many homogeneous isotropic layers bounded by parallel planes; the electromagnetic waves are plane and sinusoidal, with any orientation whatever. The problem resolves into that of determining the constants of integration for Maxwell's equations so as to satisfy the conditions at the limits. A system of $2p$ linear equations with $2p$ unknowns has thus to be solved; this is effected by means of recurrence formulas. The relation between the physical and mathematical aspects of the problem is stressed. Formulas are derived by summation of the rays reflected an odd number of times and explicit expressions are given for the complex coefficients of reflection and transmission for a stratified medium. From these coefficients, information concerning the effects of such a medium on a plane incident wave is easily deduced. Three general theorems are enunciated and briefly discussed.

538.566:551.510.52 2605
**On the Internal Reflection of Electromagnetic Waves in a Stratified Medium. Application to the Troposphere**—G. Eckart and T. Kahan. (*Compt. Rend. Acad. Sci.* (Paris), vol. 228, pp. 1373–1374; April 25, 1949.) Discussion of reflection due solely to the inhomogeneity of the medium and not to a discontinuity in the values of $\epsilon$ and $\mu$. The reflection coefficient for the stratified troposphere is calculated and shown to be proportional to $\lambda$. It appears improbable that this type of reflection can be observed with electromagnetic waves in the case of the troposphere, but since the variation of the acoustic characteristics in the troposphere is much greater than that of the values of $\epsilon$ and $\mu$, acoustic experiments might be more successful.

621.396.11:551.510.535 2606
**The Analysis of Ionospheric Reflections: Part 2**—A. H. de Voogt. (*Tijdschr. ned. Radiogenoot.*, vol. 14, pp. 73–85; May, 1949. In English.) Polarization curves for different collision frequencies are given, together with hypothetical curves for electron-density distribution and collision frequency during the daytime and in the evening. Path times are derived for positive and for negative pulses. Discussion of attenuation leads to the view that recently published values of the collision frequency are too high and that the greater part of the friction loss occurs in the *E*-layer, or even the *D*-layer. Results obtained with twin-loop receiving equipment 1,600 meters from a 2-kw transmitter are described. Signals with circular polarization gave the best results, though even these were subject to fading during evening periods. Part 1, for which corrections are given, 1381 of June.

621.396.11:551.510.535 2607
**Deviation at Vertical Incidence in the Ionosphere**—M. Cotte and G. Millington. (*Nature* (London), vol. 163, p. 810; May 21, 1949.) Comment on 1763 of July, and the author's reply.

621.396.11(98) 2608
**Short-Wave Propagation over the Polar Regions**—H. A. Hess. (*Elektron Wiss. Tech.*, vol. 3, pp. 218–226; June, 1949.) An account of results obtained at Frederikshavn during the period 1942 to 1945. Records were obtained, on quickly moving film, of direct, and reverse signals from various distant stations. In some cases, the transmission path included both the north and south polar zones. The split signals observed for transmission paths near the poles can be explained by interference between two or more waves of slightly different frequency due to a Doppler effect. When two waves of nearly equal amplitude are concerned, a pronounced beat minimum is obtained. The observed Doppler frequency shift of 5 to 30 cps at frequencies between 10 and 20 Mc indicates large movement of the reflecting layer in the polar zone.

621.396.812 2609
**Atmospheric Effects on Short-Wave Radio Propagation**—J. S. McPetrie and B. J. Starkey. (*Nature* (London), vol. 163, pp. 958–959; June 18, 1949.) The low-level atmospheric ducts discussed in 1167 of May (McPetrie and Starnecki) have little effect on the propagation of centimeter waves when the transmitter or the receiver is well above the duct, or on the propagation of meter waves for any height of transmitter or receiver. Experimental results supporting this are shown graphically and discussed.

621.396.812.3.029.64 2610
**Preliminary Analysis of Microwave Transmission Data Obtained on the San Diego Coast under Conditions of a Surface Duct**—C. L. Pekeris and M. E. Davis. (*Jour. Appl. Phys.*, vol. 18, pp. 838–842; September, 1947.) Transmission data for 63 and 170 Mc are analyzed by wave theory. Good agreement between theory and experiment was obtained for a range of 32 miles. Between 32 and 70 miles variations of intensity with height are as expected, but the theoretical horizontal decrement is less than that observed. Beyond about 80 miles the observed field tends to become uniform with height, and shows little horizontal attenuation. See also 521 of 1948, (Katzin, Bauchman, and Binnian).

621.396.812.4.029.6 2611
**Tropospheric Effects in Ionosphere-Supported Radio Transmission**—G. W. Pickard and H. T. Stetson. (PROC. I.R.E., vol. 37, pp. 596–599; June, 1949.) A statistical analysis of (a) night field strength at Newton Center, Mass., due to 1,330-kc broadcast transmissions from WBBM, Chicago, 850 miles away, (b) reception at Needham of WWV 5-Mc, XEWW 9.5-Mc, WWV 10-Mc, and W2XMN 44.1-Mc signals, for correlation with Boston weather data. Night field strength at Newton rises from a minimum one day before a temperature rise of 10° F to a maximum on the day of the rise. Similarly, a drop in field strength precedes an equal temperature fall. Night field strength of WWV 5-Mc transmissions tends to a maximum one day before a SE wind blows across the transmission path; such a wind is associated with temperature inversions. See also 1453 of 1948.

## RECEPTION

621.396.621 2612
**Extraction of Weak Signals from Noise by Integration**—H. Stockman, F. R. Dickey, Jr., and A. G. Emslie. (*Proc. N.E.C.* (Chicago), vol. 4, pp. 102–120; 1948.) Fundamental relationships concerning the detection of weak signals are obtained without recourse to the usual mathematical methods. A system is described in which a low-frequency mechanical filter interrupts the signal and gives about 24 db improvement in signal to noise ratio for an integration time of several minutes. Results obtained agree with theoretical calculations.

621.396.621 2613
**Optimum Selectivity in Superregenerators**—D. Richman. (*Proc. N.E.C.* (Chicago), vol. 4, pp. 121–131; 1948.) The selectivity of a superregenerator is determined by the variation of instantaneous sensitivity due to modulation of the resonator conductance during a quench cycle. For optimum selectivity, a conductance wave form may be selected to give narrowest skirt selectivity, or the nose of the curve may be narrowed to a degree determined by the rejection required for signals outside the pass band.

621.396.621 2614
**A Simple Far-Near Device for Radio Receivers**—H. Gibas. (*Bull. Schweiz. Elektrotech. Ver.*, vol. 39, pp. 362–367; May 29, 1948. In German.) An arrangement in which a band filter with feedback is used to increase the selectivity and sensitivity of a small receiver for the reception of signals from distant stations. The filter is short-circuited for local stations, giving a greater bandwidth and hence reception of better quality. The design of a suitable filter is discussed.

621.396.621 2615
**A Method for Distortionless Demodulation of Single-Sideband Oscillations**—E. Meinel. (*Arch. Elek.* (Übertragung), vol. 3, pp. 37–46; February, 1949.) The method is based on the fact that with quadratic rectification of single-sideband oscillations, only the first-order difference tones occur as nonlinear distortion, the amplitude of which is independent of the carrier amplitude. Since only the first-order difference tones remain after quadratic rectification of single-sideband oscillations without carrier, they can be completely eliminated in the compensation arrangement described, which consists of two symmetrical quadratic-rectifier receivers. The single-sideband oscillations with carrier are applied to one receiver and equal signals without carrier to the second receiver, the two outputs being applied in opposition in the common output circuit. Nonlinear distortion is thus eliminated so long as the modulation of the transmitter does not greatly exceed 50 per cent. The method should have wide application in single-sideband technique, including multichannel cable communication, long-wave and medium-wave broadcasting, and television.

621.396.621 2616
**Wideband Frequency Discriminator Design**—Rideout. (*See* 2483.)

621.396.621 2617

**Performance Capabilities of Superregenerative Receivers**—G. V. Eltgroth. (*Tele-Tech*, vol. 8, pp. 24–27, 57 and 40–43, 71; February and March, 1949.) Analysis with particular reference to selectivity and fidelity characteristics, signal-to-noise ratio and optimum operation conditions.

621.396.621:621.396.82 2618

**The Effect of Interference on Superregenerative Receivers**—L. S. Gutkin. (*Radiotekhnika* (Moscow), vol. 4, pp. 62–76; January and February, 1949. In Russian.) Continuation of 1738 of 1948. The effect of interference, consisting of single and repeated impulses, on the operation of a superregenerative receiver is investigated theoretically. The interference voltages at the output of the superregenerative circuit and of the low-frequency amplifier, and the effect of nonlinear operating conditions are discussed. A superregenerative receiver possesses a higher degree of discrimination with respect to impulse interference than an ordinary receiver. A general summary is given of types of interference.

621.396.621:621.396.619.11/.13 2619

**On Theoretical Signal-to-Noise Ratios in F.M. Receivers: A Comparison with Amplitude Modulation**—D. Middleton. (*Jour. Appl. Phys.*, vol. 20, pp. 334–351; April, 1949.) Signal-to-noise ratios at the output of a FM receiver are determined as functions of the input signal-to-noise ratio, clipping level, and af filter characteristics when random (fluctuation) noise accompanies the signal. Both narrow-band and broad-band FM are examined. Calculations are made for sinusoidal FM. The concept of signal-to-noise ratio is redefined. Comparison is made with AM reception using a half-wave linear rectifier. For signals less than 3 db above noise AM requires less input signal than FM for a given noise background and a given output. Only for signals at least 10 db above noise is FM superior to AM. Broad-band FM with heavy limiting is required in this case. Narrow-band FM, even with no limiting, is not better than AM at high signal levels. Limiting is detrimental for narrow-band operation, whereas it is essential for broad-band operation, in which case the shape of the if response curve is important. Curves illustrating the average and mean-square signal and noise outputs, and signal-to-noise ratios for various conditions of operation, are included.

621.396.82 2620

**Tolerable Mutual Interference of Two F.M. Broadcasting Transmitters**—T. J. Weijers. (*Tijdschr. ned. Radiogenoot.*, vol. 14, pp. 61–72; May, 1949. In Dutch.) Selectivity measurements for three different FM receivers are shown graphically and discussed. Conclusions as to the relative strengths and frequency characteristics of signals from two neighboring transmitters, consistent with satisfactory reception of the signals from one of them, are summarized.

621.396.82:537.523.3 2621

**Corona Interference with Radio Reception in Aircraft**—M. M. Newman. (*Proc. N.E.C.* (Chicago), vol. 4, pp. 91–95; 1948.) Oscillograms show typical corona pulses received on bare and on insulated antennas, and the serious effect of shock-excitation of both antennas and receiver circuits due to the sharp rate of rise of the pulses. Insulated antennas are recommended, but, even for these serious interference can be caused by other bare antennas and by charges developed on various parts of the aircraft structure.

621.396.82:551.594:551.577 2622

**The Effect of Air Speed upon Precipitation Charging of an Airplane**—H. J. Dana. (*Proc. N.E.C.* (Chicago), vol. 4, pp. 96–101; 1948.) Charging rate varies as the cube of air speed. This law was confirmed by experiment. Two types of discharger are discussed briefly.

621.396.822.029.63 2623

**Impairment of Intelligibility by Noise in Decimetre-Wave Links**—E. Dietrich. (*Fernmeldetech. Z.*, vol. 2, pp. 173–178; June, 1949.) Discussion of the various factors involved establishes that speech intelligibility suffers little reduction due to the circuit, multipath, or other noises usually met with. Decimeter-wave links can thus provide a satisfactory means of communication even without noise suppression.

621.396.828 2624

**Interference-Free Reception by means of Aerials with Screened Down-Leads**—W. Hormuth. (*Frequenz*, vol. 3, pp. 61–73; March, 1949.) Description of equipment suitable for either private dwellings or apartment houses. Particular attention is given to earthing arrangements and distribution systems.

621.396.828 2625

**Circuit Design for Reduction of Hum**—Dickerson. (*See* 2496.)

## STATIONS AND COMMUNICATION SYSTEMS

621.391.63:534.321.9:535.61-15 2626

**Ultrasonic Modulation of a Light Beam**—R. F. Humphreys, W. W. Watson, and D. L. Woernley. (*Jour. Appl. Phys.*, vol. 18, pp. 845–846; September, 1947.)

621.396(94) 2627

**Some Aspects of the Overseas Telecommunications Services Operated by the Overseas Telecommunications Commission, Australia**—A. S. McDonald. (*Proc. I.R.E.*, (Australia), vol. 9, pp. 4–8. Discussion, pp. 8–9; April, 1948.) An outline is given of the formation and functions of the Commission. A review of the present facilities includes a reference to the overseas facsimile service. Equipment and techniques are briefly described.

621.396.41:621.396.619.16 2628

**Terminal Equipment for Pulse-Time Multiplex**—A. M. Levine and D. D. Grieg. (*Proc. N.E.C.* (Chicago), vol. 4, p. 131; 1948.) Summary only. Discussion of: (a) design of terminals using pulse-amplitude, pulse-time or pulse-count modulation, (b) methods of maintaining bandwidth while improving signal-to-noise ratio by adding cross talk and distortion at the transmitting end and removing them at the receiver, (c) methods of establishing base rates and timing of the channels, (d) modulation circuits for timed channels, (e) methods of maintaining synchronism and framing, (f) channel selection and demodulation, and (g) mechanical and electrical construction. A general description of various terminal units, with photographs, is included.

621.396.41.029.63:621.396.97 2629

**Experimental Ultra-High-Frequency Multiplex Broadcasting System**—A. G. Kandoian and A. M. Levine. (PROC. I.R.E., vol. 37, pp. 694–701; June, 1949.) An 8-channel high-fidelity system in which multiplex operation is achieved by time-sharing pulse-time modulation. The main components, including modulator, transmitter antenna system and receiver, are described and their operating characteristics discussed.

621.396.44:621.315.052.63 2630

**Operational Experience with Single-Sideband Power-Line Carrier Equipment**—F. S. Beale. (*Tele-Tech*, vol. 8, pp. 32–35; June, 1949.) Single-sideband equipment is particularly useful under conditions of high circuit attenuation, high noise level, heterodyne interference, or where a limited frequency band is available.

621.396.619 2631

**Contribution to the General Theory of Modulation and Demodulation for Any Type of Characteristic**—Heymann. (*See* 2482.)

621.396.619:621.396.61 2632

**"Auto-Anode" Modulation for Radio Broadcasting Transmitters**—N. G. Kruglov. (*Radiotekhnika* (Moscow) vol. 4, pp. 7–24; March and April, 1949. In Russian.) Description of a modulation system proposed by the author and now used at several broadcasting stations in the U.S.S.R. No high-power modulator is used, but certain tubes which generate rf oscillations also serve for anode modulation. The rf output is not less than that obtained with the usual anode-modulation methods. The theory of the method is discussed and various practical circuits are suggested. The modulation efficiency is almost double that for grid modulation; an over-all transmitter efficiency of 45 per cent is possible.

621.396.619.13 2633

**Some Developments in Frequency-Modulation Techniques**—D. A. Bell. (*Strowger Jour.*, vol. 6, pp. 159–165; April, 1949.) Discussion with particular reference to signal-to-noise ratio, reactance-tube FM, relaxation oscillators, and counter circuits as frequency detectors. Simple and compact equipment for a 6-channel system is described briefly; this can be used with either cable or radio links.

621.396.619.13:621.396.029.58 2634

**On the Application of Frequency Modulation in Short-Wave Radio Technique**—H. J. Griese. (*Fernmeldetech. Z.*, vol. 2, pp. 141–146; May, 1949.) Bandwidth and signal-to-noise characteristics for AM and FM, distortion due to multipath transmissions, and fading effects are discussed. The principles of a phase-shift keying system are explained.

621.396.619.13:621.396.611.3 2635

**The Application of Coupled Systems with Distributed Constants to Frequency Modulation in the Ultra-High-Frequency Range**—Tolstikov. (*See* 2475.)

621.396.619.16 2636

**Pulse Modulation**—E. M. Deloraine. (PROC. I.R.E., vol. 37, pp. 702–705; June, 1949.) A general review of various types of pulse modulation. Application to time-division multichannel systems and to switching problems are discussed.

621.396.65:621.396.3 2637

**A 150-kc/s Carrier System for Radio Relay Applications**—J. E. Boughtwood. (*Trans. AIEE*, vol. 67, pp. 577–582; 1948.) Developed by the Western Union Telegraph Co. Thirty-two voice-band communication channels, each 3,000 cps wide, are derived in the frequency range 4 to 147 kc. Tandem stages of group modulators maintain high spectrum efficiency without crystal filters. A crystal-controlled harmonic carrier supply ensures the frequency stability required by narrow-band FM telegraph circuits. See also 2471 above.

621.396.97:621.396.619.13 2638

**Frequency-Modulation Broadcasting**—A. J. McKenzie. (*Proc. I.R.E.* (Australia), vol. 9, pp. 4–16; May, 1948. Discussion pp. 16–17.) A general review, with particular reference to experimental transmissions from Melbourne and Sydney. Various types of transmitter and typical methods of producing FM waves are discussed. Conventional antenna systems used in FM broadcasting are described and their performances are compared.

621.396.97(43) 2639
**Twenty-Five Years of Broadcasting in Germany**—A. Heilmann. (*Fernmeldetech. Z.*, vol. 2, pp. 129–134; May, 1949.) A review of technical developments.

## SUBSIDIARY APPARATUS

621-526 2640
**Evaluating Servomechanisms Performance**—G. M. Attura. (*Proc. N.E.C.* (Chicago), vol. 4, pp. 72–90; 1948.

621-526 2641
**Electronic Circuits for Control of Clutch-Type Servomechanisms**—F. E. Edwards, Jr. (*Proc. N.E.C.* (Chicago), vol. 4, pp. 54–58; 1948.) Brief description of clutch-type servomechanisms and desirable control-circuit characteristics, with details of a circuit of minimum time-lag and good stability.

621-526:621.317.79:621.396.615 2642
**Signal Generators for Servo System Measurements**—C. F. White. (*Proc. N.E.C.* (Chicago), vol. 4, pp. 59–71; 1948.)

621.3.027.3:621.316.722 2643
**A 500-50 000-Volt Regulated Power Supply**—R. E. Anderson. (*Proc. N.E.C.* (Chicago), vol. 4, pp. 315–329; 1948.) Discussion of a continuously variable dc supply unit with a maximum load current of 1 ma. A Hartley oscillator giving a frequency of about 40 kc is used with a voltage-tripler circuit. Two regulating loops in series maintain the output voltage constant within 0.2 per cent; one loop serves to control the screen-grid voltage of the rf amplifier tubes and the other to control the dc output through a dc amplifier and series regulating tube. The primary reference voltage is a thermally insulated battery from which no current is drawn.

621.314.63 2644
**A Practical Approach to Calculating Optimum Performance of Semiconductor Rectifiers**—Wilson. (*See* 2452.)

621.314.632 2645
**Twenty-Five Years of Copper/Copper-Oxide Rectifiers**—L. O. Grondahl. (*Trans. AIEE*, vol. 67, part 1, pp. 403–410; 1948.)

621.316.726 2646
**Electronic Voltage Regulator for Control of Generators**—W. J. R. Farmer. (*Elec. Times*, vol. 115, pp. 803–806; June 16, 1949.) The advantages of such regulators are discussed and the general principles of a standard type are explained in detail.

## TELEVISION AND PHOTOTELEGRAPHY

621.397.24:621.394 2647
**Western Union Teletape Facsimile**—L. G. Pollard. (*Trans. AIEE*, vol. 67, part 1, pp. 511–515; 1948.)

621.397.331.2 2648
**Cathode-Ray Tubes for Television. Operating Conditions v. Picture Brightness**—H. Moss. (*Wireless World*, vol. 55, pp. 202–205 and 261–263; June and July, 1949.) Discussion of (a) the increase of crt voltage required to maintain constant brightness as the screen diameter is increased, assuming constant resolution at the screen, constant spot size, and constant number of lines, and (b) the increase of tube voltage to maintain constant brightness as the number of scanning lines is increased, the frame frequency being unchanged.

621.397.335 2649
**The Locked Oscillator in Television Reception**—K. Schlesinger. (*Proc. N.E.C.* (Chicago), vol. 4, pp. 337–350; 1948.) Synchronization by amplitude separation of timing and picture signals does not always offer adequate noise protection. Conditions can be improved by using high-Q circuits to select a narrow spectrum around the line-scanning frequency. The number of lines effectively linked in phase is increased by using a locked oscillator tuned to the average line frequency and directly synchronized by the signal input. Q is thus increased by regeneration. Theoretical potentialities of such systems are indicated and a successful practical solution is discussed.

621.397.5:535.88 2650
**An Improved Schmidt Plate**—D. B. G. Hawkins. (*Phil. Mag.*, vol. 40, pp. 670–679; June, 1949.) The profile of an improved aspherical plate is calculated which minimizes the off-axis errors of Schmidt cameras over an given field. The color error is small compared with the off-axis errors for wide angular fields.

621.397.5:535.88 2651
**Large-Screen Television**—R. V. Little, Jr. (*Proc. N.E.C.* (Chicago), vol. 4, pp. 352–361; 1948.) Discussion of the basic elements of the direct-viewing system and the intermediate-film system.

621.397.5:535.88 2652
**Demonstration of Large-Screen Television at Philadelphia**—R. Wilcox and H. J. Schlafly. (*Jour. Soc. Mot. Pic. Eng.*, vol. 52, pp. 549–560; May, 1949.) A description of experiments with RCA equipment in the Fox-Philadelphia theatre, June, 1948. Screen brightness was increased by use of a crt voltage of 80 kv and an aluminized screen with controlled directional characteristics.

621.397.5:535.88:791.45 2653
**Theater Television System**—R. Hodgson. (*Jour. Soc. Mot. Pic. Eng.*, vol. 52, pp. 540–548; May, 1949.) A review of the development and performance of the intermediate-film method adopted by Paramount Pictures.

621.397.6:621.385.832 2654
**Mass-Production Techniques for Television Kinescopes**—D. Y. Smith. (*Proc. N.E.C.* (Chicago), vol. 4, p. 186; 1948.) Summary only.

621.397.6:778.3 2655
**Video Recording Technics**—G. H. Gordon. (*Tele-Tech*, vol. 8, pp. 31–33, 63 and 29–31, 55; May and June, 1949.) A detailed description of equipment using 16-mm film for photographing direct from a television cathode-ray tube. Film speed is 24 frames per second. The arrangements for conversion from the standard American television rate of 30 frames per second are discussed. Standard films are satisfactory.

621.397.61 2656
**Experimental Transmitting and Receiving Equipment for High-Speed Facsimile Transmission: Part 2—Details of the Transmitter**—D. Kleis, F. C. W. Slooff, and J. M. Unk. (*Philips Tech. Rev.*, vol. 10, pp. 257–264; March, 1949.) Part 1, 2338 of September. Part 3, 2657 below.

621.397.62 2657
**Experimental Transmitting and Receiving Equipment for High-Speed Facsimile Transmission: Part 3—Details of the Receiver**—F. C. W. Slooff, M. van Tol, and J. M. Unk. (*Philips Tech. Rev.*, vol. 10, pp. 265–272; March, 1949.) Part 2, 2656 above.

621.397.62 2658
**New Television Receiver without Transformers. Design with Interchangeable Units**—R. Aschen. (*TSF Pour Tous*, vol. 25, pp. 129–133, 169–173, 205–212, and 244–246; April and August, 1949.) Detailed description of a receiver comprising four units, each with its own power supply. Interaction between the four units can easily be avoided by operating them sufficiently far apart and any unit can be changed without affecting the others. The units are respectively (a) video receiver, (b) sound receiver, (c) time base unit, and (d) 7-kv supply unit for the cathode-ray tube. Stagger tuning is used in the video circuit and blocking oscillators in the line and image timebases. Detailed circuit diagrams are given in all cases. Pertinent circuit formulas and timebase refinements are discussed in an appendix.

## TRANSMISSION

621.392.53:621.396.645 2659
**Investigations on Path-Time Distortion in Carrier-Frequency Amplifiers**—Schaffstein. (*See* 2494.)

621.394.61:621.396.029.52 2660
**Valve Loading and Signal Shape for Slightly Damped Long-Wave Telegraphy Transmitters**—A. Ruhrmann. (*Fernmeldetech. Z.*, vol. 2, pp. 147–152; May, 1949.) The effect of the loading of the transmitter output tube on the signal shape is discussed. A considerable improvement in signal shape can be effected by the use of feedback. Transmitter operation is considered by reference to the equivalent circuit and the characteristics of 2-stage and 3-stage transmitters are discussed. The latter have definite practical advantages.

## VACUUM TUBES AND THERMIONICS

621.3.015.3:621.385 2661
**The Surge Testing of High-Vacuum Tubes**—H. J. Dailey. (*Proc. N.E.C.* (Chicago), vol. 4, pp. 187–199; 1948.) A method for initiating flash arcs and the results of such arcs under various conditions are described. Damage is a function of tube gas pressure, electrode configuration, and arc current. Suggestions are made for minimizing arc effects.

621.385 2662
**Operating Conditions for the Optimum Working of Output Valves in High-Power Broadcast Amplifiers**—N. L. Bezladnov. (*Radiotekhnika* (Moscow), vol. 4, pp. 5–15; January and February, 1949. In Russian.) The optimum working of a tube is secured when $\xi$, $k$, and $A$ tend simultaneously to unity, where $\xi$ is the ratio of peak voltage swing to steady anode voltage, $k$ is the ratio of maximum anode current to saturation current, and $A$ is the ratio of maximum anode current to permissible anode dissipation. Each of these conditions is examined separately and the necessary tube parameters and operating conditions for satisfying them are discussed. Practical suggestions are given.

621.385 2663
**Trends in Electron Tube Design**—W. C. White. (*Trans. AIEE*, vol. 67, part 1, pp. 796–808; 1948.) See 1827 of July.

621.385-713 2664
**A Transmitting Valve Cooler with Increased Turbulence of the Cooling Water**—M. J. Snijders. (*Philips Tech. Rev.*, vol. 10, pp. 239–246; February, 1949.) Details of a cooling system using rings of jets round the anodes of high-power tubes.

621.385.029.62 2665
**Glass Transmitting Valves of High Efficiency in the 100-Mc/sRange**—E. G. Dorgelo. (*Philips Tech. Rev.*, vol. 10, pp. 273–281; March, 1949.) Reasons for preferring a coaxial cylindrical construction are given. Special features include a spiral cathode of thoriated tungsten, a nonemissive grid, a graphite anode with horizontal cooling fins and shaped like a cotton reel, and a shield to reduce the temperature of the lower part of the all-glass envelope. In the triodes, the shield is connected to the grid, so that the tubes can be

used in grounded-grid circuits without neutrodyning even at 200 Mc. In the tetrodes, the shield is connected to the screen-grid and neutrodyning is necessary only above about 100 Mc. Details are given of the triode TB 2.5/300 and the tetrode QB 2.5/250, with anode dissipations of 135 watts and 125 watts respectively and an efficiency of 65 to 70 per cent at 100 Mc. Larger tubes, with dissipation up to 540 watts, are in course of development.

621.385.029.63/.64 2666

**On the Propagation of Waves along a Coaxial Spiral Line in the Presence of an Electron Beam**—L. N. Loshakov. (*Zh. Tekh. Fiz.*, vol. 19, pp. 578–595; May, 1949. In Russian.) A mathematical analysis. The inner conductor of the line is of spiral form. The problem was solved in a general way by the use of equivalent circuits by Pierce (2284 of 1947) and Bernier (4066 of 1947). Here a specific retardation system—the spiral line—is considered, which for centimeter waves is apparently the most suitable. From Maxwell's equations and an equation of electron travel, expressions are derived determining the field structure of waves propagated in the line. A particular case is discussed.

621.385.029.63/.64 2667

**A Periodic-Waveguide Traveling-Wave Amplifier for Medium Powers**—G. C. Dewey. (*Proc. N.E.C.* (Chicago), vol. 4, p. 253; 1948.) Summary only. The most successful waveguide for use as a power amplifier, with the best gain and bandwidth characteristics and propagating a useful slow mode, is singly corrugated coaxial transmission line with the corrugations on the inner conductor. Such an amplifier has been built giving 10 db gain at 40 watts output and a bandwidth at 4,600 Mc of 70 Mc between 3-db points. Results confirm theory to a marked degree and suggest that even better results are possible. The tube appears to be capable of 100 times the power output of the Pierce helix-type traveling-wave amplifier at any frequency.

621.385.029.63/.64:621.396.645 2668

**A Note on Filter-Type Traveling-Wave Amplifiers**—J. R. Pierce and N. Wax. (PROC. I.R.E., vol. 37, pp. 622–625; June, 1949.) Small-signal analysis of systems in which an electron beam interacts with a circuit composed of discrete filter elements. The interaction between a line beam and a series of gaps, which are capacitive elements of a filter structure, is discussed. An admittance arising from the presence of the electrons can be introduced, which is in parallel with the gap capacitance and will thus alter the propagation factor of the filter circuit. Traveling-wave solutions exist for the combination of electron beam and filter circuit; there is a solution with a positive real part, indicating that amplification will occur.

621.385.029.63./64 2669

**On the Mode of Operation of the Travelling-Wave Valve**—O. Döhler and W. Kleen. (*Arch. Elek.* (Übertragung), vol. 3, pp. 54–63 and 93–100; February and March, 1949.) The construction and operation of such tubes are briefly discussed. The power gain is of the order of 20 db. The bandwidth may exceed 100 Mc. Approximate calculations indicate that the over-all efficiency of the tube cannot exceed a few per cent. The theory for large signals shows that with present technique the maximum power that can be handled is only 0.5 to 1 watts. Discussion of space-charge effects explains the difference between measured values of amplification and values calculated without taking account of space-charge effects. See also 250 and 251 of February and 2089 of August.

621.385.032.21 2670

**Alkali-Metal Alloys for Cathodes of Power Electronic Tubes**—J. A. M. Lyon and C. E. Williams. (*Proc. N.E.C.* (Chicago), vol. 4, pp. 179–185; 1948.) An account of experiments with sodium-amalgam and potassium-amalgam cathodes in glass and in metal envelopes. A potassium-amalgam tube is described which operated satisfactorily in an inverted position for about half an hour.

621.385.032.216 2671

**Pulse Emission Decay Phenomenon in Oxide-Coated Cathodes**—G. R. Feaster. (*Jour. Appl. Phys.*, vol. 20, pp. 415–416; April, 1949.) The cathode fatigue effect which sometimes occurs during high-power pulse emission from BaO-SrO cathodes is ascribed to poisoning. Experimental evidence of this is discussed. The decay is only obtained when electrons bombard a portion of the anode containing a poisoning agent. The question whether oxygen can cause the decay is still being investigated.

621.385.2:537.525.92 2672

**Note on Space-Charge Considerations in Test-Diode Design**—E. A. Coomes and J. G. Buck. (PROC. I.R.E., vol. 37, pp. 626–627; June 1949.) For test diodes of axial symmetry, the minimum variation in the slope of the space-charge line for small variations in the anode radius $r_a$ and cathode radius $r_c$ occurs when $r_a/r_c = 3.16$.

621.385.2:621.396.822 2673

**Current Fluctuations in a Plane Diode, taking account of Space Charge and Transit Time**—A. Pérez. (*Compt. Rend. Acad. Sci.* (Paris), vol. 228, pp. 1482–1484; May 9, 1949.) Starting from published tables (2977 of 1948), new tables have been derived covering the low-frequency range. In the decimeter-wave region there should be an increase of the fluctuations with frequency, due to the Poisson emission of electrons. This may to a certain extent explain the high noise values observed.

621.385.2.032.216 2674

**Testing Cathode Materials in Factory Production**—J. T. Acker. (PROC. I.R.E., vol. 37, pp. 688–690; June, 1949.) Discussion of standard forms for reporting the results of tests of initial shrinkage, initial tube characteristics, and life tests, in order to determine a figure of merit for the material. See also 2675 below.

621.385.2.032.216 2675

**A Standard Diode for Electron-Tube Oxide-Coated Cathode-Core-Material Approval Tests**—R. L. McCormack. (PROC. I.R.E., vol. 37, pp. 683–687; June, 1949.) Report of the work of a committee set up by the American Society for Testing Materials to prepare a specification for a standard diode test. Construction details of the standard diode are tabulated and illustrated; standard parts have been made available to interested companies. A cathode-temperature emission characteristic for each test lot is taken at anode voltage 40 volts, and compared with the same characteristic for a standard material. A figure of merit is deduced. Satisfactory correlation between tests by different companies was thus achieved; in one case surface contamination of a particular sample was established as a result of the tests. Additional tests are briefly discussed. See also 2674 above.

621.385.3 2676

**The Dyotron Tube as a Very-High-Frequency Oscillator**—R. A. Dehn. (*Proc. N.E.C.* (Chicago), vol. 4, p. 220; 1948.) Summary only. See also 2979 of 1948.

621.385.832:[537.291+538.691 2677

**Electron Beam Deflection. Part 2—Applications of the Small-Angle Deflection Theory**—R. G. E. Hutter. (*Jour. Appl. Phys.*, vol. 18, pp. 797–810; September, 1947.) The theory discussed in part 1 (609 of 1948) is applied to deflection fields produced by parallel plates, parallel wires, semi-infinite coplanar sheets, and bent plates. Results are shown graphically. An electrolyte-tank potential-plotting device used for experimental verification is described. The deflection depends on the initial conditions and its relationship with field strength is slightly nonlinear. The resulting distortions of the spot and the crt pattern are calculated for several deflection fields and beam shapes, and methods of reducing such distortion are considered.

621.385.832:621.397.6 2678

**Mass-Production Techniques for Television Kinescopes**—D. Y. Smith. (*Proc. N.E.C.* (Chicago), vol. 4, p. 186; 1948.) Summary only.

621.396.615.142 2679

**Pulsed Reflex Oscillator**—(*Electronics*, vol. 22, p. 130; April, 1949.) Brief description of a rugged, miniature, v.m., external-cavity oscillator tube, Type QK-205 (RMA Type 5721), which can generate frequencies from 2,000 to 12,000 Mc. Operating characteristics are tabulated.

621.396.645:537.311.33:621.315.59 2680

**The Transistor—Its Properties and Characteristics**—W. H. Brattain and J. Bardeen. (*Proc. N.E.C.* (Chicago), vol. 4, p. 32; 1948.) Summary only. See also 264 of February.

## MISCELLANEOUS

621.38/.39(43) 2681

**German Electronics in World War II**—A. H. Sullivan, Jr. (*Elec. Eng.*, vol. 68, pp. 403–409; May, 1949.) Much effort was devoted after 1943 to radar antijamming devices, but with little success. Radio, radar, infrared, proximity fuses, tubes, ceramics, components, and navigational devices were also investigated. Apparatus of various kinds listed below is briefly discussed: (a) radar; Freya, Würzburg and Jagdschloss types, (b) radio; Type FuG 16 vhf aircraft equipment, which was extremely selective and stable; Type FuG 24, a mass-produced equipment weighing only 35 lb, with frequency range 37 to 50 Mc; the Peil G6 standard direction-finding receiver; (c) V-1 and V-2 rockets, (d) Tonschreiber and magnetophon magnetic tape recorders; (e) metal-lens, iron-core, and multi-element dielectric antennas, (f) a cathode-ray tube having two colors with different afterglow periods, (g) the Blauschrift, Mocos, and Krawinkel storage tubes, (h) carbon-film resistors, (i) inductors formed by depositing metallized coatings on ceramics, and (j) synthetic-mica and metallized-paper capacitors.

621.396 2682

**The Radio Amateur's Handbook** [Book Review]—Headquarters Staff of the American Radio Relay League. American Radio Relay League, West Hartford, Conn., 26th edition, 1949, 605 pp., 15s.6d. (*Wireless World*, vol. 55, p. 215; June, 1949.) Most of the chapters have been revised, particularly in the case of vhf, microwave, and antenna equipment. 52 pages of tube data are included. Obtainable from A. F. Bird, 66 Chandos Place, London, W.C.2, at 16s.3d., including postage, or through the Radio Society of Great Britain, New Ruskin House, Little Russell St., London, W.C.2, at 12s.6d., including postage, for delivery from America.